SYNTHESIS OF RESPONSIVE HOMO- AND BLOCK COPOLYMERS, APPLICATION TO THE GENERATION OF INORGANIC-ORGANIC NANOHYBRIDS

DISSERTATION

zur Erlangung des akademischen Grades eines
Doktors der Naturwissenschaften (Dr. rer. nat.)
in Fach Chemie der Fakultät für Biologie, Chemie und Geowissenschaften
der Universität Bayreuth

vorgelegt von

Pierre-Eric Millard

Geboren in Troyes / Frankreich

Bayreuth, 2010

Die vorliegende Arbeit wurde in der Zeit von August 2004 bis September 2008 in Bayreuth am Lehrstuhl Makromolekulare Chemie II unter der Betreuung von Herrn Prof. Dr. Axel H. E. Müller angefertigt.

Dissertation eingereicht am: 27.07.2010

Zulassung durch die Promotionskommission: 04.08.2010

Wissenschaftliches Kolloquium: 20.10.2010

Amtierender Dekan: Prof. Dr. Stephan Clemens

Prüfungsausschuss: Prof. Dr. K. Seifert (Vorsitz)

                       Prof. Dr. A. H. E. Müller (Erstgutachter)

                       Prof. Dr. A. Böker (Zweitgutachter)

                       Prof. Dr. R. Kempe

To my family

The most exciting phrase to hear in science, the one that heralds
the most discoveries, is not "Eureka!" but "That's funny..."
(Isaac Asimov)

Table of Contents

Summary

Responsive homopolymers and multi-responsive block copolymers were prepared via reversible addition-fragmentation chain transfer (RAFT) and atom transfer radical polymerization (ATRP). Self-assembly in solution depending on environmental stimuli was investigated and exploited to create responsive micelles. New cross-linking strategies were thoroughly performed in aqueous solution to allow a controlled preservation and a high shape-persistence of the colloid particles, even when exposed to non-selective environmental conditions.

The synthesis of poly(*N*-isopropylacrylamide) (PNIPAAm) was investigated by ATRP for subsequent polymer-protein nanohybrid generation. This temperature-responsive polymer was polymerized directly in pure water at a low temperature (4 ℃) by using a functional ATRP initiator which allows post-polymerization conjugation. Without the addition of Cu(II), the kinetics were extremely fast, typically less than one minute for a full conversion. By adjusting the ratio of Cu(I)/(Cu(II) and selecting a very active ligand, all polymerizations proceeded in a controlled fashion to near quantitative conversion without evidence of termination.

N-isopropylacrylamide and acrylic acid (AA) were also homopolymerized by RAFT in aqueous media using a novel strategy. Instead of using a diazo-initiator, which generally decomposed at high temperatures, γ-irradiation was used to initiate polymerization at ambient temperature. This type of radiation has many advantages. A very tiny and constant amount of radicals can be generated, which is perfect for the RAFT process. Moreover, the rate of initiation only has a low level of dependence on temperature and can be used in a wide range of temperatures. Finally, compared to UV-initiation, γ-irradiation can penetrate the reaction solution deeper and without evidence of irreversible decomposition of the dithioester end group. Therefore, RAFT polymerizations of NIPAAm and AA were achieved with a very good level of control, even at high monomer conversions.

This new process was then extended to many other water-soluble monomers for generating homopolymers and block copolymers. Among these, acrylamide, *N,N*-

dimethylacrylamide, 2-hydroxyethyl acrylate and poly(ethylene glycol) methacrylate gave the best results. This technique proved to be very efficient at generating very long and narrowly distributed polymers (up to a degree of polymerization of 10,000) and at designing block copolymers.

High molecular weight PNIPAAm-*b*-PAA copolymers, synthesized by RAFT polymerization under γ-radiation, were used to generate multi-responsive cross-linked micelles. These block copolymers were self-assembled in water at pH 7 by increasing the temperature over the lower critical solution temperature. The PNIPAAm became hydrophobic and formed the micellar core and the hydrophilic PAA block generated the corona which prevented full aggregation of the system. Then, by amidification at elevated temperatures of the carboxylic moieties via a trifunctional primary amine, the structure was found to remain even after cooling down the system. The shell-cross-linked micelles formed were utilized to generate inorganic-organic nanohybrids by the in situ reduction of gold or silver salts to generate nanoparticles inside the nanocarrier.

Another strategy of cross-linking was also investigated by using amino-functional silsesquioxane nanoparticles. In water around neutral pH values and room temperature, these particles interacted with the carboxylic groups of a high molecular weight PNIPAAm-*b*-PAA by hydrogen bonding and ionic interactions to generate an insoluble complex. Due to the presence of the hydrophilic PNIPAAm block, defined spherical micelles were obtained. The inorganic-organic particles were successfully cross-linked by subsequent amidification to preserve the structure, even at a high pH. Different temperature properties of the hybrids were observed depending on the pH value, due to the residual charge in the micellar core. At a neutral pH, shrinking of the corona was observed, while at a high pH (pH 13) a fully reversible aggregation of the system occurred.

Zusammenfassung

Responsive Homopolymere und multi-responsive Blockcopolymere wurden mit der Reversiblen Additions-Fragmentierungs-Kettenübertragungs-Polymerisation (RAFT) und Atom Transfer Radikalpolymerisation (ATRP) synthetisiert. Die Selbstorganisation - abhängig von äußeren Stimuli - wurde untersucht und genutzt, um responsive Mizellen herzustellen. Es wurden neue Vernetzungsstrategien in wässriger Lösung durchgeführt um kontrolliert stabile kolloidale Partikel zu erhalten, auch wenn sie nicht-selektiven Umgebungsbedingungen ausgesetzt sind.

Die Synthese von Poly(*N*-isoproplyacrylamid) (PNIPAAm) mit ATRP wurde untersucht für die anschließende Entwicklung von Polymer-Protein Nanohybriden. Diese temperaturresponsiven Polymere wurden direkt in Wasser bei niedrigen Temperaturen (4 °C) unter der Verwendung eines funktionellen ATRP-Initiators polymerisiert, der die Postpolymerisationskonjugation erlaubt. Ohne die Zugabe von Cu(II) verlief die Reaktion extrem schnell, typischerweise für einen vollständigen Umsatz in weniger als einer Minute. Durch die Wahl des geeigneten Cu(I)/Cu(II)-Verhältnisses und eines sehr aktiven Liganden verliefen alle Polymerisationen kontrolliert und ohne das Auftreten von Terminierungsprodukten nahezu quantitativ.

N-Isopropylacrylamid und Acrylsäure (AA) wurden mit der RAFT-Polymerisation in wässrigen Medien durch eine neuartige Strategie homopolymerisiert. Anstatt der Verwendung eines Diazo-Initiators, der sich üblicherweise bei hohen Temperaturen zersetzt, wurde γ-Strahlung verwendet um die Polymerisation bei Umgebungstemperatur zu initiieren. Diese Art von Strahlung bietet einige Vorteile. Eine ideale Voraussetzung für den RAFTprozess stellt dabei die Generierung einer sehr geringen und konstanten Menge an Radikalen dar. Desweiteren ist die Initiierungsgeschwindigkeit kaum temperaturabhängig und kann somit über einen großen Temperaturbereich verwendet werden. Im Vergleich zur UV-Initiierung hat die γ-Strahlung keinen Einfluss auf irreversible Zersetzung der Dithioester-Endgruppe. Folglich wurden NIPAAm und AA auch bei hohen Monomerumsätzen mit einer sehr guten Reaktionskontrolle polymerisiert.

Dieser neue Prozess wurde auf einige andere wasserlösliche Monomere übertragen um engverteilte Homopolymere (bis zu einem Polymerisationsgrad von 10.000) und Blockcopolymere effizient herzustellen. Darunter zeigten Acrylamid, *N,N*-Dimethylacrylamid, 2-Hydroxyethylacrylat und Ethylenglycolmethacrylat die besten Ergebnisse.

Hochmolekulare PNIPAAm-*b*-PAA Blockcopolymere, die mit γ-induzierter RAFT-Polymerisation synthetisiert wurden, wurden für die Herstellung von multiresponsiven vernetzten Mizellen verwendet. Bei Erhöhung der Temperatur oberhalb der LCST (lower critical solution temperature) tritt eine Selbstorganisation der Blockcopolymere in Wasser (pH 7) auf. Somit erhält PNIPAAm einen hydrophoben Charakter, der den mizellaren Kern bildet. Der hydrophile PAA-Block bildet die Corona aus, der die Aggregation des Systems verhindert. Die Carboxylgruppen wurden bei erhöhten Temperaturen durch ein trifunktionelles primäres Amin amidiert. Die Struktur war auch nach Erniedrigung der Temperatur stabil. Die schalen-vernetzten Mizellen wurden verwendet, um anorganisch-organische Nanohybride durch die in situ-Reduktion von Gold- und Silbersalzen im Nanocarrier herzustellen.

Eine weitere Strategie zur Vernetzung wurde unter Einsatz von aminofunktionalisierten Silsesquioxan-Nanopartikel untersucht. In Wasser - im Bereich neutraler pH-Werte und Raumtemperatur - interagieren die Partikel mit der Carboxylgruppe eines hochmolekularen PNIPAAm-*b*-PAA Blockcopolymers über Wasserstoffbrückenbindungen und ionischen Wechselwirkungen um einen unlöslichen Komplex zu generieren. Die Anwesenheit des hydrophilen PNIPAAm-Blocks verursachte die Ausbildung sphärischer Mizellen. Die anorganisch-organischen Partikel wurden erfolgreich durch die anschließende Amidierung vernetzt um auch bei hohen pH-Werten die Struktur zu erhalten. Aufgrund der noch vorhandenen Ladung im Kern konnten Temperaturabhängigkeiten bei unterschiedlichen pH-Werten der Hybride festgestellt werden. Neutrale pH-Werte bewirkte das Schrumpfen der Corona wohingegen bei hohen pH-Werten (pH 13) eine vollständig reversible Aggregation des Systems stattgefunden hat.

10

Introduction

Life is polymeric in its essence: the most important components of living cells (proteins, carbohydrates and nucleic acids) are all polymers. The salient feature of functional biopolymers is their all-or-nothing, or at least highly nonlinear, response to external stimuli. Small changes happen in response to a varying parameter until a critical point is reached and a large change occurs over a narrow range of the varying parameter. These nonlinear responses of biopolymers are caused by highly cooperative interactions. Despite the weakness of each particular interaction taking place in a separate monomer unit, when combined over hundreds and thousands of monomer units, these interactions can provide significant driving forces for the processes occurring in the whole system.

Not surprisingly, an understanding of the mechanism of cooperative interactions in biopolymers has opened the floodgates of attempts to mimic this cooperative behavior in synthetic systems. Recent decades have witnessed the appearance of synthetic functional polymers called "stimulus responsive" or "smart" polymers which respond reversibly in some desired way to a change in temperature, pH, electric or magnetic fields, or some other parameters. This new class of material has lots of applications, mainly in the biomedical domain, but they can be also used in electronic, optic, environmental or energy domains, among others.

One very fascinating area of research in the field of smart polymers is the investigation of materials which can respond to several stimuli. One way of doing this is to sequentially polymerize two or more different monomers to generate block copolymers where each block will be environmentally sensitive. To reach this goal, controlled radical polymerization is the tool of choice for obtaining the block architecture under less stringent conditions than those required for ionic polymerization in terms of oxygen and water presence or monomer functionality. Multi-responsive block copolymers generated via this technique can self-assemble reversibly into micelles in solution by applying an external trigger. These smart micelles are, for instance, intensively studied as drug carriers. However, in this particular case, due to the low stability of micelles upon high

dilutions, it is necessary to cross-link the nanocontainer to avoid non-specific drug release.

The aim of this thesis was centered on the generation of compartmentalized polymeric nanoparticles, the evaluation of their self-assembly behavior, the generation of inorganic-organic hybrid materials and the application of these for current topics in materials science such as catalysis and nanocomposite materials. Within the scope of this thesis, I made use of a variety of polymerization techniques such as controlled radical polymerization and cross-linking reactions in solution. Likewise, self-assembly in solution was rigorously exploited with the aim of utilizing these as tools for the generation of novel materials with advanced properties. Therefore, the following introduction will not contain extensive reviews on polymerization techniques since they are fundamentally understood to a large extent. On the contrary, I will stress the current state-of-the-art responsive polymers and their applications. Some of the structures researched within this thesis (cross-linked micelles and nanohybrids) are of unmatched complexity and their applications have led to the discovery of novel properties relevant for both academic research and industrial applications.

Responsive Polymers

One area of intensive research in polymer chemistry involves polymers which undergo reversible conformational changes in response to pH, ionic strength or temperature changes in physiochemical properties, for example.[1-4] These materials have lots of applications in the pharmaceutical and agricultural industries, personal care formulations, enhanced oil recovery and water remediation.[5-10]

Among the different stimuli, temperature is the most widely used in environmentally responsive polymer systems. The change in temperature is not only relatively simple to control, but it is also easily applicable both in vitro and in vivo.[11-13] One of the unique properties of temperature-responsive polymers is the presence of a critical solution temperature. The critical solution temperature is the temperature at which the phase of the polymer and solution (or the other polymer) is discontinuously changed according to their

composition. If the polymer solution (mostly water) has one phase below a specific temperature, which depends on the polymer concentration, and is phase separated above this temperature, these polymers generally have a lower critical solution temperature (LCST), which is the lowest temperature of the phase separation curve on the concentration-temperature diagram. Otherwise, it is called a higher critical solution temperature (HCST) or upper critical solution temperature (UCST). However, most applications are related to LCST-based polymer systems.

Poly(*N*-substituted acrylamides) **Poly(vinyl ethers)** **Poly(N-vinyl caprolactam)** **Poly(2-alkyl-2-oxazolines)**

Poly(propylene oxide) **Poly(oligo(ethylene oxide)methacrylates)**

P(GVGVP)

Figure 1-1. Chemical structures of the main LCST polymer families.

Intramolecular collapse occurs before the intermolecular aggregation through LCST and the collapse of individual polymer chains increases the scattering of light in solution (the cloud point). Phase separation between the collapsed polymer molecules and the expelled water follows this cloud point. Besides the relationship between the polymer and

water molecules, there is another important characteristic of a temperature-responsive polymer. This is the intermolecular interactions in the water medium, which might create hydrogel shrinkage, micelle aggregation or the physical cross-links. Generally, two types of intermolecular forces can be considered; hydrogen bonding and hydrophobic interactions. One example of an intermolecular association based on hydrogen bonding is a random coil-to-helix transition, where lowering the temperature results in two or three biopolymer chains (e.g. gelatin) forming a helix conformation which generates physical junctions to make a gel network. Another example is the hydrogen bonding association/dissociation between different pendant groups, which can be controlled by temperature. Through this mechanism, reversible swelling/deswelling of hydrogels around a critical temperature was reported in random copolymers and interpenetrating polymer networks (IPNs) composed of polyacids (proton donor at low pH) and polyacrylamide (proton accepter). On the other hand, intermolecular associations can be controlled by the balance of hydrophobic interactions and temperature.

There are different families of natural and synthetic polymers which present a LCST (Figure 1-1). Poly(*N*-substituted acrylamide) is the most studied one. Among these, poly(*N*-isopropylacrylamide) (PNIPAAm) and poly(*N*,*N*-diethylacrylamide) (PDEAAm) are the most popular due to a sharp coil-to-globule transition at temperatures close to body temperature.[14] Moreover, these polymers are easily accessible by either conventional or controlled radical polymerization for obtaining architectures such as block copolymers, gels or grafted surfaces. These particularities make them excellent candidates for many applications related to drug delivery. Vinyl ether monomers can be also used to generate LCST polymers. For example, poly(methyl vinyl ether) has a transition temperature exactly at 37 °C, which makes it very interesting for biomedical applications. Poly(*N*-vinyl caprolactam) (PVCa) has not been studied as intensively as PNIPAAm, for example, but it also possesses very interesting properties for medical and biotechnological applications, such as solubility in water and organic solvents, biocompatibility, high absorption ability and a transition temperature within the settings of these applications (33 °C).[15-17] Poly(2-alkyl-2-oxazolines) display LCST behaviors in water over a large range of temperatures depending on the alkyl chain. Polyethers and their derivatives were found to have some responses to temperature. For instance,

poly(propylene oxide) exhibited a response to temperature as short poly(ethylene oxide) (PEO) oligomers. In this case, the LCST gradually increased with the chain length. Chemists used this property to graft PEO chains to methacrylate monomers (PEOMA) after copolymerization of two PEOMAs with different lengths to be able to easily tune the LCST just by modifying the initial monomer ratio.[18, 19] Finally, polypeptides can also show LCST behaviors when hydrophilic and hydrophobic residues are well balanced.[20] A polymer made out of repeating units of the pentapeptide GVGVP exhibited a volume phase transition at 30 °C which included hydrophobic folding and assembling transitions.[21]

The pH is another important signal which can be addressed through pH-responsive materials.[22] So far, the main use of this polymer type has been in biological applications such as drug delivery.[23, 24] Indeed, physiological pH changes from 1 to 7.5 depend on the different locations in the body. Therefore, ionizable polymers with a pKa value between 3 and 10 are excellent candidates for pH-responsive systems; several examples can be found in Figure 1-2. Weak acids and bases such as carboxylic acids, phosphoric acid and amines exhibit a change in the ionization state upon variation of the pH. This leads to a conformational change of the soluble polymers and a change in the swelling behavior of coils or hydrogels when these ionizable groups are linked to the polymer structure. The pH-responsive swelling and collapsing behavior has been used to induce the controlled release of model compounds such as caffeine, drugs like insulin or doxorubicin, and proteins such as bovine serum albumin. [25-27]
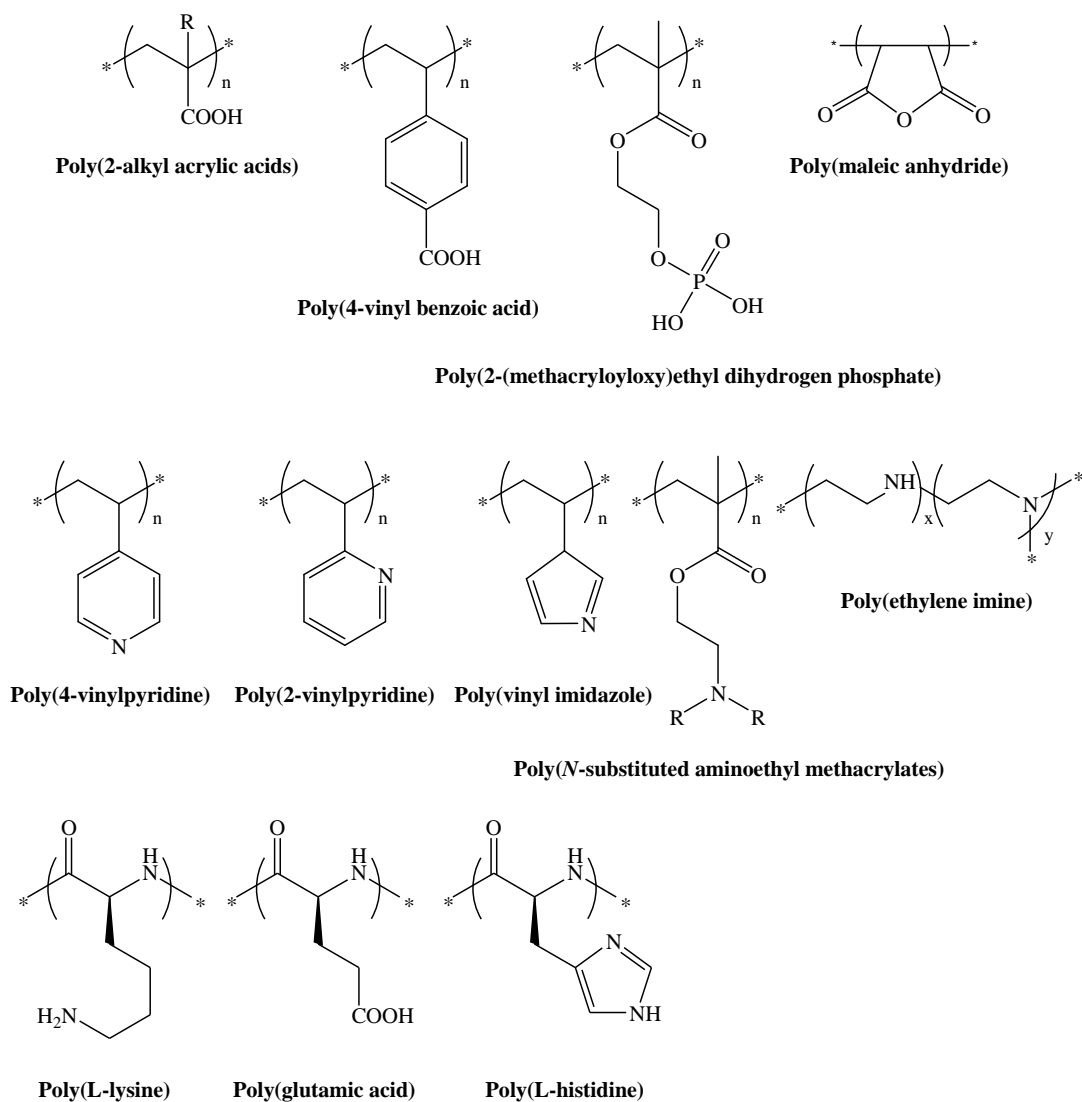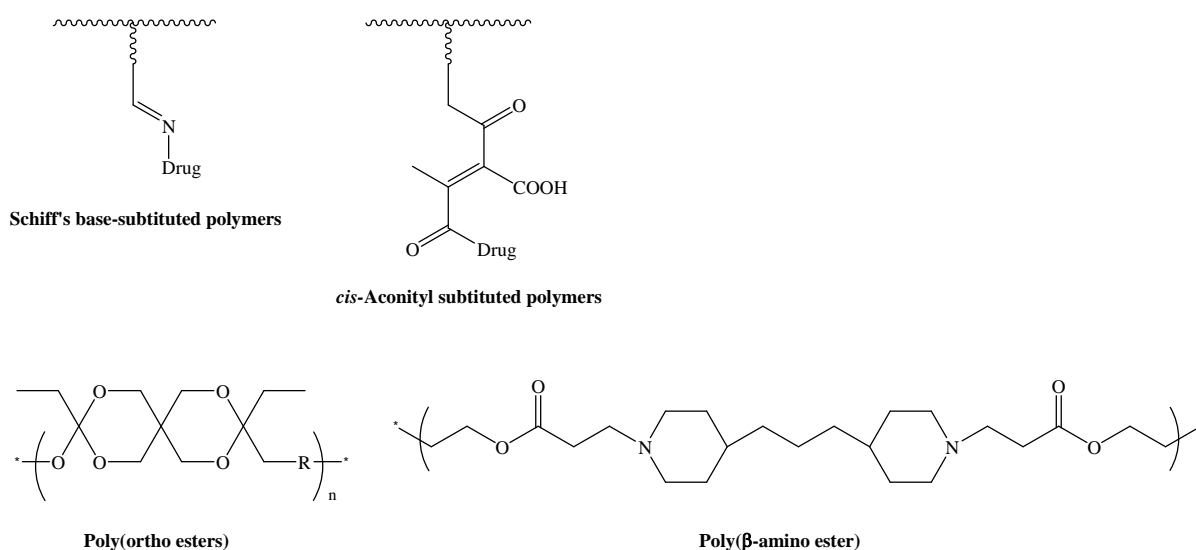
Figure 1-2. Chemical structures of the main pH-responsive polymer families.

Poly(*N,N'*-dimethyl aminoethyl methacrylate) (PDMAEMA) and poly(*N,N'*-diethyl aminoethyl methacrylate) (PDEAEMA) are examples of pH-responsive polybases. They have amine groups in their side chains. These groups gain protons under acidic conditions and release them under basic conditions. PDEAEMA has longer hydrophobic groups at the end of the amine group which cause stronger hydrophobic interactions at high pH values, and which also lead to "hypercoiled" conformations. The PDEAEMA homopolymer undergoes an abrupt precipitation above pH 7.5 due to the deprotonation of amino groups, followed by hydrophobic molecular interactions.[28] These amino polymers

have some applications, for instance in non-viral gene therapy.[29] The polycations can complex nucleotides through electrostatic interactions. The responsive characteristic of the polymer is important when the pH drops during cellular uptake as the polymer becomes increasingly charged and subsequently triggers osmotic, endosomolytic or other events. Poly(ethylene imine) (PEI) is still the golden standard against which every new polymer is tested, even though a large number of investigated polymers have performed better in terms of cytotoxicity and transfection efficiency.[30, 31] Poly(4-vinylpyridine) or poly(2-vinylpyridine) (PVP) show pH sensitivity.[32-34] These polymers undergo phase transition beneath pH 5 due to deprotonation of the pyridine groups.

The properties and applications of synthetic polymers based on natural amino acids were also investigated, including poly(L-lysine), poly(L-glutamic acid) and poly(L-histidine), due to their expected low toxicity in vitro.[35-38]

Schiff's base-subtituted polymers

***cis*-Aconityl subtituted polymers**

Poly(ortho esters)

Poly(β-amino ester)

Figure 1-3. Chemical structures of pH-responsive degradable polymer families.

Another type of pH-sensitive polymer can be defined as a polymer which can be chemically modified or degraded with pH due to its labile bonds (Figure 1-3). The main application for this type of polymer is the controlled release of drugs or active compounds. Indeed, drug molecules conjugated to a polymer are usually inactive. Therefore, these conjugates are called prodrugs.[39] This is an advantage for cytotoxic
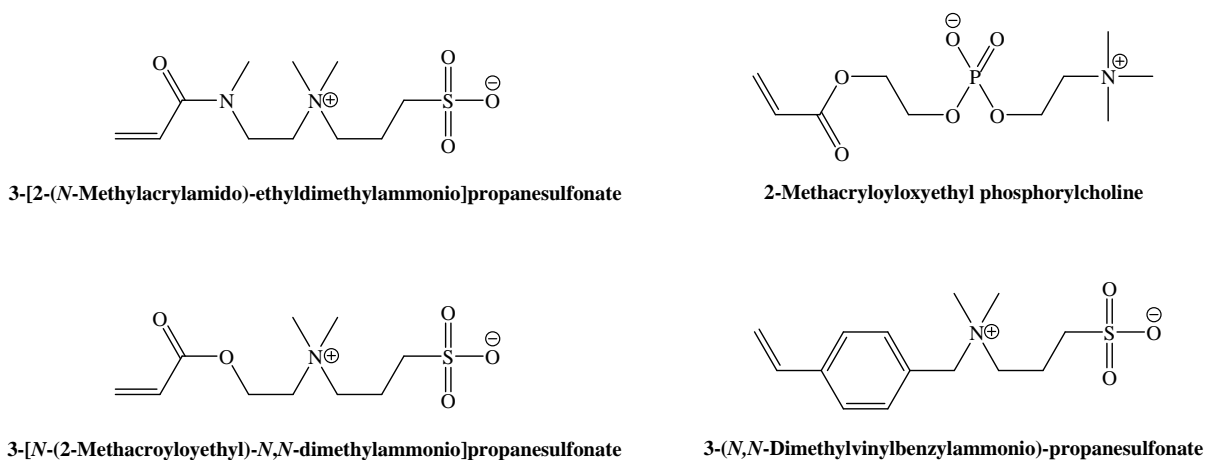
17

drugs, for example in cancer therapy, because the incorporation of a targeting system can avoid, or at least minimize, adverse side reactions due to the non-specific toxicity of these drugs. However, only an efficient release of the drug at the site of action gives these prodrugs their full advantage. Most prominent acid-labile linkers, which have been used in pH-triggered release mechanisms, are cis-aconityl acid or Schiff's-base derivatives, or polyacetals.[8, 40] Polyacetals rapidly undergo hydrolysis at acidic pH values and have potential for development as biodegradable carriers for anticancer drug delivery. Terpolymerization of divinyl ethers, serinol and PEO can be used to synthesize biodegradable, hydrolytically labile amino-pendent polyacetals suitable for drug conjugation.[41] These have been used for the conjugation of doxorubicin and have been found to be very promising.[42] Poly(ortho ester) shows fast degadation kinetics under mildly acidic conditions, while they are relatively stable at physiological pH values. This hydrolysis property was used to generate a hydrogel matrix for pulsatile insulin-delivery, and was applied in triggered drug release systems targeting weak acidic environments.[43, 44] Finally, poly(β-amino ester), an amine-containing polyester, was reported as being a pH-responsive biodegradable polymer. This polymer rapidly becomes soluble at pH values below pH 6.5. Microspheres composed of poly(β-amino ester) showed a rapid release of encapsulated material within the range of endosomal pH. Moreover, this polymer interacted electrostatically with plasmid DNA and formed nanometer-scale polymer/DNA complexes.[45] An important advantage of these polymers is that they are non-cytotoxic and degrade into non-toxic small molecular byproducts.[46, 47]
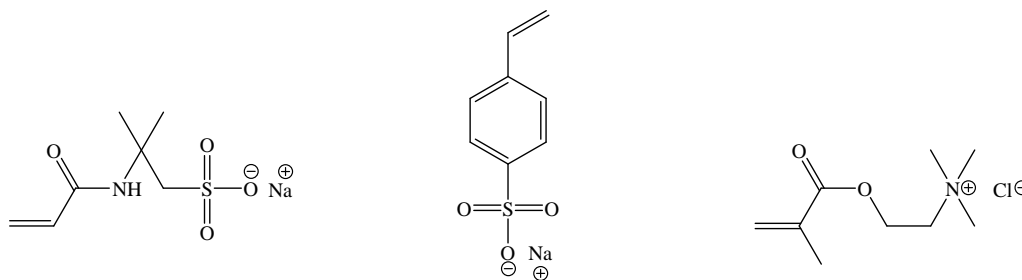
Sodium 2-acrylamido-2-methylpropanesulfonate   Sodium 4-styrenesulfonate   [2-(Methacryloyloxy)ethyl]trimethylammonium chloride

Figure 1-4. Chemical structures of ionic monomers

Many ion-containing polymers have been extensively studied due to their salt-responsive behavior in aqueous media. These ionically charged polymers can be separated into the following two groups: polyelectrolytes[48-50] and polyzwitterions.[51] Polyelectrolytes contain either anionically or cationically charged species along or pendant to the polymer backbone while polyzwitterions have both anionic and cationic charges (Figure 1-5). When the anionic and cationic charges are on different repeat units, the polyzwitterions are termed polyampholytes; if both charges are on the same repeat unit they are referred to as polybetaines. It should be noted that in addition to being salt responsive, polyampholytes and polybetaines may also be temperature or pH-responsive.[52, 53] Moreover, weak polyelectrolytes used as pH-responsive materials, such as polyacids or polybases, are also salt responsive.[54]

3-[2-(*N*-Methylacrylamido)-ethyldimethylammonio]propanesulfonate

2-Methacryloyloxyethyl phosphorylcholine

3-[*N*-(2-Methacroyloyethyl)-*N,N*-dimethylammonio]propanesulfonate

3-(*N,N*-Dimethylvinylbenzylammonio)-propanesulfonate

Figure 1-5. Chemical structures of zwitterionic monomers

Other stimuli were also intensively investigated, such as magnetic, electric or light responses, as were responses to chemicals present in the media. Electric-field-responsive polymers incorporated in hydrogels can present swelling, shrinking or bending behaviors in response to an external field.[55, 56] These polymer properties have been applied in bio-related applications such as drug delivery systems, artificial muscle and biomimetic actuators. Polymers bearing liquid crystals or comprising magnetic particles respond to external magnetic fields by changing shape.[57] Light-sensitive hydrogels have potential applications in the development of optical switches, display units and ophthalmic drug delivery devices.[58, 59] Since the light stimulus can be imposed instantly and can also be

delivered in specific amounts with high accuracy, light-sensitive hydrogels may possess special advantages over others. Chemists have also used biological compounds to induce responses in polymeric systems. For instance, glucose, antibody and antigen, urea and morphine sensitivity have already been tested.[60-63]

By using different methods of synthesis, it is possible to combine different monomers which after polymerization will generate a material which will respond to two or more stimuli.[64] Double- and multi-responsive systems can generally be distinguished based on their polymer architecture. Random copolymers are used to tailor the transition point depending on two independent parameters, for example pH and temperature.[65, 66] In contrast, block copolymers tend to self-assemble reversibly and form micelles depending on environmental conditions.[67, 68] For example, PNIPAAm-*b*-PAA can respond to temperature due to the PNIPAAm block and to pH and ionic strengths due to the PAA.[69] Depending on the environmental conditions, several morphologies can be observed, as depicted in Figure 1-6. Thus, at neutral or basic pH values and at room temperature, only unimers are present in water, whereas for the same pH but a higher LSCT, micelles with PNIPAAm cores are formed. For the same system at room temperature, but with pH < 4, a micellar state is also reached. In this particular case the core is composed of a mixture of NIPAAm and AA. Both interact by hydrogen bonding between the amide and the carboxylic moiety in a 1:1 functionality complex and become insoluble in water. In the case of unsymmetrical block copolymers the corona is then composed of an excess of moieties. These transitions are fully reversible when the stimulus changed. In the case of most vinylic monomers, the block copolymer architecture can easily be achieved by using controlled radical polymerization (CRP).
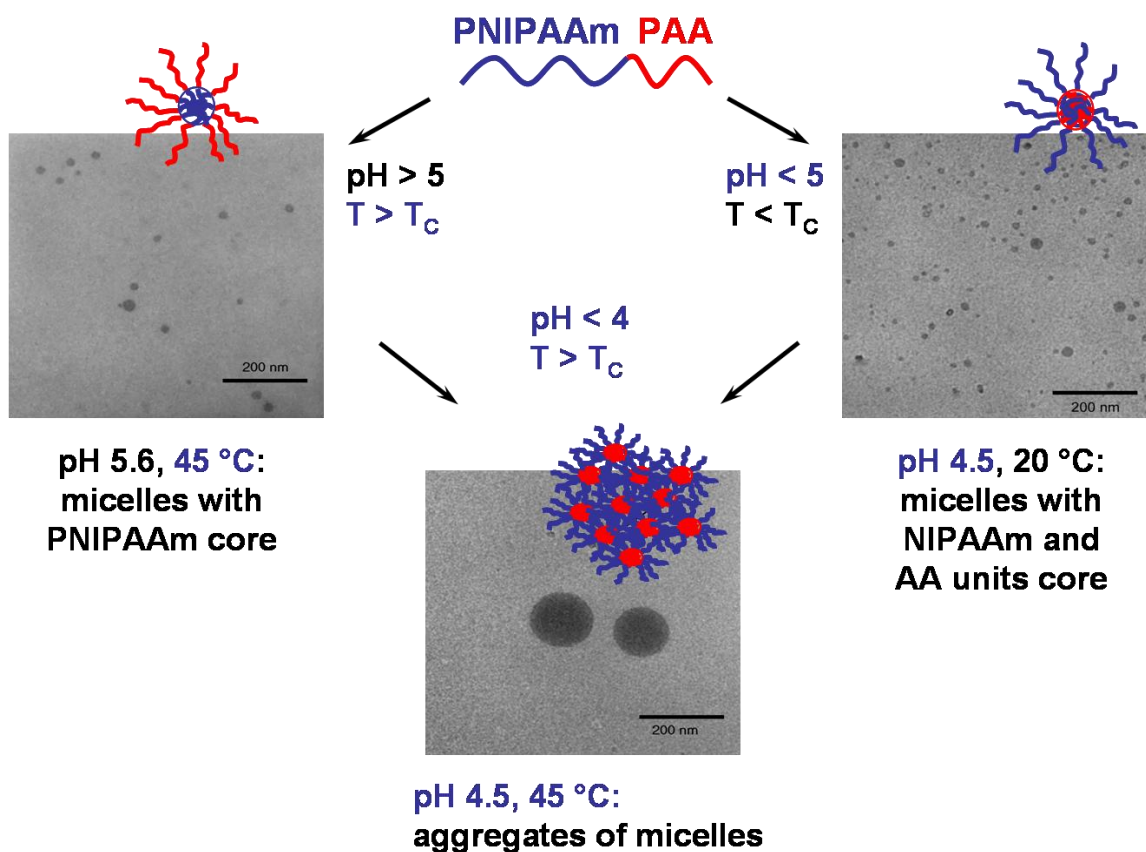
Figure 1-6. Possible modes of aggregate formation for PNIPAAm-*b*-PAA in aqueous solution depending on pH and temperature with associated cryo-TEM images.

Controlled Radical Polymerization

The different CRP techniques offer unprecedented opportunities to polymer chemists for producing material with very efficient control over the molecular weight, molecular weight distribution, microstructure, chain-end functionality and macromolecular architecture. CRP combines the utility and simplicity of conventional free radical polymerization with the kinetic and structural control obtained by ionic polymerization. As with conventional free radical polymerization, CRP can be conducted over a wide range of temperature, solvent and process conditions. It can be also applied to a huge number of vinylic monomers under less stringent conditions than required for ionic polymerization in terms of oxygen and water presence or monomer functionality. Taking into account all of these advantages, CRP is the process of choice for an ever increasing number of applications.

NMP
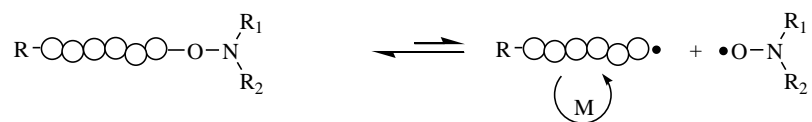
ATRP
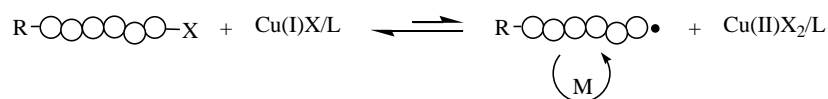
RAFT
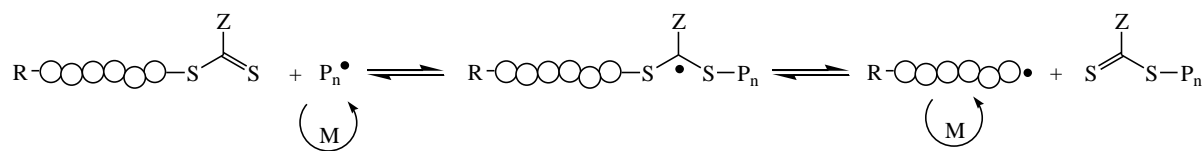
Scheme 1-1. Mechanisms of chain extension showing equilibrium between dormant and active chains for NMP, ATRP and RAFT methods.

So far, several CRP methods have been reported. Among them, three major ones have been intensively studied.[70-77] These different processes are described in Scheme 1-1. For each of these, the key feature is the existence of an equilibrium between active and dormant species which allows a controlled growth of chains while maintaining a sufficiently low concentration of chain-end radicals to minimize termination. The oldest method is the stable free radical polymerization (SFRP), which includes nitroxide-mediated polymerization (NMP). SFRP was first reported by workers at CSIRO and was subsequently developed by Georges and co-workers, as well as others.[78-82] In NMP, dormant alkoxyamines reversibly dissociate under heating to produce a propagating radical and a persistent nitroxide radical. The former adds to the monomer and re-couples with the persistent radical. Atom transfer radical polymerization (ATRP) was independently developed by Sawamoto et al. and Wang and Matyjaszewski.[83, 84] In this

22

process, the reversible cleavage of a covalently-bound halide is accomplished via a redox process catalyzed by various Cu, Ru, Fe and other transition metal complexes (the most commonly used is copper). The oxidized complex, like the nitroxide in SFRP, serves as the persistent species (not capable of addition to the monomer) which is readily accessible for recombination with the propagating species. Reversible addition-fragmentation chain transfer (RAFT) polymerization, also discovered by researchers at CSIRO, was first reported in 1998.[85] Around the same time researchers from Rhodia in France described a technique they termed MADIX, for Macromolecular Design by Interchange of Xanthate.[86] Both MADIX and RAFT operate via an identical addition-fragmentation chain transfer mechanism, i.e. they are identical processes, with MADIX referring specifically to the polymerizations mediated by xanthates. The acronym RAFT describes systems employing all other thiocarbonylthio-mediating agents. For the sake of simplicity, both systems will herein be referred to as RAFT polymerizations.

An important issue with all three CRP methods is the maintenance of chain-end functionality (nitroxide, halide or thiocarbonylthio moieties) in order to allow controlled growth during the process and to prepare, for instance, block copolymers by the subsequent addition of the second monomer (Scheme 1-1). Moreover, each CRP technique has its own advantages; however, RAFT appears to be the method of choice in situations where direct polymerization of functional monomers in aqueous media is desirable.[87-89]

As already mentioned, one area of intensive research in CRP involves responsive polymers. For example, the reversible formation of polymeric micelles and vesicles from block copolymer unimers in response to pH, ionic strength or temperature changes may now be accomplished in a facile manner. Reversible micellization can occur when a hydrophilic diblock copolymer is rendered amphiphilic in response to a stimulus.[90, 91] A large number of monomers have been used to prepare reversible micelles for applications in pharmaceutical and agricultural industries, personal care formulations, enhanced oil recovery and water remediation. In all cases the hydrophobic inner "core" of the micelle-like entities is responsible for phase transfer and sequestration of small lipophilic molecules while the outer "corona" helps stabilize the resulting structure in water.[92, 93] Of the three main CRP techniques, ATRP and RAFT have been utilized the most in

preparing stimuli-responsive block copolymers.[94-96] Success with SFRP has been limited until recently by the requirements of higher temperatures and monomer selection. However, recently discovered nitroxides with more favorable equilibria may accelerate research with this method. In all three systems, efficient block formation requires functionalized macroinitiators (SFRP and ATRP) or a macrochain transfer agent, macro-CTA, (RAFT) with appropriate reactivity for the reinitiation and formation of the second block. As is the case in CRP homopolymerization, the key is maintaining the reversible equilibrium for controlled monomer addition while avoiding possible coupling, disproportionation, and other events leading to "dead" chains. Monomer conversion must generally be limited when synthesizing macroinitiators and macro-CTAs because termination events are more likely to occur at higher conversions, thus leading to the loss of active chains. These macroinitiators and macro-CTAs are then purified and reinitiated in the presence of the second monomer, leading to the formation of a block copolymer.


Micellization

The micellization process in block copolymers mainly depends on two parameters: the critical micelle temperature (CMT) and the critical micelle concentration (CMC). If the CMT or the CMC are not reached, self-assembly will not occur and the block copolymer will behave in the solution as a unimer. On the contrary, if micelle formation is triggered, the micelles will be in thermodynamic equilibrium with the unimers. In the case of block copolymers, the CMC is generally extremely low compared to molecular surfactant. Two extremes of micellar structures can be distinguished for diblock copolymers depending on the relative length of the blocks.[97, 98] If the soluble block is larger than the insoluble one, the micelles formed consist of a small core and a very large corona, and are thus called "star-micelles".[99] In contrast, micelles with a large insoluble segment and a short soluble corona are referred to as "crew-cut micelles" (Figure 1-7).[100] However, in order to fully characterize a micellar system and to explain some other observed morphologies, several parameters have to be considered, including the equilibrium constant, the quality of the solvent, the previously mentioned CMT and CMC, the overall molar mass (Mw) of

the micelle, its aggregation number (Z) and its morphology.[101] These variables affect the hydrodynamic radius (R_H), the radius of gyration (R_G), the ratio of R_H to R_G, (which depends on the micellar shape), the core radius (R_C) and the thickness (L) of the corona.
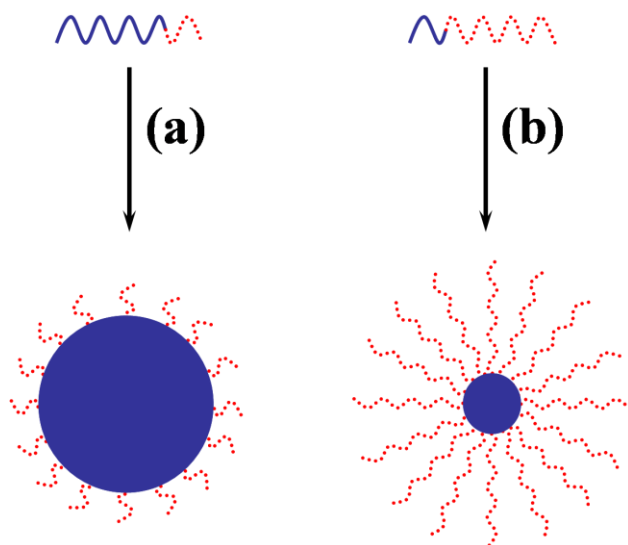
Figure 1-7. Schematic representation of two extreme morphologies of micelles depending on the relative block lengths: (a) star micelle, (b) crew-cut micelle.

The shape and the size of the aggregates are controlled by a variety of parameters which affect the balance between three major forces acting on the system. These forces reflect: the extent of the constraints between the blocks forming the core (the block will be more or less stretched depending on the solvent), the interactions between chains forming the corona, and the surface energy between the solvent and the core of the micelle.[102] Micelles can be classified into several types depending on the morphology, varying from spherical to vesicular or other less common structures, such as inverse micelles, bilayers or cylinders (Figure 1-8).[103-108] Unfortunately, these nanostructures are generally not very stable and for lot of applications such as drug delivery, the local polymer concentration decreases below the CMC which leads to micelle dissociation and to the release of unimers and the active compounds in undesired places. To avoid this problem and to create more robust carriers, one solution is to cross-link the micelles.
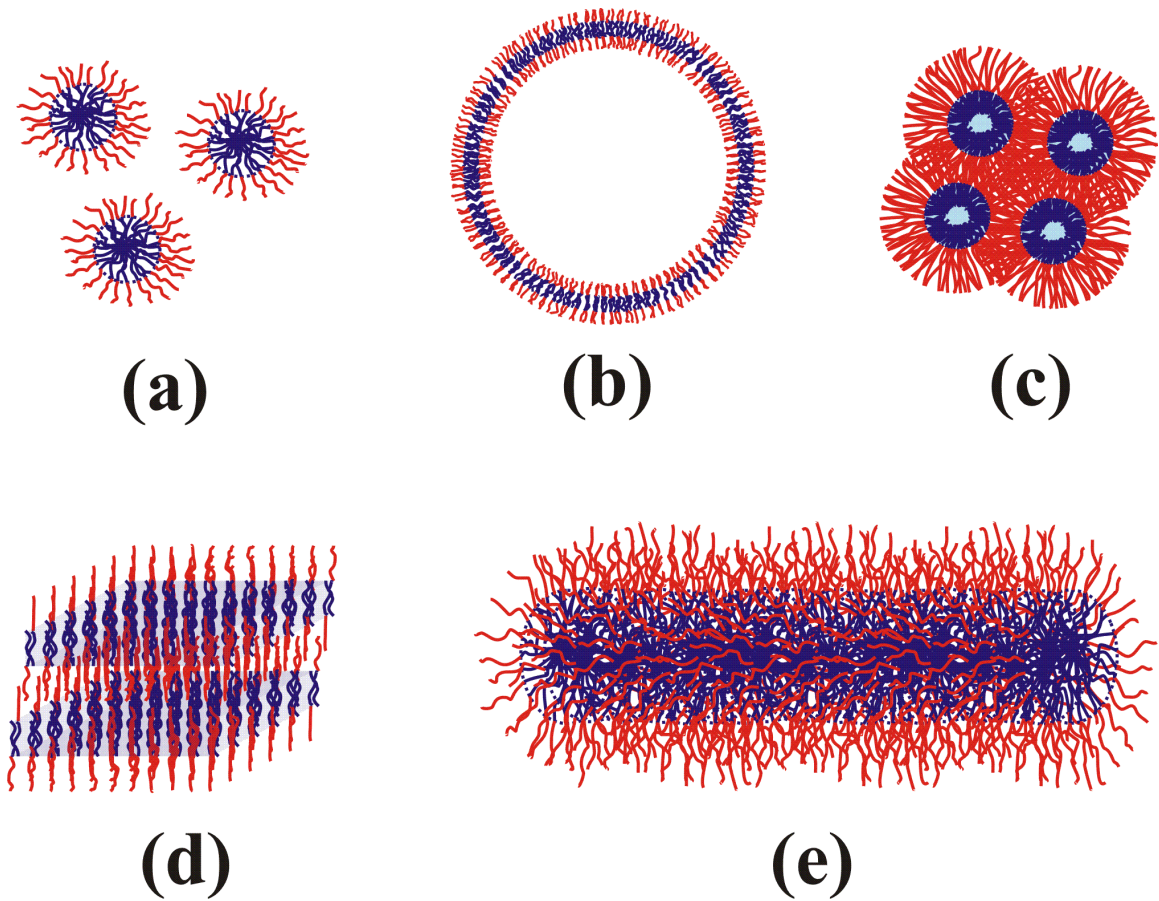
Figure 1-8. Examples of structures obtained from block copolymers: (a) direct micelles, (b) vesicles, and other morphologies: (c) inverse micelles, (d) lamellar structures and (e) cylindrical or tubular micelles.

Cross-Linking of Micelles

Many research groups work on the critical issue of cross-linking micelles and several methods have already been published. These different methods can be classified depending on the cross-linking location, such as shell or core cross-linking, or depending on the cross-linking reaction used, as described here. For instance, cross-linked micelles can be obtained by radical reactions, by chemical reactions with multifunctional compounds or by physical interactions among others. One method of cross-linking by

means of radical reactions developed by Kataoka et al. requires the free double bonds present in diblock or triblock copolymers being exposed to UV-Vis light in the presence of a radical initiator (Scheme 1-2(a)). In practice, particle-forming copolymers with a polymerizable groups at the chain-end have been prepared.[109] Starting from a heterobifunctional poly(ethylene oxide) (PEO) which could serve to grow a second hydrophobic and functionalizable block, ω-methacryloyl-polylactide-*b*-poly(ethylene oxide)-aldehyde block copolymers were obtained which were non-toxic and biodegradable. Micelles were obtained in aqueous solutions with the PLA block forming the core. The methacryloyl end-groups buried in the core could be homopolymerized to cross-link the micelles, affording stable nanospheres with aldehyde groups on the surface. Stenzel et al. recently proposed a different radical core cross-linking method.[110] In this case, they synthesized a diblock copolymer using the RAFT method which was self-assembled afterwards in a selective solvent. The RAFT end-group was present in the core of the micelles. Then, by using a divinylic cross-linker, the micellar system was stabilized via chain extension of the block copolymer as depicted in Scheme 2-2(b). In 1996, Wooley's group was the first to develop a strategy to form robust shell cross-linked (SCL) micelles in a THF-water mixture based on polystyrene-*b*-poly(4-vinyl pyridine) (PS-*b*-PVP) block copolymers.[111-113] These were prepared via anionic polymerization and the latter block was quaternized with *p*-(chloro methylstyrene), introducing hydrophilicity and cross-linkable groups at the same time. In an aqueous solution the glassy PS block formed the core of the micelle and the quaternized PVP block the shell (Scheme 1-2(c)). In the presence of a radical initiator, the shell of the resulting micelle was cross-linked via UV-irradiation. The main limitation of the SCL compared to core-cross-linked (CCL) micelles is the high dilution needed for the cross-linking reaction (typically below 0.5% solids) in order to avoid undesirable inter-micellar cross-linking, which inevitably results in micelle fusion.
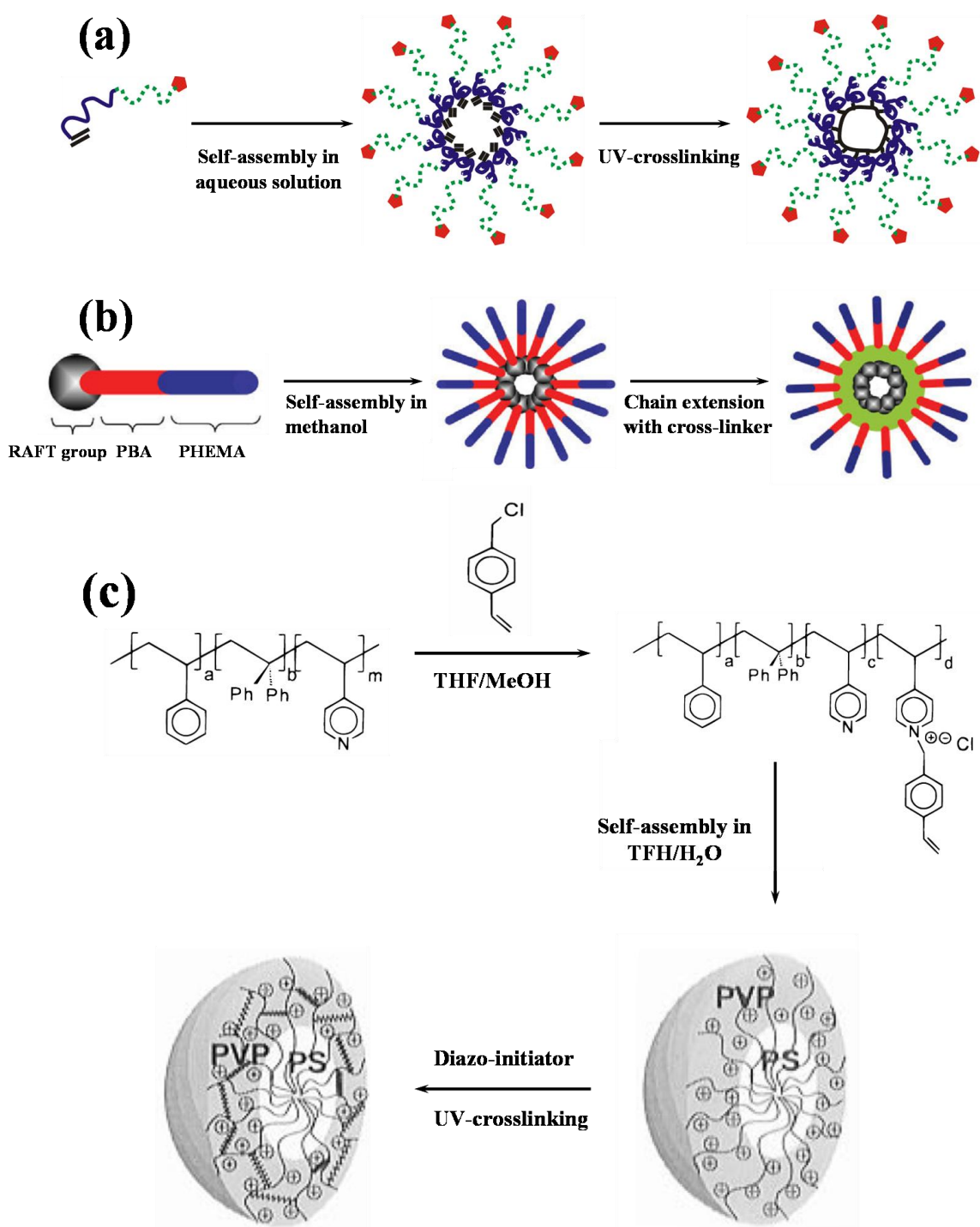
Scheme 1-2. Strategies for the preparation of cross-linked micelles via radical reactions. (a) Stabilization strategy of Kataoka et al. via self-assembly and polymerization of end-double bonds in the core. (b) Core cross-linking via RAFT polymerization. (c) Shell cross-linking developed by Wooley's group.

It is also possible to cross-link micelles by using chemical compounds which react to the functional groups present in either the core or the shell of the micelles. Depending on the polymer for cross-linking, several different cross-linkers can be used.[114-116] For example Wooley's group used water-soluble diamines to cross-link poly(carboxylic acid) blocks in aqueous solution using carbodiimide coupling (Scheme 1-3(a)).[117, 118] The SCL micelles were typically prepared via a three-step procedure. First, a polystyrene-*block*-poly(*tert*-butyl acrylate) (PS-*b*-PtBA) diblock copolymer precursor was prepared by either anionic polymerization or ATRP, followed by acid hydrolysis of the tert-butyl groups to produce a polystyrene-*block*-poly(acrylic acid) (PS-*b*-PAA) diblock copolymer.[119] This amphiphilic diblock copolymer was then dissolved in THF and micellization was induced by the addition of water. Shell cross-linking of the PAA chains in the micelle coronas was achieved by activation of the carboxylic acid groups with a water-soluble carbodiimide, 1-(3-dimethylaminopropyl)-3-ethylcarbodiimide methiodide, followed by the addition of a 2,2'-(ethylenedioxy)bis(ethylamine) cross-linker. In 1998, Bütün et al. reported another process for the synthesis of SCL micelles with tunable hydrophilic/hydrophobic cores.[120] Diblock copolymer micelles comprising partially quaternized poly(2-(dimethylamino) ethyl methacrylate-*block*-poly(2-(*N*-(morpholino) ethyl methacrylate)) (PDMAEMA-*b*-PMEMA) were cross-linked using bis(2-iodoethoxy)ethane in aqueous solution at 60 °C (Scheme 1-3(b)). This bifunctional reagent selectively quaternized the unreacted tertiary amine groups on the PDMA blocks located in the micelle coronas, leaving the thermo-responsive core-forming PMEMA block untouched. On cooling to 25 °C, the PMEMA chains passed through their LCST and hence became rehydrated. These SCL micelles thus contained micelle cores which could be reversibly hydrated or dehydrated, depending on the solution temperature.
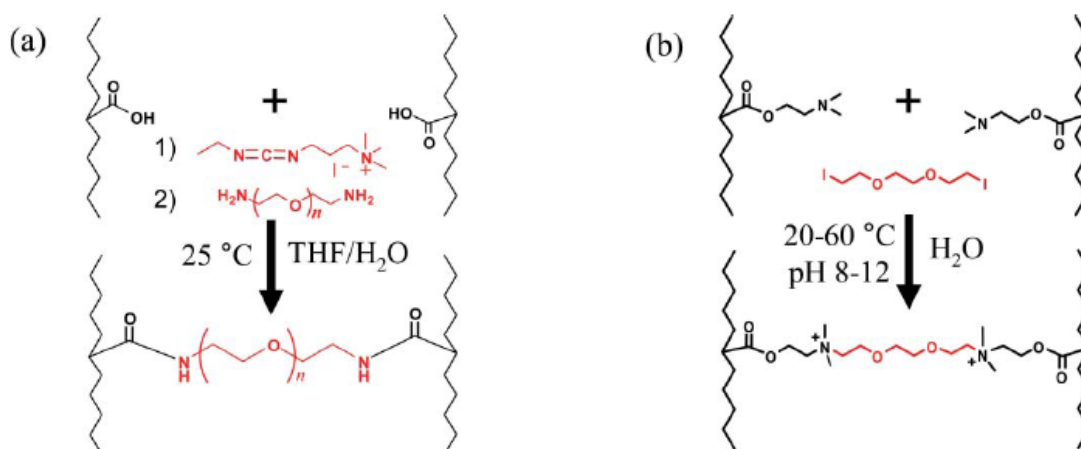
Scheme 1-3. Cross-linking chemistry of small molecule cross-linkers and appropriate monomers: (a) diamines in the presence of a carbodiimide catalyst (b) bis(2-iodoethoxy)ethane

Both methods were performed via shell cross-linking but as mentioned earlier this technique is limited to low micellar concentrations to avoid inter-micellar cross-linking. Armes and co-workers recently overcame this difficulty to produce well-defined SCL micelles at much higher copolymer concentrations by pioneering the use of ABC triblock copolymers rather than AB diblock copolymers.[121] To date, these copolymers have been typically prepared by ATRP using a poly(ethylene oxide)-based (PEO) macro-initiator. This PEO block acts as a steric stabilizer and ensures that cross-linking is confined to the inner shell (i.e. the B block) of the triblock copolymer micelles (Scheme 1-4), thus preventing inter-micelle fusion. Appropriate ABC triblocks typically comprise a permanently hydrophilic A block (e.g. PEO), a cross-linkable B block and a stimulus-responsive (i.e. tunably hydrophobic) core-forming C block. Depending on the nature of the C block, this strategy can be used to prepare SCL micelles with cores whose hydrophobicity can be tuned by varying either the solution pH or the temperature.[122, 123]
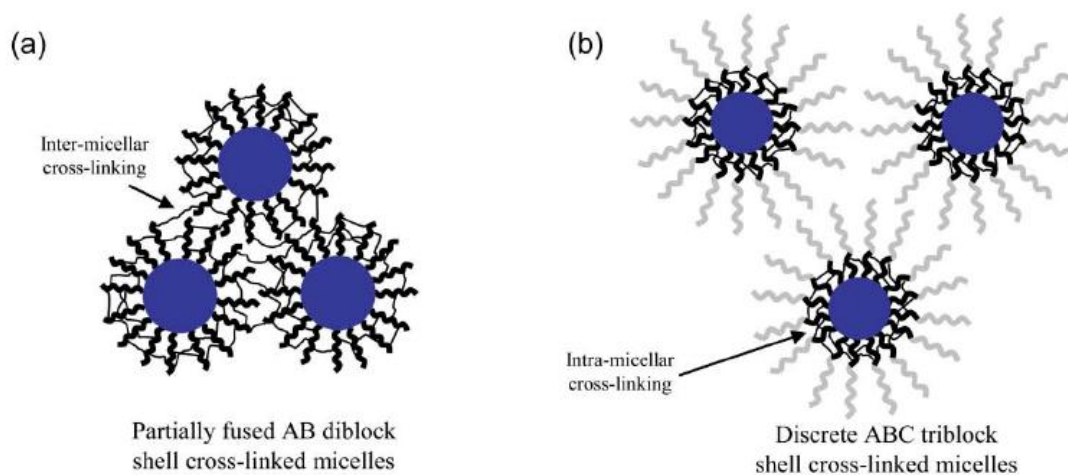
Scheme 1-4. Schematic representation of the inter-micellar and intra-micellar cross-linking for (a) AB diblock copolymer and (b) ABC triblock copolymer micelles at high copolymer concentrations (solid content > 1%).

Another way to avoid inter-micellar cross-linking is to use functional cross-linkers to cross-link the core of the micelles. Using the RAFT method, Zhang et al. synthesized poly(ethylene oxide)-*b*-poly(*N*-isopropylacrylamide-*co*-*N*-acryloxysuccinimide), PEO-*b*-P(NIPAAm-*co*-NAS), employing a poly(ethylene oxide) (PEO)-based macroRAFT agent.[124] The obtained double hydrophilic block copolymer self-assembles in water above the cloud point into spherical micelles consisting of thermoresponsive P(NIPAAm-*co*-NAS) cores and well-solvated PEO coronas. Cross-linking of the P(NIPAAm-*co*-NAS) cores was easily achieved via the reaction of NAS residues with cystamine at elevated temperatures in aqueous media, forming structurally permanent core cross-linked micelles. The P(NIPAAm-*co*-NAS) cores of the obtained CCL micelles exhibit tunable swelling/deswelling behaviors below and above the critical phase transition temperature. Moreover, the disulfide bonds within the cross-linker can be conveniently cleaved in the presence of dithiothreitol and re-formed again upon the addition of cystamine as a thiol/disulfide exchange promoter, leading to the reversible core cross-linking of micelles as depicted in Scheme 1-5.
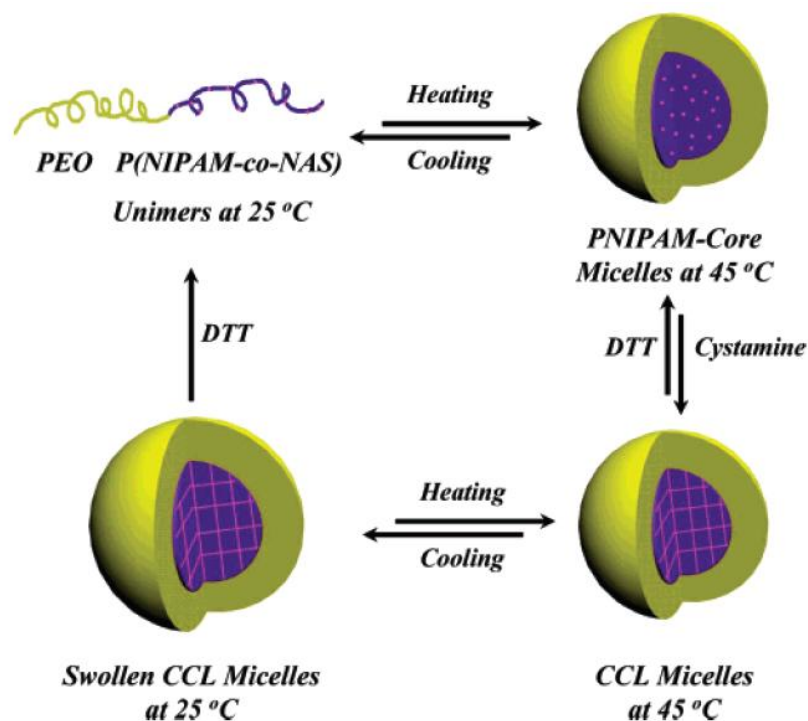
Scheme 1-5. Schematic illustration of the fabrication of reversible CCL micelles from poly(ethylene oxide)-*b*-poly(*N*-isopropylacrylamide-*co*-*N*-acryloxysuccinimide) diblock copolymers.

It is also possible to use a physical cross-linking method instead of a chemical one, as mentioned above, to stabilize the micelles, such as polyelectrolyte complexation.[125, 126] This complexation offers many advantages over other cross-linking methods: (1) most polyelectrolytes exhibit low toxicity; (2) physical cross-linking is relatively fast and should ensure that there is no chemical modification of guest molecules; (3) apart from the counter-ions that are released, no small-molecule by-products are formed so purification is straightforward; (4) in principle, such "ionic" cross-linking can be reversed by salt addition. McCormick's group reported the preparation of SCL micelles with PNIPAAm-based thermoresponsive cores using a homopolyelectrolyte cross-linker (Scheme 1-6).[127] In this study, a triblock copolymer, poly(*N,N*-dimethylacrylamide)-*block*-(*N*-acryloylalanine)-*block*-poly(*N*-isopropylacrylamide) (PDMAAm-*b*-PAAL-*b*-PNIPAAm) was first prepared by RAFT chemistry. This triblock copolymer formed

PNIPAAm-core micelles above the LCST of the PNIPAAm chains. Successful ionic cross-linking was achieved by the addition of a cationic homopolymer poly[(ar-vinylbenzyl) trimethylammonium chloride] (PVBTAC). It was also shown that the cross-linking was reversible, since micelle dissociation occurred on the addition of NaCl solution (0.4 mol · L^{-1}).
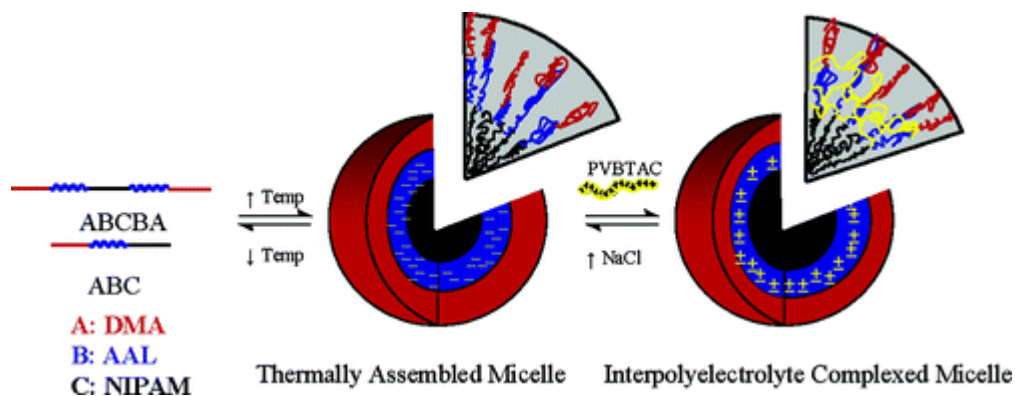
Scheme 1-6. Strategies for cross-linking via polyelectrolyte complexation of PNIPAAm-based thermoresponsive-core micelles using a poly[(ar-vinylbenzyl) trimethylammonium chloride] homopolyelectrolyte cross-linker

Inorganic-Polymer Nanohybrids

Organic-inorganic nanohybrid materials are a new class of material which present improved or unusual features and allow the development of innovative industrial applications. Being at the interface of organic and inorganic realms, these materials are highly versatile and offer a wide range of possibilities for elaborating tailor-made materials in terms of processing and chemical and physical properties. However, they are not simply physical mixtures. They can be broadly defined as nanocomposites with organic and inorganic components which are intimately mixed. Indeed, hybrids are either homogeneous systems derived from monomers and miscible organic and inorganic components, or heterogeneous systems (nanocomposites) where at least one of the components' domains has a dimension ranging from a few Å to several nanometers. It is

obvious that the properties of these materials are not just the result of the sum of the individual contributions of both phases, but rather the role of the inner interfaces could be predominant. Therefore, new properties resulting from the synergy of both components are also commonly observed.[128, 129] The nature of the interface has been used to grossly divide these materials into two distinct classes. In class I, organic and inorganic components are embedded and only weak bonds (hydrogen, van der Waals or ionic bonds) give cohesion to the whole structure. In class II materials, the two phases are linked together through strong chemical bonds (covalent or iono-covalent bonds).
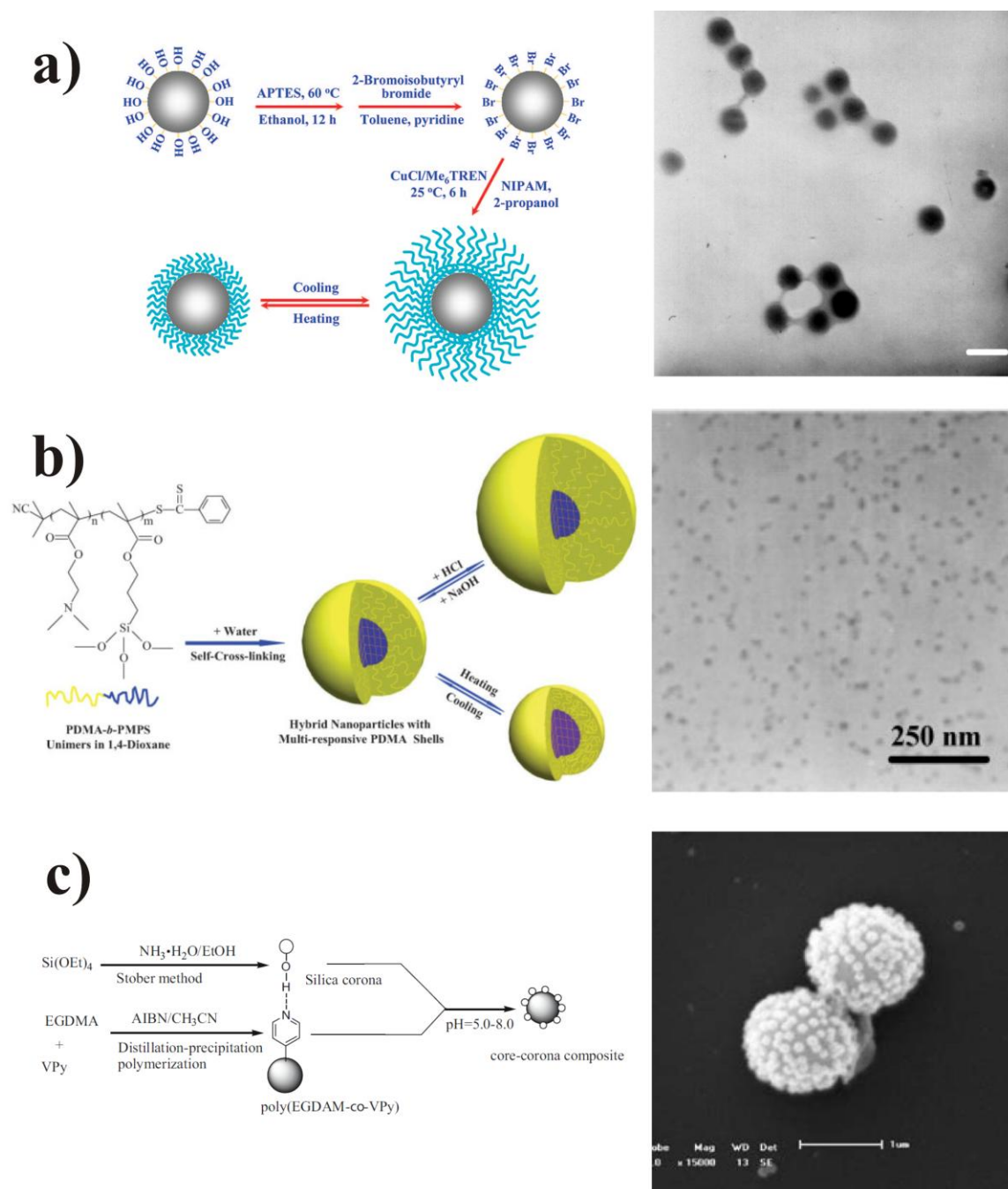
The choice of which polymer to use is mainly influenced by their mechanical and thermal behaviors. However, other properties such as hydrophobic/hydrophilic balance, chemical stability, biocompatibility, optical and/or electronic properties and chemical functionalities (i.e. solvation, wettability, templating effect) have to be considered in the choice of the organic component. In many cases the organic component also allows easy shaping and better processing of the materials. The inorganic components provide mechanical and thermal stability, but also new functionalities which depend on the chemical nature, the structure, the size and the crystallinity of the inorganic phase (silica, transition metal oxides, metallic phosphates, nanoclays, nanometals, metal chalcogenides). Indeed, the inorganic component can implement or improve electronic, magnetic and redox properties, density and the refractive index, amongst others.

Nowadays, most of the hybrid materials that have already entered the market are synthesized and processed by using conventional soft chemistry-based routes developed in the 1980s. These processes are based on: a) the copolymerization of functional organosilanes, macromonomers and metal alkoxides, b) the encapsulation of organic components within sol-gel-derived silica or metallic oxides and c) the organic functionalization of nanofillers, nanoclays or other compounds with lamellar structures.[130-133] The chemical strategies (self-assembly, nanobuilding block approaches, hybrid MOF (metal organic frameworks), integrative synthesis, coupled processes, bio-inspired strategies, amongst others) allow the development of a new vectorial chemistry, able to direct the assembly of a large variety of structurally well-defined nano-objects into complex hybrid architectures hierarchically organized in terms of structure and function.

Today, the potential of these materials is becoming real and many hybrids are entering niche markets that should expand in the future because new and stricter requirements are now being set up to achieve greater harmony between the environment and human activities. New materials and systems produced by man must in future aim toward higher levels of sophistication and miniaturization, be recyclable and respect the environment, be reliable and consume less energy. Without any doubt, these materials will open up promising applications in many areas: optics, electronics, ionics, mechanics, energy, the environment, biology, medicine (for example as membranes and separation devices), functional smart coatings, fuel and solar cells, catalysts, sensors, micro-optical and photonic components and systems, and intelligent therapeutic vectors which combine targeting, imaging, therapy and controlled-release properties, among others.[134-140]

By using smart polymers as a component of hybrids, the obtained materials will generally be able to respond to external stimuli and properties such as solubility, catalytic activity and optical properties, and will be triggered by environmental changes. Many examples can already be found in the literature. In the case of silica-based nanocomposites, a very important class of hybrid material, several strategies were developed to obtain smart silica nanoparticles.[141-144] For instance, Liu and co-workers prepared silica nanoparticles grafted with PNIPAAm via surface-initiated ATRP.[145] This process is detailed in Scheme 1-7a). They first synthesized monodispersed bare silica nanoparticles. Then, residual hydroxyl groups present on the surface were subsequently modified in an ATRP initiator via a two-step reaction. Finally, NIPAAm was polymerized in isopropanol at ambient temperature via ATRP. When these hybrids were dispersed in water, a response to the temperature was observed where the corona shrunk when the temperature was increased above cloud point. The same group also developed another strategy for generating multi-responsive silica nanoparticles (Scheme 1-7b)).[146] Poly(2-(dimethylamino)ethylmethacrylate)-*b*-poly(γ-methacryloxypropyltrimethoxysilane) (PDMAEMA-*b*-PMPS) was synthesized via consecutive RAFT polymerizations in 1,4-dioxane. Subsequent micellization of the obtained amphiphilic diblock polymer in aqueous solution led to the formation of nanoparticles consisting of hydrophobic PMPS cores and well-solvated PDMAEMA shells. Containing tertiary amine residues, PDMAEMA blocks in micelle coronas can

spontaneously catalyze the sol-gel reactions of trimethoxysilyl groups within PMPS cores, leading to the formation of hybrid nanoparticles coated with PDMAEMA brushes which were able to respond to pH and temperature. It is also possible to generate hybrid materials where the silica is not composed of the hybrid core but is adsorbed onto a polymer particle. Wang et al. prepared a raspberry-like poly(ethyleneglycoldimethacrylate-*co*-4-vinylpyridine)/silica (P(EGDMA-co-4VP)/SiO$_2$) core-corona composite. This structure was formed due to a self-assembled hetero-coagulation based on a hydrogen-bonding interaction between the pyridyl group of the poly(EGDMA-*co*-4VP) core and the active hydroxyl group of the silica corona (Scheme 1-7c)). The raspberry-like composite was stable near a neutral environment with pH values ranging from pH 5.0 to pH 8.0. By tuning the pH to either low or high pH values, the polymer-silica association can be reversibly broken.

Scheme 1-7. Examples of strategies used to obtained smart polymer-silica nanohybrids with associated micrographs of the different particles obtained. a) Grafting from an approach via surface-initiated ATRP of NIPAAm onto a silica particle, TEM image, scale bar: 100 nm. b) Self-assembly of block copolymer in water, followed by self-catalyzed core gelation, TEM image. c) Reversible self-assembly heterocoagulation via hydrogen bonding interactions near neutral pH values, SEM image.

Metal-based nanohybrids have been extensively studied due to their unique applications in many areas, such as nonlinear optics, catalysis and chemical, electronic or optical sensors.[147-152] Most of these are based on metal nanoparticles. Indeed, metal particles in the nanometric range possess unique properties which are very different compared to the bulk material. These properties are related to the size, shape and special distribution of the metal particles and are strongly dependent on the formation process.[153] However, metal nanoparticles have a strong tendency to aggregate in solution, therefore chemists have developed several new ways of synthesis via the formation of hybrid materials to prevent aggregation and enhance or modulate the properties of the metal.[154, 155] The modulation of these properties can be easily achieved using smart polymers. For instance, Choi's group synthesized gold nanoparticles/poly(*N*-isopropylacrylamide) (AuNP/PNIPAAm) core/shell hybrid structures by surface-initiated ATRP (Scheme 1-8a)).[156] Starting from AuNPs obtained by a standard reduction method using citrate, they introduced an ATRP initiator via ligand exchange. Then, the ATRP of NIPAAm was carried out in water at room temperature in the presence or absence of a cross-linker. Another method for generating metal nanohybrids is to reduce the metal inside a polymeric carrier in situ. Thus, Zhou et al. synthesized AuNPs incorporated into either core or shell cross-linked micelles based on PNIPAAm (Scheme 1-8b)).[157] Poly(*N*-isopropylacrylamide)-*b*-poly(1-(3'-aminopropyl)-4-acrylamido-1,2,3-triazole hydrochloride), PNIPAAm-*b*-PAPAT, was then synthesized via consecutive RAFT polymerizations of NIPAAm and APAT. In aqueous solution, the obtained thermoresponsive double hydrophilic block copolymer dissolves molecularly at room temperature and self-assembles into micelles with PNIPAM cores and PAPAT shells at elevated temperatures. Because of the presence of highly reactive primary amine moieties in the PAPAT block, two types of covalently stabilized nanoparticles, either core cross-linked or shell cross-linked micelles with "inverted" core-shell nanostructures, were easily prepared upon the addition of glutaric dialdehyde at 25 °C and 50 °C, respectively. In addition, the obtained fixed-structure micelles were incorporated with gold nanoparticles via the in situ reduction of preferentially loaded $HAuCl_4$. Another potential carrier for metal nanoparticles is hydrogel. For instance, Ballauff and co-workers easily

generated microgels with a polystyrene core and cross-linked PNIPAAm shells by photo-emulsion. This robust carrier was used for the reduction of many metal nanoparticles such as gold and silver, as depicted in Scheme 1-8c).[158, 159] They proved that the nanoparticles present in the shell are able to catalyze different organic reactions. Moreover, by tuning the temperature, the activity of the metal catalyst can be modified, but not totally suppressed, due to the collapse of the PNIPAAm shell onto the nanoparticles at elevated temperatures.[160]
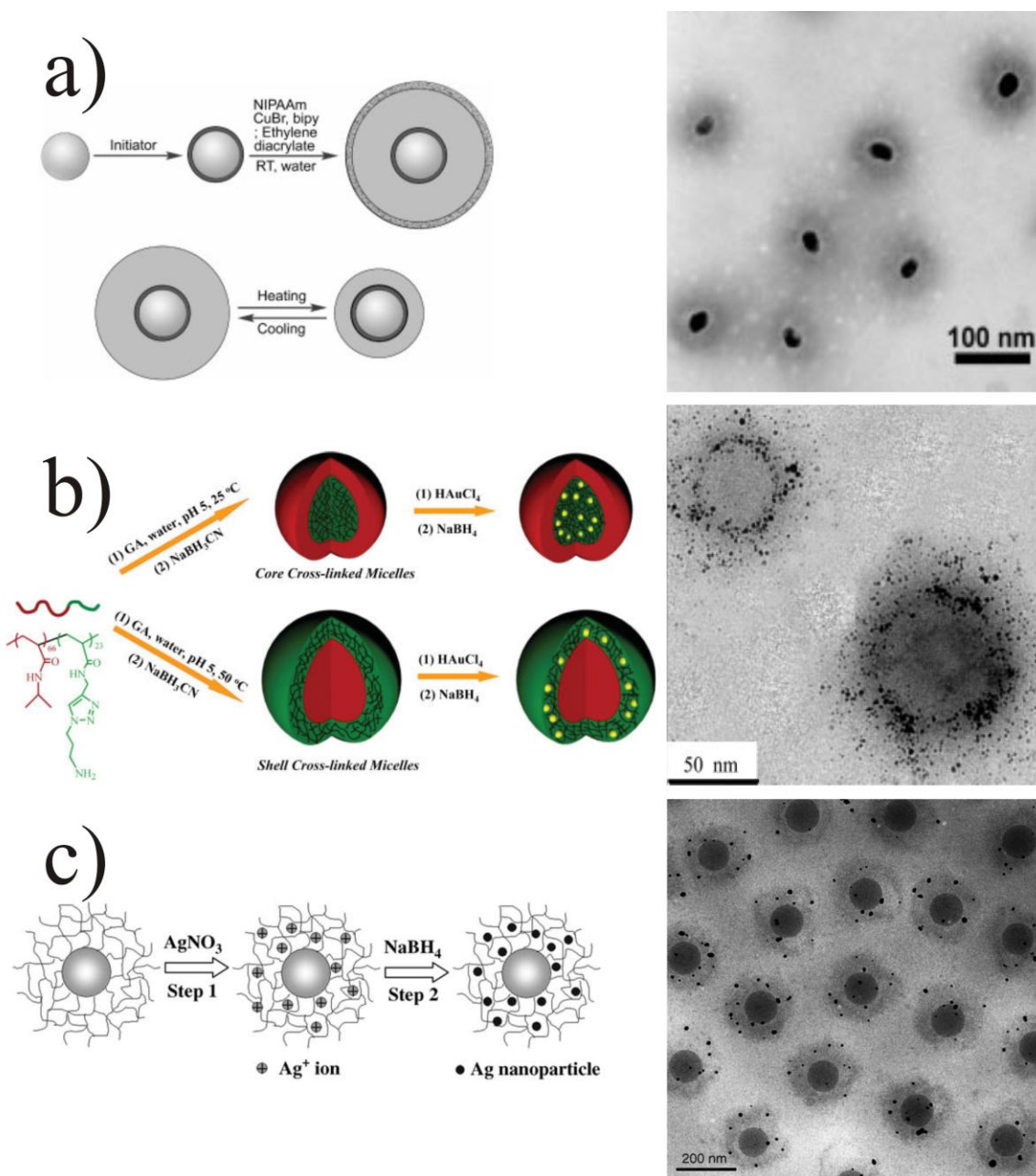
Scheme 1-8. Examples of strategies used to obtain smart polymer-metal nanohybrids with associated micrographs of the different particles obtained. a) Grafting from approach via surface-initiated ATRP of NIPAAm onto a gold particle, TEM image. b) Self-assembly of block copolymer and cross-linking using glutaric dialdehyde either at room temperature (upper part) or at 50 °C (bottom part) to obtain core or shell cross-linked micelles, respectively, followed by reduction of auryl salt, HRTEM image of SCL micelles. c) Absorption of silver ions inside the PS-PNIPAAm core-shell system followed by reduction to produce silver nanoparticles immobilized in the PNIPAAm network, cryo-TEM image.

Other types of nanohybrids based on smart polymers have been described, such as magnetic nano-hybrids.[161-165] An example is the multi-responsive pH- and temperature-responsive Janus magnetic nanoparticles synthesized by Hatton's group:[166] 5 nm magnetite nanoparticles coated on one side with a pH-dependent polymer (PAA) and functionalized on the other side by a second polymer which is a temperature-dependent polymer (PNIPAAm). These Janus nanoparticles are stably dispersed as individual particles at high pH values and low temperatures, but they can self-assemble at low pH values leading to a full aggregation, or at high temperatures (>31 °C) (PNIPAAm) to form stable dispersions of clusters of approximately 80-100 nm in hydrodynamic diameter.

Objective of this Thesis

The objective of this thesis was to broaden the scope of multi-responsive block copolymers with respect to their stimuli and possible applications in materials science. In addition, the generation of inorganic-organic hybrid materials based on these developed structures was of interest. One focus of this thesis was certainly the synthesis of these block copolymers in pure water or in aqueous solution via controlled radical polymerization in a large range of molecular weights. Furthermore, functional initiators (ATRP) or RAFT agents were used to allow post reactions with drugs or proteins to generate smart vectors for bio-applications. Self-assembly into micelles depending on the environmental trigger of the synthesized block copolymers was also investigated. To

generate robust responsive carriers, different ways of cross-linking were developed via shell or core cross-linking strategies by using multifunctional cross-linkers which insured a strong cohesion to the obtained structure. This is of particular importance for biotechnological applications where the concentration can decrease below the CMC leading to a total disintegration of the micelle and an uncontrolled release of the encapsulated drug. To further push smart micelles into applications, for example in materials science, inorganic-organic colloidal hybrid formation was investigated. The in situ reduction of metal nanoparticles was realized to explore the possibility of using this nanostructure as smart catalyst carriers. Taking advantage of simple polymerization conditions and efficient cross-linking reactions, we want to show that multi-responsive cross-linked micelles are useful and efficient nano-objects for the generation of novel materials with advanced properties.

References

[1] S.-K. Ahn, R. M. Kasi, S.-C. Kim, N. Sharma, and Y. Zhou, *Soft Matter*, 2008, **4**, 1151.

[2] E. S. Gil and S. M. Hudson, *Progress in Polymer Science*, 2004, **29**, 1173.

[3] C. L. McCormick, S. E. Kirkland, and A. W. York, *Polymer Reviews*, 2006, **46**, 421

[4] S. Minko, *Polymer Reviews*, 2006, **46**, 397

[5] C. Alexander and K. M. Shakesheff, *Advanced Materials*, 2006, **18**, 3321.

[6] A. K. Bajpai, S. K. Shukla, S. Bhanu, and S. Kankane, *Progress in Polymer Science*, 2008, **33**, 1088.

[7] L. R. Fogueri and S. Singh, *Recent Patents on Drug Delivery & Formulation*, 2009, **3**, 40.

[8] S. Ganta, H. Devalapally, A. Shahiwala, and M. Amiji, *Journal of Controlled Release*, 2008, **126**, 187.

[9] Y. Qiu and K. Park, *Advanced Drug Delivery Reviews*, 2001, **53**, 321.

[10] M. Yoshida, R. Langer, A. Lendlein, and J. Lahann, *Polymer Reviews*, 2006, **46**, 347

[11] A. Chilkoti, M. R. Dreher, D. E. Meyer, and D. Raucher, *Advanced Drug Delivery Reviews*, 2002, **54**, 613.

[12] D. Crespy and R. M. Rossi, *Polymer International*, 2007, **56**, 1461.

[13] N. Nath and A. Chilkoti, *Advanced Materials*, 2002, **14**, 1243.

[14] H. G. Schild, *Progress in Polymer Science*, 1992, **17**, 163.

[15] A. S. Dubovik, E. E. Makhaeva, V. Y. Grinberg, and A. R. Khokhlov, *Macromolecular Chemistry and Physics*, 2005, **206**, 915.

[16] A. Imaz and J. Forcada, *Journal of Polymer Science Part A: Polymer Chemistry*, 2008, **46**, 2510.

[17] M. Prabaharan, J. J. Grailer, D. A. Steeber, and S. Gong, *Macromolecular Bioscience*, 2008, **8**, 843.

[18] J.-F. Lutz and A. Hoth, *Macromolecules*, 2006, **39**, 893.

[19] J.-F. Lutz, *Journal of Polymer Science Part A: Polymer Chemistry*, 2008, **46**, 3459.

[20] D. W. Urry, *The Journal of Physical Chemistry B*, 1997, **101**, 11007.

[21] H. Nuhn and H.-A. Klok, *Biomacromolecules*, 2008, **9**, 2755.

[22] S. Dai, P. Ravi, and K. C. Tam, *Soft Matter*, 2008, **4**, 435.

[23] R. C. A. Schellekens, F. Stellaard, D. Mitrovic, F. E. Stuurman, J. G. W. Kosterink, and H. W. Frijlink, *Journal of Controlled Release*, 2008, **132**, 91.

[24] E. R. Gillies and J. M. J. Frechet, *Bioconjugate Chemistry*, 2005, **16**, 361.

[25] K. M. Wood, G. M. Stone, and N. A. Peppas, *Biomacromolecules*, 2008, **9**, 1293.

[26] B. Kim, S. H. Lim, and W. Ryoo, *Journal of Biomaterials Science, Polymer Edition*, 2009, **20**, 427.

[27] Z. Jie, L. Xiaohui, Z. Daijia, and X. Zhilong, *Journal of Applied Polymer Science*, 2008, **110**, 2488.

[28] A. S. Lee, V. Bütün, M. Vamvakaki, S. P. Armes, J. A. Pople, and A. P. Gast, *Macromolecules*, 2002, **35**, 8540.

[29] J. M. Layman, S. M. Ramirez, M. D. Green, and T. E. Long, *Biomacromolecules*, 2009, **10**, 1244.

[30] M. Morille, C. Passirani, A. Vonarbourg, A. Clavreul, and J.-P. Benoit, *Biomaterials*, 2008, **29**, 3477.

[31] S. Xu, M. Chen, Y. Yao, Z. Zhang, T. Jin, Y. Huang, and H. Zhu, *Journal of Controlled Release*, 2008, **130**, 64.

[32] B. Qi and Z. Yue, *Journal of Polymer Science Part A: Polymer Chemistry*, 2006, **44**, 1734.

33   F. Liu and A. Eisenberg, *Journal of the American Chemical Society*, 2003, **125**, 15059.

34   A. Kyriazis, T. Aubry, W. Burchard, and C. Tsitsilianis, *Polymer*, 2009, **50**, 3204.

35   L. Wei, C. Cai, J. Lin, and T. Chen, *Biomaterials*, 2009, **30**, 2606.

36   L. Minhyung and K. Sung Wan, *Polymeric Gene Delivery*, 2005, **Ed. Mansoor M. Amiji**, 79.

37   P. Midoux, C. Pichon, J.-J. Yaouanc, and P.-A. Jaffrès, *British Journal of Pharmacology*, 2009, **157**, 166.

38   E. S. Lee, K. T. Oh, D. Kim, Y. S. Youn, and Y. H. Bae, *Journal of Controlled Release*, 2007, **123**, 19.

39   T. Minko, J. J. Khandare, and S. Jayant, *Macromolecular Engineering*, 2007, **4**, 2541.

40   S. E. Paramonov, E. M. Bachelder, T. T. Beaudette, S. M. Standley, C. C. Lee, J. Dashe, and J. M. J. Fréchet, *Bioconjugate Chemistry*, 2008, **19**, 911.

41   E. Schacht, V. Toncheva, K. Vandertaelen, and J. Heller, *Journal of Controlled Release*, 2006, **116**, 219.

42   R. Tomlinson, J. Heller, S. Brocchini, and R. Duncan, *Bioconjugate Chemistry*, 2003, **14**, 1096.

43   X. Guo and F. C. Szoka, *Bioconjugate Chemistry*, 2001, **12**, 291.

44   J. Heller, A. C. Chang, G. Rood, and G. M. Grodsky, *Journal of Controlled Release*, 1990, **13**, 295.

45   D. M. Lynn and R. Langer, *Journal of the American Chemical Society*, 2000, **122**, 10761.

46   G. T. Zugates, N. C. Tedford, A. Zumbuehl, S. Jhunjhunwala, C. S. Kang, L. G. Griffith, D. A. Lauffenburger, R. Langer, and D. G. Anderson, *Bioconjugate Chemistry*, 2007, **18**, 1887.

47   D. Jere, C.-X. Xu, R. Arote, C.-H. Yun, M.-H. Cho, and C.-S. Cho, *Biomaterials*, 2008, **29**, 2535.

48   P. Kaewsaiha, K. Matsumoto, and H. Matsuoka, *Langmuir*, 2007, **23**, 7065.

49   Y. Mei, K. Lauterbach, M. Hoffmann, O. V. Borisov, M. Ballauff, and A. Jusufi, *Physical Review Letters*, 2006, **97**, 158301.

50   S.-I. Yusa, Y. Yokoyama, and Y. Morishima, *Macromolecules*, 2009, **42**, 376.

51   A. B. Lowe and C. L. McCormick, *Chemical Reviews*, 2002, **102**, 4177.

52   P. Mary, D. D. Bendejacq, M.-P. Labeau, and P. Dupuis, *The Journal of Physical Chemistry B*, 2007, **111**, 7767.

53   J. F. Michael, J. K. Bridges, G. K. Matthew, D. H. Roger, and L. M. Charles, *Journal of Applied Polymer Science*, 2004, **94**, 24.

54   G. Lina, F. Chun, Y. Dong, L. Yaogong, H. Jianhua, L. Guolin, and H. Xiaoyu, *Journal of Polymer Science Part A: Polymer Chemistry*, 2009, **47**, 3142.

55   W. Lehmann, H. Skupin, C. Tolksdorf, E. Gebhard, R. Zentel, P. Kruger, M. Losche, and F. Kremer, *Nature*, 2001, **410**, 447.

56   R. Shankar, T. K. Ghosh, and R. J. Spontak, *Soft Matter*, 2007, **3**, 1116.

57   A. M. Schmidt, *Macromolecular Rapid Communications*, 2006, **27**, 1168.

58   Y. Yu, T. Maeda, J.-i. Mamiya, and T. Ikeda, *Angewandte Chemie International Edition*, 2007, **46**, 881.

59   T. Ikeda, J.-i. Mamiya, and Y. Yu, *Angewandte Chemie International Edition*, 2007, **46**, 506.

60   S. I. Kang and Y. H. Bae, *Journal of Controlled Release*, 2003, **86**, 115.

61   T. Miyata, N. Asami, and T. Uragami, *Nature*, 1999, **399**, 766.

62   T. Ahuja, D. Kumar, and Rajesh, *Sensor Letters*, 2008, **6**, 663.

63   K. V. Roskos, J. A. Tefft, B. K. Fritzinger, and J. Heller, *Journal of Controlled Release*, 1992, **19**, 145.

64   I. Dimitrov, B. Trzebicka, A. H. E. Müller, A. Dworak, and C. B. Tsvetanov, *Progress in Polymer Science*, 2007, **32**, 1275.

65   C.-L. Lo, K.-M. Lin, and G.-H. Hsiue, *Journal of Controlled Release*, 2005, **104**, 477.

66   J. Huang and X. Y. Wu, *Journal of Polymer Science Part A: Polymer Chemistry*, 1999, **37**, 2667.

67   W. Zhang, L. Shi, R. Ma, Y. An, Y. Xu, and K. Wu, *Macromolecules*, 2005, **38**, 8850.

68   S. Reinicke, J. Schmelz, A. Lapp, M. Karg, T. Hellweg, and H. Schmalz, *Soft Matter*, 2009, **5**, 2648.

69   C. M. Schilli, M. Zhang, E. Rizzardo, S. H. Thang, Y. K. Chong, K. Edwards, G. Karlsson, and A. H. E. Müller, *Macromolecules*, 2004, **37**, 7861.

70   C. J. Hawker, A. W. Bosman, and E. Harth, *Chemical Reviews*, 2001, **101**, 3661.

71   V. Sciannamea, R. Jérôme, and C. Detrembleur, *Chemical Reviews*, 2008, **108**, 1104.

72   V. Coessens, T. Pintauer, and K. Matyjaszewski, *Progress in Polymer Science*, 2001, **26**, 337.

73   W. A. Braunecker and K. Matyjaszewski, *Progress in Polymer Science*, 2007, **32**, 93.

74   N. V. Tsarevsky and K. Matyjaszewski, *Chemical Reviews*, 2007, **107**, 2270.

75   F. J. Xu, K. G. Neoh, and E. T. Kang, *Progress in Polymer Science*, 2009, **34**, 719.

76   A. Favier and M.-T. Charreyre, *Macromolecular Rapid Communications*, 2006, **27**, 653.

77   G. Moad, E. Rizzardo, and S. H. Thang, *Australian Journal of Chemistry*, 2006, **59**, 669.

78   D. H. Solomon, E. Rizzardo, and P. Cacioli, *U.S. Patent*, 1986, US4581429.

79   M. K. Georges, R. P. N. Veregin, P. M. Kazmaier, and G. K. Hamer, *Macromolecules*, 1993, **26**, 2987.

80   C. Dire, S. Magnet, L. Couvreur, and B. Charleux, *Macromolecules*, 2009, **42**, 95.

81   B. Clément, T. Trimaille, O. Alluin, D. Gigmes, K. Mabrouk, F. Féron, P. Decherchi, T. Marqueste, and D. Bertin, *Biomacromolecules*, 2009, **10**, 1436.

82   F. Aldabbagh, P. B. Zetterlund, and M. Okubo, *Macromolecules*, 2008, **41**, 2732.

83   M. Kato, M. Kamigaito, M. Sawamoto, and T. Higashimura, *Macromolecules*, 1995, **28**, 1721.

84   J.-S. Wang and K. Matyjaszewski, *Journal of the American Chemical Society*, 2002, **117**, 5614.

85   J. Chiefari, Y. K. Chong, F. Ercole, J. Krstina, J. Jeffery, T. P. T. Le, R. T. A. Mayadunne, G. F. Meijs, C. L. Moad, G. Moad, E. Rizzardo, and S. H. Thang, *Macromolecules*, 1998, **31**, 5559.

86   P. Corpart, D. Charmot, T. Biadatti, S. Zard, and D. Michelet, 1998, WO 9858974.

87   C. L. McCormick and A. B. Lowe, *Accounts of Chemical Research*, 2004, **37**, 312.

88   A. B. Lowe and C. L. McCormick, *Progress in Polymer Science*, 2007, **32**, 283.

89   C. L. McCormick, B. S. Sumerlin, B. S. Lokitz, and J. E. Stempka, *Soft Matter*, 2008, **4**, 1760.

90   N. Suchao-in, S. Chirachanchai, and S. Perrier, *Polymer*, 2009, **50**, 4151.

91   J. Li, W.-D. He, N. He, S.-C. Han, X.-L. Sun, L.-Y. Li, and B.-Y. Zhang, *Journal of Polymer Science Part A: Polymer Chemistry*, 2009, **47**, 1450.

92   P. Bawa, V. Pillay, Y. E. Choonara, and L. C. du Toit, *Biomedical Materials*, 2009, **4**, 022001.

93   H. Wei, S.-X. Cheng, X.-Z. Zhang, and R.-X. Zhuo, *Progress in Polymer Science*, 2009, **34**, 893

94   F.-J. Xu, E.-T. Kang, and K.-G. Neoh, *Biomaterials*, 2006, **27**, 2787.

95   J. M. Rathfon and G. N. Tew, *Polymer*, 2008, **49**, 1761.

96   B. Liu and S. Perrier, *Journal of Polymer Science Part A: Polymer Chemistry*, 2005, **43**, 3643.

97   X. André, M. Zhang, and A. H. E. Müller, *Macromolecular Rapid Communications*, 2005, **26**, 558.

98   K. Zhu, R. Pamies, A.-L. Kjøniksen, and B. Nyström, *Langmuir*, 2008, **24**, 14227.

99   S. Kirkland-York, K. Gallow, J. Ray, Y.-l. Loo, and C. McCormick, *Soft Matter*, 2009, **5**, 2179.

100 J. Zhao, G. Zhang, and S. Pispas, *Journal of Polymer Science Part A: Polymer Chemistry*, 2009, **47**, 4099.

101 C.-M. Lin, Y.-Z. Chen, Y.-J. Sheng, and H.-K. Tsao, *Reactive and Functional Polymers*, 2009, **69**, 539.

102 C.-J. Huang and F.-C. Chang, *Macromolecules*, 2008, **41**, 7041.

103 A. Sinaga, T. A. Hatton, and K. C. Tam, *Macromolecules*, 2007, **40**, 9064.

104 G. Li, L. Shi, Y. An, W. Zhang, and R. Ma, *Polymer*, 2006, **47**, 4581.

105 H. Xu, F. Meng, and Z. Zhong, *Journal of Materials Chemistry*, 2009, **19**, 4183.

106 S. Zhong, H. Cui, Z. Chen, K. L. Wooley, and D. J. Pochan, *Soft Matter*, 2008, **4**, 90.

107 Z. Li, M. A. Hillmyer, and T. P. Lodge, *Nano Letters*, 2006, **6**, 1245.

108 J. Rodríguez-Hernández, F. Chécot, Y. Gnanou, and S. Lecommandoux, *Progress in Polymer Science*, 2005, **30**, 691.

109 M. Iijima, Y. Nagasaki, T. Okada, M. Kato, and K. Kataoka, *Macromolecules*, 1999, **32**, 1140.

110 L. Zhang, K. Katapodi, T. Davis, P., C. Barner-Kowollik, and M. Stenzel, H., *Journal of Polymer Science Part A: Polymer Chemistry*, 2006, **44**, 2177.

111 K. B. Thurmond, T. Kowalewski, and K. L. Wooley, *Journal of the American Chemical Society*, 1996, **118**, 7239.

112 K. B. Thurmond, T. Kowalewski, and K. L. Wooley, *Journal of the American Chemical Society*, 1997, **119**, 6656.

113 E. E. Remsen, K. B. Thurmond, and K. L. Wooley, *Macromolecules*, 1999, **32**, 3685.

114 L. Zhang, J. Bernard, T. Davis, P., C. Barner-Kowollik, and M. Stenzel, H., *Macromolecular Rapid Communications*, 2008, **29**, 123.

115 L. Zhang, W. Liu, L. Lin, D. Chen, and M. H. Stenzel, *Biomacromolecules*, 2008, **9**, 3321.

116 J. Zhang, Y. Zhou, Z. Zhu, Z. Ge, and S. Liu, *Macromolecules*, 2008, **41**, 1444.

117 H. Huang, K. L. Wooley, and E. E. Remsen, *Chemical Communications*, 1998, 1415.

118 Q. Zhang, E. E. Remsen, and K. L. Wooley, *Journal of the American Chemical Society*, 2000, **122**, 3642.

119 H. Huang, T. Kowalewski, E. E. Remsen, R. Gertzmann, and K. L. Wooley, *Journal of the American Chemical Society*, 1997, **119**, 11653.

120 V. Bütün, N. C. Billingham, and S. P. Armes, *Journal of the American Chemical Society*, 1998, **120**, 12135.

121 V. Bütün, X. S. Wang, M. V. de Paz Báñez, K. L. Robinson, N. C. Billingham, S. P. Armes, and Z. Tuzar, *Macromolecules*, 1999, **33**, 1.

122 S. Liu, J. V. M. Weaver, Y. Tang, N. C. Billingham, S. P. Armes, and K. Tribe, *Macromolecules*, 2002, **35**, 6121.

123 S. Liu and S. P. Armes, *Journal of the American Chemical Society*, 2001, **123**, 9910.

124 J. Zhang, X. Jiang, Y. Zhang, Y. Li, and S. Liu, *Macromolecules*, 2007, **40**, 9125.

125 J. V. M. Weaver, Y. Tang, S. Liu, P. Iddon, D., R. Grigg, N. C. Billingham, S. P. Armes, R. Hunter, and S. P. Rannard, *Angewandte Chemie International Edition*, 2004, **43**, 1389.

126 Y. Li, B. S. Lokitz, and C. L. McCormick, *Angewandte Chemie International Edition*, 2006, **45**, 5792.

127 B. S. Lokitz, A. J. Convertine, R. G. Ezell, A. Heidenreich, Y. Li, and C. L. McCormick, *Macromolecules*, 2006, **39**, 8594.

128 B. D. Yang, K. H. Yoon, and K. W. Chung, *Materials Chemistry and Physics*, 2004, **83**, 334.

129 F. Leroux, G. Goward, W. P. Power, and L. F. Nazar, *Journal of The Electrochemical Society*, 1997, **144**, 3886.

130 H.-C. Kuan, S.-L. Chiu, C.-H. Chen, C.-F. Kuan, and C.-L. Chiang, *Journal of Applied Polymer Science*, 2009, **113**, 1959.

131 Q. Dou, X. Zhu, K. Peter, D. Demco, M. Möller, and C. Melian, *Journal of Sol-Gel Science and Technology*, 2008, **48**, 51.

132 A. Pomogailo, *Colloid Journal*, 2005, **67**, 658.

133 A. Pomogailo, *Russian Chemical Reviews*, 2000, **69**, 53.

134 X. Liu, M. Zhu, S. Chen, M. Yuan, Y. Guo, Y. Song, H. Liu, and Y. Li, *Langmuir*, 2008, **24**, 11967.

135 Y. Wada, T. Kobayashi, H. Yamasaki, T. Sakata, N. Hasegawa, H. Mori, and Y. Tsukahara, *Polymer*, 2007, **48**, 1441.

136 T.-Y. Liu, S.-H. Hu, K.-H. Liu, D.-M. Liu, and S.-Y. Chen, *Journal of Magnetism and Magnetic Materials*, 2006, **304**, e397.

137 Y. Bai, B. Teng, S. Chen, Y. Chang, and Z. Li, *Macromolecular Rapid Communications*, 2006, **27**, 2107.

138 M. Zhang, C. Estournès, W. Bietsch, and A. H. E. Müller, *Advanced Functional Materials*, 2004, **14**, 871.

139 F. Yang, Y. Li, Z. Chen, Y. Zhang, J. Wu, and N. Gu, *Biomaterials*, 2009, **30**, 3882.

140 D. R. Paul and L. M. Robeson, *Polymer*, 2008, **49**, 3187.

141 Y. Zhu, J. Shi, W. Shen, X. Dong, J. Feng, M. Ruan, and Y. Li, *Angewandte Chemie International Edition*, 2005, **44**, 5083.

142 F. J. Xu, S. P. Zhong, L. Y. L. Yung, E. T. Kang, and K. G. Neoh, *Biomacromolecules*, 2004, **5**, 2392.

143 H. Wei, ChengCheng, C. Chang, W.-Q. Chen, S.-X. Cheng, X.-Z. Zhang, and R.-X. Zhuo, *Langmuir*, 2008, **24**, 4564.

144 D. Li, G. L. Jones, J. R. Dunlap, F. Hua, and B. Zhao, *Langmuir*, 2006, **22**, 3344.

145 T. Wu, Y. Zhang, X. Wang, and S. Liu, *Chemistry of Materials*, 2007, **20**, 101.

146 Y. Zhang, W. Gu, H. Xu, and S. Liu, *Journal of Polymer Science Part A: Polymer Chemistry*, 2008, **46**, 2379.

147 G. Hou, L. Zhu, D. Chen, and M. Jiang, *Macromolecules*, 2007, **40**, 2134.

148 Y. Kang and T. A. Taton, *Angewandte Chemie International Edition*, 2005, **44**, 409.

149 X. Chen, Y. An, D. Zhao, Z. He, Y. Zhang, J. Cheng, and L. Shi, *Langmuir*, 2008, **24**, 8198.

150 I. Gorelikov, L. M. Field, and E. Kumacheva, *Journal of the American Chemical Society*, 2004, **126**, 15938.

151 D. Suzuki and H. Kawaguchi, *Langmuir*, 2005, **21**, 8175.

152 V. Biju, T. Itoh, A. Anas, A. Sujith, and M. Ishikawa, *Analytical and Bioanalytical Chemistry*, 2008, **391**, 2469.

153 M. Pelton, J. Aizpurua, and G. Bryant, *Laser & Photonics Review*, 2008, **2**, 136.

154 D. Astruc, F. Lu, and J. R. Aranzaes, *Angewandte Chemie International Edition*, 2005, **44**, 7852.

155 J. Shan and H. Tenhu, *Chemical Communications*, 2007, 4580.

156 D. J. Kim, S. M. Kang, B. Kong, W.-J. Kim, H.-j. Paik, H. Choi, and I. S. Choi, *Macromolecular Chemistry and Physics*, 2005, **206**, 1941.

157 Y. Zhou, K. Jiang, Y. Chen, and S. Liu, *Journal of Polymer Science Part A: Polymer Chemistry*, 2008, **46**, 6518.

158 Y. Lu, Y. Mei, M. Drechsler, and M. Ballauff, *Angewandte Chemie International Edition*, 2006, **45**, 813.

159 Y. Lu, S. Proch, M. Schrinner, M. Drechsler, R. Kempe, and M. Ballauff, *J. Mater. Chem.*, 2009, **19**, 3955.

160 Y. Lu, Y. Mei, M. Ballauff, and M. Drechsler, *The Journal of Physical Chemistry B*, 2006, **110**, 3930.

161 S. Lecommandoux, O. Sandre, F. Chécot, and R. Perzynski, *Progress in Solid State Chemistry*, 2006, **34**, 171.

162 J. Guo, W. Yang, C. Wang, J. He, and J. Chen, *Chemistry of Materials*, 2006, **18**, 5554.

163 H. Furukawa, R. Shimojyo, N. Ohnishi, H. Fukuda, and A. Kondo, *Applied Microbiology and Biotechnology*, 2003, **62**, 478.

164 M. Talelli, C. J. F. Rijcken, T. Lammers, P. R. Seevinck, G. Storm, C. F. van Nostrum, and W. E. Hennink, *Langmuir*, 2009, **25**, 2060.

165 R. Narain, M. Gonzales, A. S. Hoffman, P. S. Stayton, and K. M. Krishnan, *Langmuir*, 2007, **23**, 6299.

166 T. Isojima, M. Lattuada, J. B. Vander Sande, and T. A. Hatton, *ACS Nano*, 2008, **2**, 1799.

Overview of this Thesis

This dissertation contains five publications presented in Chapters 3 to 7. This thesis is connected by the common theme of studying stimuli responsive polymers and their applications for generating hybrid nanoparticles. My research efforts focused on new synthesis pathways for creating smart block copolymers, an investigation of the self-assembly behaviors into micelles, the realization of robust organic-inorganic nanohybrids and an evaluation of the stimuli responsiveness of these colloids.

Synthesis of the required polymers was accomplished via two controlled radical polymerization techniques: radical addition-fragmentation chain transfer polymerization (RAFT) and atom transfer radical polymerization (ATRP). Self-assembly in solution under various external stimuli was exploited for preparation of the micellar nanoparticles. Applications based on multi-responsive particles require kinetically stabilized systems; therefore, a facile cross-linking strategy in solution was investigated. The evaluation of solution properties before and after locking the structure was accomplished by several light scattering and imaging techniques (scanning force microscopy, transmission electron microscopy) to allow monitoring of the ensemble behavior, to quantify the response to stimuli and to determine the shape of these objects.

The application studies were focused on the formation of inorganic-organic hybrid materials. Different procedures were developed depending on the nature of the object. Metal-polymer hybrids involved the conjugation of metal salts as precursors onto the micelle and their subsequent reduction to obtain tiny catalytically active metal nanoparticles inside the colloid. Silica-polymer hybrids were generated by self-assembly of silica nanoparticles and polymers via hydrogen bonding and ionic interactions.

The chapters can to some extent be subdivided into two main topics. Chapters $3-5$ deal with the synthesis of smart and other water-soluble homo- and block copolymers in aqueous media. Chapters 6 and 7 are comprised of investigations concerning the self-assembly behavior of poly(N-isopropylacrylamide)-b-poly(acrylic acid) block copolymers into spherical micelles under various stimuli, their cross-linking abilities, the synthesis of nanohybrids and the environmental response of these new objects.

In the following sections, I will present a summary of the key results obtained within the scope of this thesis. Complete coverage of the experimental results and conclusions can be found in the respective chapters.

Smart Polymer Synthesis by RAFT Polymerization

The synthesis of responsive polymers was achieved using reversible addition-fragmentation chain transfer (RAFT) polymerization and atom transfer radical polymerization (ATRP). These controlled radical polymerization (CRP) techniques were chosen because they combine the utility and simplicity of conventional free radical polymerization with the kinetic and structural control obtained by ionic polymerization. CRP can be conducted over a wide range of temperatures, solvents and process conditions. It can be also applied to a huge number of vinylic monomers under less stringent conditions than ionic polymerization in terms of oxygen and water presence or monomer functionality. Finally, as with living ionic polymerization, materials with very efficient control over molecular weight, molecular weight distribution, microstructure, chain-end functionality and complex macromolecular architecture can be obtained.

Among the large choice of smart polymers, poly(*N*-isopropylacrylamide) (PNIPAAm) and poly(acrylic acid) (PAA), respectively a thermo- and a pH-responsive polymer, were selected as model compounds for investigating the control of the RAFT polymerization in aqueous media. PNIPAAm exhibits a lower critical solution temperature (LCST) in water and a sharp reversible phase transition is observed at 32 °C, close to the human body temperature, which makes this polymer very attractive and popular for biological applications. PAA responds to changes in pH and ionic strength by changing coil dimensions and solubility. Performing RAFT polymerization directly in water presents the advantage of working in an environmentally friendly solvent where the rate of polymerization is much higher than in organic solvents. However, when a LCST polymer is synthesized, the reaction has to be performed below this temperature to enable good control. The classic azo-initiators generally used in this process do not work at ambient temperature. Therefore, γ-radiation was employed to initiate RAFT polymerization of these smart monomers in aqueous solution due to the small temperature dependence of the initiation rate in this case. This radiation type can initiate most vinylic monomers and can penetrate the reaction solution more deeply than UV initiation.
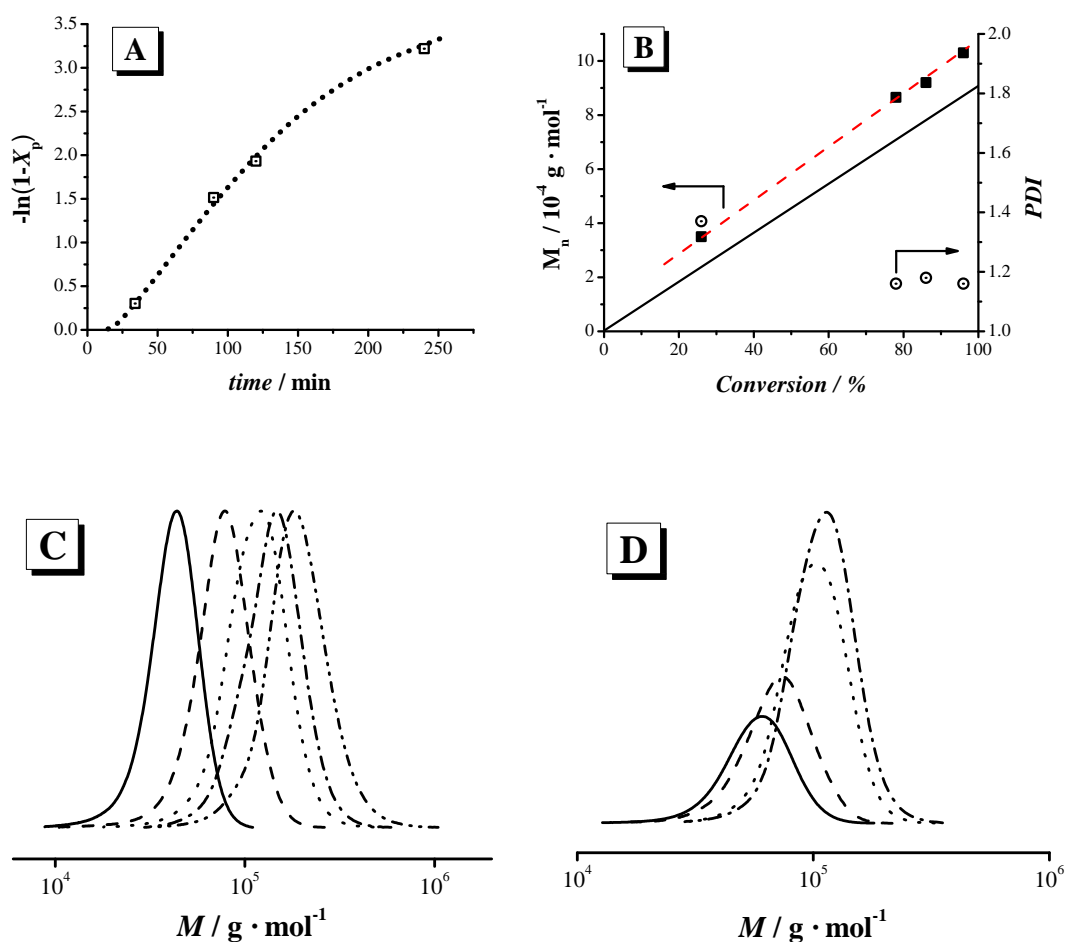
Figure 2-1. RAFT polymerization of NIPAAm under γ-radiation in water (1.5 mol·L^{-1}) using S,S-bis(α,α'-dimethyl-α"-acetic acid)trithiocarbonate (TRITT) at ambient temperature. (A) First-order time-conversion plot for $[M]_0/[CTA]_0 = 800$, (• • •) extrapolation. (B) Apparent number-average molecular weight (■) and polydispersity index (⊙) versus monomer conversion for $[M]_0/[CTA]_0 = 800$, (– –) extrapolation, (——) theoretical number-average molecular weight evolution. (C) Dependence of the molecular weight distribution, $w(\log M)$, on the ratio of monomer/CTA. $[M]_0/[CTA]_0 =$ (——) 200, (– –) 400, (• • •) 600, (– • –) 800, (– • • –) 1200. (D) Molecular weight distributions, $w(\log M)$, obtained in chain extension of PNIPAAm macro-CTA synthesized with TRITT as CTA under γ-radiation. $[M]_0 = 0.4$ mol·L^{-1}, $[M]_0/[$macro-CTA$]_0 = 368$. (——) precursor, (– –) 24%, (• • •) 76% and (– • –) 94% of monomer conversion.

The RAFT polymerizations of NIPAAm and AA were mediated in the presence of two trithiocarbonate chain transfer agents (CTAs), i.e. S,S-bis(α,α'-dimethyl-α''-acetic acid)trithiocarbonate (TRITT) and 3-benzylsulfanylthiocarbonylsulfanyl propionic acid (BPATT) (see Chapter 3). Both carry carboxylic moieties which make them soluble in aqueous media. However, when TRITT is soluble in water, even at a high concentration, BPATT, due to the presence of an aromatic ring, needs the use of a co-solvent like acetone to obtain homogenous solutions. Both CTAs allow the excellent control of either NIPAAm or AA polymerizations, as illustrated in Figure 2-1 in the case of NIPAAm with TRITT. After a generally short induction period, the first-order plot is linear up to 90% conversion, which indicates that the main equilibrium is rapidly established and is operative during the major part of the reaction (Figure 2-1A). Moreover, the molecular weight increases linearly with conversion (Figure 2-1B) and the polydispersity indices (PDI) are low (PDI<1.2) even at a high conversion (>95%) and for a high monomer/RAFT agent ratio of up to 2,000. The size exclusion chromatography (SEC) traces display unimodal, symmetrical and narrow peaks (Figure 2-1C) which indicate a low influence or an absence of termination or other side-reactions during the process. Finally, to further demonstrate the retention of the trithiocarbonate functionality, chain extension experiments using two macro-CTAs of PNIPAAm and PAA were attempted. In both cases, as highlighted in Figure 2-1D, when a PNIPAAm macro-CTA based on TRITT is used, the reaction is nearly quantitative. The SEC traces show a distinct increase in molecular weight and do not present a shoulder or a tailing, which when combined with a low PDI suggest that the large majority of the macro-CTAs exhibit living characteristics.

Extension to the Synthesis of Water-Soluble Homopolymers and Block Copolymers

Taking into account all the benefits of using γ-initiation at ambient temperature in aqueous media to obtain well-defined smart polymers over a large range of molecular

weights by RAFT, several other water-soluble monomers were tested to develop this process (Chapter 4). Poly(2-(dimethylamino)ethyl methacrylate) (PDMAEMA), a pH and temperature responsive polymer, poly(2-acrylamido-2-methylpropane sulfonic acid) (PAMPS), an ionic strength responsive polymer, poly(N, N-dimethylacrylamide) (PDMAAm), poly(acrylamide) (PAAm) and poly(poly(ethylene glycol)methacrylate) (PPEGMA), all three permanent water-soluble polymers, and poly(2-hydroxyethyl acrylate) (PHEA), a functional polymer which can be easily modified via ester chemistry, were synthesized as summarized in Table 2-1. In all cases, a good control was reached with a low PDI even when close to full monomer conversion (>99%). Moreover, this technique was shown to be really efficient at generating extremely long polymers, as we demonstrated for PAA, PAAm and PDMAAm when well-defined polymers with a theoretical degree of polymerization (DP) close to 10,000 were obtained.

Furthermore, an added advantage of this process is the solvent selected. In addition to being an environmentally friendly solvent, the aqueous solution proved to be more efficient compared to the organic solvent in terms of kinetics and control. Figure 2-2 shows that in the case of DMAAm polymerization using the same monomer/BPATT ratio and the same conditions, a long induction period of 3 h was required in dioxane, whereas this phenomenon was not observed in the aqueous solution (Figure 2-2A). Moreover, when the first-order dependence on monomer conversion is observed, the apparent rate coefficient associated with the rate of polymerization is more than 2.5 times higher in the aqueous solvent than in organic solvent, which demonstrates a faster addition of the monomer in water-based media. Finally, even though in both systems the molecular weight increased linearly with the conversion, a broader polymer distribution was obtained in dioxane (Figure 2-2C).

Table 2-1. RAFT polymerization under γ-initiation of water soluble monomers in aqueous media at ambient temperature.

Mono-mer[a]	CTA	$\dfrac{[M]_0}{[CTA]_0}$	Acetone %Vol	Time min	x_p [b] %	$\overline{M}_{n,th}$ [c] kg/mol	$\overline{M}_{n,exp}$ kg/mol	PDI
HEA	TRITT	400	-	420	91	43	72[d]	1.15[d]
HEA	BPATT	200	25	1 440	97	22.8	50[d]	1.12[d]
AAm	TRITT	400	-	300	89	25.6	17[e]	1.19[e]
AAm	BPATT	800	22	2 720	>99	57	37[e]	1.19[e]
AA	TRITT	800	-	1 200	98	57	87[e]	1.14[e]
AA	BPATT	1 200	16	1 520	98	85	98[e]	1.10[e]
NIPAAm	TRITT	500	-	180	98	56	74[d]	1.10[d]
NIPAAm	BPATT	1 000	15	310	88	100	105[d]	1.12[d]
AMPS	TRITT	800	-	220	90	131	178[d]	1.16[d]
AMPS	BPATT	200	30	1 440	96	40	57[d]	1.19[d]
OEGMA	CPADB	100	15	140	16	8.7	10[d]	1.05[d]
OEGMA	CPADB	100	15	240	73	38.7	50[d]	1.07[d]
DMAEMA	CPADB	100	10	240	79	12.7	17.5[d]	1.20[d]

[a] HEA = 2-hydroxyethyl acrylate, AAm = acrylamide, AA = acrylic acid, NIPAAm = N-isopropylacrylamide, AMPS = 2-acrylamido-2-methylpropane sulfonic acid, OEGMA = oligo(ethylene glycol) methacrylate, DMAEMA = 2-(dimethylamino)ethyl methacrylate [b] Determined by ^{1}H NMR spectroscopy in D$_2$O. [c] $\overline{M}_{n,th} = M_M \cdot X_p \cdot [M]_0/[CTA]_0 + M_{CTA}$. [d] Measured by SEC using PS standards in N,N-dimethylacetamide (DMAc). [e] Measured by SEC using PEO standards in water.

Figure 2-2. Influence of the solvent on the RAFT polymerization of DMAAm under γ-radiation at ambient temperature using BPATT as CTA for an initial ratio of $[M]_0/[CTA]_0$ of 1,000 and $[M]_0 = 1.5$ mol·L^{-1}. (A) First-order time-conversion plot in the water-acetone mixture 85/15 (v/v) (■) and in pure dioxane (●). (– –) and (• • •) are extrapolations to guide the reader's eyes, (B) (⊡) and (⊙) are apparent number-average molecular weights and PDI obtained in the water-acetone mixture 85/15 (v/v), respectively, and (– –) is the corresponding extrapolation of apparent number-average molecular weights. (■) and (●) are apparent number-average molecular weight and PDI obtained in dioxane, respectively, and (• • •) is the corresponding extrapolation of apparent number-average molecular weights.

RAFT polymerization in aqueous solution under γ-radiation is not only the technique of choice for obtaining water-soluble homopolymers with a very efficient control, but it can also be extended to the synthesis of well-defined block copolymers. A high number of diblocks were reached using different macro-RAFT agents (Chapter 4). Selected results are shown in Table 2-2 and Figure 2-3. A good control was obtained for most of these (Table 2-2). Among the large choice in terms of monomers investigated for synthesizing our block copolymers, PNIPAAm-*b*-PAA was a very attractive material due to its multi-responsive behavior to temperature, pH and ionic strength. This block copolymer type cannot be generated directly in water due to the complexation by hydrogen bonding between the carboxylic and the amide groups present which lead to a

full collapse of the system and a loss of control. However, this problem was fully overcome by using an organic co-solvent. Then, narrow and monomodal molecular weight distributions were usually found, even when a high monomer/macro-CTA was used (Figure 2-3A). None or only a few remaining precursors were noticed in the GPC traces. This was due to an extremely low amount or an absence of side reactions during the reaction to obtain the macro-CTAs; a good retention of the RAFT functionality is observed and almost all the polymer chains are available for the chain extension. This characteristic was even noticed when the macro-CTA was generated at almost full conversion. Finally, as with the homopolymers, this technique is also very attractive for generating very long diblock copolymers. Different long PAA precursors were used to polymerize NIPAAm over a monomer/PAA ratio up to 2,000. In all cases, well-defined PNIPAAm-*b*-PAA block copolymers were generated (Figure 2-3B).
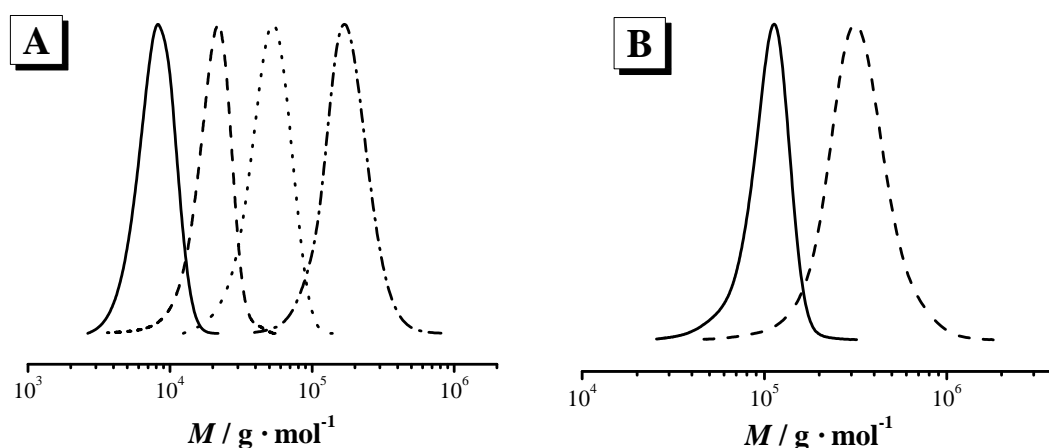
Figure 2-3. Dependence of the molecular weight distributions, $w(\log M)$, on the ratio of $[NIPAAm]_0/[PAA\text{-}CTA]_0$ in the RAFT polymerization of NIPAAm under γ-radiation in aqueous solution using PAA macro-CTAs. (A) Using a PAA macro-CTA B1 (DP = 26). PAA precursor (—), after chain extension with $[M]_0/[CTA]_0 = 50$ (– –), 300 (• • •) and 1,000 (– • –). (B) Using a PAA macro-CTA based on B4 (DP = 500). PAA precursor (—), after chain extension with $[M]_0/[CTA]_0 = 2,000$ (– –).

Table 2-2. Chain extension with different monomers of various macro-CTAs by RAFT polymerization in aqueous media at ambient temperature under γ-initiation.

Monomer	CTA	$\dfrac{[M]_0}{[CTA]_0}$	$[M]_0$ mol/L	Cosolvent %V	Time min	$x_p^{(j)}$ %	$\overline{M}_{n,th}^{(k)}$ kg/mol	$\overline{M}_{n,exp}$ kg/mol	PDI
AAm	B1[a]	405	2	22[g]	1 620	>99	31	23[l]	1.23[l]
AAm	B2[b]	155	2	35[g]	1 515	97	14.1	17[l]	1.10[l]
NIPAAm	B3[c]	2000	0.6	50[h]	1440	>99	241	217[m]	1.24[m]
NIPAAm	B5[d]	1000	0.4	50[h]	1440	>99	257	343[m]	1.40[m]
DMAAm	B2[b]	300	1	4[i]	2540	>99	33.2	41[m]	1.11[m]
DMAAm	PNIPAAm[e]	400	1	-	2540	>99	57	55[n]	1.15[n]
DMAAm	PEO$_{2k}$-BPATT[f]	600	1.7	20[i]	2500	>99	62	62[l]	1.09[l]
AA	PEO$_{2k}$-BPATT[f]	600	1.7	20[i]	2500	>99	45.5	69[l]	1.15[l]

[a] Using asymmetric PAA-macro-CTA B1 of DP_n = 26. [b] Using asymmetric PAA-macro-CTA B2 of DP_n = 42. [c] Using asymmetric PAA-macro-CTA B3 of DP_n = 200. [d] Using asymmetric PAA-macro-CTA B5 of DP_n = 2,000. [e] Using asymmetric PNIPAAm macro-CTA of DP_n = 152. [b] Using asymmetric PEO macro-CTA of molecular weight 2,000 g·mol^{-1}. [g] Ethanol. [h] Dioxane. [i] Acetone. [j] Monomer conversion is calculated by ^{1}H NMR in D$_2$O. [k] The theoretical number-average molecular weight is calculated according to the equation, $\overline{M}_{n,th} = M_M * X_p * [M]_0/[CTA]_0 + M_{CTA}$. [l] Apparent number-average molecular weight and PDI, as measured by SEC using PEO standards in water. [m] Apparent number-average molecular weights and PDIs, as measured by SEC using PS standards in *N,N*-dimethylacetamide (DMAc). [n] Apparent number-average molecular weights and PDIs, as measured by SEC using PS standards in 2-*N*-methylpyrrolidone (NMP).

ATRP of *N*-Isopropylacrylamide in Water

Reversible addition-fragmentation chain transfer polymerization is not the only controlled radical polymerization technique available for obtaining well-defined PNIPAAm directly in water. Atom transfer radical polymerization (ATRP) was also investigated (Chapter 5). A careful selection of the initiator and of the experimental conditions is compulsory in order to reach a good control. Bromo-2-methylpropionic acid (BIBA) was selected due to its high solubility in water compared to the usual ATRP initiator. In addition, it has the advantage of introducing a carboxylic group to allow protein modification by active ester chemistry to create polymer-protein hybrids or to allow other post-polymerization modifications. The highly exothermic characteristic of the polymerization in water, which leads to a collapse of the PNIPAAm during the reaction by temperatures rising higher than the LCST, was overcome by using a rather low monomer concentration, typically $[M]_0 = 0.5$ mol·L^{-1} and an ice bath. After having solved this crucial prerequisite step to the experiment, the influences of the ligand, the catalyst system and Cu(I)/Cu(II) ratio were examined. The most efficient system was determined to be tris(2-dimethylaminoethyl)amine (Me$_6$TREN), a very active ligand in combination with CuBr/CuBr$_2$ catalysts, with a high amount of CuBr$_2$ to slow down the kinetics which would otherwise take less than a minute to reach full conversion.

A kinetic study was realized using a $[NIPAAm]_0/[BIBA]_0/[CuBr]_0/[CuBr_2]_0/[Me_6TREN]_0$ ratio of 50/1/0.5/0.5/1. In these conditions, the first-order time-conversion plot (Figure 2-4A) is linear up to at least 90%, which indicates an absence of side reactions. Moreover, the molecular weight increases linearly with the conversion demonstrating the controlled fashion of this process (Figure 2-4B). The resulting polydispersity indices are low (PDI<1.2) and decrease with the conversion. The SEC traces are unimodal and symmetrical and do not exhibit any trace of termination by the recombination of growing radicals, even at an extremely high monomer conversion.
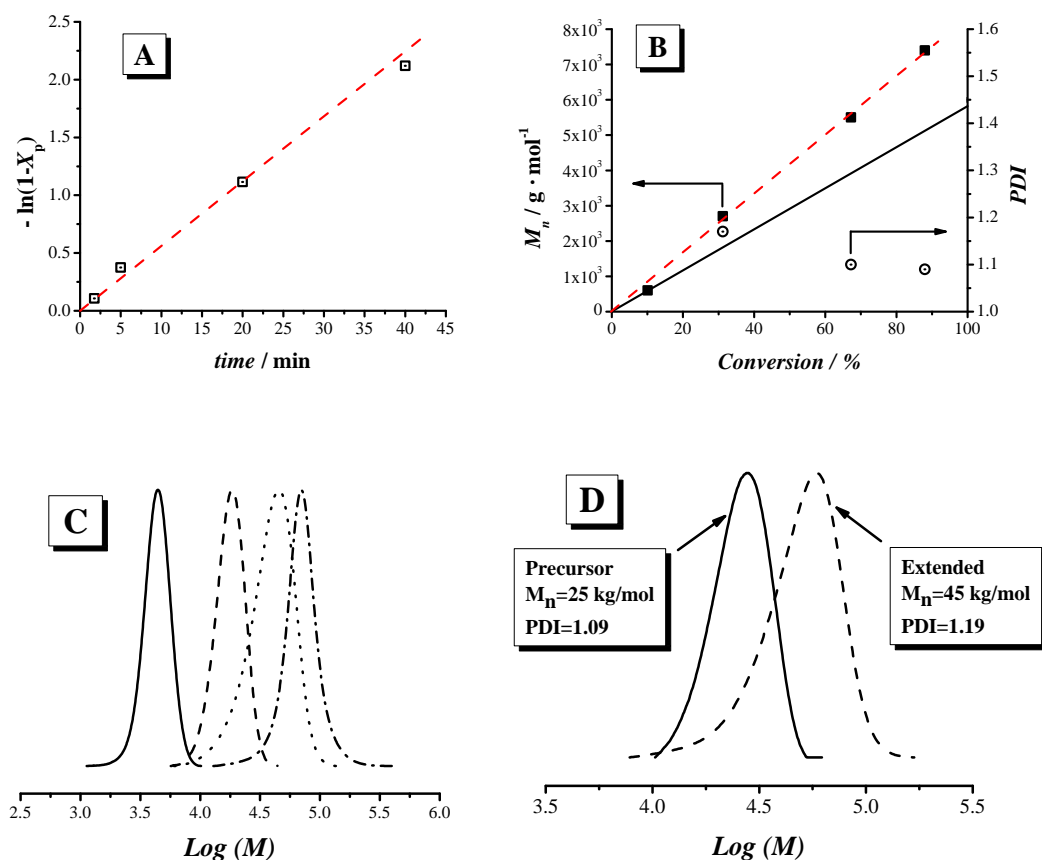
Figure 2-4. Kinetic of NIPAAm ATRP (0.5 mol·L^{-1}) in water at 4 °C with [M]$_0$/[BIBA]$_0$/[CuBr]$_0$/[CuBr$_2$]$_0$/[Me$_6$TREN]$_0$ = 50/1/0.5/0.5/1. (A) First-order time-conversion plot (�). (– –) Extrapolation. (B) Molecular weight and polydispersity index vs. conversion (■). (– –) Extrapolation of the molecular weight, (——) theoretical number-average molecular weight evolution. (C) Dependence of the molecular weight distribution, $w(\log M)$, depending on the monomer/initiator ratio for the ATRP of NIPAAm (0.5 mol·L^{-1}) in water at 4 °C with [BIBA]$_0$/[CuBr]$_0$/[CuBr$_2$]$_0$/[Me$_6$TREN]$_0$ = 1/0.7/0.3/1 with [M]$_0$/[BIBA]$_0$ = (——) 30, (– –) 100, (• • •) 200 and (– • –) 400. (D) Molecular weight distribution, $w(\log M)$, for the chain extension of PNIPAAm by ATRP in water at 4 °C. [M]$_0$ = 0.5 mol·L^{-1}, [M]$_0$/[PNIPAAm$_{120}$-Cl]$_0$ = 300. (——) Precursor, (– –) extension after 40% conversion.

To prove the versatility of the process, different molecular weights of PNIPAAm were synthesized over a large range from rather low (DP = 30) to rather high (DP = 400). It

was found that an increase of the NIPAAm/BIBA ratio leads (at comparable monomer conversions) to a linear increase in the molecular weight. The GPC traces (Figure 2-4C) display monomodal and narrow peaks (PDI < 1.2) without any trace of termination at full conversion.

The livingness was further demonstrated by chain extension of an initial PNIPAAm obtained by using a [NIPAAm]$_0$/[BIBA]$_0$/[CuCl]$_0$/[CuCl$_2$]$_0$/[Me$_6$TREN]$_0$ ratio of 120/1/1.6/0.4/2. Then, the block copolymer was synthesized by the sequential addition of a degassed aqueous monomer solution without purification of the macro-initiator, which was polymerized at full conversion. A CuCl-based catalyst was chosen to avoid halogen abstraction by nucleophilic substitution, which can occur in water. The resulting polymer-halide bound C-Cl is much stronger and less sensitive to abstraction than C-Br. The GPC chromatograms before and during chain extension (Figure 2-4D) show a distinct increase in the molecular weight. However, a small tailing can be observed which might be due to the partial loss of a terminal chloride of the precursor. Nevertheless, the large majority of the PNIPAAm precursors retained functionality and were available for subsequent chain extensions.
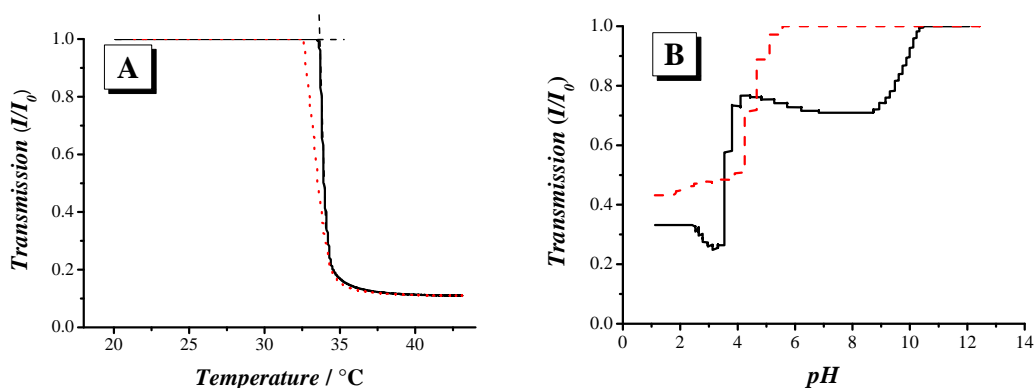
Figure 2-5. Self-assembly properties of PNIPAAm-b-PAA under various stimuli. (A) Determination of the cloud point, T_{cl}, from turbidity measurements of PNIPAAm$_{2000}$-b-PAA$_{300}$ in pure water at pH 7, (——) heating and (• • •) cooling. The cloud point is defined as the intercept of the tangents (– –) upon heating. (B) Response of PNIPAAm$_{1000}$-b-PAA$_{2000}$ in water to pH (——) and in the presence of amino-silsesquioxane nanoparticles with a [NH$_2$]/[AA] ratio of 5 (– –).

Self-Assembly of PNIPAAm-*b*-PAA under various Stimuli and its Cross-Linking Strategies

After investigating different efficient strategies of synthesizing smart homo and block copolymers in aqueous solution, attention was drawn to possible applications of the multi-responsive PNIPAAm-*b*-PAA. This block copolymer can self-assemble in water under various triggers (Figure 2-5). Due to the PNIPAAm block, which exhibits a LCST above the cloud point (T_{cl}) in neutral or basic pH, spherical micelles are formed. The core is composed of hydrophobic PNIPAAm and the hydrophilic PAA block generates the corona which prevents full aggregation of the system. Figure 2-5A depicts the determination of the cloud point for PNIPAAm$_{2000}$-*b*-PAA$_{500}$: a very sharp transition occurs at 33.3 ºC. The phase transition is fully reversible and, after cooling down, the solution is fully transparent again. The pH can be also used to create micelles. In acidic conditions at ambient temperature, a complex based on hydrogen bonding interactions between the carboxylic group of the PAA and the amide group of the NIPAAm is obtained. For PNIPAAm$_{1000}$-*b*-PAA$_{2000}$ (Figure 2-5B), this reversible phenomenon starts at pH 5.5 over one unit of pH. Stable aggregates are then formed. This pH transition is modified in the presence of amino functionalized silsesquioxane, where a first complexation between the PAA block and the amino groups can already be observed at pH 10.5. Spherical micelles with a core made of a mixture of PAA and silica particles are created. The PNIPAAm block is present in the corona and prevents full collapse via steric interactions. When the pH decreases below pH 4, another transition is observed and the system aggregates.
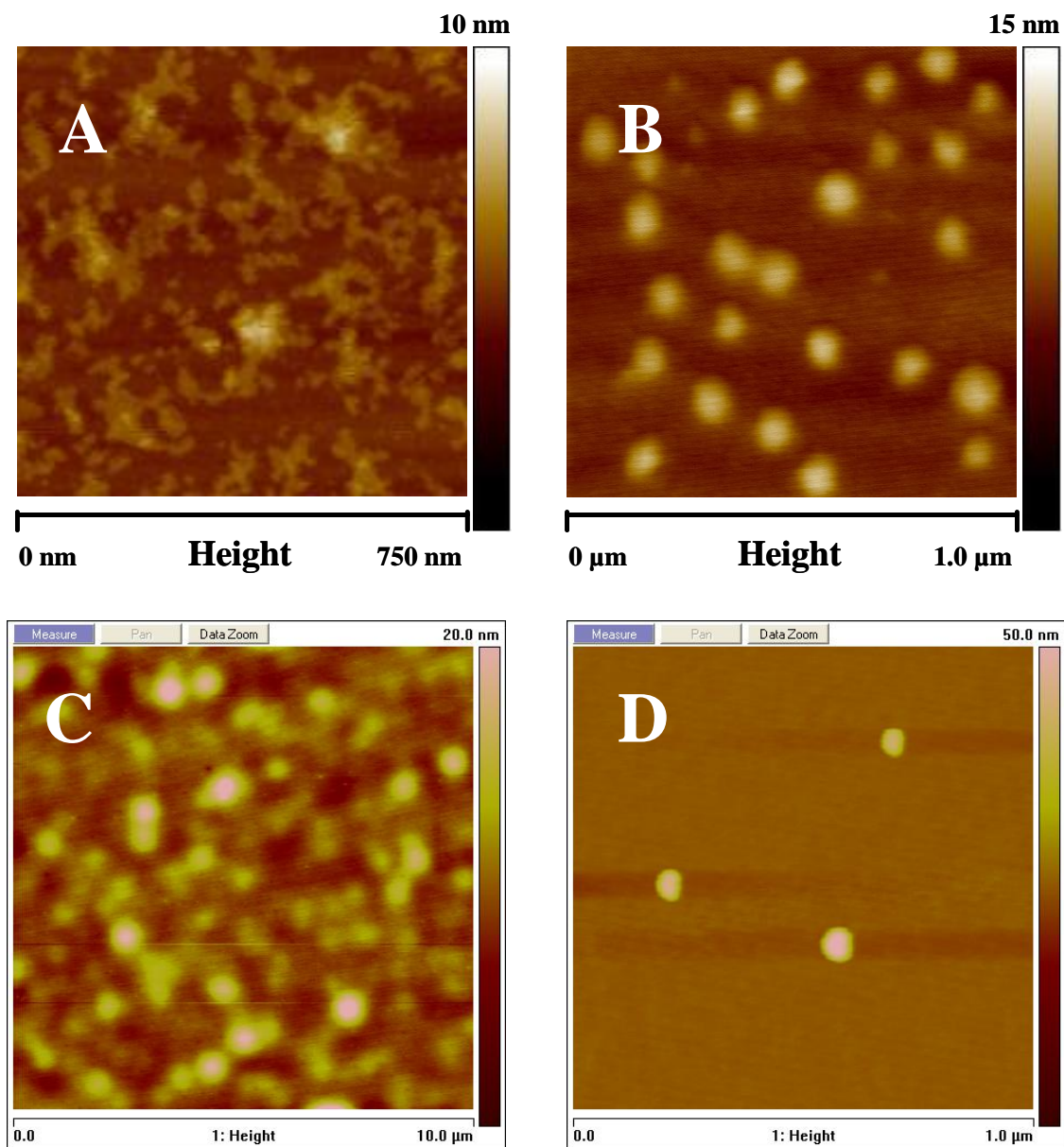
Figure 2-6. Cross-linking of PNIPAAm-*b*-PAA in the presence of EDC as investigated by scanning force microscopy. (A) PNIPAAm$_{2000}$-*b*-PAA$_{500}$ solution in water at pH 7 before cross-linking was measured at 25 ºC. (B) Shell cross-linked PNIPAAm$_{2000}$-*b*-PAA$_{500}$ solution in water at pH 7 measured at 25 ºC. (C) PNIPAAm$_{1000}$-*b*-PAA$_{2000}$ and amino-silsesquioxane nanoparticle complex with a [NH$_2$]/[AA] ratio of 5 in aqueous solution, pH 7, before cross-linking. (D) Core cross-linked micelles composed of PNIPAAm$_{2000}$-*b*-PAA$_{1000}$ and amino-silsesquioxane nanoparticles with a [NH$_2$]/[AA] ratio of 5 in water at pH 7.

For many applications, like drug delivery, micelles stability is a critical issue. Below the critical micelle concentration (cmc), micelles will inevitably disintegrate into unimers. To solve this handicap we investigated cross-linking procedures based on amidification of the carboxylic group of PAA (see Chapters 6-7). Two distinct strategies were studied to obtain either shell cross-linked (SCL) micelles or core cross-linked (CCL) micelles. The first process was carried out at 45 ºC, above the LCST of PNIPAAm. The block copolymer is then in a micellar state and PAA is present in the corona. By using tris(2-aminoethyl)amine (TREN) as a tri-functional cross-linker in the presence of a water-soluble carbodiimide (EDC), a network was formed, as proven by scanning force microscopy (SFM). An inhomogeneous film can be seen before the cross-linking at ambient temperature, when a solution of PNIPAAm-*b*-PAA is deposited (coil state) (Figure 2-6A). Micelles were observed after this reaction, even at a low temperature, which demonstrates the efficiency of the cross-linking (Figure 2-6B).

The core cross-linking was realized with amino functionalized silsesquioxane. In this case, at neutral pH, composite micelles composed of PAA and silica particles in the core were generated. By adding EDC to the system, nice cross-linked objects were created. The original complex, as measured by SFM (Figure 2-6C), shows large and not very defined objects which are quite flat. After the procedure, the structure is more defined and robust CCL micelles are seen with a greater height (Figure 2-6D).

Applications for the Synthesis of Smart Polymer-Metal Hybrids

Organic-inorganic nanohybrids are a new class of material which present improved or unusual features and allow the development of innovative industrial applications. Being at the interface of organic and inorganic realms, these compounds are highly versatile and offer a wide range of possibilities for elaborating tailor-made materials in terms of processing and chemical and physical properties. The PNIPAAm-*b*-PAA SCL micelles were used as nanoreactors for the synthesis of metal nanoparticles; they then acted as a robust vessel to support inorganic materials (Chapter 6). Gold or silver salts, which are

able to complex the micelles, were reduced using sodium borohydride. The TEM revealed that almost monodispersed, small nanoparticles were generated inside the SCL micelle of both metals (Figure 2-7A). A characteristic absorption peak was always observed by UV-vis spectrometry (Figure 2-7B).
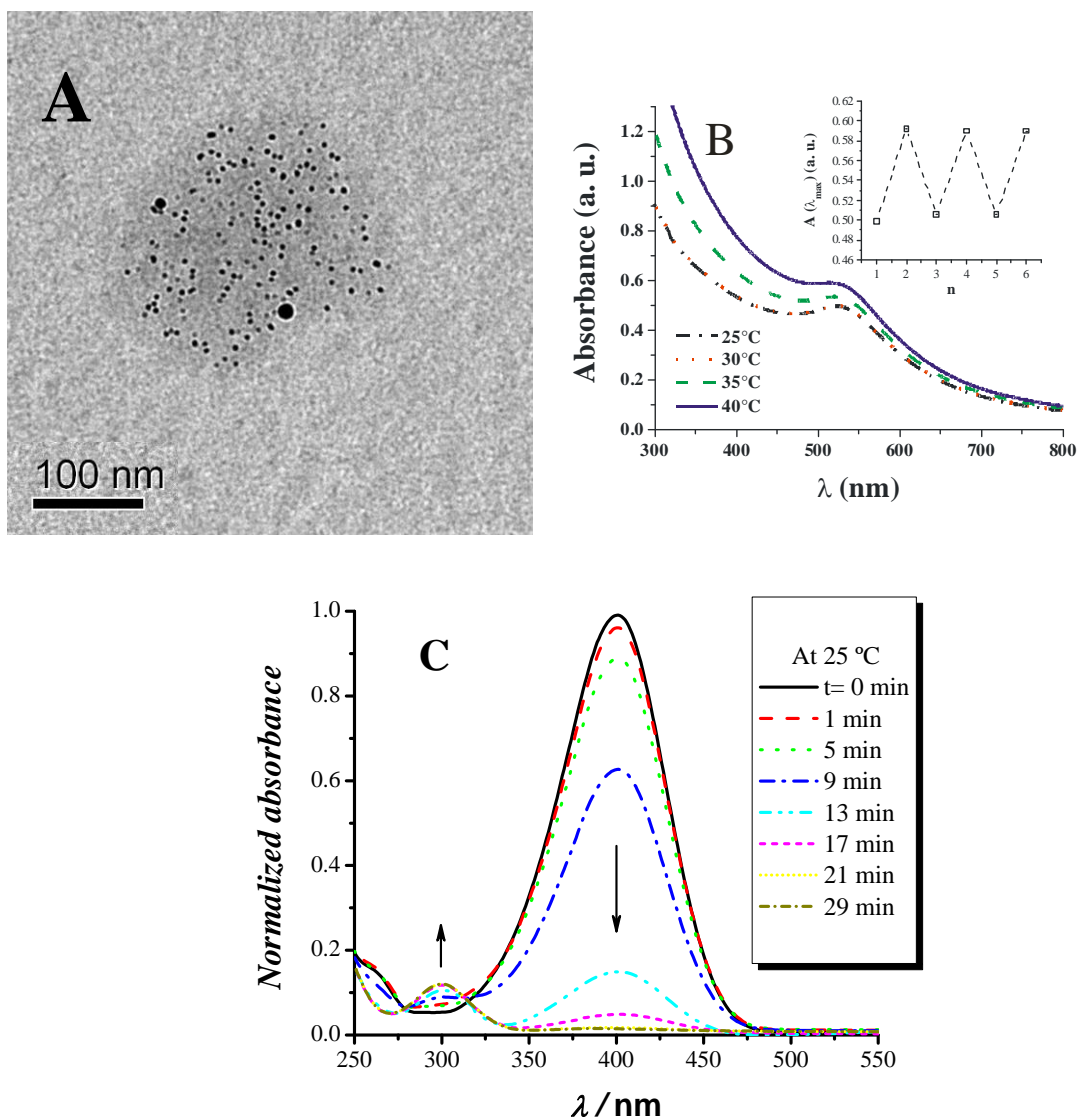

Figure 2-7. PNIPAAm-*b*-PAA-metal hybrid characterization. (A) Transmission electron microscopy (TEM) of gold nanoparticle-PNIPAAm$_{2000}$-*b*-PAA$_{500}$ hybrid. (B) Absorption spectra of PNIPAAm$_{2000}$-*b*-PAA$_{500}$ after reduction of gold nanoparticles depending on the temperature (• – •) 25 ℃, (• • •) 30 ℃, (– –) 35 ℃ and (——) 40 ℃. In the inset, variation of the absorbance maximum (λ_{max}= 523 nm) at 25 ℃ and 40 ℃ over three heating-

cooling cycles. (C) Catalytic reduction of 4-nitrophenol by $NaBH_4$ in the presence of silver nanoparticle-PNIPAAm$_{2000}$-b-PAA$_{300}$ hybrids. UV-vis spectra measured at different times.

Moreover, the response to temperature was also studied. As with the SCL micelles alone, nanohybrids aggregate at elevated temperatures. The reversibility of this technique was demonstrated by monitoring several cycles. The values of the resulting absorbances obtained at low and elevated temperatures exhibited good reproducibility over subsequent cycles and constant values were noticed (Figure 2-7B inset). Finally, the catalytic potential of these metal-polymer particles was studied. The reduction of 4-nitrophenol into 4-aminophenol by an excess of $NaBH_4$ was chosen as model reaction. The kinetics of this reaction can be monitored by UV-vis spectroscopy. From the spectra depicted in Figure 2-7C, it can be seen that the reaction was completed in around 21 min. This proves the accessibility and the capacity of the metal nanoparticles inside the SCL micelles in catalyzing reactions.

Smart polymer-silica hybrids

Core cross-linked silica/PNIPAAm-b-PAA was synthesized using a new process starting from tiny silsesquioxane functional particles (Chapter 7). These silica nanoparticles which wear residual amino groups can complex the PAA block by hydrogen bonding and ionic interactions depending on the pH. PNIPAAm is present in the corona and prevents the full aggregation of the system. Moreover, silsesquioxane particles act as a really powerful multifunctional cross-linkers during the amidification of the residual carboxylic groups of PAA. The obtained CCL micelles are well defined and monodispersed. The size of the particles can be influenced by modifying the [NH$_2$]/[AA] ratio (Figure 2-10). The higher the ratio the bigger the particles will be. However, superstructures can be observed at a high [NH$_2$]/[AA] ratio (≥ 5).
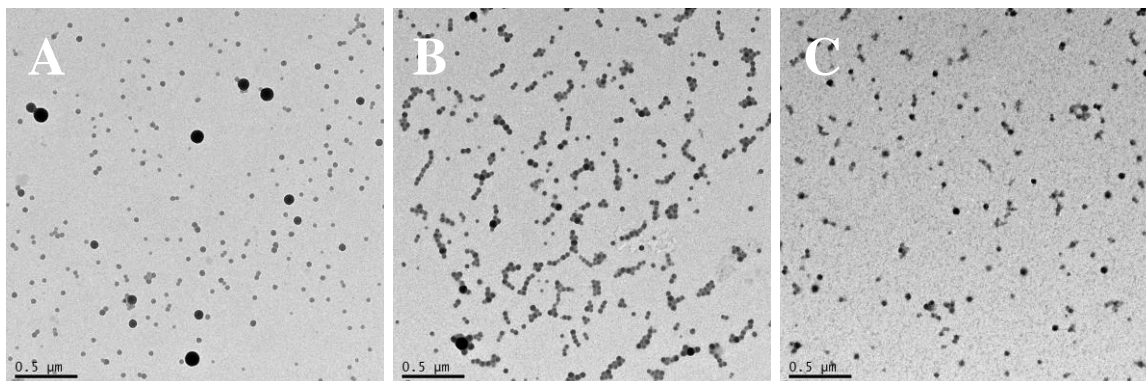
Figure 2-10. Silica-PNIPAAm$_{1000}$-b-PAA$_{2000}$ core cross-linked micelles at different [NH$_2$]/[AA] ratios. (A) [NH$_2$]/[AA]=5. (B) [NH$_2$]/[AA]=2. (C) [NH$_2$]/[AA]=1.

Table 2-3. Response to temperature of silica-PNIPAAm$_{1000}$-b-PAA$_{2000}$ core-cross-linked micelles at [NH$_2$]/[AA]=10 in water investigated by zeta-sizer measurements.

Conditions	$\dfrac{R_H}{nm}$	$\dfrac{\zeta}{mV}$
25 ℃, pH 7	173	+18
40 ℃, pH 7	124	+60
25 ℃, pH 13	139	+1
40 ℃, pH 13	Aggregation	——

The response to temperature of these robust micelles was also explored. The behavior can be tuned depending on the pH. At a neutral pH the hydrodynamic radius decreases above the LCST, whereas at a high pH the hybrids aggregate (Table 2-3). This can be explained by the charges present in the micelle, as demonstrated by electrophoretic mobility measurements. At pH 7, the residual amino groups are protonated and a charge is observed (ζ= +18 mV at 25 ℃) which prevents the aggregation when the temperature is raised. In a basic solution (pH 13), the hybrids are stable and do not disintegrate, which proves the efficiency of the cross-linking. Moreover, the amino groups are deprotonated

and no charge is detected ($\zeta = +1$mV at 25 ºC) which would avoid destabilization of the system at elevated temperature.

Individual Contributions to Joint Publications

The results presented in this thesis were obtained in collaboration with others and published as indicated below. In the following, the contributions of all the coauthors to the different publications are specified. The asterisk denotes the corresponding author.

Chapter 3

This work is published in MACROMOLECULAR RAPID COMMUNICATIONS (**2006**, 27(11), 821-828) under the title:

"RAFT Polymerization of _N_-Isopropylacrylamide and Acrylic Acid under γ-Irradiation in Aqueous Media"

By Pierre-Eric Millard, Leonie Barner, Martina H. Stenzel, Thomas P. Davis, Christopher Barner-Kowollik[*] and Axel H. E. Müller[*]

I conducted all experiments and wrote the publication.

Exceptions are stated in the following:

L. Barner was involved in operating the γ-source and discussion.

M. Stenzel and T. Davis were involved in scientific discussion.

C. Barner-Kowollik and A. Müller were involved in scientific discussion and correcting the manuscript.

Chapter 4

This work is published in POLYMER (**2010**, 51(19), 4319-4328) under the title:

"Synthesis of Water-Soluble Homo- and Block Copolymers by RAFT Polymerization under γ-Irradiation in Aqueous Media"

By Pierre-Eric Millard, Leonie Barner, Jürgen Reinhardt, Michael R. Buchmeiser, Christopher Barner-Kowollik[*] and Axel H. E. Müller[*]

I conducted all experiments and wrote the publication.

Exceptions are stated in the following:

J. Reinhardt was involved in operating the γ-source and discussion.

L. Barner was involved in operating the γ-source and correcting the manuscript.

M. Buchmeiser was involved in correcting the manuscript.

C. Barner-Kowollik and A. Müller were involved in scientific discussion and correcting the manuscript.

Chapter 5

This work is published in CONTROLLED/LIVING RADICAL POLYMERIZATION: PROGRESS IN ATRP (**2009**, ACS Washington DC, Ed.: Matyjaszewski, K.; 1023, 127-137) under the title:

"Controlling the Fast ATRP of *N*-Isopropylacrylamide in Water"

By Pierre-Eric Millard, Nathalie C. Mougin, Alexander Böker and Axel H. E. Müller[*]

This is a joint project between the chairs PC2 and MC2.

I conducted all experiments and wrote the publication.

Exceptions are stated in the following:

N. Mougin conducted preliminary experiments under my supervision.

A. Böker and A. Müller were involved in scientific discussion and correcting the manuscript.

Chapter 6

This work is in preparation under the title:

"Poly(*N*-Isopropylacrylamide)-*b*-Poly(Acrylic Acid) Shell Cross-Linked Micelles Formation and Application to the Synthesis of Metal-Polymer Hybrids"

By Pierre-Eric Millard,[*] Jérôme J. Crassous, Adriana Mihut, Jiayin Yuan and Axel H. E. Müller[*]

I conducted all experiments, assisted in the analytics and wrote the publication.

Exceptions are stated in the following:

J. Crassous performed some UV-Vis experiments, was involved in scientific discussion and correcting the manuscript.

A. Mihut performed scanning force microscopy experiments.

J. Yuan performed transmission electron microscopy experiments.

A. Müller was involved in scientific discussion and correcting the manuscript.

Chapter 7

This work is in preparation under the title:

"New Water Soluble Smart Polymer-Silica Hybrids Based on Poly(*N*-Isopropylacrylamide)-*b*-Poly(Acrylic Acid)"

By Pierre-Eric Millard,[*] Jérôme J. Crassous, Jiayin Yuan, Adriana Mihut, Andreas Hanisch and Axel H. E. Müller[*]

I conducted all experiments, assisted in the analytics and wrote the publication.

Exceptions are stated in the following:

J. Crassous was involved in scientific discussion and correcting the manuscript.

A. Mihut performed scanning force microscopy experiments.

J. Yuan performed transmission electron microscopy experiments.

A. Hanisch synthesized the silsesquioxane nanoparticles.

A. Müller was involved in scientific discussion and correcting the manuscript.

3. RAFT Polymerization of N-Isopropylacrylamide and Acrylic Acid under γ-Irradiation in Aqueous Media

Pierre-Eric Millard,[1] Leonie Barner,[2] Martina H. Stenzel,[2] Thomas P. Davis,[2] Christopher Barner- Kowollik,[2,3] and Axel H. E. Müller[1]

[1] Makromolekulare Chemie II and Zentrum für Kolloide und Grenzflächen, Universität Bayreuth, 95440 Bayreuth, Germany,

pierre-eric.millard@basf.com; axel.mueller@uni-bayreuth.de

[2] Centre for Advanced Macromolecular Design, School of Chemical Engineering and Industrial Chemistry, The University of New South Wales, Sydney, NSW 2052, Australia

[3] Current address: Preparative Macromolecular Chemistry, Karlsruhe Institute of Technology (KIT), Institut für Technische Chemie und Polymerchemie, Engesser Str. 18, 76128 Karlsruhe, Germany,

christropher.barner-kowollik@kit.de
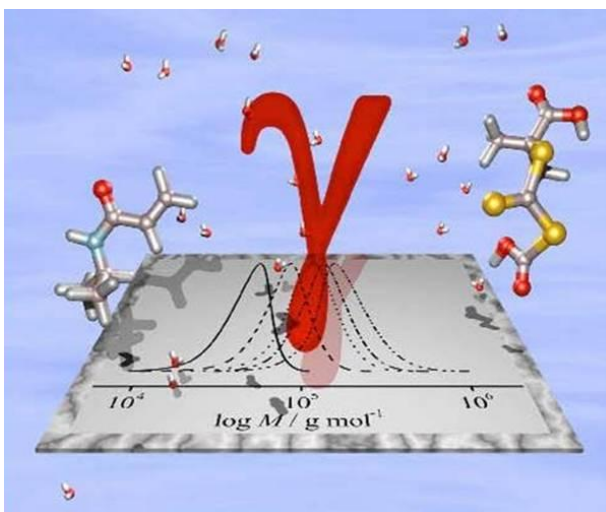
Abstract

The ambient temperature (20°C) reversible addition-fragmentation chain transfer (RAFT) polymerization of *N*-isopropylacrylamide (NIPAAm) and acrylic acid (AA) conducted directly in aqueous media under γ-initiation (at dose rates of 30 Gy · h^{-1}) proceeds in a controlled fashion (typically, $\overline{M}_w / \overline{M}_n < 1.2$) to near quantitative conversions and up to number-average molecular weights of 2.5 × 10^5 g · mol^{-1} for PNIPAAm and 1.1 × 10^5 g · mol^{-1} for PAA via two water-soluble trithiocarbonate chain transfer agents, i.e. S,S-bis(α,α'-dimethyl-α"-acetic acid)trithiocarbonate (TRITT) and 3-benzylsulfanylthio-carbonylsulfanyl propionic acid (BPATT). The generated polymers were successfully chain extended, suggesting that the RAFT agents are stable throughout the polymerization process so that complex and well-defined architectures can be obtained.

Introduction

'Smart' polymers respond with large property changes to a small environmental stimuli.[1] Among them pH, ionic strength, temperature, light, electric and magnetic fields have been the most studied stimuli over the past two decades.[2, 3] These types of polymers find a vast array of biomedical applications in the delivery of therapeutics, bioseparations and biosensors.[3-8] Two of them, i.e. poly(*N*-isopropylacrylamide) (PNIPAAm) and poly(acrylic acid) (PAA), have been intensively investigated for their stimuli-responsive properties. PNIPAAm exhibits a lower critical solution temperature (LCST) in aqueous solution and a sharp reversible phase transition is observed at 32 °C in water.[9] PAA responds to changes in pH and ionic strength by changing coil dimensions and solubility. Combining these two polymers in PNIPAAm-*b*-PAA copolymers generates a material which responds to several stimuli and has micellisation properties that depend on the solvent, temperature, pH, block lengths and salt concentration.[10, 11]

Except via the reversible addition-fragmentation chain transfer (RAFT) technique, the polymerization of AA is difficult to carry out directly in a controlled fashion without recourse to protective group chemistry.[12] To obtain PNIPAAm-*b*-PAA block copolymers, we developed a synthesis via thermal initiation by diazo-compounds under RAFT control in organic solvents.[11] An alternative strategy is to work directly in aqueous solution. Indeed, the rate of polymerization for AA is much higher in water and has the added advantage of occurring in an environmentally friendly solvent.[13] On the other hand, working in water also presents some disadvantages, especially for polymers that exhibit a low LCST because the polymerization has to be carried out below this temperature. Several teams have developed strategies to carry out NIPAAm polymerization at low temperatures. Kizhakkedathu *et al*. employed atom transfer radical polymerization (ATRP) to control the NIPAAm polymerization in water at room temperature.[14] Subsequently, McCormick's group has succeed in obtaining well-defined PNIPAAm via RAFT by employing an azo-initiator with a low decomposition temperature.[15] In this case, the solvent used was dimethylformamide (DMF) to achieve sufficient solubility of the RAFT agent, the initiator and the monomer. Here, for the first

time the RAFT polymerization of NIPAAm and AA in aqueous solution at ambient temperature (20 °C) is described and it is demonstrated that a wide array of block lengths of PAA and PNIPAAm can be obtained with very low polydispersities.

To initiate the polymerizations, γ-radiation is employed instead of an azo-initiator. γ-Radiation has previously been applied to initiate polymerization reactions, to graft polymer chains onto polymeric backbones, to modify polymer blends, to cross-link polymers, and to prepare interpenetrating polymer networks.[16-19] Another application, which is also intensively studied, is the generation of smart polymer hydrogels.[20, 21] However, γ-radiation can initiate most vinylic monomers, such as acrylates, methacrylates and styrenics. Thus, in the past few years, γ-irradiation has been increasingly used in the context of the RAFT process to obtain well-defined (living) polymers.[22-25] The mechanism of the RAFT process has been detailed elsewhere and the complexities of its mechanism will not be reiterated inhere.[26] While the present study employs radiolysis to generate the initiating radicals, there is no difference between γ-initiated and thermally initiated polymerization.[27] The rate of initiation has a small temperature dependence only and can be used at ambient temperature. In comparison with UV-initiation,[28, 29] the γ-irradiation can penetrate the reaction solution more deeply and there is no irreversible decomposition of the dithioester end group as in UV-initiation as described earlier by Quinn et al.[30]

In the current study, a novel strategy to obtain PNIPAAm and PAA via RAFT polymerization in water with γ-initiation is reported. The advantages of this technique to access these polymers with an excellent control and without irreversible termination even at high conversion is detailed, and the livingness of the process is demonstrated by sequential block extension.

Experimental

Materials

All chemicals and solvents where purchased from Sigma-Aldrich, Acros and Fluka at the highest available purity and were used as received unless otherwise noted. NIPAAm was purified by two recrystallizations in a mixture of *n*-hexane and benzene. AA was distilled under vacuum and used immediatly. The syntheses of the RAFT agents S,S-bis(α,α'-dimethyl-α''-acetic acid)trithiocarbonate (TRITT) and 3-benzylsulfanyl thiocarbonylsulfanyl propionic acid (BPATT) have been described elsewhere.[31, 32]

Polymerization Procedure

NIPAAm or AA were dissolved with TRITT or BPATT in pure water or in a mixture of water/acetone, respectively. The monomer concentrations and the monomer/chain transfer agent (CTA) ratios are given in Tables 1-3. After complete dissolution the stock solution was divided and transferred into glass sample vials, containing ca. 3 to 4 mL solution. The vials were capped with rubber septa and deoxygenated by purging with nitrogen gas for 15 min each. The samples were placed in an insulated room with a ^{60}Co source with a dose rate of 30 Gy · h^{-1} at ambient temperature (typically close to 20 °C). Samples were taken after pre-selected time intervals to follow the monomer-to-polymer conversion. All the samples were freeze-dried after their respective polymerization time was reached. PNIPAAm was purified by precipitation from a dioxane solution into a 20-fold excess of diethyl ether before further analysis. PAA was analyzed directly after freeze-drying. The conversion of each sample was determined directly from the solution by ^{1}H NMR (in D_2O) from the relative integration of peaks associated with the monomer in relation to those associated with the polymer. For NIPAAm, the monomer peak chosen as reference was its vinylic peak at δ = 5.72-5.8 ppm (dd, CH(H)=), which was compared to the CH peak of the isopropyl group at 4.1-3.8 ppm (m, $CH(CH_3)_2$) of the polymer and monomer. In the case of AA, the monomer vinyl peak at 5.95-6.03 ppm (dd, CH) was employed, while the polymer peak used was the methylene resonance with a chemical shift of 1.4-2.1 ppm (m, CH_2).

Characterization

^{1}H-NMR spectra were recorded on a Bruker spectrometer (300 MHz) in D_2O (residual peak $\delta = 4.79$ ppm). Gel permeation chromatography (GPC) analysis of PNIPAAm was performed in *N,N*-dimethylacetamide (DMAc) (0.03% w/v LiBr, 0.05% BHT stabilizer) at 50 °C (flow rate: 0.85 mL · min^{-1}) using a Shimadzu modular system comprising a DGU-12A solvent degasser, an LC-10AT pump, a CTO-10A column oven, and an RID-10A refractive index detector. The system was equipped with a Polymer Laboratories 5.0 μm bead-size guard column (50×7.8 mm[2]) followed by four 300×7.8 mm[2] linear PL columns (10^5, 10^4, 10^3, and 500 Å). Calibration was performed with low polydispersity polystyrene standards ranging from 500 to 10^6 g · mol^{-1}. PAA was analyzed by GPC in water (0.1 mol · L^{-1} NaN_3, 0.01 mol · L^{-1} NaH_2PO_4, pH = 6.3) at 35 °C (flow rate: 1 mL · min^{-1}) using a Gynkotek model 300 pump, an ERC column oven, and a Bischoff 8110 refractive index detector. The system was equipped with a Polymer Laboratories (PL) PLaquagel-OH 8 μm bead-size guard column (50×7.5 mm[2]) followed by two 300×7.5 mm[2] columns, a PLaquagel-OH mix 8 μm and a PLaquagel-OH 30, 8 μm. Calibration was performed with low polydispersity poly(ethylene oxide) standards ranging from 2 000 to 85 000 g · mol^{-1}.

Results and Discussion

Polymerization of *N*-Isopropylacrylamide

N-Isopropylacrylamide was polymerized in the presence of two trithiocarbonate CTAs, i.e. BPATT and TRITT (see Scheme 3-1) at various ratios of monomer to CTA. The results of selected polymerizations using TRITT as CTA are summarized in the Table 3-1 and Figure 3-1. TRITT, a symmetrical trithiocarbonate, has already been used as a CTA for the RAFT polymerization of several monomers, such as acrylates, methacrylates, styrenics, and acrylamides.[32-36] Inspection of the data given in Figure 3-1A and B clearly indicates that TRITT allows for excellent control of NIPAAm polymerization. With a NIPAAm/TRITT ratio of 800, the first-order time-conversion plot (Figure 3-1A) displays a small induction period of close to 20 min Such induction periods are often observed in the RAFT process. However for a trithiocarbonate such an induction period is not generally anticipated, but may occur under certain polymerization conditions.[37] After the induction period, the first-order plot is linear up to 90% conversion, which indicates that the main RAFT equilibrium is rapidly established and an apparent first-order dependence on monomer concentration is operative during the major part of the polymerization. Figure 3-1B depicts the molecular weight and the polydispersity index evolutions with the conversion. It is obvious that the molecular weight increases linearly with conversion which demonstrates the controlled fashion of the process. The difference between the theoretical and the experimental molecular weight can be assigned to the calibration of the SEC on the basis of polystyrene equivalents. The resulting polydispersity indices are low (PDI < 1.2) except at the early stage of the polymerization. Even at high conversions (> 95%) and very high molecular weights ($\overline{M}_{n,exp} > 1.4 \times 10^5$ g · mol^{-1}), the PDI is low (PDI = 1.16) and no bimodalities are observed.

BPATT   **TRITT**
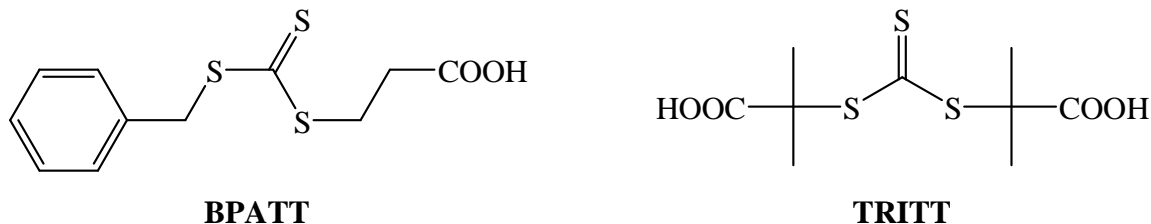
Scheme 3-1. Trithiocarbonate RAFT agents employed in the present study.

Table 3-1. Influence of the monomer/CTA ratio in the RAFT polymerization of NIPAAm in water during γ-initiation at room temperature with TRITT as RAFT agent. $[M]_0 = 1.5$ mol $\cdot$ L^{-1}.

$\dfrac{[M]_0}{[CTA]_0}$	x_p [a] %	Time min	$\overline{M}_{n,th}$ [b] kg/mol	$\overline{M}_{n,exp}$ [c] kg/mol	PDI[c]
200	97	1 440	22.2	38	1.10
400	96	265	43.7	62.5	1.14
600	96	265	65.5	88.5	1.17
800	96	240	87.2	103	1.16
1 200	97	240	132	143	1.20

[a] Monomer conversion is calculated by ^{1}H NMR spectroscopy in D$_2$O. [b] The theoretical number-average molecular weight is calculated according to the equation, $\overline{M}_{n,th} = M_M \times \text{conv} \times [M]_0/[CTA]_0 + M_{CTA}$. [c] The experimental number-average molecular weight, $\overline{M}_{n,exp}$, and the polydispersity index, PDI, were measured by SEC using polystyrene standards in DMAc (0.03% w/v LiBr, 0.05% BHT).

Table 3-1 and Figure 3-1C indicate that an increase of the monomer/CTA ratio leads (at a comparable conversion) to an increase of the molecular weight. The SEC traces display unimodal and narrow peaks. Even at a high ratio of monomer to CTA, the polydispersity index remains below 1.2 at almost complete conversion. It will be demonstrated below that the TRITT-generated PNIPAAm macroRAFT agents can be readily chain extended, which indicates that most of the chains have a trithiocarbonate central group. All these criteria indicate the controlled fashion of the PNIPAAm RAFT polymerization under γ-radiation.
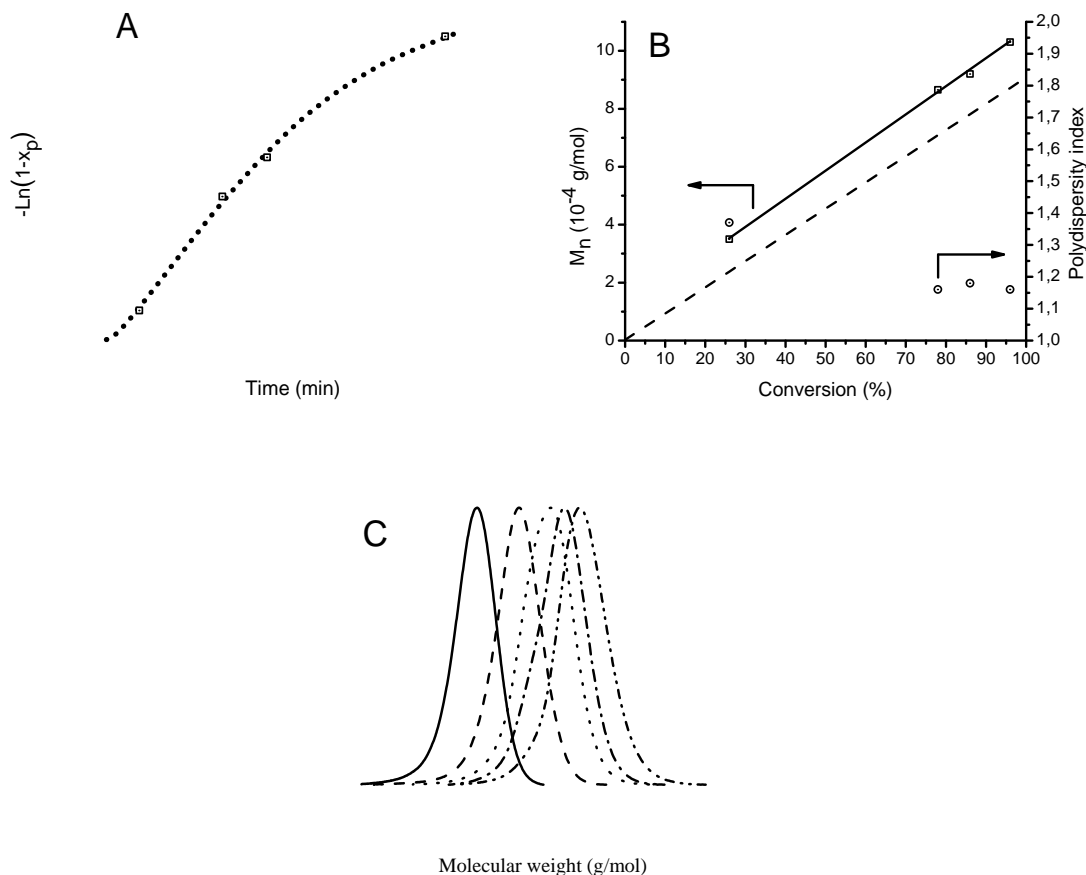
Figure 3-1. RAFT polymerization of NIPAAm under γ-radiation in water (1.5 mol · L^{-1}) using TRITT at ambient temperature. (A) First-order time-conversion plot for $[M]_0/[CTA]_0 = 800$. (• • •) Extrapolation. (B) Molecular weight and polydispersity index vs conversion for $[M]_0/[CTA]_0 = 800$. (– –) Theoretical number average molecular weight evolution. (C) Dependence of the molecular weight distribution on the monomer/CTA ratio. $[M]_0/[CTA]_0 = $ (——) 200, (– –) 400, (• • •) 600, (– • –) 800 and (– • • –) 1200.

The unsymmetrical CTA BPATT is also employed in the γ-radiation initiated polymerization of water-soluble monomers. BPATT has already been used for the polymerization of different styrenics, acrylates and acrylamides monomers.[38-40] An added advantage of this CTA is the ability to easily link it via the carboxylic group to generate different architectures, such as hyperbranched or star polymers.[31, 41, 42] The main problem of BPATT is its poor solubility in pure water due to the aromatic ring. The

carboxylic group at the neutral pH of the polymerization is protonated and is not able to make the CTA fully soluble even for a high monomer/CTA ratio. To dissolve it fully, the addition of a cosolvent is required. Here, the addition of 15 vol.-% acetone is sufficient for any monomer/CTA ratio to obtain a homogenous solution.

The principal experimental data for the BPATT-mediated polymerizations are collected in the Supporting Information section (Table 3-S1 and Figure 3-S1). As in the case of TRITT, even for a high monomer/CTA ratio of 1 000 the control of the PNIPAAm polymerization is very good. The PDI is low and close to 1.1 in all conducted polymerizations, even at high conversions. The molecular weight evolution with conversion depicted in Figure 3-S1B exhibits a linear increase. A comparison of the activity of TRITT and BPATT is not easy because TRITT is a symmetrical CTA while BPATT is unsymmetrical. Via the use of TRITT an ABA triblock copolymer can be synthesized in two steps, whereas BPATT allows for the synthesis of AB diblock copolymers in two subsequent reaction steps. However, an additionally important parameter is the position of the active trithiocarbonate group. Whereas a macroRAFT agent based on BPATT has the trithiocarbonate group at the end of the block, one based on TRITT displays it in the middle of the block. As a consequence, the steric hindrance is different and depends on the chain length. A symmetrical CTA may lead to a low accessibility of the thiocarbonyl group for the propagating radical at high molecular weights. Thus, depending on the polymerization conditions, an increase of the polydispersity or even a complete loss of control has been observed.[37] According to the kinetic data, the reactivity of these two RAFT agents seems different, evident as a discrepancy in the corresponding induction times. Even when the concentration of CTA is not equal, the inhibition period is smaller than 20 min in the TRITT system with a higher concentration of RAFT agent, compared to that of around 90 min observed in the BPATT mediated polymerizations (see Figure 3-S1A). Moreover, the apparent rate coefficient associated with the rate of polymerization, k_p^{app} (estimated from the slope of the linear part of the first-order time-conversion plot) exhibits a slight difference. In the case of TRITT (see Figure 3-1A) the polymerization seems to be marginally faster compared to the corresponding BPATT system. A k_p^{app} of 3.6×10^{-4} s^{-1} is determined for TRITT-mediated polymerizations, which is higher than the 2.7×10^{-4} s^{-1} deduced form

the BPATT system. However, the control is better with BPATT and a lower PDI can be reach for the same concentration of CTA in the polymerization solution.

To obtain well-defined blocks of high molecular weight by increasing the monomer/CTA ratio is a considerable challenge. BPATT is a good candidate for the RAFT polymerization of NIPAAm under γ-radiation to obtain a large block with good control. The associated experimental data are collected in Table 3-S1 and Figure 3-S1C of the Supporting Information. Two monomer/CTA ratios of 1 500 and 2 000 were investigated and compared to the corresponding polymerizations employing a monomer/CTA ratio of 1 000. The SEC traces and the polydispersity indices indicate good control of the polymerization even at a very low concentration of RAFT agent and high conversion. The molecular weight distributions are unimodal and no side reactions – as potentially evident in tailing or multimodalities – seem to occur.

Table 3-2. Influence of the monomer/CTA ratio for the RAFT polymerization of AA in water during γ-initiation at room temperature with TRITT as RAFT agent. $[M]_0 = 2.5$ mol $\cdot$ L^{-1}.

CTA	$\dfrac{[M]_0}{[CTA]_0}$	$\dfrac{\text{Time}}{\text{min}}$	$\dfrac{x_p{}^{(b)}}{\%}$	$\dfrac{\overline{M}_{n,th}{}^{(c)}}{\text{kg/mol}}$	$\dfrac{\overline{M}_{n,exp}{}^{(d)}}{\text{kg/mol}}$	PDI$^{(d)}$
TRITT$^{(a)}$	100	1 380	93	7	24	1.07
TRITT	200	1 440	95	14	34	1.10
TRITT	400	1 440	98	28.5	59	1.12
TRITT	800	1 200	98	56.8	87	1.15
TRITT	1 200	545	91	79	107	1.11

[a] Polymerization in a mixture of water/acetone (v/v) 85/15. [b] Monomer conversion is calculated by ^{1}H NMR spectroscopy in D$_2$O. [c] The theoretical number-average molecular weight is calculated according to the equation, $\overline{M}_{n,th} = M_M \times \text{conv} \times [M]_0 / [CTA]_0 + M_{CTA}$. [d] The experimental number-average molecular weight, $\overline{M}_{n,exp}$, and the polydispersity index, PDI, were measured by SEC using poly(ethylene oxide) standards in water (0.1 mol $\cdot$ L^{-1} NaN$_3$, 0.01 mol $\cdot$ L^{-1} NaH$_2$PO$_4$).
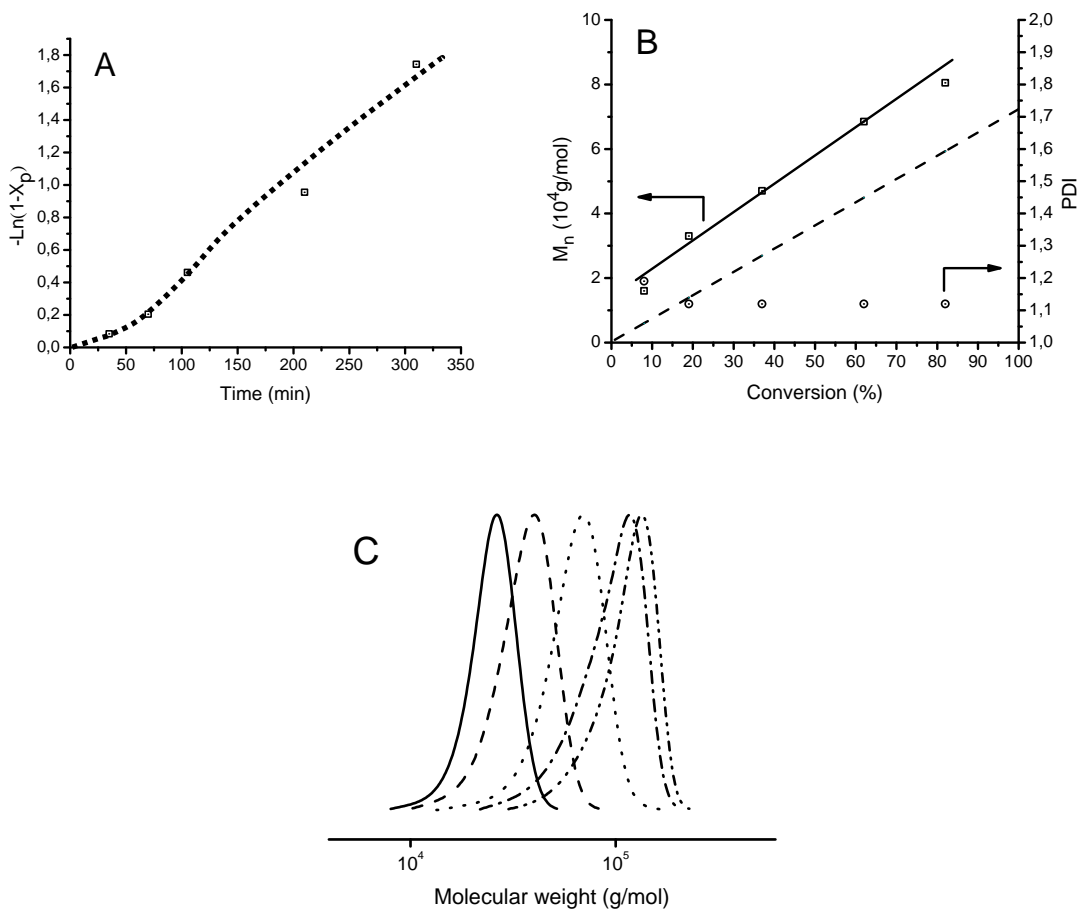
Figure 3-2. RAFT polymerization of AA under γ-radiation in a mixture water/acetone 85/15 (2.5 mol · L^{-1}) using BPATT at ambient temperature. (A) First-order time-conversion plot for $[M]_0/[CTA]_0 = 1\ 000$. (• • •) Extrapolation. (B) Molecular weight and polydispersity index versus conversion for $[M]_0/[CTA]_0 = 1\ 000$. (– –) Theoretical number average molecular weight evolution. (C) Dependence of the molecular weight distribution on the ratio monomer/CTA using TRITT as CTA. $[M]_0 = 2.5$ mol · L^{-1}, $[M]_0/[CTA]_0 = $ (——) 100, (– –)200, (• • •) 400, (– • –) 800 and (– • • –) 1 200.

Polymerization of Acrylic Acid

Similar to NIPAAm, the RAFT polymerization of acrylic acid under γ-radiation with TRITT and BPATT is investigated. The experimental conditions and the results are detailed in Table 3-2 and Figure 3-2. The PAA synthesized using BPATT as CTA with

an initial monomer/CTA ratio of 1 000 exhibits good control. Indeed, except in the early stage of the polymerization, the polydispersity is low and stays close to 1.1 even up to high conversions. Moreover, the molecular weight increases linearly with conversion (see Figure 3-2B), which demonstrates the controlled fashion of the AA RAFT polymerization. The differences between experimental and expected molecular weights may be a result of the poly(ethylene oxide) calibration used. The first-order time-conversion plot (see Figure 3-2A) exhibits an absence or only a very short induction time associated with the first-order monomer concentration dependence throughout the polymerization. As in the NIPAAm RAFT polymerizations, the molecular weight distributions are monomodal even at very high conversion, which indicates the absence of undesired side reactions.

The influence of the monomer/CTA ratio is also studied. TRITT is used at different concentrations at a constant concentration of AA. The experimental data are collated in Table 3-2 and plotted in Figure 3-2C and indicate the generation of well-defined PAA even at a high monomer/CTA ratio. The PDI increases with decreasing amounts of TRITT, but stays lower than 1.15 and the molecular weight distributions (see Figure 3-2C) are unimodal, symmetrical and narrow.

Because of the low dose rate ($30 \, Gy \cdot h^{-1}$) of the source and according to the low polydispersity of the two different monomers polymerization, it is assumed that in presence of these two CTAs no or an insignificant amount only of chain scission and cross-linking can occur. To prove this assumption an experiment with an aqueous solution of NIPAAm ($1.5 \, mol \cdot L^{-1}$) and without RAFT agent was carried out and after less than 2 h a gel was obtained. Moreover, in the system here, the initiating radical can be generated from different molecules, like water and monomer. It is well known that water under γ-radiation produces various radicals like OH and H.[43, 44] Detailed studies of which radicals initiate the polymerization and in which proportion is currently underway.

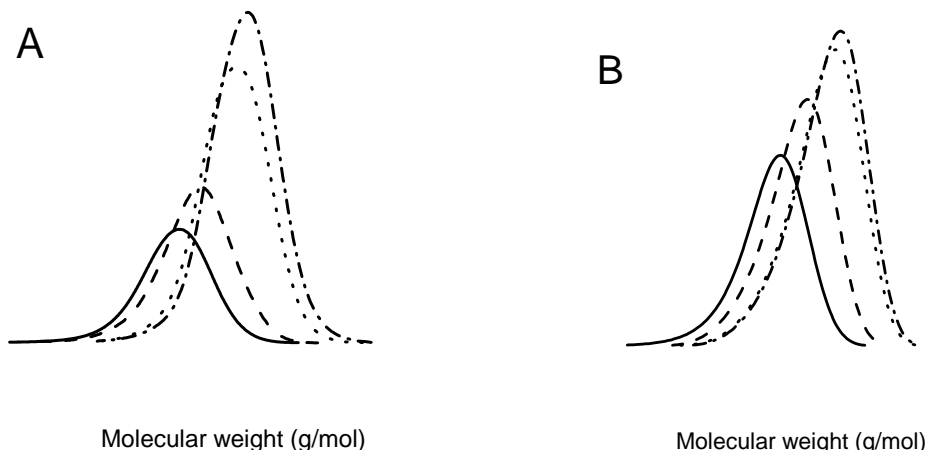**Table 3-3**. Block extension of PNIPAAm and PAA by γ-initiation at room temperature in water.

	Monomer	$\dfrac{[M]_0}{[CTA]_0}$	$\dfrac{Time}{min}$	$\dfrac{x_p\,^{(c)}}{\%}$	$\dfrac{\overline{M}_{n,th}\,^{(d)}}{kg/mol}$	$\dfrac{\overline{M}_{n,exp}\,^{(e)}}{kg/mol}$	PDI[e]
Precursor[a]	NIPAAm	400	95	83	37.9	50	1.12
Extension	NIPAAm	368[a]	35	24	47.8	58.5	1.13
Extension	NIPAAm	368[a]	95	76	69.5	84	1.11
Extension	NIPAAm	368[a]	300	94	77	91	1.12
Precursor[b]	AA	400	300	72	21	42.5	1.08
Extension	AA	300[b]	35	33	28.1	52.5	1.08
Extension	AA	300[b]	300	70	36.1	65	1.09
Extension	AA	300[b]	390	80	38.3	67.5	1.09

[a] PNIPAAm macroCTA synthesized by RAFT under γ-radiation with TRITT as CTA. $[M]_0 = 1.5$ mol $\cdot$ L^{-1}. [b] PAA macroCTA synthesized by RAFT under γ-radiation with TRITT as CTA. $[M]_0 = 2.5$ mol $\cdot$ L^{-1} [c] Monomer conversion is calculated by ^{1}H NMR spectroscopy in D$_2$O. [d] The theoretical number-average molecular weight is evaluated according to the formula, $\overline{M}_{n,th} = M_M \times conv \times [M]_0/[CTA]_0 + M_{CTA}$. [e] The experimental number-average molecular weight, $\overline{M}_{n,exp}$, and the polydispersity index, PDI, were measured by SEC using poly(ethylene oxide) standards in water (0.1 mol $\cdot$ L^{-1} NaN$_3$, 0.01 mol $\cdot$ L^{-1} NaH$_2$PO$_4$)

Chain Extension Experiments

To further demonstrate the retention of the trithiocarbonate functionality and the controlled nature of the above discussed polymerizations, two macroCTAs of PNIPAAm and PAA are synthesized. In both cases TRITT is used as RAFT agent at a ratio of 1/400 compared to the monomer. The experimental data and the principal results are detailed in Table 3-3 and Figure 3-3. After purification, the resulting macroCTAs are chain extended with NIPAAm and AA, respectively. The chain extension of the PNIPAAm and PAA macroCTAs is nearly quantitative. The GPC chromatograms during the block extension show a distinct increase of the molecular weight. Moreover, even for a high conversion of the first block (83% for PNIPAAm and 72% for PAA) throughout chain extension, there is no trace of a shoulder or tailing of the molecular weight distributions. Such evidence

combined with a low PDI suggests that the large majority of the macroCTAs retain the trithiocarbonate functionality and are available for subsequent chain extension.

Molecular weight (g/mol)   Molecular weight (g/mol)

Figure 3-3. Chain extension of PNIPAAm and PAA macroCTA synthesized with TRITT as CTA. (A) Molecular weight distributions obtained in the block extension of PNIPAAm under γ-radiation. $[M]_0 = 0.4$ mol $\cdot$ L^{-1}, $[M]_0/[macroCTA]_0 = 368$. (——) precursor, (– –) 24%, (• • •) 76% and (– • –) 94% of monomer conversion. (B) Block extension of PAA under γ-radiation. $[M]_0 = 0.6$ mol $\cdot$ L^{-1}, $[M]_0/[macroCTA]_0 = 300$. (——) precursor, (– –) 33%, (• • •) 70% and (– • –) 80% of conversion.

Conclusions

It is demonstrated for the first time that RAFT polymerizations of NIPAAm and AA can be carried out directly in water at room temperature under γ-radiation. Under these conditions, the controlled/living characteristics are proven for two CTAs, i.e. TRITT and BPATT for a large range of monomer/RAFT agent ratios. Moreover, even at monomer conversion exceeding 90%, polymerization control is maintained. The living character of the generated macroRAFT agents is confirmed by subsequent chain extension. During chain extension, no side reactions are observed and the polydispersity remains low throughout the polymerization. Given the environmental benefits associated with aqueous

87

polymerizations at room temperature, and the possibility to tailor a large variety of block lengths, it is believed that the method reported in the present study represents a significant advance in the ability to prepare complex architectures for smart polymers, including other water-soluble monomers to be included in the present investigation.

Acknowledgements

References

[1]   A. S. Hoffman, P. S. Stayton, *Macromolecular Symposia* **2004**, *207*, 139.
[2]   T. Shimoboji, E. Larenas, T. Fowler, A. S. Hoffman, P. S. Stayton, *Bioconjugate Chemistry* **2003**, *14*, 517.
[3]   K. L. Christman, H. D. Maynard, *Langmuir* **2005**, *21*, 8389.
[4]   R. Lupitskyy, Y. Roiter, C. Tsitsilianis, S. Minko, *Langmuir* **2005**, *21*, 8591.
[5]   S. Chen, J. Singh, *International journal of pharmaceutics* **2005**, *295*, 183.
[6]   H. Rauter, V. Matyushin, Y. Alguel, F. Pittner, T. Schalkhammer, *Macromolecular Symposia* **2004**, *217*, 109.
[7]   S. Kulkarni, C. Schilli, A. H. E. Müller, A. S. Hoffman, P. S. Stayton, *Bioconjugate Chemistry* **2004**, *15*, 747.
[8]   I. Yu. Galaev, B. Mattiasson, Editors, *Smart Polymers for Bioseparation and Bioprocessing*, Taylor & Francis, London, New York, **2002**.
[9]   H. Yang, R. Cheng, Z. Wang, *Polymer* **2003**, *44*, 7175.
[10]   X. André, M. Zhang, A. H. E. Müller, *Macromolecular Rapid Communications* **2005**, *26*, 558.
[11]   C. M. Schilli, M. Zhang, E. Rizzardo, S. H. Thang, Y. K. Chong, K. Edwards, G. Karlsson, A. H. E. Müller, *Macromolecules* **2004**, *37*, 7861.
[12]   F. A. Plamper, H. Becker, M. Lanzendörfer, M. Patel, A. Wittemann, M. Ballauff, A. H. E. Müller, *Macromolecular Chemistry and Physics* **2005**, *206*, 1813.
[13]   F.-D. Kuchta, A. M. Van Herk, A. L. German, *Macromolecules* **2000**, *33*, 3641.
[14]   J. N. Kizhakkedathu, R. Norris-Jones, D. E. Brooks, *Macromolecules* **2004**, *37*, 734.
[15]   A. J. Convertine, N. Ayres, C. W. Scales, A. B. Lowe, C. L. McCormick, *Biomacromolecules* **2004**, *5*, 1177.
[16]   T. Caykara, M. S. Eroglu, O. Guven, *Journal of Applied Polymer Science* **1999**, *73*, 141.
[17]   E. M. El-Nesr, *Polymers for Advanced Technologies* **2002**, *13*, 626.
[18]   Z. Liu, M. Yi, M. Zhai, H. Ha, Z. Luo, X. Xiang, *Journal of Applied Polymer Science* **2004**, *92*, 2995.
[19]   Z. S. Nurkeeva, G. A. Mun, V. V. Khutoryanskiy, A. B. Dzhusupbekova, *Radiation Physics and Chemistry* **2004**, *69*, 205.
[20]   V. Kumar, C. V. Chaudhari, Y. K. Bhardwaj, N. K. Goel, S. Sabharwal, *European Polymer Journal* **2006**, *42*, 235.
[21]   Y. Zhuang, G. Wang, H. Yang, Z. Zhu, J. Fu, W. Song, H. Zhao, *Polymer International* **2005**, *54*, 617.
[22]   D. Hua, K. Cheng, R. Bai, W. Lu, C. Pan, *Polymer International* **2004**, *53*, 821.
[23]   L. Barner, J. F. Quinn, C. Barner-Kowollik, P. Vana, T. P. Davis, *European Polymer Journal* **2003**, *39*, 449.
[24]   J. F. Quinn, L. Barner, E. Rizzardo, T. P. Davis, *Journal of Polymer Science, Part A: Polymer Chemistry* **2001**, *40*, 19.
[25]   C.-Y. Hong, Y.-Z. You, R.-K. Bai, C.-Y. Pan, G. Borjihan, *Journal of Polymer Science, Part A: Polymer Chemistry* **2001**, *39*, 3934.

[26] P. Vana, T. P. Davis, C. Barner-Kowollik, *Macromolecular Theory and Simulations* **2002**, *11*, 823.

[27] J. F. Quinn, L. Barner, T. P. Davis, S. H. Thang, E. Rizzardo, *Macromolecular Rapid Communications* **2002**, *23*, 717.

[28] L. Lu, N. Yang, Y. Cai, *Chemical Communications (Cambridge, United Kingdom)* **2005**, 5287.

[29] K. Ishizu, R. A. Khan, T. Furukawa, M. Furo, *Journal of Applied Polymer Science* **2004**, *91*, 3233.

[30] J. F. Quinn, L. Barner, C. Barner-Kowollik, E. Rizzardo, T. P. Davis, *Macromolecules* **2002**, *35*, 7620.

[31] M. H. Stenzel, T. P. Davis, *Journal of Polymer Science, Part A: Polymer Chemistry* **2002**, *40*, 4498.

[32] J. T. Lai, D. Filla, R. Shea, *Macromolecules* **2002**, *35*, 6754.

[33] A. J. Convertine, B. S. Lokitz, A. B. Lowe, C. W. Scales, L. J. Myrick, C. L. McCormick, *Macromolecular Rapid Communications* **2005**, *26*, 791.

[34] V. Lima, X. Jiang, J. Brokken-Zijp, P. J. Schoenmakers, B. Klumperman, R. Van Der Linde, *Journal of Polymer Science, Part A: Polymer Chemistry* **2005**, *43*, 959.

[35] D. B. Thomas, A. J. Convertine, L. J. Myrick, C. W. Scales, A. E. Smith, A. B. Lowe, Y. A. Vasilieva, N. Ayres, C. L. McCormick, *Macromolecules* **2004**, *37*, 8941.

[36] Z. Szablan, A. A. Toy, T. P. Davis, X. Hao, M. H. Stenzel, C. Barner-Kowollik, *Journal of Polymer Science, Part A: Polymer Chemistry* **2004**, *42*, 2432.

[37] R. Wang, C. L. McCormick, A. B. Lowe, *Macromolecules* **2005**, *38*, 9518.

[38] M. Hernandez-Guerrero, T. P. Davis, C. Barner-Kowollik, M. H. Stenzel, *European Polymer Journal* **2005**, *41*, 2264.

[39] M. H. Stenzel, C. Barner-Kowollik, T. P. Davis, H. M. Dalton, *Macromolecular Bioscience* **2004**, *4*, 445.

[40] T. S. C. Pai, C. Barner-Kowollik, T. P. Davis, M. H. Stenzel, *Polymer* **2004**, *45*, 4383.

[41] X. Hao, C. Nilsson, M. Jesberger, M. H. Stenzel, E. Malmström, T. P. Davis, E. Östmark, C. Barner-Kowollik, *Journal of Polymer Science, Part A: Polymer Chemistry* **2004**, *42*, 5877.

[42] M. Jesberger, L. Barner, M. H. Stenzel, E. Malmström, T. P. Davis, C. Barner-kowollik, *Journal of Polymer Science, Part A: Polymer Chemistry* **2003**, *41*, 3847.

[43] J. W. T. Spinks, R. J. Woods, *An Introduction to Radiation Chemistry. 3rd Ed*, John Wiley, New York, **1990**.

[44] A. Chapiro, Editor, *Radiation Chemistry of Polymeric Systems*, Interscience, New York, **1962**.

Supporting Information

Table 3-S1. RAFT polymerization of NIPAAm in water by γ-initiation at room temperature with BPATT as RAFT agent. $[M]_0 = 1.5$ mol · L^{-1}.

$\dfrac{[M]_0}{[CTA]_0}$	$\dfrac{\text{Time}}{\text{min}}$	$\dfrac{x_p^{(a)}}{\%}$	$\dfrac{\overline{M}_{n,th}^{(b)}}{\text{kg/mol}}$	$\dfrac{\overline{M}_{n,exp}^{(c)}}{\text{kg/mol}}$	$PDI^{(c)}$
1 000[d]	105	23	26.3	49	1.13
1 000[d]	150	63	71.6	84	1.09
1 000[d]	210	79	89.7	96.5	1.09
1 000[d, e]	310	88	100	105	1.12
1500[e]	185	92	157	191	1.21
2000[e]	265	93	210.7	249	1.28

[a] Monomer conversion is calculated by ^{1}H NMR spectroscopy in D_2O. [b] The theoretical number-average molecular weight is calculated according to the equation, $\overline{M}_{n,th} = M_M \times \text{conv} \times [M]_0/[CTA]_0 + M_{CTA}$. [c] The experimental number-average molecular weight, $\overline{M}_{n,exp}$, and the polydispersity index, PDI, were measured by SEC using polystyrene standards in DMAc (0.03% w/v LiBr, 0.05% BHT). [d] Kinetic study with samples collected at pre-selected reaction times. [e] Final samples of experiments with varying ratios monomer/CTA.
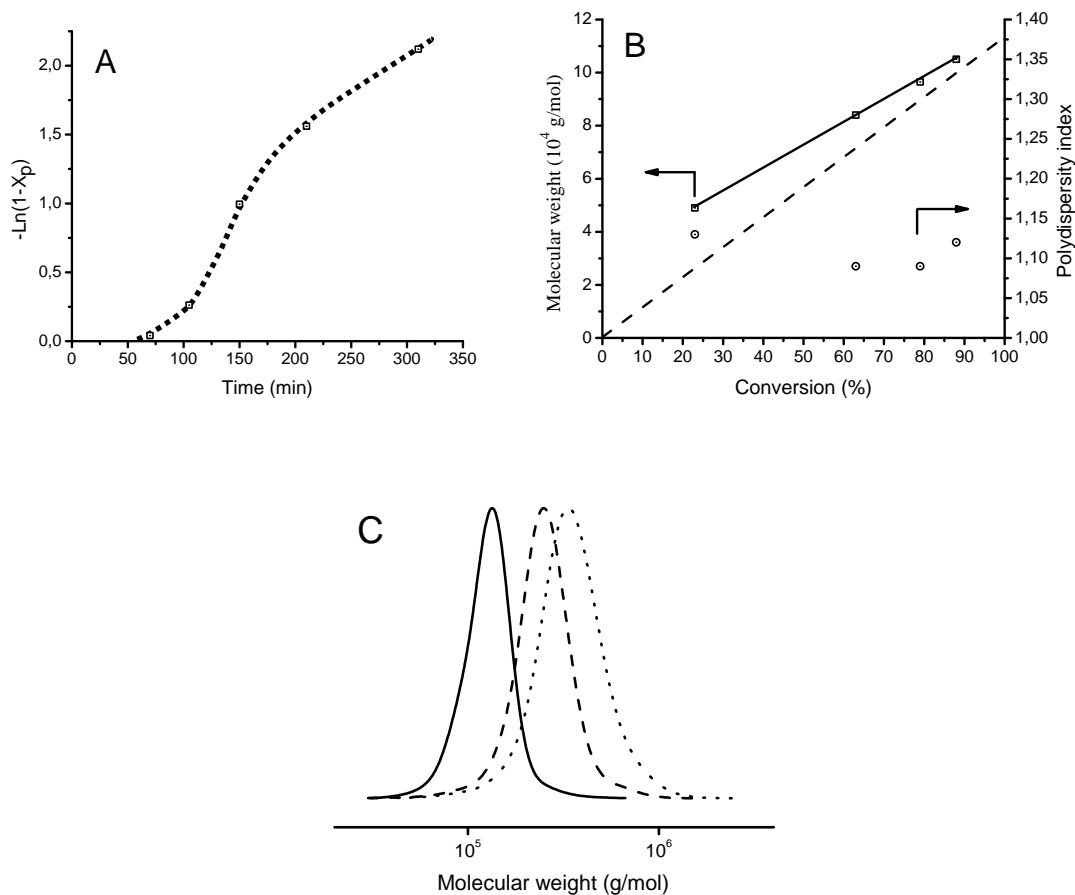
Figure 3-S1. RAFT polymerization of NIPAAm under γ-radiation in water (1.5 mol · L$^-$^{1}) using BPATT at ambient temperature. (A) First-order time-conversion plot for $[M]_0/[CTA]_0 = 1\ 000$. (• • •) Extrapolation. (B) Molecular weight and polydispersity index versus conversion for $[M]_0/[CTA]_0 = 1\ 000$. (– –) Theoretical number average molecular weight evolution. (C) Dependence of the molecular weight distribution on the monomer/CTA ratio. $[M]_0/[CTA]_0 =$ (——) 1 000, (– –) 1 500 and (• • •) 2 000.

4. Synthesis of Water-Soluble Homo- and Block Copolymers by RAFT Polymerization under γ-Irradiation in Aqueous Media

Pierre-Eric Millard,[1] Leonie Barner,[2,4] Jürgen Reinhardt,[3] Michael R. Buchmeiser,[3,5] Christopher Barner-Kowollik[2,6] and Axel H. E. Müller[1]

[1] Makromolekulare Chemie II and Zentrum für Kolloide und Grenzflächen, Universität Bayreuth, 95440 Bayreuth, Germany,

pierre-eric.millard@basf.com; axel.mueller@uni-bayreuth.de

[2] Centre for Advanced Macromolecular Design, School of Chemical Engineering and Industrial Chemistry, The University of New South Wales, Sydney, NSW 2052, Australia

[3] Leibniz-Institut für Oberflächenmodifizierung e.V., Permoserstraße 15, D-04318 Leipzig, Germany

[4] Fraunhofer Institute for Chemical Technology, Joseph-von-Fraunhofer Str. 7, 76327 Pfinztal (Berghausen), Germany,

leonie.barner@ict.fraunhofer.de

[5] Current address: Institut für Polymerchemie, Universität Stuttgart, Pfaffenwaldring 55, 70550 Stuttgart, Germany

[6] Current address: Preparative Macromolecular Chemistry, Karlsruhe Institute of Technology (KIT), Institut für Technische Chemie und Polymerchemie, Engesser Str. 18, 76128 Karlsruhe, Germany,

christopher.barner-kowollik@kit.edu
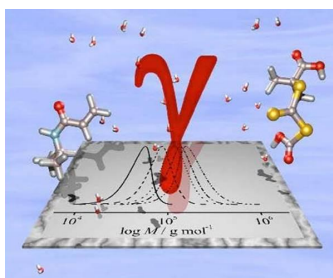
Abstract

The ambient temperature (20 °C) reversible addition-fragmentation chain transfer (RAFT) polymerization of several water-soluble monomers conducted directly in aqueous media under γ-initiation (at dose rates of 30 Gy·h^{-1}) proceeds in a controlled fashion. Using functional trithiocarbonates, i.e., *S,S*-bis(α,α'-dimethyl-α''-acetic acid)trithiocarbonate (TRITT), 3-benzylsulfanyl thiocarbonylsulfanyl propionic acid (BPATT), and dithioester, i.e., 4-cyanopentanoic acid dithiobenzoate (CPADB), as chain transfer agents, fully water-soluble polymers of monomers such as *N,N*-dimethylacrylamide, 2-hydroxyethyl acrylate, acrylamide or oligo(ethylene glycol) methacrylate and stimuli-responsive polymers of monomers such as acrylic acid, *N*-isopropylacrylamide, 2-(dimethylamino)ethyl methacrylate or 2-acrylamido-2-methylpropane sulfonic acid can be obtained over a wide range of degrees of polymerization up to 10,000 with low polydispersity (typically $\overline{M}_w / \overline{M}_n < 1.2$) to near quantitative conversions. Well-defined block copolymers between these monomers, based on several asymmetric macro-RAFT agents, can be obtained, suggesting that the RAFT agents are stable throughout the polymerization process so that complex and well-defined architectures can be obtained.

Introduction

Water soluble polymers are a highly interesting class of materials which have found numerous applications especially in biotechnology [1]. Among them, over the past two decades, delivery of therapeutics [2, 3], bioseparations [4, 5], or biosensors [6] have been intensively studied. For many purposes, these polymers have to be synthesized via a controlled fashion to obtain targeted molecular weights, narrow molecular weight distributions and well-defined complex architectures. Several techniques can be used to achieve this goal. Anionic polymerization generally gives very good results in terms of molecular weight and polydispersity control [7, 8]. However, it is also an experimentally demanding technique, due to the necessity to conduct the reaction with highly pure monomers and solvents. In addition, anionic polymerization cannot be performed directly in water and protic monomers have to be protected first.

Therefore, since the mid-nineties, controlled/living free radical polymerization techniques such as atom transfer radical polymerization (ATRP) [9-13], nitroxide-mediated polymerization (NMP) [14, 15] and reversible addition fragmentation chain transfer (RAFT) polymerization [16-19] have received considerable attention due to their relative ease of operation and versatility in synthesizing complex macromolecules with well-defined architectures, controlled molecular weights and low polydispersity. Among these techniques, RAFT polymerization shows particular promise because it possesses significant advantages such as its applicability to a wide variety of monomers (including functional styrenic, acrylate and methacrylate monomers), the performance under a wide array of reaction conditions (e.g. wide range of solvents, including water, ambient temperature, UV- or γ-initiation) and processes (e.g. bulk, solution or emulsion). In addition, it allows for the facile preparation of polymers with complex architectures including block, graft and star copolymers [20].

Recently, significant progress has been made in living/controlled free radical polymerization at ambient temperature in aqueous solution, especially via RAFT polymerization. This strategy combines the advantages of working in an environmentally friendly solvent without the necessity to heat the polymerization system. It is also

essential in bioconjugate chemistry to work in aqueous systems at low temperature as proteins or viruses require generally mild temperatures ($T \leq 40\ °C$) and the absence of organic solvents to avoid denaturation [21-24]. Thus, several strategies have been developed to achieve this goal. For instance, Convertine *et al.* successfully carried out the aqueous RAFT polymerizations of acrylamide (AAm) and *N,N*-dimethylacrylamide (DMAAm) at 25 °C using *S,S*-bis(α,α'-dimethyl-α''-acetic acid)trithiocarbonate (TRITT) as RAFT agent and 2,2'-azobis[(2-carboxyethyl)-2-methylpropion-amidine] (VA-057) as initiator [25]. They obtained well-defined polymers with very low polydispersity (polydispersity index, *PDI* < 1.1). These authors employed the same process to synthesize thermally responsive poly(*N,N*-dimethylacrylamide)-*b*-poly(*N*-isopropylacrylamide) (PDMAAm-*b*-PNIPAAm) diblock and PDMAAm-*b*-PNIPAAm-*b*-PDMAAm triblock copolymers [26]. In both cases, an azo initiator with a low decomposition temperature was used. Nevertheless, this type of initiator is relatively expensive and difficult to ship and stock due to its inherently low decomposition temperature.

To overcome these disadvantages, other initiating systems were developed. Zhang and coworkers demonstrated that a mixture of potassium persulfate ($K_2S_2O_8$) and sodium thiosulfate ($Na_2S_2O_3$) can be used as redox initiator for RAFT polymerization in aqueous media at ambient temperature [27]. With such a system, these authors were able to polymerize NIPAAm and AAm with good control even at high conversions (> 90%). Another possibility of initiation is UV-radiation. Recently Cai's group detailed the RAFT polymerization of *N*-(2-acryloyloxyethyl) pyrrolidone (NAP) and 2-hyroxyethyl acrylate (HEA) monomers in pure water initiated by the photolysis of (2,4,6-trimethylbenzoyl)-diphenyl phosphine oxide (TPO) with visible light [28]. Rapid and well-controlled polymerizations were obtained in both cases. Interestingly the reaction exhibited an on/off character: when the irradiation was stopped, the polymerization essentially came to a standstill. Turning on the light again led to another rapid polymerization process with the same kinetics. In addition, Muthukrishnan *et al.* reported the first RAFT polymerization of acrylic acid (AA) initiated under ultraviolet radiation at a specific wavelength of 365 nm in aqueous solution to achieve PAA with very low polydispersities [29]. In this process, the solution is free of initiator and radicals are generated directly by

partial photolysis of the monomer. The chain transfer agent TRITT was used to control the polymerization effectively at conversions as high as 50% without efficient control. However, many RAFT agents, in particular aromatic ones, are UV-sensitive and can decompose under UV irradiation.

Thus, an alternative is initiation by γ-irradition. Quinn *et al.* as well as Bai *et al.* showed that RAFT polymerization can be initiated with γ-irradition at ambient temperature under full conservation of the control of the polymerization and that the preparation of block copolymers is possible under these conditions [30-34]. This radiation type can initiate most vinylic monomers, such as acrylates, methacrylates and styrenics [35-39]. Barner *et al.* as well as Barsbay *et al.* also applied γ-initiated RAFT polymerization to graft polymers from solid surfaces, e.g. polypropylene lanterns [35, 40, 41] and cellulose [36, 42]. Thus, in the past few years, γ-irradiation has been increasingly used in the context of the RAFT process to obtain well-defined (living) polymers [42-45]. Recently, the RAFT polymerization of the water-soluble monomers NIPAAm and AA under γ-irradiation in aqueous media was reported [46]. γ-Initiation was also successfully used to generate a conjugate PNIPAAm-bovine serum albumin via a grafting from approach without any degradation of the protein [47]. It is important to note that while the initiation process under γ-radiation may include a serie of species (the initial RAFT agent, the solvent as well as the monomer), a RAFT process is nevertheless in operation (see for example ref. [48, 49]). In here, we describe the generalization of the process to a large variety of water-soluble monomers. We also prove that this technique is an excellent tool to obtain well-defined polymers and block copolymers with very low polydispersity up to full conversion and even for very high degrees of polymerization (DP_n up to 10,000).

Experimental Part

Materials

All chemicals and solvents where purchased from Sigma-Aldrich, Acros and Fluka at the highest available purity and used as received unless otherwise noted. NIPAAm was purified by two recrystallizations in a mixture of n-hexane and benzene. AA was distilled under vacuum and used freshly. AAm was purified by two recrystallizations in acetone. 2-Hydroxyethyl acrylate, oligo(ethylene glycol) methacrylate (OEGMA, M = 526 g·mol^{-1}, ~10 ethylene glycol units) and 2-(dimethylamino)ethyl methacrylate (DMAEMA) were passed through a column of neutral alumina to remove the inhibitor prior to use. The syntheses of the RAFT agents S,S-bis(α,α'-dimethyl-α''-acetic acid)trithiocarbonate (TRITT), 3-benzylsulfanyl thiocarbonylsulfanyl propionic acid (BPATT) and 4-cyanopentanoic acid dithiobenzoate (CPADB) have been described elsewhere [50-52]. Poly(ethylene oxide) modified benzylsulfanylthiocarbonylsulfanyl propionate (PEO$_{2k}$-BPATT) was synthesized according to the following procedure. 8 g (4 mmol) of poly(ethylene glycol) monomethyl ether were dissolved in 40 mL water-free N,N-dimethylacetamide (DMAc) in presence of 0.39 mL of anhydrous pyridine (4.8 mmol). The solution was cooled with a water/acetone (1/1 v%) ice bath. 1.396 g (4.8 mmol) of 3-benzylsulfanyl thiocarbonylsulfanyl propionic acid chloride (BPATT-COCl) was then added dropwise under stirring. Details of the BPATT-COCl synthesis have been described elsewhere [51]. The solution was allowed to warm to room temperature and was stirred overnight. The mixture was concentrated under reduced pressure and precipitated in cold hexane. After filtering, the yellow solid (BPATT-COCl) was dried under high vacuum for 24 h prior to use.

Polymerization Procedure

Homopolymers and block copolymers were synthesized following the same procedure described here. Monomers were dissolved with the CTA in pure water or in a mixture of water/organic co-solvent, respectively at the desired concentration. After complete dissolution the stock solution was divided and transferred into glass sample vials,

containing approximately 3 to 4 mL solution. The vials were capped with rubber septa and deoxygenated by purging with nitrogen gas for 15 min each. The samples were placed in an insulated room with a ^{60}Co source at ambient temperature (typically close to 20 °C) at a dose rate of 30 Gy · h^{-1}. Samples were taken after pre-selected time intervals to follow the monomer conversion. The conversion of each sample was determined directly from the solution by ^{1}H-NMR (in D_2O) from the relative integration of peaks associated with the monomer vinyl group in relation to those associated with the polymer. Subsequently, all samples were freeze-dried and purified by precipitation before SEC measurements or subsequent block extension.

Characterization

^{1}H-NMR spectra were recorded on a Bruker spectrometer (300 MHz) in D_2O (residual peak $\delta = 4.79$ ppm). Depending on the nature of the polymer, *Size Exclusion Chromatography (SEC)* analyses were performed in *N,N*-dimethylacetamide (DMAc) (0.03% w/v LiBr, 0.05% BHT stabilizer) at 50 °C (flow rate: 0.85 mL·min^{-1}) using a PL50 compact modular system comprising a DGU-12A solvent degasser, an LC-10AT pump, a CTO-10A column oven, and an RID-10A refractive index detector. The system was equipped with a 5.0 μm bead-size guard column (50×7.8 mm) followed by four 300×7.8 mm linear PL columns (10^5, 10^4, 10^3, and 500 Å). Calibration was performed with low polydispersity polystyrene standards ranging from 500 to 10^6 g·mol^{-1}. The polymers were also characterized by SEC using a Gynkotek model 300 pump, a Bischoff 8110 RI detector, a Waters 486 UV detector ($\lambda = 270$ nm), and a 0.05 M solution of LiBr in 2-*N*-methylpyrrolidone (NMP) as eluent. PSS GRAM columns (300×8 mm, 7 μm): 10^3, 10^2 Å (PSS, Mainz, Germany) were thermostated at 70 °C. A 0.4 wt % (20 μL) polymer solution was injected at an elution rate of 0.72 mL·min^{-1}. Polystyrene standards were used to calibrate the columns, and methyl benzoate was used as an internal standard. Finally GPC in water was also used to analyze some polymers (0.1 mol·L^{-1} NaN$_3$, 0.01 mol·L^{-1} NaH$_2$PO$_4$, pH = 6.3) at 35 °C (flow rate: 1 mL·min^{-1}) using a Gynkotek model 300 pump, an ERC column oven, and a Bischoff 8110 refractive index detector. The system was equipped with a Polymer Laboratories (PL) PLaquagel-OH 8 μm bead-size

guard column (50×7.5 mm) followed by two 300×7.5 mm columns, a PLaquagel-OH mix 8 μm and a PLaquagel-OH 30, 8 μm. Calibration was performed with low polydispersity poly(ethylene oxide) standards ranging from 2000 to 85 000 g·mol⁻¹. *Liquid Adsorption Chromatography at Critical Conditions of Adsorption* (LACCC) was conducted on a chromatographic system composed of a degasser ERC 3415R, a pump P4000 (TSP), and an autosampler AS3000 (TSP). Two detectors were used: a UV detector UV6000LP (TSP) with two wavelengths (λ = 230 and 261 nm) and an evaporative light scattering detector (ELSD) EMD 960 (Polymer Laboratories) operating at 80 °C with a gas flow rate of 6.8 L·min⁻¹. Two reversed phase columns C18, 250×4.6 mm i.d., with 5 μm average particle size were employed, one with 120 Å (YMC) and the other with 300 Å pore diameters (Macherey-Nagel). The solvents, acetonitrile (ACN) and water (H_2O), were HPLC grade and used freshly. The critical solvent composition for polyethylene glycol monomethyl ether (PEO-OH) determined for this system was ACN/H_2O 38.8/61.2 (v/v) at 23 °C with a flow rate of 0.5 mL·min⁻¹. Samples were dissolved in the critical mix at a concentration of 0.2 wt %. Then 20 μL was injected. Modified PEO-OH appeared in adsorption mode due to the low polarity of the end group. To obtain a narrow and well-defined peak, a gradient was used after the elution time of remaining PEO-OH. The composition sequence is detailed here. The critical composition was maintained for 16 min. Then, over 16 min, a linear gradient up to 60% of ACN was realized. This percentage was decreased directly to the critical composition over 1 min also with a linear gradient. Finally, this proportion was kept for 60 min to equilibrate the system before the next measurement.

Results and Discussion

Homopolymerizations

Polymerization of N,N-dimethylacrylamide (DMAAm). DMAAm is a very important water-soluble monomer which is widely used [53-55]. DMAAm was polymerized in the presence of two trithiocarbonate CTAs, i.e. BPATT and TRITT (see Scheme 4-1) at various ratios of monomer to CTA. The results of selected polymerizations are summarized in Tables 4-S1-S2 and Figure 4-1 as well as Figures 4-S1-S2 (see supporting information). Inspection of the kinetic data given in Figure 4-1 clearly indicates that TRITT allows for an excellent control of DMAAm polymerization in pure water. This RAFT agent was selected for its good solubility in water, even at high concentration, due to the presence of the two carboxylic moieties. It is also known to allow a good control of acrylate-based monomers [56-58]. With an initial DMAAm/TRITT ratio of 400, the first-order time-conversion plot (Figure 4-1A) displays a short induction time, close to 15 min. Such induction phenomena are often observed in the RAFT process [59-62]. After the induction period, the first-order plot is linear up to 90% conversion indicating that the main RAFT equilibrium is rapidly established and an apparent first-order dependence on monomer concentration is operative during the major part of the polymerization. Figure 4-1B depicts the evolutions of the apparent number-average molecular weight and the polydispersity index with the conversion. It is obvious that the molecular weight increases linearly with conversion demonstrating the controlled fashion of the process. The difference between the theoretical and the experimental molecular weight can be assigned to the calibration of the SEC on the basis of polystyrene equivalents. The resulting polydispersity indices, *PDI,* are low (*PDI* < 1.2) except at the early stage of the polymerization and they decrease throughout the polymerization. Even at high conversions (>95%) the *PDI* is low (*PDI* = 1.07) and mono-modal molecular weight distributions are observed (results not shown).

BPATT **TRITT** **CPADB**
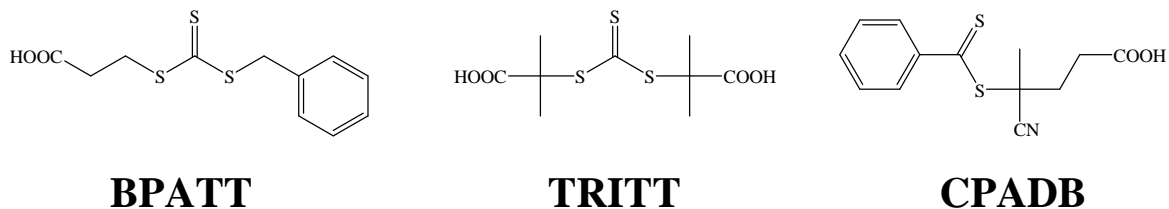
Scheme 4-1. RAFT agents employed in the present study. From left to right, 3-benzyl sulfanylthiocarbonylsulfanyl propionic acid (BPATT)), (*S,S*-bis(α,α'-dimethyl-α''-acetic acid)trithiocarbonate (TRITT) and 4-cyanopentanoic acid dithiobenzoate (CPADB).
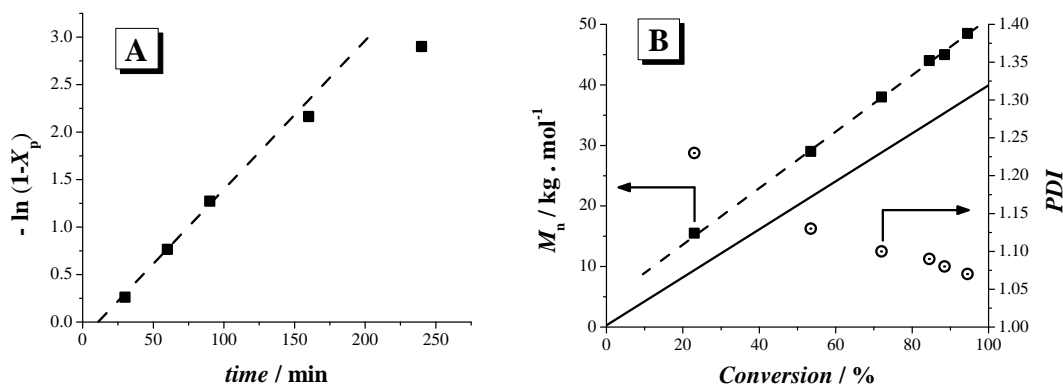
Figure 4-1. Kinetics of the RAFT polymerization of DMAAm under γ-radiation (dose rate = 30 Gy·h^{-1}) in pure water at ambient temperature using TRITT as CTA for an initial ratio $[M]_0/[CTA]_0 = 400$ with $[M]_0 = 1.5$ mol·L^{-1}. (A) First-order time-conversion plot (■), (– –) extrapolation. (B) Apparent number-average molecular weight (■) and *PDI* (⊙) versus monomer conversion measured by SEC using PS standards, (– –) extrapolation, (——) theoretical number-average molecular weight evolution determined according to the equation $\overline{M}_{n,\,th} = [M]_0 / [CTA]_0 \cdot X_p \cdot M_M + M_{CTA}$.

The asymmetric CTA 3-benzylsulfanylthiocarbonylsulfanyl propionic acid (BPATT) was also employed in the γ-radiation initiated polymerization of DMAAm. An added advantage of this CTA is the ability to easily link it via the carboxylic group to surfaces or to small molecules to generate star polymers [42, 55, 63, 64]. However, the main problem of BPATT is its poor solubility in pure water due to the aromatic ring. To

dissolve it completely, the addition of a cosolvent is required. Here, the addition of acetone at different volume ratios is used to obtain a homogenous solution. Acetone was chosen due to its low boiling point, which makes it easy to remove by distillation to finally obtain the polymer in pure water.

The fundamental experimental data for BPATT-mediated polymerizations of DMAAm are collected in Table 4-S1 and Figure 4-S1 (see supporting information). As in the case of TRITT, the control of the DMAAm polymerization is very good. When a monomer/CTA ratio of 200 is used, an induction period close to 3 h is observed. Subsequently, the first-order time-conversion plot exhibits a linear relationship during a major part of the polymerization (Figure 4-S1A). Moreover – as depicted in Figure 4-S1B – the molecular weight increases linearly with monomer conversion and the *PDI* decreases up to 1.05, which indicates the absence of undesired side reactions. Obtaining well-defined blocks of high molecular weight by increasing the monomer/CTA ratio is a considerable challenge. BPATT is an excellent candidate for the RAFT polymerization of DMAAm under γ-radiation to obtain a large variety of chain lengths from $DP_n = 60$ up to 4,000 with good control (Figure 4-S1C and Table 4-S1). The SEC traces and the polydispersity indices indicate good control of the polymerizations even at a very low concentration of RAFT agent up to high conversions. The molecular weight distributions are unimodal except in few cases where a small evidence of termination by recombination of radicals is noticed when the monomer conversion is almost complete.

In addition of being an environmental friendly and cheap solvent, water also improves the kinetics and the control of the RAFT polymerization of DMAAm compared to organic solvents. For the same DMAAm/BPATT ratio (1,000/1), kinetic studies were conducted in aqueous media and in 1,4-dioxane. The respective results are summarized in Figure 4-S2 and Table 4-S2 (see supporting information). Dioxane is well-known to be a solvent of choice to polymerize DMAAm and other (meth)acrylamide derivatives and good results were already obtained by different research groups [61, 65-67]. For instance, Liu et al. used this solvent to synthesize narrowly distributed PDMAAm and PDMAAm-*b*-PNIPAAm [68]. The generated block copolymers were used afterwards for surface modification of multi-walled carbon nanotubes via a *Click* chemistry approach. However, in case of γ-initiation, a long induction period close to 3 h was observed when dioxane

was used as can be seen in Figure 4-S2A. This effect was almost not noticed when the polymerization was conducted in aqueous solution at this high monomer/CTA ratio. Moreover, the apparent rate coefficient associated with the rate of polymerization, k_p^{app} (estimated from the slope of the linear part of the first-order time–conversion plot) exhibits a difference. In dioxane, the polymerization seems much slower in comparison to aqueous media. An apparent rate coefficient of $k_p^{app} = 6.1 \cdot 10^{-5}$ s^{-1} was determined for the organic solvent which is more than 2.5 time lower compared to the one estimated at the same conditions in aqueous media ($k_p^{app} = 16 \cdot 10^{-5}$ s^{-1}). Thus, to reach a monomer conversion of 96%, a reaction time of less than 7 h is needed in aqueous solution while more than 18 h is necessary in dioxane. The low rate of polymerization in dioxane may result from two factors: (i) compared to water, the radical concentration may be lower in dioxane due to a less efficient radiolysis of this solvent compared to water [69] and (ii) protic solvents such as water activate the propagating radical to react faster with monomers present in the media [70, 71]. It is also important to note that the control obtained in dioxane is not as good as in aqueous media (Figure 4-S2B). Low polydisperse PDMAAm samples were obtained in a water-based system with a *PDI* close to 1.10 even close to full conversion. In dioxane, although the molecular weight increases linearly with the conversion, as in aqueous media, the polydispersity index did not decrease below 1.20. It should be noted that a certain loss of control may be caused by potentially peroxide containing solvents such as tetrahydrofuran and dioxane, which may cause the thio carbonylthio moiety to be oxidized or even removed [72, 73].

Taking into account all the benefits of using γ-initiation at ambient temperature in aqueous media to polymerize water-soluble monomers by RAFT, a large range of monomers was tested. Selected results are collected in Table 4-1 and in the supporting information section (see Tables 4-S3-S5 and Figures 4-S3-S6).

Polymerization of 2-hydroxyethyl acrylate (HEA). HEA was polymerized in presence of two CTAs, i.e. TRITT and BPATT. When the polymerization is conducted using BPATT as RAFT agent with an initial HEA/BPATT ratio of 200 in a mixture of water/acetone, good control is reached. The first-order time-conversion plot (Figure 4-S3A) exhibits linearity up to a conversion higher than 95%, which indicates that the radical

concentration is approximately constant over the duration of the polymerization. It also seems that no induction period can be determined by extrapolation of the linear part. Moreover, it is clear from the Figure 4-S3B that the apparent number-average molecular weight of the polymer increases linearly with the monomer conversion. The linearity, associated with a low *PDI* which decreases over the polymerization to reach a value close to 1.1, demonstrates the controlled fashion of the process. The SEC traces (Figure 4-S3C) are monomodal and symmetric at low conversion, yet when a conversion higher than 60% is reached a shoulder can be detected at high molecular weights. This phenomenon can be explained by a possible termination by recombination of two growing radicals. By using TRITT as RAFT agent, it was possible to conduct the polymerization in pure water (see Table 4-S3). Similar results were obtained and a good control was achieved. The first-order time-conversion plot and the apparent molecular weight increase linearly respectively with the time and the monomer conversion (Figure 4-S4)**.** Again no induction period was detected and the polydispersity index was almost always lower than 1.2 except at low conversion. The obtained low *PDIs* prove – as for BPATT – that the polymerization of HEA, initiated by γ-irradiation at ambient temperature, proceeds in a controlled manner.

Table 4-1. RAFT polymerization under γ-initiation of water soluble monomers in aqueous media at ambient temperature.

Mono-mer[a]	CTA	$\dfrac{[M]_0}{[CTA]_0}$	Acetone %Vol	Time min	x_p[b] %	$\overline{M}_{n,th}$[c] kg/mol	$\overline{M}_{n,exp}$ kg/mol	PDI
HEA	TRITT	400	-	420	91	43	72[d]	1.15[d]
HEA	BPATT	200	25	1 440	97	22.8	50[d]	1.12[d]
AAm	TRITT	400	-	300	89	25.6	17[e]	1.19[e]
AAm	BPATT	800	22	2 720	>99	57	37[e]	1.19[e]
AA	TRITT	800	-	1 200	98	57	87[e]	1.14[e]
AA	BPATT	1 200	16	1 520	98	85	98[e]	1.10[e]
NIPAAm	TRITT	500	-	180	98	56	74[d]	1.10[d]
NIPAAm	BPATT	1 000	15	310	88	100	105[d]	1.12[d]
AMPS	TRITT	800	-	220	90	131	178[d]	1.16[d]
AMPS	BPATT	200	30	1 440	96	40	57[d]	1.19[d]
OEGMA	CPADB	100	15	140	16	8.7	10[d]	1.05[d]
OEGMA	CPADB	100	15	240	73	38.7	50[d]	1.07[d]
DMAEMA	CPADB	100	10	240	79	12.7	17.5[d]	1.20[d]

[a] HEA = 2-hydroxyethyl acrylate, AAm = acrylamide, AA = acrylic acid, NIPAAm = *N*-isopropylacrylamide, AMPS = 2-acrylamido-2-methylpropane sulfonic acid, OEGMA = oligo(ethylene glycol) methacrylate, DMAEMA = 2-(dimethylamino)ethyl methacrylate [b] Determined by ^{1}H NMR spectroscopy in D$_2$O. [c] $\overline{M}_{n,th}=M_M \cdot X_p \cdot [M]_0/[CTA]_0+M_{CTA}$. [d] Measured by SEC using PS standards in *N,N*-dimethylacetamide (DMAc). [e] Measured by SEC using PEO standards in water.

Polymerization of acrylamide (AAm). The influence of the monomer/CTA ratio was investigated for the RAFT polymerization of AAm mediated by BPATT. Table 4-S4 and Figure 4-S5 summarize the results. By modifying the monomer/CTA ratio, a large range of targeted degrees of polymerization from 120 to 10,000 was obtained with a good control even at nearly full monomer conversion (>99%). The apparent number-average molecular weight increases linearly with the ratio AAm/BPATT up to 4,000 (Figure 4-S5A). The difference between the theoretical and the experimental molecular weights can be assigned to the calibration of the SEC on the basis of poly(ethylene oxide) standards. It can be also seen that every polymerization exhibits a polydispersity index lower than 1.2. An important reason to explain the low polydispersity is the high dilution (less than 0.5 mol·L^{-1}) used when high molecular weight polymers were desired. Indeed, all reactions were performed in a static environment without stirring the solutions. Thus, only Brownian motion allows the monomer and the polymer coils to move. The control of the system is therefore significantly depending on the diffusion of the reactants and on the system viscosity. By using a dilute solution, a reasonably low viscosity was observed and better results were obtained (results not shown). All AAm polymerizations were conducted for a longer time than necessary according to the kinetic results to be sure to reach full conversion. As depicted in Figure 4-S5B, all molecular weight distributions are monomodal and do not exhibit a shoulder at high molecular weight due to the termination by recombination of growing radicals. Therefore, the RAFT polymerization initiated by γ-radiation is a very useful and versatile tool to obtain well-defined polymers with exactly targeted molecular weight without having a precise knowledge of the polymerization kinetics.

Polymerization of acrylic acid (AA). Poly(acrylic acid) (PAA) has been intensively investigated for its stimuli-responsive properties. PAA responds in water to changes in pH and ionic strength by changing coil dimensions and solubility. Therefore it finds a vast array of applications, especially in the biomedical area [74-76]. Kinetic details of the RAFT polymerization at ambient temperature in aqueous media under γ-irradiation mediated by TRITT and BPATT have been previously reported by us [46]. Both RAFT agents successfully controlled the polymerization. The first-order time conversion plot

exhibits a linear relationship associated with an absence or only a very short induction period. The apparent molecular weights increase linearly with the monomer conversion and the *PDI* decreases throughout the polymerization to reach a value close to 1.10. Moreover, the molecular weight distributions are monomodal even at very high conversion, which indicates the absence of undesired side reactions. Finally, we demonstrated the living character of the process by subsequent chain extension. We now investigated the ability of BPATT-mediated RAFT polymerization in aqueous media under γ-irradiation to generate well-defined PAA with very high molecular weight. The results are summarized in Table 4-S5 and Figure 4-S6. As in the case of AAm, high molecular weight PAA with DP_n up to 10,000 and narrow molecular weight distributions (*PDI* < 1.20) were obtained via this process. It is also important to note that this technique can be applied over an extremely high range of AA/BPATT ratios from 42 to 10,000 without sacrificing the control. As depicted in Figure 4-S6A, the apparent molecular weight increases linearly with the initial monomer to CTA ratio up to a *DP* of 300. Afterwards, a deviation is observed which can be attributed to the calibration of the SEC on the basis of poly(ethylene oxide) (PEO) equivalents. Indeed there is a strong difference in behavior between non-ionic PEO and our polyanion PAA during the SEC measurement. However, as can be seen from Figure 4-S6B, it is clear that all molecular weight distributions are monomodal, symmetric and do not exhibit any visible termination even at nearly full conversion.

Polymerization of other water-soluble monomers. The polymerization of two other acrylamides and two methacrylate-based monomers were investigated Selected conditions and results are collected in Table 4-1 and Figure 4-S7. Poly(*N*-isopropylacrylamide) (PNIPAAm), a thermo-responsive polymer, was already successfully polymerized by us using BPATT or TRITT as RAFT agent via γ-initiation in aqueous media [46]. With both CTAs, narrow distributed polymers were synthesized over a large range of degrees of polymerization. For instance, it can be seen for a polymerization carried out in water with an initial NIPAAm/TRITT ratio of 500 (Table 4-1), that the reaction reaches a conversion of 98% within 3 h, which highlights the fast character of NIPAAm polymerization in water. However, thanks to the good transfer

108

ability of the RAFT agent, a narrow, a symmetric and monomodal molecular weight distribution was obtained (Figure 4-S7A). The polymerization of 2-acrylamido-2-methylpropane sulfonic acid (AMPS) also exhibits a good control when BPATT or TRITT is used (Figure 4-S7B).

Oligo(ethylene glycol) methacrylate (OEGMA) and 2-(dimethylamino)ethyl methacrylate (DMAEMA) cannot be polymerized in a controlled manner when TRITT or BPATT are used. Indeed these RAFT agents are commonly employed for the synthesis of acrylate-based polymers. Due to the low stability of the original radical $R^\bullet$ generated from the CTA compared to the growing radical, the fragmentation step of the R group is unlikely. In addition – and more importantly – the propensity of the C=S double bond towards methacrylic radical attack is low. The consequence is a poor control when BPATT or TRITT is used to mediate the polymerization of methacrylates. Therefore, we selected 4-cyanopentanoic acid dithiobenzoate (CPADB) as RAFT agent to polymerize OEGMA and DMAEMA. CPADB has a highly reactive C=S double bond and generates a more stable but reactive tertiary radical $R^\bullet$ after fragmentation and allows a good control of methacrylate-based monomers [77-82]. Moreover it features a carboxylic group which allows good solubility in aqueous solution with the use of only a limited amount of organic cosolvent. The RAFT polymerizations of OEGMA and DMAEMA mediated by CPADB showed a good control. Monomodal and narrow molecular weight distribution were obtained in both cases (Table 4-1 and Figures 4-S7 C, D)

Synthesis of Block Copolymers with Acrylic Acid

Synthesis of poly(acrylic acid) macro-CTAs. To further demonstrate the retention of the RAFT functionality and the controlled nature of the above discussed polymerizations, several block copolymers were synthesized. Selected results are summarized in Table 4-2 and Figures 4-2-5. A number of PAA macro-CTAs was synthesized using BPATT under γ-irradiation. Since BPATT is an asymmetric CTA, it allows the generation of AB diblock copolymers. After purification, these macro-CTAs were used to polymerize various monomers.

Table 4-2: RAFT Synthesis of poly(acrylic acid) (PAA) macro-CTAs for the synthesis of block copolymers; γ-initiation at room temperature using BPATT as CTA.

Run	$\dfrac{[M]_0}{[CTA]_0}$	$\dfrac{[M]_0}{mol/L}$	$\dfrac{Acetone}{\% Vol}$	$\dfrac{Time}{min}$	$\dfrac{x_p^{(a)}}{\%}$	$\dfrac{\overline{M}_{n,th}^{(b)}}{kg/mol}$	$\dfrac{\overline{M}_{n,exp}^{(c)}}{kg/mol}$	PDI[c]
B1	42	2.5	50	1620	63	2.2	7.9	1.10
B2	42	2.5	50	2500	>99	3.4	11	1.08
B3	200	2.5	23	1520	>99	14.4	45	1.08
B4	500	2.5	20	1520	>99	36.3	87	1.11
B5	2 000	2.0	15	1520	>99	144	230	1.26

[a] Determined by ^{1}H NMR spectroscopy in D_2O. [b] $\overline{M}_{n,th}=M_M\cdot X_p\cdot[M]_0/[CTA]_0+M_{CTA}$. [c] Apparent number-average molecular weights and *PDIs*, as measured by SEC using PEO standards in water.

Block copolymers with acrylamide (AAm). Two different PAA CTAs were used to polymerize acrylamide at different AAm/PAA ratios of up to 1,000. The results are given in Table 4-3 and Figure 4-2. For all ratios good control was found. Monomodal molecular weight distributions were obtained even at high conversion and no remaining PAA precursor was observed in the SEC traces as inspection of Figure 4-2A reveals. However, the distributions are not completely symmetric and a tailing towards low molecular weights can be noticed. Such a phenomenon may be associated with the slow establishment of the pre-equilibrium between the PAAm growing radicals and the PAA macro-CTA. Very well-defined block copolymers PAAm$_x$-*b*-PAA$_y$ were synthesized even when a PAA macro-CTA obtained at full monomer conversion was employed. According to the SEC traces, no residual PAA seems to be present and only a small amount of recombination was observed at extremely high conversion (>99%) for the diblock copolymers. These experiments show that RAFT polymerization under γ-irradiation is a simple process to generate well-controlled block copolymers in aqueous solutions. Due to the extremely low amount of bimolecular termination or other side reactions, precursors and extended polymers can be polymerized up to full conversion which allows a precise control of the targeted DP_n over a wide range.

Table 4-3. Chain extension with acrylamide (AAm) of various poly(acrylic acid) (PAA) macro-CTAs by RAFT polymerization in aqueous media at ambient temperature under γ-initiation.

PAA macro-CTA	$\dfrac{[M]_0}{[CTA]_0}$	$[M]_0$ mol/L	Ethanol %Vol	Time min	$x_p^{(c)}$ %	$\overline{M}_{n,th}^{(d)}$ kg/mol	$\overline{M}_{n,exp}^{(e)}$ kg/mol	PDI[e]
B1	105[a]	2	40	1 620	95	9.3	12	1.14
B1	205[a]	2	30	1 620	98	16.4	17	1.25
B1	405[a]	2	22	1 620	>99	31	23	1.23
B1	1 000[a]	1.5	20	1 440	>99	73.3	37	1.27
B2	155[b]	2	35	1 515	97	14.1	17	1.10
B2	300[b]	2	25	1 515	99	24.7	25	1.17
B2	610[b]	2	15	1 515	>99	46.8	38	1.23

[a] Using asymmetric PAA-macro-CTA B1 of DP_n = 26. [b] Using asymmetric PAA-macro-CTA B2 of DP_n = 42. [c] Determined by ^{1}H NMR spectroscopy in D_2O. [d] $\overline{M}_{n,th} = M_M \cdot X_p \cdot [M]_0/[CTA]_0 + M_{CTA}$. [e] Apparent number-average molecular weights and *PDIs*, as measured by SEC using PEO standards in water.
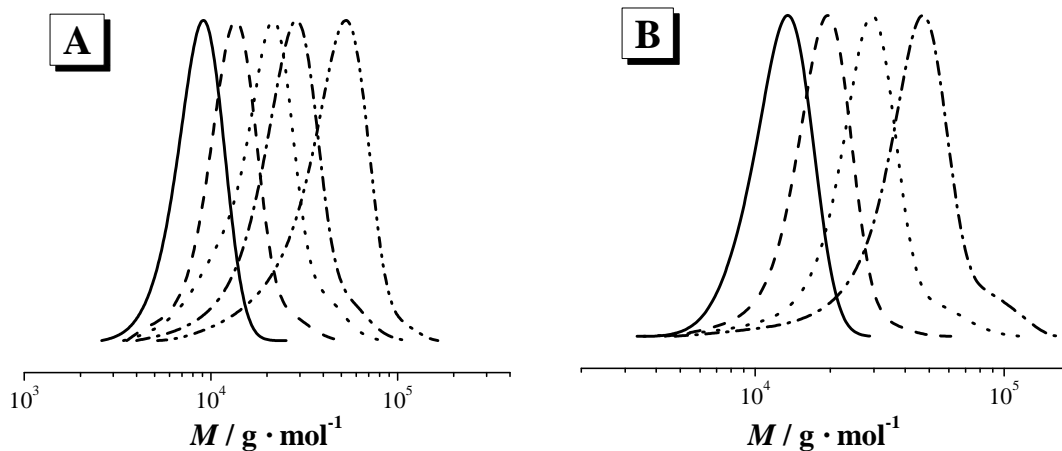
Figure 4-2. Dependence of the molecular weight distributions, $w(\log M)$, on the ratio $[AAm]_0/[PAA\text{-}CTA]_0$ in the RAFT polymerization of AAm under γ-radiation in water at ambient temperature using PAA macro-CTAs. (A) Using a PAA macro-CTA B1. PAA precursor (—), after chain extension with $[M]_0/[CTA]_0$= 105 (– –), 205 (• • •), 405 (– • –) and 1 000 (– • • –). (B) Using a PAA macro-CTA B2. PAA precursor (—), after chain extension with $[M]_0/[CTA]_0$= 155 (– –), 300 (• • •) and 610 (– • –).

Block copolymers with N-isopropylacrylamide (NIPAAm). AB block copolymers were synthesized from PAA precursors. Selected results are collected in Table 4-4 and Figure 4-3. PNIPAAm-*b*-PAA responds to both temperature and pH and it is known to form hydrogen bonds between the carboxylic groups of the acrylic acid unit and the amide groups of NIPAAm [83]. When the polymerizations were carried out in pure water, the complexation leads to a full collapse of the block copolymers which results in a loss of control. To avoid this loss, an organic solvent dioxane was added in the media to prevent the aggregation.

Two low molecular weight PAAs with a degrees of polymerization of 26 and 42, respectively were used to generate different block copolymers over a very large range of NIPAAm/macro-CTA ratios of up to 1,000. In all cases, the obtained polymers were narrowly distributed ($PDI \leq 1.20$). The SEC traces did not exhibit any traces of residual precursor as evident from Figures 4-3A and 3B. Moreover, the molecular weight distributions are symmetrical and even at high conversion no termination by coupling was detected. Three further PAA macro-CTAs produced at near quantitative monomer conversions and having DP_ns of of 200, 500 and 2,000, respectively, were also used to generate high molecular weight PNIPAAm-*b*-PAA block copolymers. As previously observed for the short chain PAA, well-defined block copolymers were obtained in all cases. A clear shift of the molecular weights and an absence of residual macro-RAFT agent were found for the molecular weight distributions for the samples prepared with the PAA$_{196}$ and PAA$_{500}$ as depicted in Figure 4-3C, which demonstrate the possibility to generate very high molecular weight block copolymers (up to 250 kg·mol^{-1}) with this technique.

Table 4-4. Chain extension with NIPAAm of various PAA macro-CTAs by RAFT polymerization in aqueous media (50 v% dioxane) at ambient temperature under γ-initiation.

PAA macro-CTA	$\dfrac{[M]_0}{[CTA]_0}$	$[M]_0$ mol/L	Time min	$x_p^{(f)}$ %	$\overline{M}_{n,th}^{(g)}$ kg/mol	$\overline{M}_{n,exp}^{(h)}$ kg/mol	PDI[h]
B1	50[a]	1	1440	81	6.8	17.5	1.14
B1	100[a]	1	1440	89	12.2	24	1.12
B1	200[a]	1	1440	98	24.5	38	1.12
B1	300[a]	1	1440	99	35.8	50	1.14
B1	1000[a]	1	1440	>99	115	130	1.20
B2	200[b]	1	1440	98	25.6	38	1.15
B2	1000[b]	1	1440	>99	116	102	1.30
B3	2000[c]	0.6	1440	>99	241	217	1.24
B4	2000[d]	0.5	1440	>99	262	254	1.28
B5	1000[e]	0.4	1440	>99	257	343	1.40

[a] Using asymmetric PAA-macro-CTA B1 of DP_n = 26. [b] Using asymmetric PAA-macro-CTA B2 of DP_n = 42. [c] Using asymmetric PAA-macro-CTA B3 of DP_n = 200. [d] Using asymmetric PAA-macro-CTA B4 of DP_n = 500. [e] Using asymmetric PAA-macro-CTA B5 of DP_n = 2 000. [f] Determined by ^{1}H NMR in D$_2$O. [g] $\overline{M}_{n,th}=M_M \cdot X_p \cdot [M]_0/[CTA]_0+M_{CTA}$. [h] Apparent number-average molecular weights and *PDIs*, as measured by SEC using polystyrene standards in *N*,*N*-dimethylacetamide (DMAc).
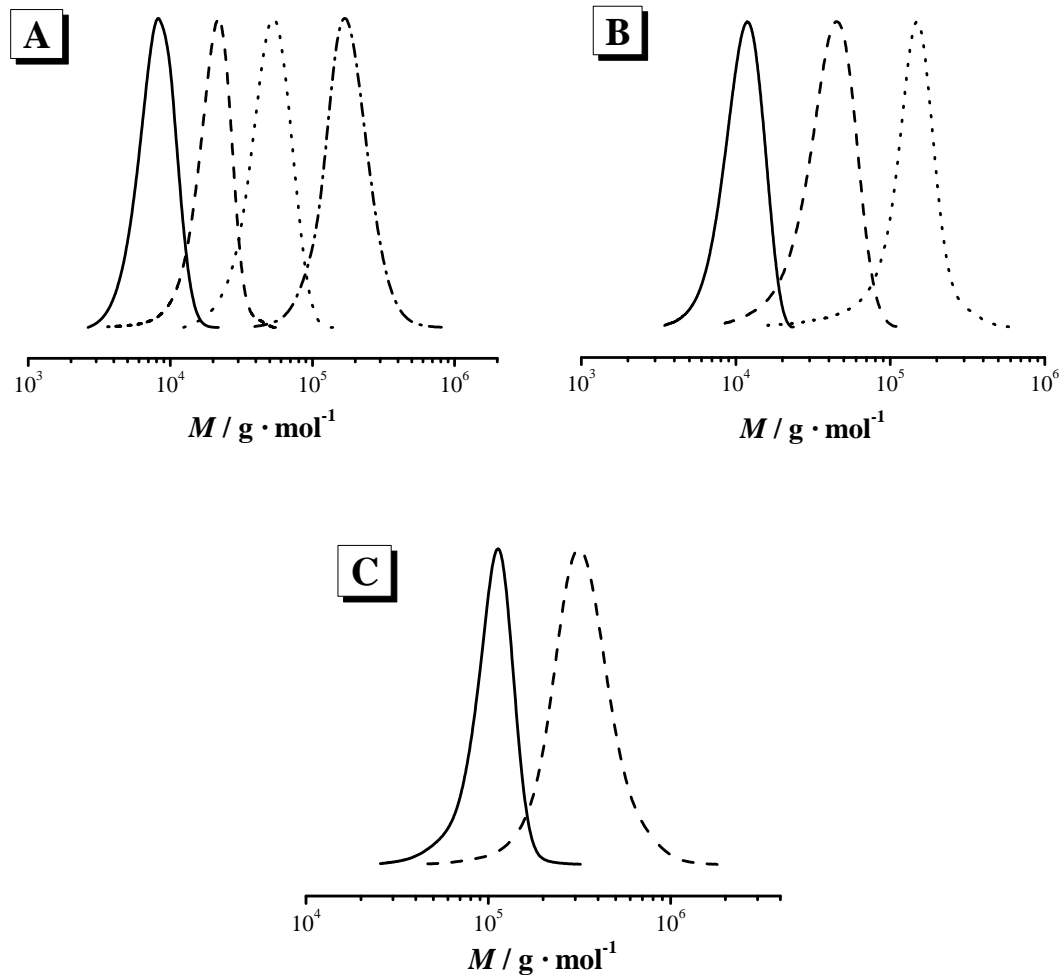
Figure 4-3. Dependence of the molecular weight distributions, $w(\log M)$, on the ratio [NIPAAm]$_0$/[PAA-CTA]$_0$ in the RAFT polymerization of NIPAAm under γ-radiation in aqueous solution using PAA macro-CTAs. (A) Using a PAA macro-CTA B1. PAA precursor (—), after chain extension with [M]$_0$/[CTA]$_0$ = 50 (– –), 300 (• • •) and 1 000 (– • –). (B) Using a PAA macro-CTA B2. PAA precursor (—), after chain extension with [M]$_0$/[CTA]$_0$ = 200 (– –) and 1 000 (• • •). (C) Using a PAA macro-CTA based on B4. PAA precursor (—), after chain extension with [M]$_0$/[CTA]$_0$= 2 000 (– –).

Block copolymers with N,N-dimethylacrylamide (DMAAm) were also generated by RAFT using γ-irradiation to initiate the process. Again different PAA precursors were used.

Selected results are highlighted in Table 4-5 and Figure 4-4. When short PAA macro-CTAs based on BPATT were employed, the following results were obtained. The SEC traces of the block copolymers depicted in Figures 4-4A and 4B exhibit a clear shift in molecular weight compared to the macro-RAFT agent. The molecular weight distributions are monomodal and narrowly distributed (*PDI* generally below 1.15). It should be noticed that often a small tailing can be observed in the range of the low molecular weight. This phenomenon, also observed in the case of PAA-*b*-PAAm, may find its origin in a slow fragmentation of the original macro-CTA where the PAA macro-radical is found to be less stable than PDMAAm or the PAAm macro-radical, respectively. However this phenomenon plays a minor role and well-defined polymers were produced at the end. Finally, all the block copolymers were synthesized at almost full monomer conversion and no or only very minor termination was observed.

Table 4-5. Chain extension with DMAAm ($[M]_0 = 1$ mol·L^{-1}) of various PAA macro-CTAs by RAFT polymerization in aqueous media at room temperature under γ-initiation.

PAA macro-CTA	$\dfrac{[M]_0}{[CTA]_0}$	Acetone %Vol	Time min	$x_p^{(c)}$ %	$\overline{M}_{n,th}^{(d)}$ kg/mol	$\overline{M}_{n,exp}^{(e)}$ kg/mol	PDI$^{(e)}$
B1	100$^{(a)}$	17	2540	>99	12.1	23	1.09
B1	200$^{(a)}$	13	2540	>99	22	31	1.10
B1	300$^{(a)}$	10	2540	>99	32	38	1.16
B2	100$^{(b)}$	13	2540	>99	13.4	25	1.08
B2	200$^{(b)}$	10	2540	>99	23.3	32	1.12
B2	300$^{(b)}$	4	2540	>99	33.2	41	1.11
B2	1 000$^{(b)}$	4	1440	>99	102.5	88	1.31

$^{(a)}$ Using asymmetric PAA-macro-CTA B1 of DP_n = 26. $^{(b)}$ Using asymmetric PAA-macro-CTA B2 of DP_n = 42. $^{(c)}$ Determined by ^{1}H NMR spectroscopy in D$_2$O. $^{(d)}$ $\overline{M}_{n,th}=M_M \cdot X_p \cdot [M]_0/[CTA]_0 + M_{CTA}$. $^{(e)}$ Apparent number-average molecular weights and *PDIs*, as measured by SEC using PS standards in *N,N*-dimethylacetamide (DMAc).
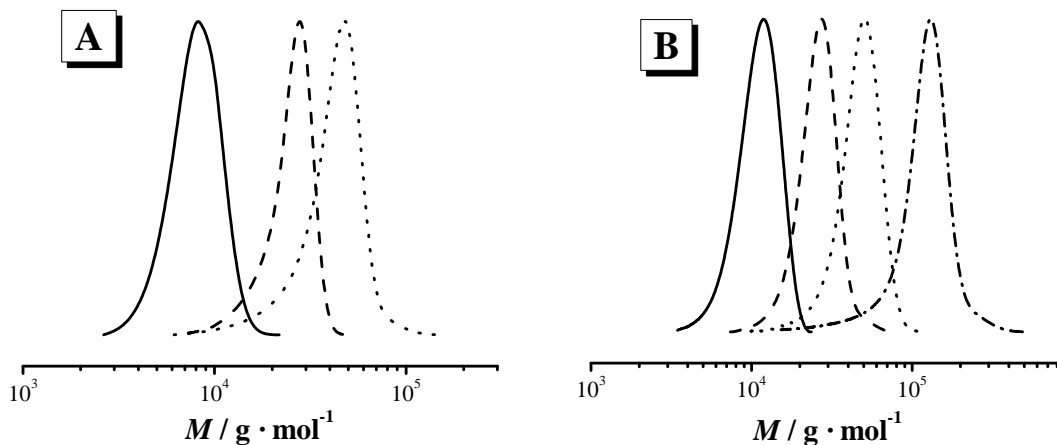
Figure 4-4. Dependence of the molecular weight distributions, $w(\log M)$, on the ratio $[DMAAm]_0/[PAA\text{-}CTA]_0$ in the RAFT polymerization of DMAAm under γ-radiation in aqueous solution at ambient temperature using PAA macro-CTAs. (A) Using a PAA macro-CTA B1. PAA precursor (—), after chain extension with $[M]_0/[CTA]_0=100$ (– –), 300 (• • •). (B) Using a PAA macro-CTA B2. PAA precursor (—), after chain extension with $[M]_0/[CTA]_0=100$ (– –), 300 (• • •) and 1 000 (– • –).

RAFT Synthesis of PNIPAAm-*b*-PDMAAm

PNIPAAm was also evaluated as macro-RAFT agent to generate PDMAAm-*b*-PNIPAAm diblock copolymers. The obtained results are summarized in Table 4-6 and Figure 4-5A. The syntheses were carried out in pure water due to the solubility of all components in this solvent at ambient temperature. Both reactions were carried out close to full conversions and present rather low polydispersities. However, the SEC traces depicted in Figure 4-5A indicate some residual PNIPAAm precursors, maybe due to a slow establishment of the RAFT equilibrium compared to propagation.

Table 4-6. Chain extension with DMAAm or AA of poly(*N*-isopropylacrylamide) (PNIPAAm) and poly(ethylene oxide) (PEO$_{2k}$-BPATT) macro-CTAs by RAFT polymerization in aqueous media at ambient temperature under γ-irradiation.

Monomer	CTA	$\dfrac{[M]_0}{[CTA]_0}$	$\dfrac{[M]_0}{mol/L}$	Acetone %Vol	Time min	$x_p^{(c)}$ %	$\overline{M}_{n,th}^{(d)}$ kg/mol	$\overline{M}_{n,exp}$ kg/mol	PDI
NIPAAm	BPATT	200	1.5	25	1440	76	17.5	25[e]	1.07[e]
DMAAm	PNIPAAm[a]	400	1	-	2540	>99	57	55[e]	1.15[e]
DMAAm	PNIPAAm[a]	1 000	1	-	1440	>99	116	78[e]	1.27[e]
DMAAm	PEO$_{2k}$-BPATT[b]	600	1.7	20	2500	>99	62	62[f]	1.09[f]
AA	PEO$_{2k}$-BPATT[b]	600	1.7	20	2500	>99	45.5	69[f]	1.15[f]

[a] Using asymmetric PNIPAAm macro-CTA of $DP_n = 152$. [b] Using asymmetric PEO macro-CTA of molecular weight 2 000 g·mol^{-1}. [c] Determined by ^{1}H NMR in D$_2$O. [d] $\overline{M}_{n,th} = M_M \cdot X_p \cdot [M]_0/[CTA]_0 + M_{CTA}$. [e] Apparent number-average molecular weights and *PDIs*, as measured by SEC using PS standards in 2-*N*-methylpyrrolidone (NMP). [f] Apparent number-average molecular weight and *PDI*, as measured by SEC using PEO standards in water.
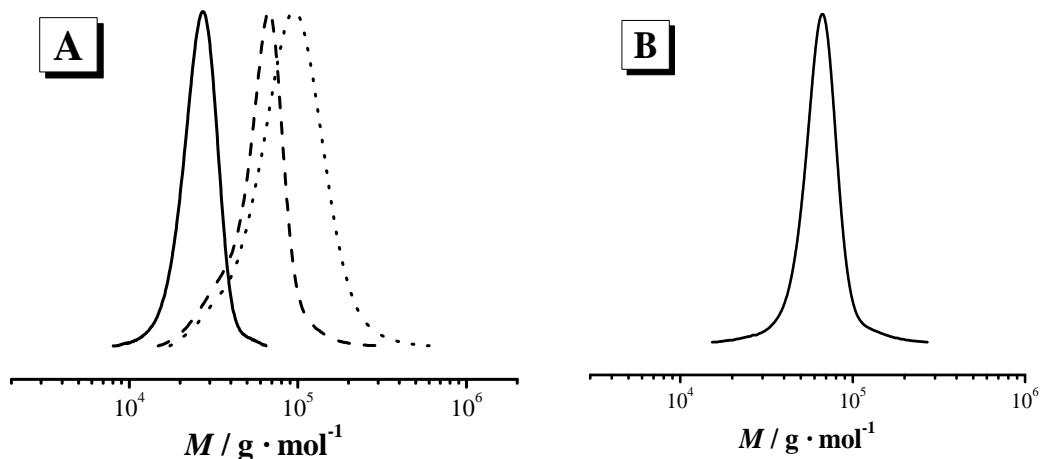
Figure 4-5. (A) Dependence of the molecular weight distributions, $w(\log M)$, on the ratio $[\text{DMAAm}]_0/[\text{PNIPAAm-CTA}]_0$ in the RAFT polymerization of DMAAm under γ-radiation in water at ambient temperature using PNIPAAm macro-CTA. PNIPAAm precursor (—), after chain extension with $[M]_0/[CTA]_0 = 400$ (– –) and 1 000 (• • •). (B) Molecular weight distribution, $w(\log M)$, of PEO-*b*-PDMAAm synthesized by RAFT polymerization of DMAAm under γ-radiation in aqueous solution at ambient temperature using PEO_{2k}-BPATT macro-CTA.
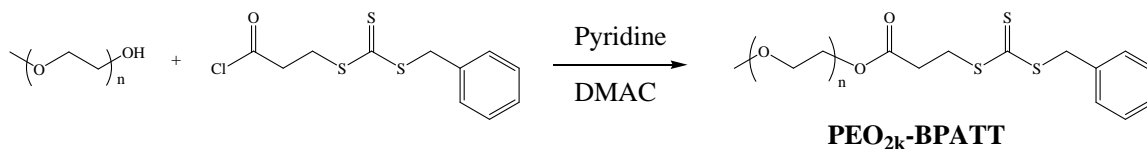
Scheme 4-2. Synthetis of a PEO-based macro-RAFT agent.

RAFT Synthesis of PEO-*b*-PDMAAm and PEO-*b*-PAA

Finally, other types of block copolymers were synthesized using a poly(ethylene oxide)-based CTA (PEO_{2k}-BPATT). The synthetic access to the RAFT agent is outlined in Scheme 4-2. A monohydroxy-functional PEO (PEO_{2k}-OH) with $DP = 45$ was reacted with an acyl chloride-modified BPATT in anhydrous dimethylacetamide in the presence of pyridine to generate PEO-BPATT. To characterize this macro-CTA, liquid adsorption

chromatography under critical conditions (LACCC) was performed. This method has been successfully used to analyze PEO end-capped with a RAFT agent [84]. LACCC is one of the few techniques that is exclusively sensitive to modifications of the end group of a polymer molecule when keeping the side groups or repeating units unreacted [85-87]. Figure 4-S8 displays the LACCC traces of two hydroxyl-functionalized PEO of 2,000 and 5,000 g·mol^{-1}, under the critical conditions of PEO (acetonitrile/water 38.8/61.2 at 23 °C); both traces overlay perfectly. By end-capping BPATT onto PEO-OH with 2,000 g·mol^{-1}, a clear shift in the elution volume is observed. The reaction is quantitative and no remaining unmodified PEO$_{2k}$-OH can be detected. In addition, the presence of only one peak proves that no side product is generated during the synthesis of the PEO$_{2k}$-BPATT.

The PEO$_{2k}$-BPATT macro-CTA was used as precursor to generate PEO-*b*-PDMAAm and PEO-*b*-PAA. Acetone was added, especially for PEO-*b*-PAA, to minimize the formation of hydrogen bonding complexes between the acrylic acid and the ethylene oxide units during the reaction. Strong aggregation of the block copolymer was observed in pure water which leads to an uncontrolled polymerization. When a PEO with a longer block is utilized, the hydrogen bonding is more pronounced and block copolymers were synthesized in pure organic solvent (results not shown). For both PEO-*b*-PDMAAm and PEO-*b*-PAA, monomodal and narrow distributions were obtained after polymerization (see Figure 4-5B) and no traces of unreacted PEO was detected by SEC, congruent with the LACCC measurements. The traces are symmetric and no undesired termination was detected even at high conversion, which underpins the high efficiency of this process to generate well-defined block copolymers. All these examples prove the excellent ability of RAFT polymerization initiated under γ-irradiation to generate a large variety of block copolymers in term of monomers composition and molecular weights.

Conclusions

We have demonstrated that RAFT polymerization of several water-soluble acrylic monomers can be carried out in aqueous media under γ-radiation. Under these conditions, the controlled/living characteristics are proven for three CTAs, i.e., TRITT, BPATT, and CPADB (Scheme 4-1) for a large range of monomer/RAFT agents ratios. For most of the monomers, monomodal distributions and the virtual absence of termination or side-reaction was observed even near to quantitative conversion. These specifications allow for the synthesis of precisely tailored block copolymers. Moreover, associated with the benefit of using an environmentally friendly solvent, the polymerization rates in aqueous media are higher and better controlled than in organic solvents, as demonstrated in the case of DMAAm. The living character of the generated macro-RAFT agents was confirmed by subsequent chain extension with various acrylamides. During the block formation process the polydispersity remained low and well-defined block copolymers are generated. Side-reactions and bimolecular termination were observed to a very minor extent. The presented polymerization technique thus constitutes a powerful tool for the straightforward preparation of complex macromolecular architectures constituted of smart polymers.

Acknowledgements

References

[1]   Maitland GC. Current Opinion in Colloid & Interface Science 2000;5(5-6):301-311.

[2]   Wiradharma N, Zhang Y, Venkataraman S, Hedrick JL, and Yang YY. Nano Today 2009;4(4):302-317.

[3]   Stenzel MH. Chemical Communications 2008(30):3486-3503.

[4]   Porfiri MC, Braia M, Farruggia B, Picó G, and Romanini D. Process Biochemistry 2009;44(9):1046-1049.

[5]   Kulkarni S, Schilli C, Grin B, Müller AHE, Hoffman AS, and Stayton PS. Biomacromolecules 2006;7(10):2736-2741.

[6]   Teles FRR and Fonseca LP. Materials Science and Engineering: C 2008;28(8):1530-1543.

[7]   Baskaran D and Müller AHE. Progress in Polymer Science 2007;32(2):173-219.

[8]   Hadjichristidis N, Pitsikalis M, Pispas S, and Iatrou H. Chemical Reviews 2001;101(12):3747-3792.

[9]   Braunecker WA and Matyjaszewski K. Progress in Polymer Science 2007;32(1):93-146.

[10]   Coessens V, Pintauer T, and Matyjaszewski K. Progress in Polymer Science 2001;26(3):337-377.

[11]   Matyjaszewski K and Xia J. Chemical Reviews 2001;101(9):2921-2990.

[12]   Ouchi M, Terashima T, and Sawamoto M. Chemical Reviews 2009;109(11):4963-5050.

[13]   Patten TE, Xia J, Abernathy T, and Matyjaszewski K. Science 1996;272(5263):866-868.

[14]   Hawker CJ, Bosman AW, and Harth E. Chemical Reviews 2001;101(12):3661-3688.

[15]   Sciannamea V, Jerome R, and Detrembleur C. Chemical Reviews 2008;108(3):1104-1126.

[16]   Barner-Kowollik C and Perrier S. Journal of Polymer Science Part A: Polymer Chemistry 2008;46(17):5715-5723.

[17]   Favier A and Charreyre M-T. Macromolecular Rapid Communications 2006;27(9):653-692.

[18]   Lowe AB and McCormick CL. Progress in Polymer Science 2007;32(3):283-351.

[19]   Moad G, Rizzardo E, and Thang SH. Australian Journal of Chemistry 2005;58(6):379-410.

[20]   Barner-Kowollik C. Handbook of RAFT Polymerization 2008;Ed. Barner-Kowollik, Christopher:Wiley-VCH, Weinheim.

[21]   Gauthier MA and Klok H-A. Chemical Communications 2008(23):2591-2611.

[22]   Heredia KL, Bontempo D, Ly T, Byers JT, Halstenberg S, and Maynard HD. Journal of the American Chemical Society 2005;127(48):16955-16960.

[23]   Bontempo D and Maynard HD. Journal of the American Chemical Society 2005;127(18):6508-6509.

[24]   Boyer C, Bulmus V, Liu J, Davis TP, Stenzel MH, and Barner-Kowollik C. Journal of the American Chemical Society 2007;129(22):7145-7154.

[25] Convertine AJ, Lokitz BS, Lowe AB, Scales CW, Myrick LJ, and McCormick CL. Macromolecular Rapid Communications 2005;26(10):791-795.

[26] Convertine AJ, Lokitz BS, Vasileva Y, Myrick LJ, Scales CW, Lowe AB, and McCormick CL. Macromolecules 2006;39(5):1724-1730.

[27] Bai W, Zhang L, Bai R, and Zhang G. Macromolecular Rapid Communications 2008;29(7):562-566.

[28] Shi Y, Liu G, Gao H, Lu L, and Cai Y. Macromolecules 2009;42(12):3917-3926.

[29] Muthukrishnan S, Pan EH, Stenzel MH, Barner-Kowollik C, Davis TP, Lewis D, and Barner L. Macromolecules 2007;40(9):2978-2980.

[30] Bai R-K, You Y-Z, and Pan C-Y. Macromolecular Rapid Communications 2001;22(5):315-319.

[31] Bai R-K, You Y-Z, Zhong P, and Pan C-Y. Macromolecular Chemistry and Physics 2001;202(9):1970-1973.

[32] Quinn JF, Barner L, Davis TP, Thang SH, and Rizzardo E. Macromolecular Rapid Communications 2002;23(12):717-721.

[33] Quinn JF, Barner L, Rizzardo E, and Davis TP. Journal of Polymer Science Part A: Polymer Chemistry 2002;40(1):19-25.

[34] You Y-Z, Bai R-K, and Pan C-Y. Macromolecular Chemistry and Physics 2001;202(9):1980-1985.

[35] Barner L, Quinn JF, Barner-Kowollik C, Vana P, and Davis TP. European Polymer Journal 2003;39(3):449-459.

[36] Barsbay M, Güven O, Stenzel MH, Davis TP, Barner-Kowollik C, and Barner L. Macromolecules 2007;40(20):7140-7147.

[37] Han D-H and Pan C-Y. Macromolecular Chemistry and Physics 2006;207(9):836-843.

[38] Hu Z and Zhang Z. Macromolecules 2006;39(4):1384-1390.

[39] Hua D, Ge X, Tang J, Zhu X, and Bai R. European Polymer Journal 2007;43(3):847-854.

[40] Barner L. Australian Journal of Chemistry 2003;56(10):1091-1091.

[41] Barner L, Perera S, Sandanayake S, and Davis TP. Journal of Polymer Science Part A: Polymer Chemistry 2006;44(2):857-864.

[42] Barsbay M, Güven O, Davis TP, Barner-Kowollik C, and Barner L. Polymer 2009;50(4):973-982.

[43] Zhang X, Li J, Li W, and Zhang A. Biomacromolecules 2007;8(11):3557-3567.

[44] Wang S, Qiang Y, Zhang Z, and Wang X. Colloids and Surfaces A: Physicochemical and Engineering Aspects 2006;281(1-3):156-162.

[45] Hua D, Ge X, Tang J, Zhu X, Bai R, and Pan C. Journal of Polymer Science Part A: Polymer Chemistry 2007;45(14):2847-2854.

[46] Millard P-E, Barner L, Stenzel MH, Davis TP, Barner-Kowollik C, and Müller AHE. Macromolecular Rapid Communications 2006;27(11):821-828.

[47] Liu J, Bulmus V, Herlambang D, L., Barner-Kowollik C, Stenzel MH, and Davis TP. Angewandte Chemie International Edition 2007;46(17):3099-3103.

[48] Hart-Smith G, Lovestead TM, Davis TP, Stenzel MH, and Barner-Kowollik C. Biomacromolecules 2007;8(8):2404-2415.

[49] Lovestead TM, Hart-Smith G, Davis TP, Stenzel MH, and Barner-Kowollik C. Macromolecules 2007;40(12):4142-4153.

[50]   Lai JT, Filla D, and Shea R. Macromolecules 2002;35(18):6754-6756.

[51]   Stenzel MH and Davis TP. Journal of Polymer Science Part A: Polymer Chemistry 2002;40(24):4498-4512.

[52]   Thang SH, Chong YK, Mayadunne RTA, Moad G, and Rizzardo E. Tetrahedron Letters 1999;40(12):2435-2438.

[53]   Pai TSC, Barner-Kowollik C, Davis TP, and Stenzel MH. Polymer 2004;45(13):4383-4389.

[54]   Donovan MS, Lowe AB, Sumerlin BS, and McCormick CL. Macromolecules 2002;35(10):4123-4132.

[55]   Stenzel MH, Zhang L, and Huck W, T. S. Macromolecular Rapid Communications 2006;27(14):1121-1126.

[56]   Sogabe A and McCormick CL. Macromolecules 2009;42(14):5043-5052.

[57]   Kirkland SE, Hensarling RM, McConaughy SD, Guo Y, Jarrett WL, and McCormick CL. Biomacromolecules 2007;9(2):481-486.

[58]   Wang R, McCormick CL, and Lowe AB. Macromolecules 2005;38(23):9518-9525.

[59]   Barner-Kowollik C, Buback M, Charleux B, Coote ML, Drache M, Fukuda T, Goto A, Klumperman B, Lowe AB, Mcleary JB, Moad G, Monteiro MJ, Sanderson RD, Tonge MP, and Vana P. Journal of Polymer Science Part A: Polymer Chemistry 2006;44(20):5809-5831.

[60]   Chernikova E, Morozov A, Leonova E, Garina E, Golubev V, Bui C, and Charleux B. Macromolecules 2004;37(17):6329-6339.

[61]   Favier A, Charreyre M-T, and Pichot C. Polymer 2004;45(26):8661-8674.

[62]   Schilli C, Lanzendörfer MG, and Müller AHE. Macromolecules 2002;35(18):6819-6827.

[63]   Bernard J, Hao X, Davis TP, Barner-Kowollik C, and Stenzel MH. Biomacromolecules 2005;7(1):232-238.

[64]   Zhang L and Stenzel MH. Australian Journal of Chemistry 2009;62(8):813-822.

[65]   Akimoto J, Nakayama M, Sakai K, and Okano T. Journal of Polymer Science Part A: Polymer Chemistry 2008;46(21):7127-7137.

[66]   Arotcarena M, Heise B, Ishaya S, and Laschewsky A. Journal of the American Chemical Society 2002;124(14):3787-3793.

[67]   Relógio P, Charreyre M-T, Farinha JPS, Martinho JMG, and Pichot C. Polymer 2004;45(26):8639-8649.

[68]   Liu J, Nie Z, Gao Y, Adronov A, and Li H. Journal of Polymer Science Part A: Polymer Chemistry 2008;46(21):7187-7199.

[69]   Hentz RR and Sherman WV. Journal of Physical Chemistry 1968;72(7):2635-2641.

[70]   Millard P-E, Mougin Nathalie C, Böker A, and Müller AHE. Controlling the Fast ATRP of N-Isopropylacrylamide in Water. Controlled/Living Radical Polymerization: Progress in ATRP. Washington DC: American Chemical Society, 2009. pp. 127-137.

[71]   Shi Y, Gao H, Lu L, and Cai Y. Chemical Communications 2009(11):1368-1370.

[72]   Gruendling T, Dietrich M, and Barner-Kowollik C. Australian Journal of Chemistry 2009;62(8):806-812.

[73]   Gruendling T, Pickford R, Guilhaus M, and Barner-Kowollik C. Journal of Polymer Science Part A: Polymer Chemistry 2008;46(22):7447-7461.

[74]   Schmaljohann D. Advanced Drug Delivery Reviews 2006;58(15):1655-1670.

[75]   Richter A, Paschew G, Klatt S, Lienig L, Arndt K-F, and Adler H-JP. Sensors 2008;8(1):561-581.

[76]   Dai S, Ravi P, and Tam KC. Soft Matter 2008;4(3):435-449.

[77]   Pelet JM and Putnam D. Macromolecules 2009;42(5):1494-1499.

[78]   Vijayakrishna K, Jewrajka SK, Ruiz A, Marcilla R, Pomposo JA, Mecerreyes D, Taton D, and Gnanou Y. Macromolecules 2008;41(17):6299-6308.

[79]   Deng Z, Bouchékif H, Babooram K, Housni A, Choytun N, and Narain R. Journal of Polymer Science Part A: Polymer Chemistry 2008;46(15):4984-4996.

[80]   Hu YQ, Kim MS, Kim BS, and Lee DS. Journal of Polymer Science Part A: Polymer Chemistry 2008;46(11):3740-3748.

[81]   Liu L, Wu C, Zhang J, Zhang M, Liu Y, Wang X, and Fu G. Journal of Polymer Science Part A: Polymer Chemistry 2008;46(10):3294-3305.

[82]   Albertin L, Stenzel MH, Barner-Kowollik C, and Davis TP. Polymer 2006;47(4):1011-1019.

[83]   Schilli CM, Zhang M, Rizzardo E, Thang SH, Chong YK, Edwards K, Karlsson G, and Müller AHE. Macromolecules 2004;37(21):7861-7866.

[84]   Walther A, Millard P-E, Goldmann AS, Lovestead TM, Schacher F, Barner-Kowollik C, and Müller AHE. Macromolecules 2008;41(22):8608-8619.

[85]   Ahmed H, Trathnigg B, Kappe CO, and Saf R. European Polymer Journal 2009;45(8):2338-2347.

[86]   Gorbunov A and Trathnigg B. Journal of Chromatography A 2002;955(1):9-17.

[87]   Macko T and Hunkeler D. Advances in Polymer Science 2003;163:61-136.
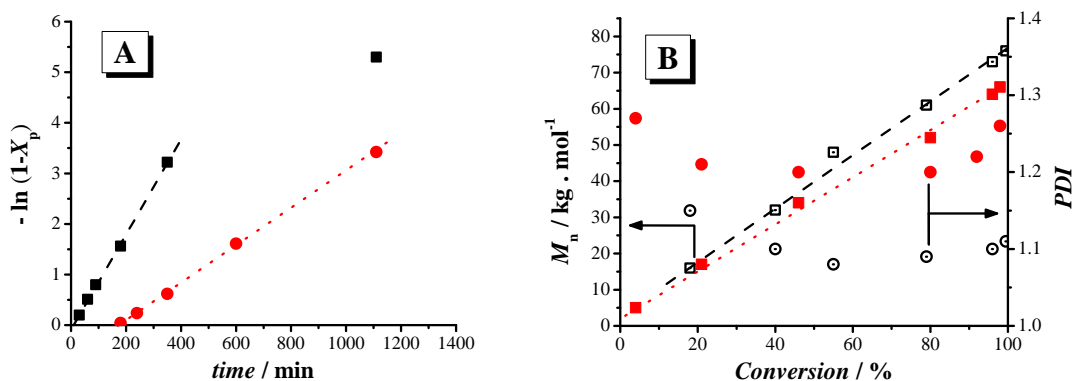
Supporting Information
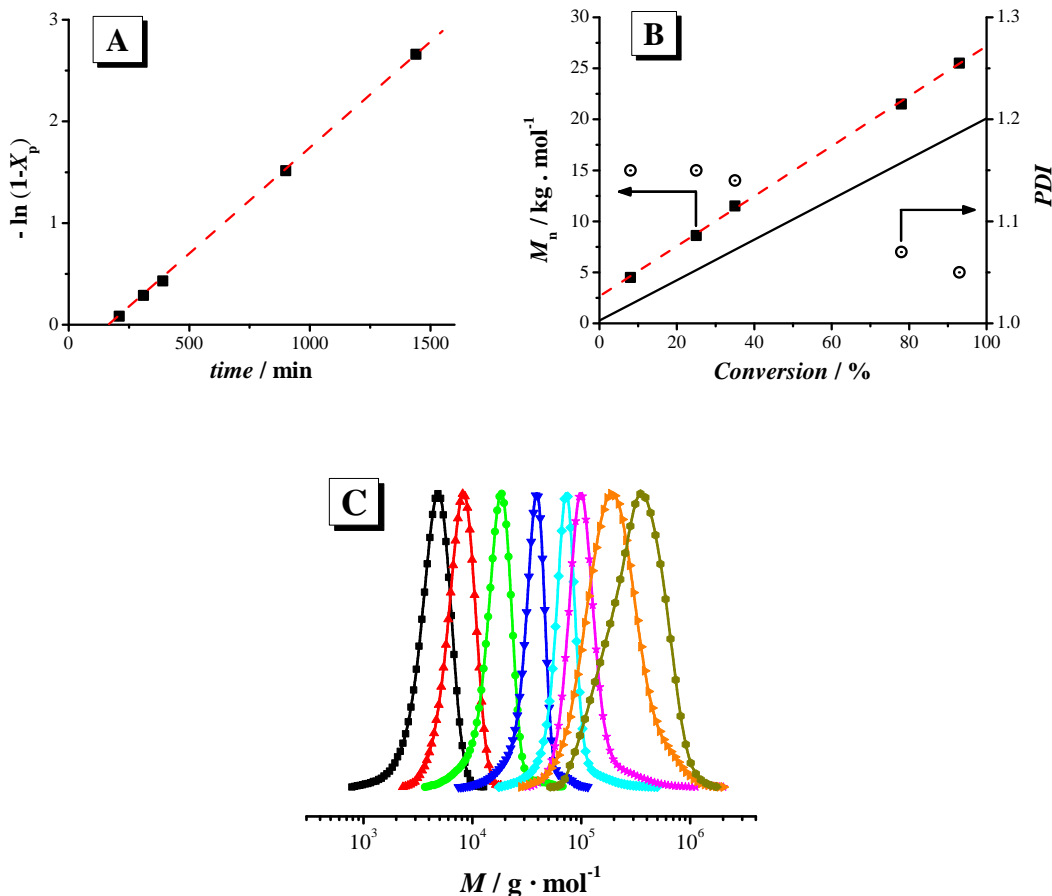
Figure 4-S1. RAFT polymerization of DMAAm under γ-radiation in a mixture water/acetone 85/15 (v/v) at ambient temperature using BPATT as CTA for an initial ratio $[M]_0/[CTA]_0$ of 200 and $[M]_0=1.5$ mol·L^{-1}. (A) First-order time-conversion plot (■), extrapolation (– –). (B) Apparent number-average molecular weight (■) and polydispersity index (⊙) versus monomer conversion measured by SEC using PS standards in DMAc, (– –) extrapolation, (——) theoretical number-average molecular weight evolution determined according to the equation $\overline{M}_{n,\ th} = [M]_0 / [CTA]_0 \cdot X_p \cdot M_M + M_{CTA}$. (C) Dependence of the molecular weight distribution, $w(\log M)$, on the ratio $[DMAAm]_0/[BPATT]_0$. With $[M]_0/[CTA]_0= 60$ (–■–), 100 (–▲–), 200 (–●–), 400 (– ▼–), 800 (–◆–), 1300 (–★–), 2100 (–▶–) and 4000 (–⬣–).

126

Table 4-S1. Influence of the ratio monomer/CTA in the RAFT polymerization of DMAAm ($[M]_0$ = 1.5 mol·L^{-1}) in aqueous media under γ-initiation at ambient temperature with BPATT as RAFT agent.

$\dfrac{[M]_0}{[CTA]_0}$	Acetone %V	Time min	x_p [a] %	$\overline{M}_{n,th}$ [b] kg/mol	$\overline{M}_{n,exp}$ [c] kg/mol	PDI[c]
60	33	1620	93	5.8	4.1	1.14
100	20	1620	95	9.7	7.3	1.09
200	18	1620	97	19.5	16	1.12
400	15	1620	99	39.5	34	1.09
800	15	1290	>99	80	67	1.12
1300	12	1520	>99	129	99	1.17
2100	10	1520	>99	208	161	1.39
3000	10	1260	>99	298	215	1.35
4000	10	165	95	377	268	1.37

[a] Determined by ^{1}H NMR in D_2O. [b] $\overline{M}_{n,th}$ = $[M]_0/[CTA]_0 * X_p * M_M + M_{CTA}$. [c] Apparent number-average molecular weights and *PDIs*, as measured by SEC using PS standards in 2-*N*-methylpyrrolidone (NMP).
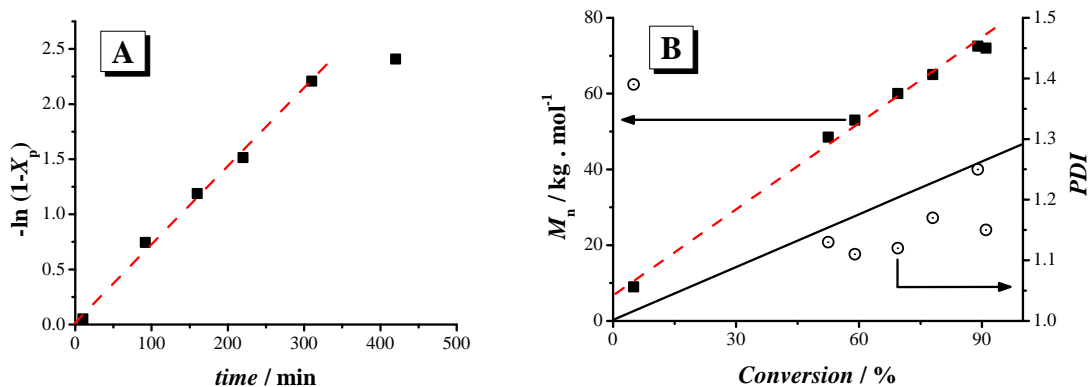
Figure 4-S2. Influence of the solvent on the RAFT polymerization of DMAAm under γ-radiation at ambient temperature using BPATT as CTA for an initial ratio $[M]_0/[CTA]_0$ of 1000 and $[M]_0=1.5$ mol·L^{-1}. (A) First-order time-conversion plot in water-acetone mixture 85/15 (v/v) (■) and in pure dioxane (●). (– –) and (• • •) are extrapolations to guide reader eyes, (B) (⊡) and (⊙) are respectively apparent number-average molecular weight and PDI obtained in water-acetone mixture 85/15 (v/v) and (– –) is the corresponding extrapolation of apparent number-average molecular weights. (■) and (●) are respectively apparent number-average molecular weight and PDI obtained in dioxane and (• • •) is the corresponding extrapolation of apparent number-average molecular weights.

Table 4-S2. Influence of the solvent on the kinetics of DMAAm RAFT polymerization via γ-initiation at ambient temperature with BPATT as RAFT agent with a DMAAm/BPATT ratio of 1000 and $[M]_0 = 1.5$ mol·L^{-1}.

Solvent	$\dfrac{\text{Time}}{\text{min}}$	$\dfrac{x_p{}^{(a)}}{\%}$	$\dfrac{\overline{M}_{n,th}{}^{(b)}}{\text{kg/mol}}$	$\dfrac{\overline{M}_{n,exp}{}^{(c)}}{\text{kg/mol}}$	PDI$^{(c)}$
Acetone 15%	30	18	18	16	1.15
Acetone 15%	60	40	40	32	1.10
Acetone 15%	90	55	55	48	1.08
Acetone 15%	180	79	79	61	1.09
Acetone 15%	350	96	96	73	1.10
Acetone 15%	1110	>99	99	76	1.11
Dioxane	180	4	4.2	5	1.27
Dioxane	240	21	21	17	1.21
Dioxane	350	46	46	34	1.2
Dioxane	600	80	79	52	1.2
Dioxane	1110	96	96	64	1.22
Dioxane	1600	98	97	66	1.26

$^{(a)}$ Determined by ^{1}H NMR in D$_2$O. $^{(b)}$ $\overline{M}_{n,th} = [M]_0/[CTA]_0 * X_p * M_M + M_{CTA}$. $^{(c)}$ Apparent number-average molecular weight and *PDIs*, as measured by SEC using PS standards in 2-*N*-methylpyrrolidone (NMP).

Table 4-S3. Kinetic data of the RAFT polymerization of 2-hydroxyethyl acrylate (HEA) via γ-initiation at ambient temperature with BPATT or TRITT as RAFT agent and $[M]_0$ = 1.5 mol·L^{-1}.

CTA	$\dfrac{[M]_0}{[CTA]_0}$	Acetone %V	Time min	x_p [a] %	$\overline{M}_{n,th}$ [b] kg/mol	$\overline{M}_{n,exp}$ [c] kg/mol	PDI[c]
BPATT	200	25	35	8.5	2.2	7	1.22
BPATT	200	25	210	35	8.4	20.5	1.16
BPATT	200	25	300	60	14.2	32	1.15
BPATT	200	25	390	66	15.6	35.5	1.13
BPATT	200	25	1440	97	22.8	50	1.12
TRITT	400	-	10	5	2.6	9	1.39
TRITT	400	-	90	52	24.5	48	1.13
TRITT	400	-	160	69	33	53	1.11
TRITT	400	-	220	78	36	60	1.12
TRITT	400	-	420	91	43	72	1.15

[a] Determined by ^{1}H NMR in D$_2$O. [b] $\overline{M}_{n,th} = M_M * X_p * [M]_0/[CTA]_0 + M_{CTA}$. [c] Apparent number-average molecular weight and PDIs, as measured by SEC using PS standards in *N,N*-dimethylacetamide (DMAc).
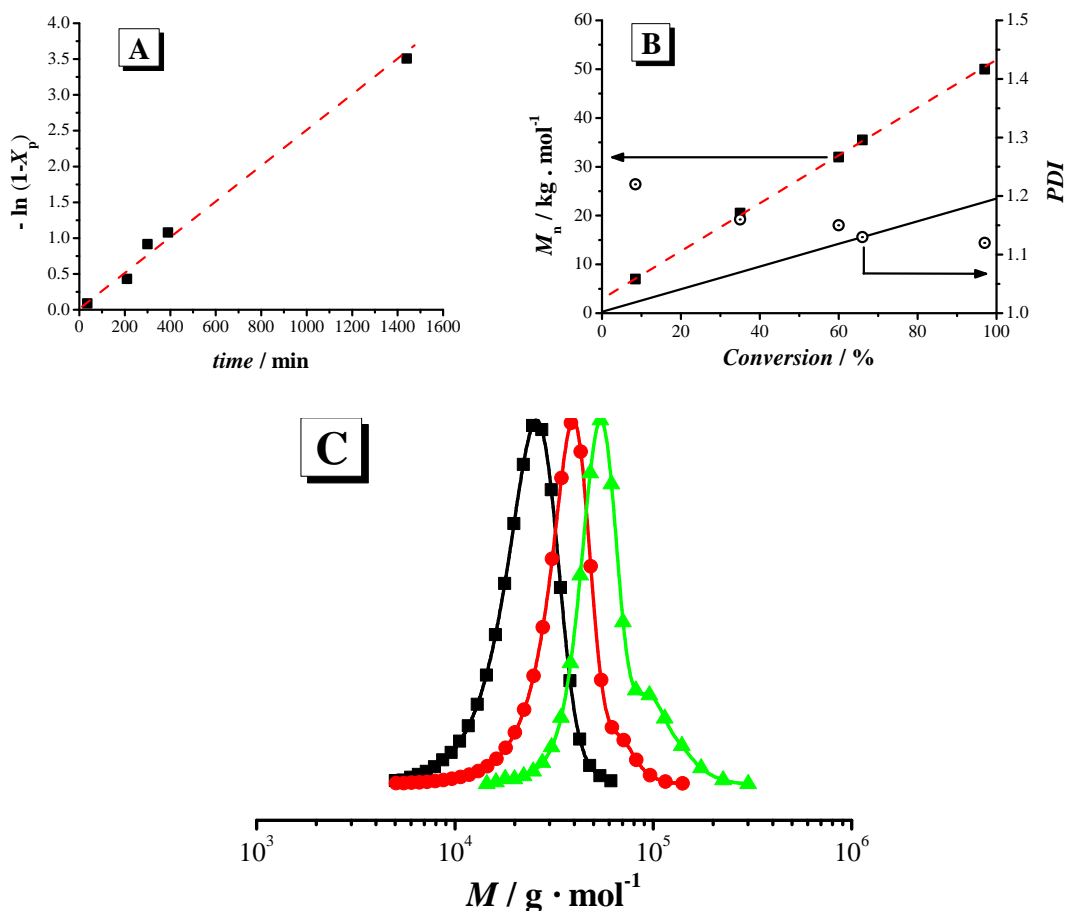
Figure 4-S3. RAFT polymerization of HEA under γ-radiation in a mixture water/acetone 75/25 at ambient temperature using BPATT as CTA for an initial ratio $[M]_0/[CTA]_0$ of 200 and $[M]_0 = 1.5$ mol·L^{-1}. (A) First-order time-conversion plot (■), (– –) extrapolation. (B) Apparent number-average molecular weight (■) and PDI (⊙) versus monomer conversion measured by SEC using PS standards in DMAc, (– –) extrapolation, (——) theoretical number-average molecular weight evolution determined according to the equation $\overline{M}_{n,\,th} = [M]_0 / [CTA]_0 \cdot X_p \cdot M_M + M_{CTA}$. (C) Molecular weight distributions, $w(\log M)$, of PHEA after 35% (■), 60% (●) and 97% of monomer conversion (▲).

Figure 4-S4. RAFT polymerization of HEA under γ-radiation in water at ambient temperature using TRITT as CTA for an initial ratio $[M]_0/[CTA]_0$ of 400 and $[M]_0 = 1.5$ mol·L^{-1}. (A) First-order time-conversion plot (■), (– –) extrapolation. (B) Apparent number-average molecular weight (■) and PDI (⊙) versus monomer conversion measured by SEC using PS standards in DMAc, (– –) extrapolation, (——) theoretical number-average molecular weight evolution determined according to the equation $\overline{M}_{n,\,th}$ $= [M]_0 / [CTA]_0 \cdot X_p \cdot M_M + M_{CTA}$.

Table 4-S4. Influence of the ratio monomer/CTA in the RAFT polymerization of acrylamide (AAm) in aqueous media via γ-initiation at ambient temperature with BPATT as RAFT agent.

$\dfrac{[M]_0}{[CTA]_0}$	$\dfrac{[M]_0}{mol/L}$	$\dfrac{Acetone}{\%V}$	$\dfrac{Time}{min}$	$\dfrac{x_p{}^{(a)}}{\%}$	$\dfrac{\overline{M}_{n,th}{}^{(b)}}{kg/mol}$	$\dfrac{\overline{M}_{n,exp}{}^{(c)}}{kg/mol}$	PDI$^{(c)}$
120	2	41	2720	99	8.7	3.6	1.17
200	2	35	2720	>99	14.5	7.4	1.12
300	2	36	2720	>99	21.5	12	1.16
400	2	27	1620	98	28	17	1.27
500	2	25	2540	>99	36	20	1.24
800	2	22	2720	>99	57	37	1.19
1300	2	18	1620	>99	93	47	1.3
2000	2	15	1620	>99	142	75	1.18
3000	1	10	2720	>99	214	110	1.15
4000	1	10	2720	>99	285	136	1.12
6000	0.5	5	1620	>99	427	162	1.16
10000	0.5	5	1620	>99	711	183	1.19

$^{(a)}$ Determined by ^1H NMR in D_2O. $^{(b)}$ $\overline{M}_{n,th}=M_M*X_p*[M]_0/[CTA]_0+M_{CTA}$. $^{(c)}$ Apparent number-average molecular weights and *PDIs*, as measured by SEC using PEO standards in water.
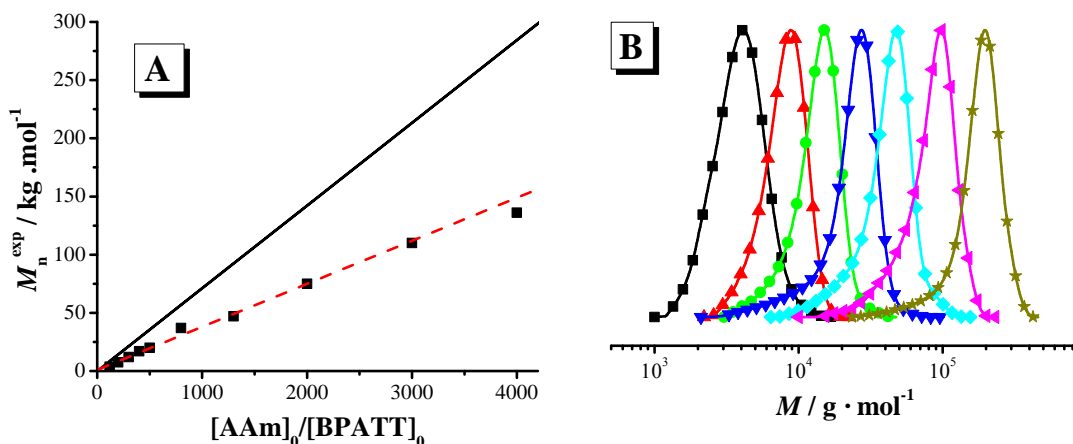
Figure 4-S5. Dependence of the apparent number-average molecular weight and molecular weight distributions, $w(\log M)$, on the ratio $[AAm]_0/[BPATT]_0$ in the RAFT polymerization of AAm under γ-radiation in a mixture water/acetone at ambient temperature using BPATT as CTA. (A) Apparent number-average molecular weight (■) measured by SEC using PEO standards in water versus initial AAm/BPATT ratio, ($-$ $-$) extrapolation and ($-$) theoretical number average molecular weight evolution determined according to the equation $\overline{M}_{n, th} = [M]_0 / [CTA]_0 \cdot X_p \cdot M_M + M_{CTA}$. (B) Dependence of the molecular weight distribution on the ratio $[AAm]_0/[BPATT]_0$. With $[M]_0/[CTA]_0 = 120$ ($-$■$-$), 200 ($-$▲$-$), 300 ($-$●$-$), 500 ($-$▼$-$), 800 ($-$◆$-$), 2000 ($-$◀$-$) and 6000 ($-$★$-$).

Table 4-S5. Influence of the ratio monomer/CTA in the RAFT polymerization of acrylic acid (AA) in aqueous media via γ-initiation at ambient temperature with BPATT as RAFT agent.

$\dfrac{[M]_0}{[CTA]_0}$	$\dfrac{[M]_0}{mol/L}$	$\dfrac{Acetone}{\%V}$	$\dfrac{Time}{min}$	$\dfrac{x_p{}^{(a)}}{\%}$	$\dfrac{\overline{M}_{n,th}{}^{(b)}}{kg/mol}$	$\dfrac{\overline{M}_{n,exp}{}^{(c)}}{kg/mol}$	PDI[c]
42	2.5	50	1620	90	3	8.1	1.09
60	2.5	32	1440	92	4.3	10.4	1.12
100	2.5	26	1440	93	7	14.8	1.15
150	2.5	25	1485	95	10.5	23	1.10
200	2.5	23	1520	97	14.3	31	1.09
250	2.5	22	1410	98	18.9	35	1.07
300	2.5	21	1520	99	21.7	43	1.09
500	2.5	20	1520	>99	36.3	60	1.1
800	1.5	18	1520	>99	57.9	79	1.12
1380	1	15	1410	>99	100	113	1.09
3070	0.7	10	1410	>99	221	152	1.08
10000	0.7	5	1620	>99	711	183	1.19

[a] Determined by ^{1}H NMR in D_2O. [b] $\overline{M}_{n,th} = M_M * X_p * [M]_0/[CTA]_0 + M_{CTA}$. [c] Apparent number-average molecular weight and *PDIs*, as measured by SEC using PEO standards in water.
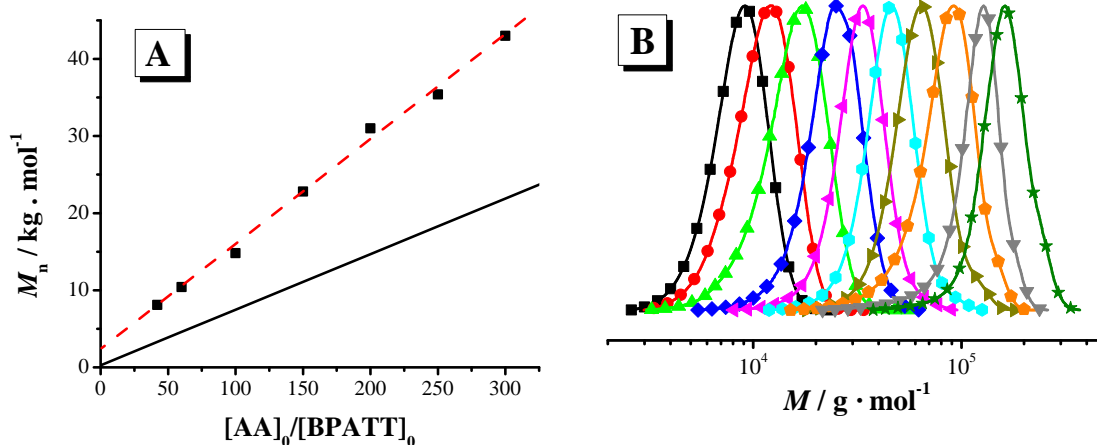
Figure 4-S6. Dependence of the apparent number-average molecular weight and molecular weight distributions, $w(\log M)$, on the ratio $[AA]_0/[BPATT]_0$ in the RAFT polymerization of AA under γ-radiation in a mixture water/acetone at ambient temperature using BPATT as CTA. (A) Apparent number-average molecular weight (■) measured by SEC using PEO standards in water versus initial AAm/BPATT ratio, (– –) extrapolation and (——) theoretical number average molecular weight evolution determined according to the equation $\overline{M}_{n,th} = [M]_0 / [CTA]_0 \cdot X_p \cdot M_M + M_{CTA}$. (B) Dependence of the molecular weight distribution on the ratio $[AA]_0/[BPATT]_0$. With $[M]_0/[CTA]_0 = 42$ (–■–), 60 (–●–), 100 (–▲–), 150 (–◆–), 200 (–◄–), 300 (–●–), 500 (–►–), 800 (–⬟–), 1380 (–▼–) and 3070 (–★–).
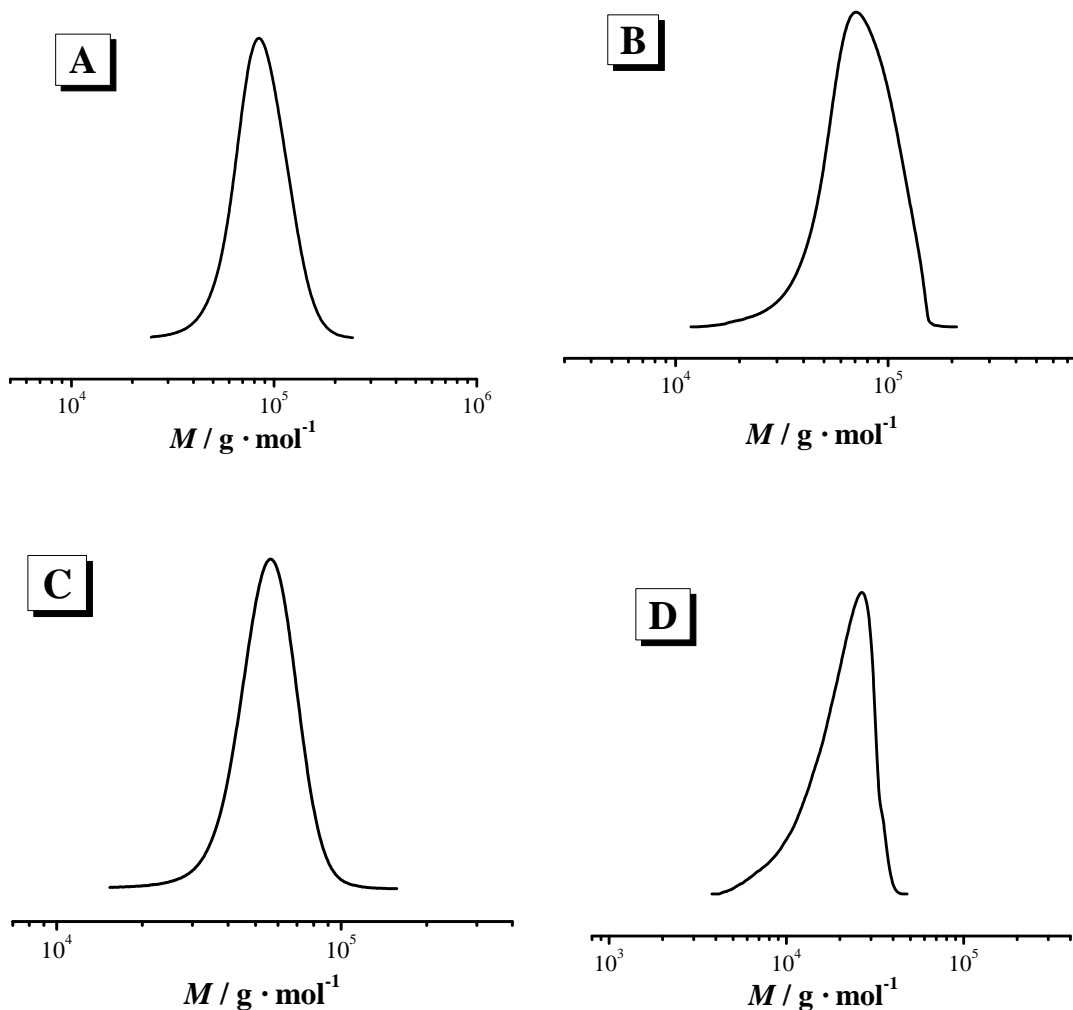
Figure 4-S7. Molecular weight distributions, $w(\log M)$, of polymers obtained by RAFT polymerization at ambient temperature under γ-irradiation based on four different monomers. (A) Poly(N-isopropylacrylamide (PNIPAAm) synthesized in pure water in presence of TRITT for an initial ratio $[M]_0/[CTA]_0$ of 500. (B) Poly(2-acrylamido-2-methylpropane sulfonic acid) (PAMPS) synthesized in mixture of water/acetone in presence of BPATT for an initial ratio $[M]_0/[CTA]_0$ of 200. (C) Poly(oligo(ethylene glycol) methacrylate) (POEGMA) synthesized in mixture of water/acetone in presence of CPADB for an initial ratio $[M]_0/[CTA]_0$ of 100 after 73% of monomer conversion. (D) Poly(2-(dimethylamino)ethyl methacrylate) (PDMAEMA) synthesized in mixture of water/acetone in presence of CPADB for an initial ratio $[M]_0/[CTA]_0$ of 100.
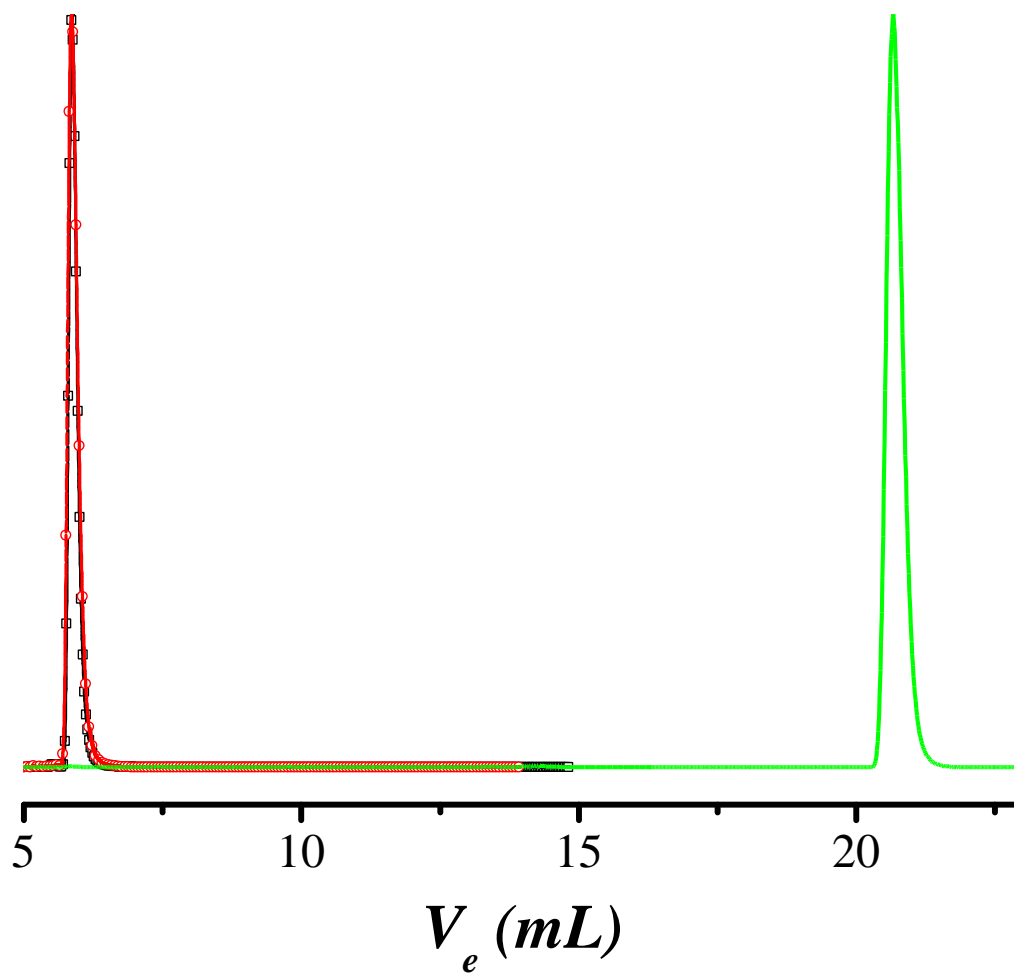
Figure 4-S8. LACCC traces of various end-group-modified PEOs. PEO$_{2k}$-OH (–□–) and PEO$_{5k}$-OH (–O–) were measured in a mixture water/acetonitrile 38.8/61.2 (v/v) at room temperature. A solvent gradient was applied after 16 minutes in order to force elution of PEO$_{2k}$-BPATT (—) and minimize the measurement time.

5. Controlling the Fast ATRP of *N*-Isopropylacrylamide in Water

Pierre-Eric Millard,[1] Nathalie C. Mougin,[2] Alexander Böker,[2,3] Axel H. E. Müller[1]

[1] Makromolekulare Chemie II, [2] Physikalische Chemie II, Universität Bayreuth, D-95440 Bayreuth, Germany,

pierre-eric.millard@basf.com; axel.mueller@uni-bayreuth.de

[3] Current address: Lehrstuhl für Makromolekulare Materialien und Oberflächen and DWI an der RWTH Aachen e.V., RWTH Aachen University, 52056 Aachen, Germany

Abstract

The atom transfer radical polymerization (ATRP) of *N*-isopropylacrylamide (NIPAAm) conducted in pure water at low temperature (4 °C) proceeds in a controlled fashion ($M_n/M_w \leq 1.2$) to near quantitative conversion. Different initiators, ligands, copper halides and ratios of copper (I) to copper (II) were investigated to enhance the control and reduce the termination. The reaction proceeds with a very fast kinetics and a high amount of Cu(II) is needed to slow down the polymerization. The generated polymers were successfully chain extended suggesting that well defined and complex architectures can be obtained.

Introduction

Poly(*N*-isopropylacrylamide) (PNIPAAm) is a well-known thermo-responsive polymer and exhibits a lower critical solution temperature (LCST) of 32°C in water.[1] It assumes a random coil structure (hydrophilic state) below the LCST and a collapsed globular structure (hydrophobic state) above. Because of this sharp reversible transition, this polymer finds a vast array of applications, e.g., in the delivery of therapeutics, bioseparations and biosensors.[2-4] NIPAAm is generally polymerized via free radical polymerization. However, conventional free radical polymerization does not allow control of the molecular weight and to reach a narrow molecular weight distribution (MWD). For sophisticated PNIPAAm-containing materials, defined molecular weight and end-group but also low polydispersity index are highly desirable.

Controlled free radical polymerization techniques have been intensively investigated during the past ten years. Nitroxide-mediated polymerization (NMP),[5-7] reversible addition fragmentation chain transfer (RAFT) polymerization[8-10] and atom transfer radical polymerization (ATRP)[11, 12] are the main radical polymerization techniques that allow the preparation of polymers with defined molecular weights and narrow polydispersities. Several teams have developed strategies to carry out NIPAAm polymerization with a good control. Schulte *et al.* performed this synthesis via NMP with a sterically hindered alkoxyamine and detailed mass spectrometry analysis.[6] In our laboratory we employed RAFT polymerization, in pure water, to obtain high molecular weight PNIPAAm with a very good control and without irreversible termination even at high conversion.[13]

Working in water is a great challenge and exhibits a high potential; it is an environmentally friendly solvent and also allows the presence of biological compounds like viruses, polypeptides or proteins in the polymerization process.[14-17] The synthesis of well-defined bioconjugates for biomedical applications has been an active area of research for many years. However before investigating the synthesis of biohybrids based on PNIPAAm, the homopolymerization in pure water has to be optimized to reach the best possible control. During the past few years, several studies have been realized in this field. Among them, Masci and co-workers were the first to report the successful ATRP of

NIPAAm using a DMF/water mixture. However the experiment performed in pure water failed and a gel was formed immediately after the addition of the catalyst.[18] Because of the low solubility in water of usual ATRP initiators like methyl 2-bromopropionate or ethyl 2-bromoisobutyrate, a pure organic solvent or an aqueous mixture are commonly used yielding satisfactory results. Thus, Stöver and co-workers studied the influence of different alcohols and demonstrated good polymerization control especially in isopropanol by using CuCl/Me$_6$TREN as catalyst system.[19] Nevertheless, to perform the polymerization in pure water another strategy used was to start from a macroinitiator, which is soluble in water. Kim *et al.* have succeeded to prepare linear PEG-*b*-PNIPAAm diblock copolymers and also hydrogel nanoparticles by ATRP of NIPAAm in water at 25 ºC and 50 ºC using a PEG macro-initiator.[20] Another example was recently described by Kizhakkedathu and co-workers. They synthesized mikto-arm star copolymers of poly(di-methylacrylamide) (PDMAAm) and PNIPAAm by sequential RAFT and ATRP from a multi-initiator-functionalized polyglycerol. The ATRP of NIPAAm was conducted after the RAFT polymerization of DMAAm in pure water in the presence of CuCl/Me$_6$TREN. Monomodal and narrow MWD were achieved.[21] Additionally, several studies were performed to polymerize NIPAAm from surfaces, like gold, carbon black, polystyrene (PS) or dextran particles, directly in water.[22-26] Brooks and co-workers prepared PNIPAAm brushes by surface-initiated ATRP from polystyrene particles. High molecular weights (up to 800 kg/mol) and narrow MWD were obtained. [27, 28] However to the best of our knowledge, there is no report on the polymerization of NIPAAm via ATRP in pure water with low molecular weight water-soluble initiators.

Therefore, in the current study, we describe a novel strategy to obtain PNIPAAm via ATRP in pure water by using a fully soluble low molecular weight initiator. We detail the influence of the ratio CuBr/CuBr$_2$ or CuCl/CuCl$_2$ and of the choice of the ligand, to access this polymer with an excellent control, without irreversible termination even at high conversion and demonstrate the livingness of the process by a successful chain extension.

Experimental

Materials

All chemicals and solvents where purchased from Sigma-Aldrich, Acros and Fluka at the highest available purity and used as received unless otherwise noted. NIPAAm (99%, Acros) was purified by two recrystallizations in a mixture of *n*-hexane and benzene. CuBr (98%, Aldrich) and CuCl (97%, Aldrich) were purified by stirring with acetic acid overnight. After filtration, they were washed with ethanol and ether and then dried in vacuum oven. N,N,N',N'',N''-pentamethyldiethylenetriamine (PMDETA; 99%, Aldrich) and 1,1,4,7,10,10-hexamethyltriethylenetetramine (HMTETA; 97%, Aldrich) were distilled before use. Tris(2-dimethylaminoethyl)amine (Me$_6$TREN) was prepared as described in the literature.[29] Water was obtained from a Milli-Q PLUS (Millipore) apparatus.

Polymerization Procedure

 NIPAAm and 2-bromo-isobutyric acid (BIBA) were dissolved in 19 mL of pure water. Then CuBr/CuBr$_2$ or CuCl/CuCl$_2$, respectively were added. Monomer concentrations and monomer/BIBA/Cu(I)/Cu(II)/Ligand ratios are given in Tables 1 and 2. The vial was capped with a rubber stopper to allow addition of the ligand and placed in an ice bath. In a second small flask, 2mL of aqueous ligand solution was prepared. Then both were deoxygenated by purging with nitrogen gas for 15 min. Afterwards 1mL of ligand solution was withdrawn with a degassed syringe and placed in the polymerization flask to start the reaction. The reaction was stopped after pre-selected time and quenched with air. PNIPAAm samples were purified by freeze-drying to remove the solvent. Then the solid was dissolved in dichloromethane and passed through a silica gel column to remove the ATRP catalyst. Finally PNIPAAm was precipitated from this solution into a 20-fold excess of diethyl ether before further analysis The conversion of each sample was determined directly after freeze-drying by ^{1}H-NMR (in CDCl$_3$) from the relative integration of peaks associated with the monomer in relation to those associated with the polymer. For NIPAAm, the monomer peak chosen as reference was its vinyl peak at δ =

5.72-5.8 ppm (dd, C$\underline{H}$(H)=), which was compared to the proton peak of the isopropyl group at 4.1-3.8 ppm (m, C$\underline{H}$(CH$_3$)$_2$) of the polymer and monomer.

Characterization

Polymers were characterized by size exclusion chromatography (SEC) using a 0.05 M solution of LiBr in 2-*N*-methylpyrrolidone (NMP) as eluent. PSS GRAM columns (300 mm * 8 mm, 7 μm): 10^3, 10^2 Å (PSS, Mainz, Germany) were thermostated at 70 °C. A 0.4 wt % (20 μL) polymer solution was injected at an elution rate of 0.72 mL/min. RI and UV (λ = 270 nm) were used for detection. Polystyrene standards were used to calibrate the columns, and methyl benzoate was used as an internal standard. ^{1}H-NMR spectra were recorded on a Bruker AC-25 spectrometer in CDCl$_3$ (reference peak δ = 7.26 ppm) at room temperature.

Results and Discussion

Homopolymerization of *N*-isopropylacrylamide

N-Isopropylacrylamide (NIPAAm) was polymerized in the presence of 2-bromo-isobutyric acid (BIBA). This initiator was mainly chosen due to its high solubility in water. In addition, it has the advantage to introduce a carboxylic group to allow protein modification by active ester chemistry or post-polymerization modification.[16] Common ATRP initiators like methyl 2-bromopropionate and ethyl 2-bromoisobutyrate were also used but the resulting polymers always exhibited a high polydispersity index (PDI > 1.7) and a multimodal distribution (results not shown). This absence of control can be explained by the very poor solubility of these initiators in water which leads to a slow initiation. Another important parameter allowing for a successful polymerization is the reaction temperature. When polymerizations were carried out at room temperature with Cu(I) or with a high ratio Cu(I)/Cu(II), kinetics were extremely fast, typically less than a minute for full conversion. This very high rate of polymerization was also observed by Narumi *et al.* in DMF/water at 20 ºC. In this less polar solvent mixture, conversions of 98% where obtained after 30 min only.[30] Moreover, due to the exothermic character of the propagation, the temperature in the medium increased drastically which accelerated the rate of polymerization but more important, the temperature raised at least above the LCST of PNIPAAm, leading to polymer collapse and a total loss of control. This increase in temperature during the polymerization of NIPAAm via ATRP was already described by Kuckling and co-workers for a DMF/water system. However for this solvent mixture, an increase of 5-10 K was observed which was not sufficient to observe the collapse of PNIPAAm.[31] To avoid this problem, a rather low monomer concentration, typically $[M]_0 = 0.5$ M and an ice bath were used to control the heat evolution. Under these conditions all polymerizations were successfully achieved even in the absence of Cu(II).

A suitable choice of the ligand is crucial to reach a good control of NIPAAm polymerization.[32] Inspection of the data given in Table 5-1 clearly indicates that N,N,N',N'',N''-pentamethyldiethylenetriamine (PMDETA) and 1,1,4,7,10,10-hexamethyltriethylenetetramine (HMTETA) are not the right choice to obtain a polymer with a low polydispersity when CuCl$_2$ is not present in the media. The SEC profiles of

the polymers made in the presence of PMDETA and HMTETA with CuCl only is strongly skewed towards low molecular weights, which might indicate a slow initiation step. Moreover, the polymers have a higher molecular weight as compared to that made in presence of Me_6TREN. A reasonable explanation is a low efficiency of this initiator in presence of these two former ligands. This problem was already described in the case of BIBA.[33] By adding Cu(II) to the system, for PMDETA and HMTETA, kinetics slow down and the molecular weight distributions of the resulting polymers become sharper but still not below 1.2 (results not shown). Under these conditions, these two ligands do not seem to be suitable to obtain PNIPAAm with a good control. Me_6TREN globally yields the best results for the different ratios of $[CuCl]_0/[CuCl_2]_0$ employed and was the ligand of choice for the continuation of the study. This ligand is known to be very active for ATRP compared to HMTETA and PMDETA.[32] Unfortunately it is also highly sensitive to oxygen which can drastically slow down the kinetics. Hence, kinetic reproducibility was difficult to achieve. However, the ATRP of NIPAAm in water did not exhibit any or less than few percents of termination even at full conversion. This property allowed us to solve the reproducibility problem. Therefore the reactions were always carried out at longer times than normally required to follow the kinetics, and then well defined polymers with narrow molecular weight distribution at full conversion were obtained.

Table 5-1. Influence of the ligand on the ATRP of NIPAAm in water at 4 °C.[a]

Ligand	Time (min)	$M_{n,exp}$[b] (kg/mol)	PDI[b]
PMDETA	95	32	1.79
HMTETA	130	29	1.94
Me_6TREN	76	23	1.30

[a] $[M]_0 = 0.5$ mol*L^{-1} with $[M]_0/[BIBA]_0/[CuCl]_0/[L]_0 = 100/1/1/1$. Monomer conversion, determined by ^{1}H NMR in $D_2O > 99\%$. The theoretical-number-average molecular weight, evaluated according to the formula, $M_n^{th} = M_M*conv*[M]_0/[BIBA]_0 + M_{BIBA} = 11.5$ kg/mol. [b] measured by size-exclusion chromatography (SEC) using polystyrene standards in 2-N-methylpyrrolidone (NMP) as eluent.

The influence of the catalyst system was also investigated by comparing CuCl- and CuBr-based systems at different ratios of [Cu(I)]/[Cu(II)]. The results are summarized in Table 5-2. In all cases CuBr provides a narrower molecular weight distribution of the resulting polymer than CuCl for the ATRP of NIPAAm in water, independent of the ratio [Cu(I)]/[Cu(II)] used. This effect is generally observed for acrylate polymerization.[34] When CuCl is used the low rate of activation of the dormant species combined with the high reactivity of the secondary propagating radical lead to a lower control as compared to CuBr. In the case of the bromide system, already without addition of $CuBr_2$ to the reaction mixture, the polydispersity index is lower than 1.2. Here, already the addition of only a small amount of $CuBr_2$ leads to a drop in PDI to around 1.1. This proves the excellent ability of this system to polymerize NIPAAm in a controlled fashion. For the chloride-based ATRP the MWD is broader but narrows by raising the amount of $CuCl_2$. For both catalytic systems and for all the different ratios of [Cu(I)]/[Cu(II)], the SEC traces are monomodal and symmetrical. However, at full monomer conversion, especially for a low concentration of $CuBr_2$, some SEC traces of CuBr mediated ATRP show a small amount of coupling which is the predominant termination reaction for acrylamide-based monomers. This termination was never detected even at full conversion in the case of CuCl mediated ATRP.

Based on the above results, the CuBr-based catalyst with BIBA as initiator was chosen to study the kinetics due to its excellent ability to control the polymerization of NIPAAm in water at low temperature. The results are summarized in Figure 5-1. The polymerization was carried out in presence of Me_6TREN and with a ratio [CuBr]/[$CuBr_2$] = 1/1. This relatively high amount of $CuBr_2$ is needed to slow down the kinetics which otherwise proceeds in less than a minute. This very fast ATRP in water was already observed for several types of monomers like poly(ethylene glycol) methacrylate, sodium 4-vinylbenzoate or dimethylacrylamide.[35] Tsarevsky *et al.* explained this phenomenon by some side reactions which occur during the ATRP in protic media, such as reversible dissociation and substitution (by a solvent or possibly by a polar monomer molecule) of the halide ligand from the deactivating Cu(II) complex. These reactions lead to inefficient deactivation and therefore to faster polymerizations with unsatisfactory control.[36]

Table 5-2. Influence of the ratio Cu(I)/Cu(II) on the ATRP of NIPAAm with Me_6TREN as ligand in water at 4 °C[a]

Catalyst	$[BIBA]_0/[Cu(I)]_0/[Cu(II)]_0/[L]_0$	Time min	$M_{n,exp}^b$ kg/mol	PDI[b]
$CuCl/CuCl_2$	1/1/0/1	76	23	1.30
$CuCl/CuCl_2$	1/0.6/0.4/1	85	16	1.25
$CuCl/CuCl_2$	1/0.5/0.5/1	90	16.5	1.20
$CuBr/CuBr_2$	1/1/0/1	60	17	1.19
$CuBr/CuBr_2$	1/0.85/0.15/1	100	18.5	1.08
$CuBr/CuBr_2$	1/0.7/0.3/1	115	18	1.08
$CuBr/CuBr_2$	1/0.6/0.4/1	130	19	1.09

[a] $[M]_0 = 0.5$ mol*L^{-1} and $[M]_0/[BIBA]_0=100$. Monomer conversion, determined by ^{1}H NMR in D_2O > 99%. The theoretical-number-average molecular weight, evaluated according to the formula, $M_n^{th}=M_M*conv*[M]_0/[BIBA]_0+M_{BIBA}$ = 11.5 kg/mol. [b] measured by size-exclusion chromatography (SEC) using polystyrene standards in 2-*N*-methylpyrrolidone (NMP) as eluent.
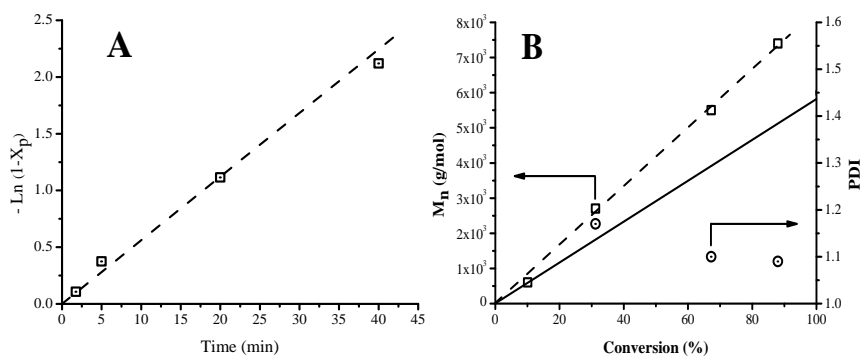
Figure 5-1. Kinetics of ATRP of NIPAAm (0.5 M) in water at 4 °C with $[M]_0/[BIBA]_0/[CuBr]_0/[CuBr_2]_0/[Me_6TREN]_0$ = 50/1/0.5/0.5/1. (A) First-order time-conversion plot. (B) Molecular weight and polydispersity index vs conversion. (——) theoretical number average molecular weight.

In our case the first-order time-conversion plot (Figure 5-1A) is linear at least up to 90% and an apparent first-order dependence on monomer concentration can be found

during the major part of the polymerization. This tendency indicates the absence of side reactions. Figure 5-1B depicts the molecular weight and the polydispersity index evolution with the conversion. It is obvious that the molecular weight increases linearly with conversion demonstrating the controlled fashion of the process. The difference between the theoretical and the experimental molecular weight can be assigned to the calibration of the SEC on the basis of polystyrene standards. The resulting polydispersity indices are low (PDI < 1.2) and decrease with the conversion. Even at high conversions (close to 90%), the PDI is low (< 1.1). Moreover the SEC traces (not shown here) are always unimodal and symmetrical and do not show any trace of termination by recombination of growing radicals.

To prove the versatility of this process, different molecular weights of PNIPAAm were synthesized. Figure 5-2 indicates that an increase of the ratio of monomer/initiator leads (at a comparable conversion) to a linear increase of the molecular weight. The SEC traces display unimodal and narrow peaks. Moreover a large range of molecular weights from rather low (DP = 30) to rather high (DP = 400) were achieved. In all cases the PDI remains below 1.2 at full conversion, without any trace of termination. All these criteria indicate the controlled fashion of the ATRP of NIPAAm in water.
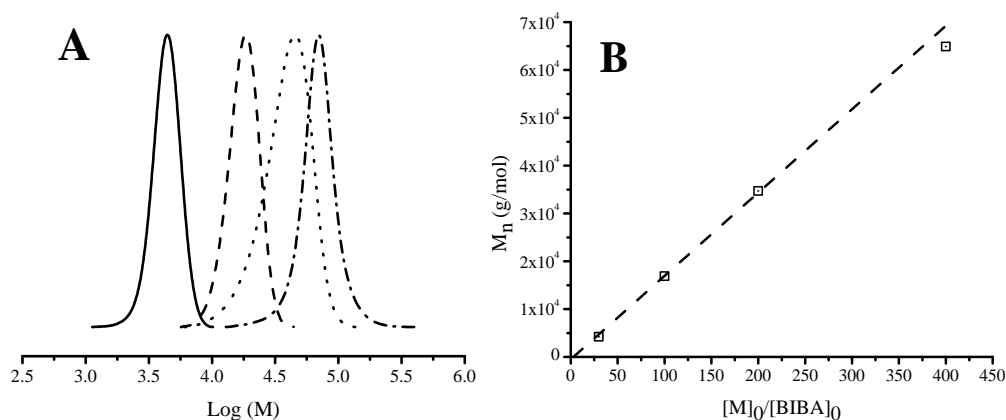
Figure 5-2. Influence of the ratio [monomer]/[initiator] for the ATRP of NIPAAm (0.5 M) in water at 4 °C with $[BIBA]_0/[CuBr]_0/[CuBr_2]_0/[Me_6TREN]_0 = 1/0.7/0.3/1$. (A) MWD at a ratio $[M]_0/[BIBA]_0 = $ (——) 30, (– –) 100, (• • •) 200, (– • –) 400. (B) Dependence of M_n on the ratio $[M]_0/[BIBA]_0$

Chain Extension Experiments

To further demonstrate the livingness of the process a chain extension of PNIPAAm was carried out. The initial block was obtained by using a ratio $[M]_0/[BIBA]_0/[CuCl]_0/[CuCl_2]_0/[Me_6TREN]_0$ of 120/1/1.6/0.4/2 with a NIPAAm concentration of 0.5 M. Then the block copolymer was synthesized by sequential addition after 38 min of a degassed aqueous solution of monomer (0.5 M) without purification of the macro-initiator. A CuCl-based catalyst was chosen to perform the reaction to avoid any termination. Indeed, in water, bromide-terminated polymers can be sensitive to halogen abstraction by nucleophilic substitution. Then with CuCl the resulting polymer-halide bound C-Cl is much stronger and there is less possibility of halogen abstraction. We also sometimes observed a tiny amount of termination by recombination of growing radical in the ATRP of NIPAAm with CuBr at full conversion. This termination was not really detected on any SEC traces in the case of CuCl catalyst. Because, for the chain extension, we used a strategy of direct addition of a second monomer solution, the first block has to be polymerized up to full conversion. Therefore to reduce these two different types of termination CuCl combined with Me_6TREN was selected as catalyst system.
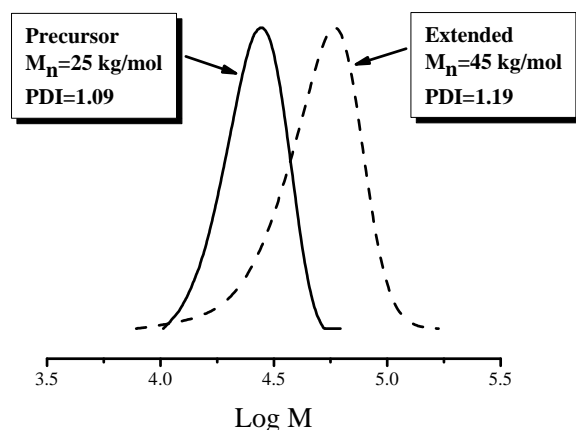
Figure 5-3. Molecular weight distribution for the chain extension of PNIPAAm by ATRP in water at 4°C. $[M]_0=0.5$ M, $[M]_0/[PNIPAAm_{120}-Cl]_0=300$. (——) precursor, (– –) extension after 40% conversion.

Figure 5-3 depicts the MWDs during the process. As for the homopolymerization, even for a full conversion of the first block, throughout chain extension, there is no

appearance of a shoulder due to the termination by recombination. However a small tailing can be observed which might be due to a loss of terminal chloride of the precursor. Nevertheless, such evidence combined with a low PDI suggests that the large majority of the PNIPAAm precursor retained the functionality and was available for subsequent chain extension.

Conclusions

We have demonstrated for the first time that ATRP of NIPAAm can be carried out in water at low temperature by using a low molecular weight water-soluble initiator. We also showed that by choosing an appropriate ligand and catalyst system a well-controlled polymerization can be achieved. Under these conditions, the controlled/living characteristics were proven when BIBA, CuBr/CuBr and Me$_6$TREN were used for a large range of monomer/initiator ratios. Moreover, even at full conversion the polymerization control is maintained. The living character of the generated PNIPAAm was confirmed by subsequent chain extension directly by addition of a second portion of degassed monomer solution. During chain extension, no side reactions were observed and the polydispersity remained low throughout the polymerization. Finally, due to the terminal carboxylic end group present on the polymer, post polymerization treatments like protein conjugation are possible. Given the environmental benefits associated with aqueous polymerizations at low temperature and the possibility to tailor a large variety of block lengths, we believe that the method reported in the present study represents a significant advance in the ability to prepare complex architectures based on this smart polymer. Results of the conjugation of PNIPAAm to proteins will be given in subsequent publications.

Acknowledgements

References

1 H. G. Schild, *Progress in Polymer Science*, 1992, **17**, 163.

2 D. C. Coughlan and O. I. Corrigan, *Int J Pharm*, 2006, **313**, 163.

3 S. Kulkarni, C. Schilli, A. H. E. Müller, A. S. Hoffman, and P. S. Stayton, *Bioconjugate Chemistry*, 2004, **15**, 747.

4 C.-C. Yang, Y. Tian, A. K. Y. Jen, and W.-C. Chen, *Journal of Polymer Science, Part A: Polymer Chemistry*, 2006, **44**, 5495.

5 C. J. Hawker, A. W. Bosman, and E. Harth, *Chemical Reviews (Washington, D. C.)*, 2001, **101**, 3661.

6 T. Schulte, K. O. Siegenthaler, H. Luftmann, M. Letzel, and A. Studer, *Macromolecules*, 2005, **38**, 6833.

7 A. Studer and T. Schulte, *Chemical Record*, 2005, **5**, 27.

8 A. Favier and M.-T. Charreyre, *Macromolecular Rapid Communications*, 2006, **27**, 653.

9 G. Moad, Y. K. Chong, A. Postma, E. Rizzardo, and S. H. Thang, *Polymer*, 2005, **46**, 8458.

10 M. J. Monteiro, *Journal of Polymer Science, Part A: Polymer Chemistry*, 2005, **43**, 3189.

11 K. Matyjaszewski, J. Spanswick, and B. S. Sumerlin, *Living and Controlled Polymerization: Synthesis, Characterization and Properties of the Respective Polymers and Copolymers*, 2006, 1.

12 K. Matyjaszewski and J. Xia, *Chemical Reviews (Washington, D. C.)*, 2001, **101**, 2921.

13 P.-E. Millard, L. Barner, M. H. Stezel, D. T. P., C. Barner-Kowollik, and A. H. E. Müller, *Macromolecular Rapid Communications*, 2006, **27**, 821.

14 K. L. Heredia, D. Bontempo, T. Ly, J. T. Byers, S. Halstenberg, and H. D. Maynard, *J. Am. Chem. Soc.*, 2005, **127**, 16955.

15 X. Lou, C. Wang, and L. He, *Biomacromolecules*, 2007, **8**, 1385.

16 P.-E. Millard, N. C. Mougin, A. Böker, and A. H. E. Müller, *Polymer Preprints (American Chemical Society, Division of Polymer Chemistry)*, 2008, **49**, 121.

17 N. C. Mougin, A. H. E. Müller, and A. Böker, *PMSE Preprints*, 2008, **99**, 713.

18 G. Masci, L. Giacomelli, and V. Crescenzi, *Macromolecular Rapid Communications*, 2004, **25**, 559.

19 Y. Xia, X. Yin, N. A. D. Burke, and H. D. H. Stöver, *Macromolecules*, 2005, **38**, 5937.

20 K. H. Kim, J. Kim, and W. H. Jo, *Polymer*, 2005, **46**, 2836.

21 K. Ranganathan, R. Deng, R. K. Kainthan, C. Wu, D. E. Brooks, and J. N. Kizhakkedathu, *Macromolecules (Washington, DC, United States)*, 2008, **41**, 4226.

22 J. Cheng, L. Wang, J. Huo, H. Yu, Q. Yang, and L. Deng, *Journal of Polymer Science, Part B: Polymer Physics*, 2008, **46**, 1529.

23 D. J. Kim, J.-y. Heo, K. S. Kim, and I. S. Choi, *Macromolecular Rapid Communications*, 2003, **24**, 517.

24 D. J. Kim, S. M. Kang, B. Kong, W.-J. Kim, H.-j. Paik, H. Choi, and I. S. Choi, *Macromolecular Chemistry and Physics*, 2005, **206**, 1941.

25 V. Mittal, N. B. Matsko, A. Butte, and M. Morbidelli, *European Polymer Journal*, 2007, **43**, 4868.

26   A. Mizutani, A. Kikuchi, M. Yamato, H. Kanazawa, and T. Okano, *Biomaterials*, 2008, **29**, 2073.

27   J. N. Kizhakkedathu, K. R. Kumar, D. Goodman, and D. E. Brooks, *Polymer*, 2004, **45**, 7471.

28   J. N. Kizhakkedathu, R. Norris-Jones, and D. E. Brooks, *Macromolecules*, 2004, **37**, 734.

29   M. Ciampolini and N. Nardi, *Inorg. Chem.*, 1966, **5**, 41.

30   A. Narumi, K. Fuchise, R. Kakuchi, A. Toda, T. Satoh, S. Kawaguchi, K. Sugiyama, A. Hirao, and T. Kakuchi, *Macromolecular Rapid Communications*, 2008, **29**, 1126.

31   S. Mendrek, A. Mendrek, H.-J. Adler, W. Walach, A. Dworak, and D. Kuckling, *Journal of Polymer Science, Part A: Polymer Chemistry*, 2008, **46**, 2488.

32   W. Tang and K. Matyjaszewski, *Macromolecules*, 2006, **39**, 4953.

33   X. Zhang, J. Xia, S. G. Gaynor, and K. Matyjaszewski, *Polymeric Materials Science and Engineering*, 1998, **79**, 409.

34   W. A. Braunecker and K. Matyjaszewski, *Progress in Polymer Science*, 2007, **32**, 93.

35   S. Perrier and D. M. Haddleton, *Macromolecular Symposia*, 2002, **182**, 261.

36   N. V. Tsarevsky, T. Pintauer, and K. Matyjaszewski, *Macromolecules*, 2004, **37**, 9768.

6. Poly(N-Isopropylacrylamide)-b-Poly(Acrylic Acid) Shell Cross-Linked Micelles Formation and Application to the Synthesis of Metal-Polymer Hybrids

Pierre-Eric Millard,[1] Jerome J. Crassous,[2] Adriana M. Mihut,[2] Jiayin Yuan[1] and Axel H. E. Müller[1]

[1]Makromolekulare Chemie II, [2]Physikalische Chemie I, Universität Bayreuth, 95440 Bayreuth, Germany,

pierre-eric.millard@basf.com; axel.mueller@uni-bayreuth.de
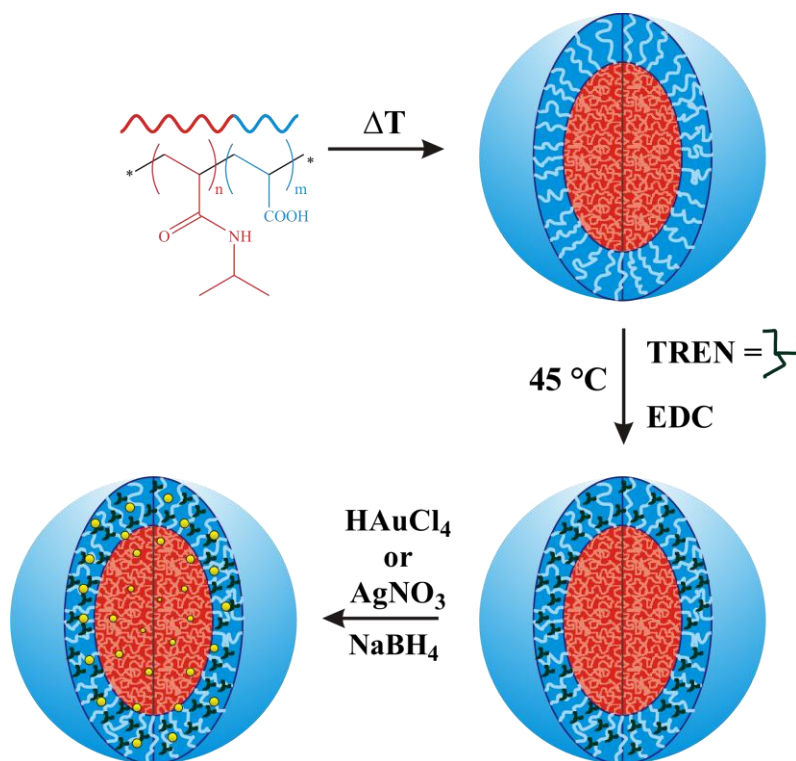
In preparation

Abtract

The self-assembly of two different poly(N-isopropylacrylamide)-b-poly(acrylic acid) multi-responsive block copolymers, PNIPAAm$_{2000}$-b-PAA$_{300}$ and PNIPAAm$_{2000}$-b-PAA$_{500}$, was investigated at elevated temperature in neutral water. The PAA coronas of the obtained spherical micelles were cross-linked at 45 ºC via amidification of the carboxylic groups using tris(2-aminoethyl)amine (TREN). These particles were subsequently utilized as nano-carriers for silver or gold nanoparticles obtained via *in situ* reduction of silver nitrate or tetrachloroauric acid by sodium borohydride. The generated silver-PNIPAAm$_{2000}$-b-PAA$_{300}$ nano-hybrids were tested as catalyst for the reduction of 4-nitrophenol suggesting that these responsive particles can be attractive for catalysis applications.

Introduction

Double hydrophilic block copolymers (DHBCs) can play an important role in diverse fields such as drug delivery, biosensing, soft actuators/valves, and catalysis among others.[1-7] When one or both blocks are made from a responsive polymer, these copolymers can form colloidal aggregates in solution. Responsive or "smart" polymers respond with large property changes to small environmental stimuli. [8-10] This type of polymers finds a vast array of biomedical applications in the delivery of therapeutics, bioseparations and biosensors.[9,11-15] Two of them, i.e. poly(*N*-isopropylacrylamide) (PNIPAAm) and poly(acrylic acid) (PAA), have been intensively investigated for their responsive properties.[16] PNIPAAm exhibits a lower critical solution temperature (LCST) in aqueous solution and a sharp reversible phase transition is observed at 32 °C in water.[17] PAA responds on changes in pH and ionic strength by changing coil dimensions and solubility.[18,19] Combining these two polymers in PNIPAAm-*b*-PAA block copolymers generates a material which responses to several stimuli and has micellisation properties depending on the solvent, temperature, pH, block lengths and salt concentration.[20,21]

To obtain this diblock copolymer or other DHBCs, controlled/"living" radical polymerization[22] including nitroxide-mediated polymerization,[23] atom transfer radical polymerization (ATRP),[24] and reversible addition-fragmentation chain transfer (RAFT) polymerization [25] are the most effective techniques. Although each technique has its own characteristics and advantages, RAFT is arguably the most versatile since it is compatible with most functional monomers under conditions that are similar to conventional free radical polymerization. In the particular case of PNIPAAm-*b*-PAA, we developed in our laboratory two different strategies to obtain this block copolymer. Originally the synthesis was performed via thermal initiation using an azo-initiator under RAFT control in organic solvents.[20] However more recently, we found a very interesting pathway to obtain this material via RAFT polymerization in aqueous media with γ-initiation.[26] This technique allows us access to a large number of hydrophilic homopolymers and block

copolymers with an excellent control, with an absence or a very tiny amount of termination even at very high conversion.

An important consideration concerning the practical applications of responsive DHBCs is the stability of the micelles in solution. This is a key property for example in drug delivery or catalytic application where the overall material concentration is really low. The micelles will inevitably disintegrate into unimers when the copolymer concentration falls below the critical micelle concentration (cmc). For therapeutics application, this will lead to premature release of the active compounds.[27] To solve this handicap, different research groups developed cross-linking procedures to maintain the micelle configuration. We can distinguish two types of cross-linked micelles depending on the location of the network: the core[28] or the shell cross-linked[29] (SCL) micelles. Many new potential applications were investigated included, as already mentioned, targeted drug delivery but also emulsification, sequestration of metabolites and entrapment of environmental pollutants.[3,30-37] To date, several methods have been employed for shell cross-linking. 1,2-Bis(2-iodoethoxy)ethane has been used by Armes and co-workers to cross-link 2-(dimethylamino)ethyl methacrylate residues via quaternization.[38] Wooley's group has reported carbodiimide coupling chemistry to link carboxylic acid groups via diamines.[39] Moreover they developed a cross-linking based on click chemistry.[40] Liu et al. utilized divinyl sulfone to successfully cross-link hydroxylated blocks.[41] Other cross-linking methods including UV-induced coupling[42] and ionically induced polyelectrolyte complexation[43] have also been reported.

Cross-linked micelles are an interesting class of materials to generate hybrid inorganic-organic materials.[41,44-46] Indeed gold, silver, and other noble metal nanoparticles have attracted a great interest in recent years because of their unique optical, electronic and catalytic properties.[47-51] They find their origin in the particle size, the shape and the interparticle distance and their properties are derived from quantum confinement effects and from the large surface areas relative to the volume of the nanoparticles.[52,53] Therefore these materials have totally different properties compared to the bulk metal as already widely demonstrated in both experimental and theoretical investigations. These nanoparticles are commonly prepared from salt precursors using various chemical and photochemical reduction methods in solution.[54-56] However without

stabilization metal nanoparticles create insoluble aggregates that cannot be redispersed. To improve their stability as well as their handling many strategies were created like ligands,[57,58] homo-[59,60] and block copolymers,[61-65] hydrogels[66-68] and spherical[69,70] and cylindrical[71,72] polyelectrolyte brushes protection among other. For this particular reason, SCMs could be very promising containers for nanoparticles because they can act as nanoreactors during the synthesis and also as robust vessels to support inorganic materials. Therefore we believe these nano-hybrids can find many applications in electronics, magnetic, optical, spectroscopic, catalytic and biomedical materials.

In this study, we report a novel type of SCM based on PNIPAAm-*b*-PAA block copolymers. The cross-linking was performed at 45 ºC when the PNIPAAm block is collapsed by using a new multifunctional cross-linker. The evidence of reaction was demonstrated by NMR, dynamic light scattering (DLS), scanning force microscopy (SFM) and transmission electron microscopy (TEM). Then these SCMs were used as nanoreactors for the reduction of gold and silver nanoparticles. Well-distributed particles of few nanometers were obtained inside the SCMs. The overall process is described in Scheme 6-1. The characterization of these metal-polymer hybrids was performed by UV-visible spectroscopy and TEM. Finally the catalytic activity of these nanocarriers was proven in the case of the silver nanoparticles by the reduction of 4-nitrophenol to 4-aminophenol.
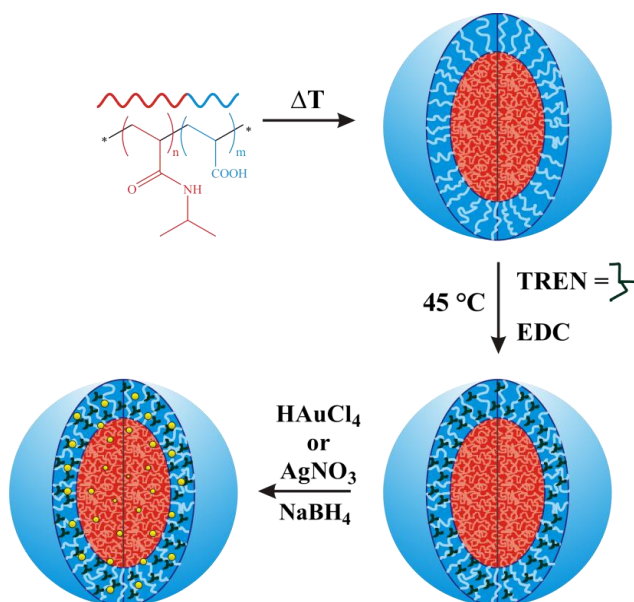
Scheme 6-1. Preparation of PNIPAAm-*b*-PAA-metal nano-hybrids.

Experimental

Materials

All chemicals and solvents where purchased from Sigma-Aldrich, Acros and Fluka at the highest available purity and used as received. The two different PNIPAAm-*b*-PAA described here were obtained by reversible addition fragmentation chain transfer (RAFT) polymerization. 3-Benzylsulfanyl thiocarbonylsulfanyl propionic acid (BPATT) was used as chain transfer agent (CTA) and the process was carried out in two steps by first synthesis and purification of a PAA macroCTA and then polymerization of the PNIPAAm block. The all procedure was done in aqueous media at ambient temperature by using γ-irradiation to initiate the polymerization. Details of the polymerization process have been described elsewhere.[73]

Cross-Linking Procedure

In a typical procedure 400 mg of PNIPAAm-b-PAA was dissolved in deionized water. The pH was raised to 12 by addition of KOH solution and an ultra-sonic bath filled with cold water was used to accelerate the process. After full dissolution, the pH was adjusted to 7 by addition of a dilute HCl solution. Then the solution was transferred to a round bottom flask and the polymer concentration was adjusted to 4 g · L^{-1} by addition of deionized water. The flask was sealed with a rubber septum and heated to 45 °C under stirring to allow the self-assembly into spherical micelles. When the solution was turbid, tris(2-aminoethyl)amine (TREN) was added to the system. For PNIPAAm$_{2000}$-*b*-PAA$_{300}$ and PNIPAAm$_{2000}$-*b*-PAA$_{500}$ the amount introduced was adjusted to have a ratio [NH$_2$]/[AA] = 2. After few minutes, two molar equivalent compared to the acrylic acid unit of 1-[3-(dimethylamino)propyl]-3-ethylcarbodiimide methiodide (EDC) powder were introduced. This last addition was repeated three other times every 2 hours to complete the cross-linking process. 2 hours after the last addition the temperature was allowed decreased to room temperature. The solution was then dialyzed several days against water to remove the residual urea compound generated from the EDC and the

unreacted TREN. The different cross-linked micelles were then stored as stock solutions directly after the dialysis prior to additional reaction.

Generation of Au and Ag nanoparticles

In a typical procedure, 10 mg of cross-linked PNIPAAm-*b*-PAA micelles from the stock were diluted in 20 mL of deionized water in 40 mL vial. Then 2.5 mg of $HAuCl_4$ was added. The vial was covered with aluminum foil to avoid the reduction by UV light and stirred for 2 hours. Afterwards the solution was dialyzed against water in the dark for 2 days to remove the excess of $HAuCl_4$ which did not generate a complex with the micelles. Finally the gold salt was reduced by a one quick addition of 300 μL of 10 mM of sodium borohydride ($NaBH_4$) solution added under intensive stirring. The solution was then dialyzed to remove the unreacted $NaBH_4$ prior to analysis.

To obtain Ag nanoparticles, in a typical procedure, 10 mg of cross-linked PNIPAAm-*b*-PAA micelles from the stock were diluted in 20 mL of deionized water in a 40 mL vials. Then 0.75 mg of $AgNO_3$ from a concentrated aqueous solution was added. The vial was covered with aluminum foil to avoid the reduction by UV light and stirred for 2 hours. Then silver nanoparticles were obtained by direct addition of 150 μL of 10 mM of sodium borohydride ($NaBH_4$) solution added under intensive stirring. The solution was then dialyzed against water to remove the unreacted $NaBH_4$ prior to analysis.

Catalytic Reduction of 4-Nitrophenol

An aqueous solution of sodium borohydride (10 mM, 0.05 mL) was added to a solution of 4-nitrophenol (0.1 mM, 2.95 mL). A defined amount of silver/PNIPAAm$_{2000}$-*b*-PAA$_{300}$ nano-hybrid (5×10^{-3} g · L^{-1}) was then added to this solution. Immediately after the addition of silver nanoparticles, UV spectra of the mixture were recorded with a UV/VIS spectrometer. The kinetic study of the reaction was performed by measuring the change in intensity of the absorbance at 400 nm with time. The spectra were recorded every 1.5 minutes in the range 250–550 nm.

Characterization

^{1}H-NMR spectra were recorded on a Bruker spectrometer (300 MHz) in D_2O (residual peak δ = 4.75 ppm). The determination of the *cloud points* was achieved by turbidity measurements using a titrator (Titrando 809, Metrohm, Herisau, Switzerland) equipped with a turbidity sensor (λ_0 = 523 nm, Spectrosense, Metrohm). In addition, a temperature sensor (Pt 1000, Metrohm) was used. The temperature program (1K / min) was run by a thermostat (LAUDA RE 306 and Wintherm_Plus software), using a home-made thermostable vessel. We defined the cloud point as the intercept of the tangents of the transmittance-temperature dependence at the onset of turbidity. *Dynamic Light Scattering (DLS)* was performed at 25 °C using an ALV DLS/SLS-SP 5022F compact goniometer system with an ALV 5000/E correlator and a He-Ne laser (λ = 632.8 nm; Peters ALV, Lange n, Germany). The intensity fluctuations were detected at 90°. By means of CONTIN analysis of the intensity autocorrelation functions the intensity weighted hydrodynamic radii were derived from the collective diffusion coefficients by the Stokes-Einstein relation. *Scanning force microscopy (SFM)* measurements were performed with a Dimension 3100 Metrology SFM (Digital Instruments, Veeco Metrology Group) operated in tapping mode by using silicon tips with a spring constant of $40 \text{ N} \cdot \text{m}^{-1}$ and a resonance frequency in the range between 200 and 300 kHz. Scan rates were between 0.5 and 1 Hz and a resolution of 256×256 were used for image recording. Samples were prepared on silicon wafers by spin-casting at 2000 rpm from 0.1 wt% polymer solution in water. *Transmission electron microscopy (TEM)* images were taken on a Zeiss 922 EM EF-TEM instrument operated at 200 kV. A 5μL droplet of a dilute solution (~ $0.01 \text{ g} \cdot \text{L}^{-1}$) in water, was dropped onto a copper grid (200 mesh) coated with carbon film, followed by drying at room temperature for a short time. UV-vis spectra were measured on a Perkin-Elmer Lambda 25 spectrometer.

Results and Discussion

Shell Cross-Linked PNIPAAm-*b*-PAA micelles

RAFT initiated by γ-radiation has proven to be a very powerful process to obtain very high molecular weight polymers with narrow molecular weight distribution and with a low amount of termination even at high conversion.[26] The results of selected polymers are summarized in Table 6-1. Both polymers exhibit a rather low polydispersity with an absence or a very tiny amount of termination. Moreover no trace of residual precursor was detected by size exclusion chromatography. All these criteria proved that the polymerization proceeds in a controlled fashion.

Table 6-1. Characteristics of the different PNIPAAm-*b*-PAA

Polymer	$\overline{M}_{n,th}$[a] kg/mol	$\overline{M}_{n,exp}$[b] kg/mol	PDI[b]	T_{Cl}[c] °C	R_H (45 °C)[d] nm
PNIPAAm$_{2000}$-*b*-PAA$_{300}$	241	217	1.24	33.7	132
PNIPAAm$_{2000}$-*b*-PAA$_{500}$	262	254	1.28	33.3	77

[a] $\overline{M}_{n,th} = M_M \cdot X_p \cdot [M]_0/[CTA]_0 + M_{CTA}$. [b] Measured by SEC using PS standards in *N,N*-dimethylacetamide (DMAc). [c] Cloud points are defined as the intercept of the tangents in the turbidity measurements. [d] Hydrodynamic radii were estimated from dynamic light scattering measurements.
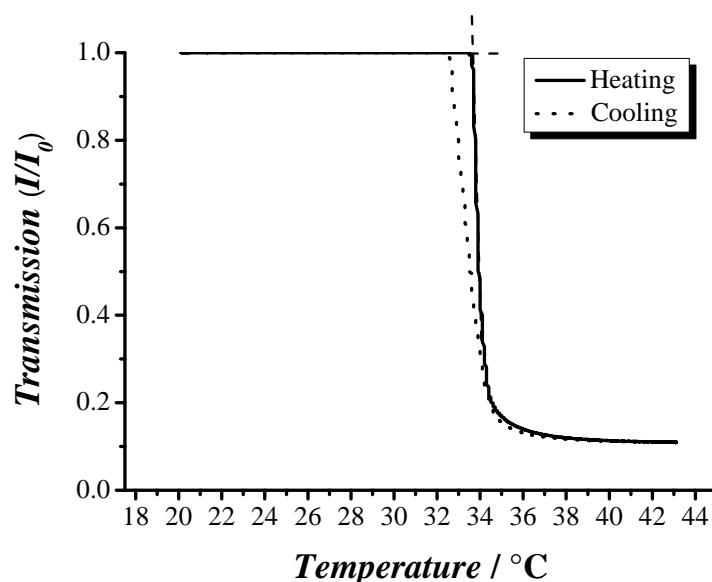
Figure 6-1. Determination of the cloud point, T_{cl}, from turbidity measurements. PNIPAAm$_{2000}$-b-PAA$_{300}$ (concentration 1 g · L^{-1}) in pure water at pH 7. The cloud point is defined as the intercept of the tangents (– –) at heating.

Due to the PNIPAAm block, these block copolymers are thermo-responsive and exhibit a lower critical solution temperature (LCST). In aqueous media above the cloud point (T_{cl}) in neutral or basic pH spherical micelles are formed.[20,74] The hydrophobic PNIPAAm forms the micellar core and the hydrophilic PAA block generates the corona preventing the full aggregation of the system. Figure 6-1 depicts the determination of the cloud point for PNIPAAm$_{2000}$-b-PAA$_{500}$; a very sharp transition occurs at 33.3 °C. Because of the very long PNIPAAm used, the size of the core is rather large and the objects scatter enough light to drop the relative intensity I/I_0 to near zero after the transition. The phase transition is fully reversible and after cooling down, the solution is again fully transparent. However a small hysteresis was observed. This phenomenon is common for PNIPAAm and was already observed for PNIPAAm based micelles and hydrogels.[75] Figure 6-2 shows the count rate and the hydrodynamic radius (R_H) obtained by dynamic light scattering (DLS) as a function of the temperature. The transition temperatures are comparable to those observed by turbidity measurement. Below T_{cl}, a

very low count rate was reached and no reliable R_H could be estimated. Above this temperature, the count rate increases drastically and narrowly distributed micelles are formed (Figure 6-4).
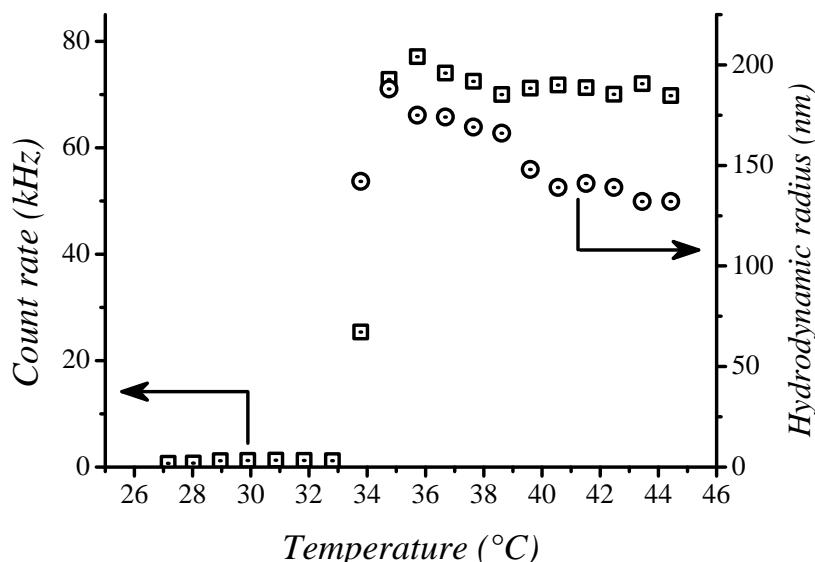
Figure 6-2. Evolution of the count rate (▫) and the hydrodynamic radius (⊙), obtained by DLS, with the temperature, for PNIPAAm$_{2000}$-*b*-PAA$_{300}$.

To stabilize this micellar structure even at room temperature the shell was cross-linked at 45 °C by using tris(2-aminoethyl)amine (TREN). This triamine compound is fully water-soluble and can react with the carboxylic groups present on the PAA to generate an amide bound in presence of the water-soluble carbodiimide EDC. TREN was found to be more effective than 2,2′-(ethylenedioxy)bis(ethylamine) (EO$_2$DA) which is commonly used due to of the trifunctionality of TREN compared to the difunctional EO$_2$DA (results not shown). Moreover, several equivalents of EDC were added sequentially to obtain sufficient cross-linking efficiency. For both cross-linkers, after the addition of only one or two equivalent of EDC, the micellar structure was not fully maintained at room temperature. This phenomenon can be explained by the poor stability of EDC in water at elevated temperature. However after several additions of EDC and cooling down the reaction mixture, in all cases, the solutions remained highly turbid. This is a first

indication that the cross-linking was efficient to maintain the micellar structure. Moreover to increase the probability of reaction between the amino and carboxylic groups, an excess of TREN was used. For both polymers a ratio $[NH_2]/[AA] = 2$ was selected. The reaction between TREN and the carboxylic groups of the PAA corona was characterized by ^{1}H-NMR. Figure 6-3 depicts the NMR spectra of PNIPAAm-*b*-PAA in D_2O. After cross-linking and purification by dialysis to remove unreacted TREN and urea compounds generated from the EDC, a clean spectrum is obtained (upper spectrum). However, a new peak in the range of 2.6-3.5 ppm appears which comes from the attachment of TREN to the polymer and the amide formation. The chemical shift observed is in a good agreement to the ethyl protons of TREN after modification of the NH_2 groups into amide[76] and also of the ethyl protons of TREN present in unmodified NH_2. These residual unreacted amino moieties are protonated (NH3+) at neutral or acidic pH, and they contribute to the solubility of the shell cross-linked micelles in water.[77]
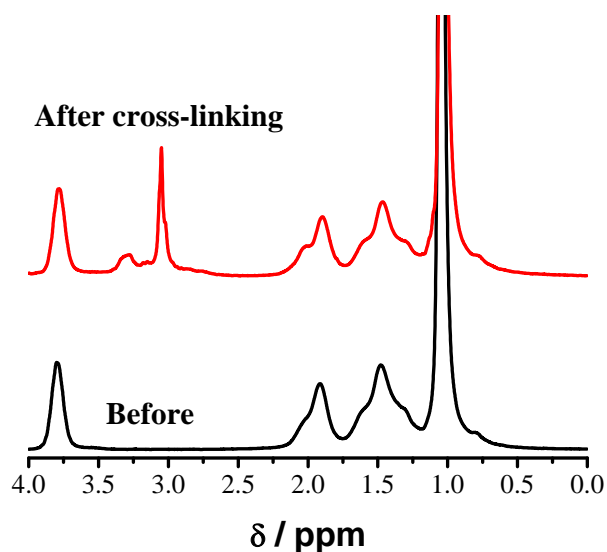

Figure 6-3. ^{1}H-NMR spectrum of PNIPAAm$_{2000}$-*b*-PAA$_{500}$ in D_2O before and after cross-linking

The generated shell cross-linked micelles were also analyzed by DLS at 25 °C. Figure 6-4 illustrates the tendency observed by this technique. For both systems, the hydrodynamic radius distribution presents two peaks. The main one is centered on the

initial peak before cross-linking but is somewhat more polydisperse. The difference of hydrodynamic radii is very small (R_H(45 °C) = 132 nm and R_H(25 °C) = 134 nm) for PNIPAAm$_{2000}$-b-PAA$_{300}$ indicating that the structure generated at high temperature is kept after cross-linking. A second small peak, at around 10 nm, may find its origin in some fragments of partially cross-linking PNIPAAm-b-PAA. In addition, the osmotic pressure generated by rehydratation of the PNIPAAm core after cooling may lead to the rupture of bonds. Finally, DLS shows no peak with a higher hydrodynamic radius which proves that no aggregates are formed during the cross-linking reaction and no intermicellar cross-linking was observed.
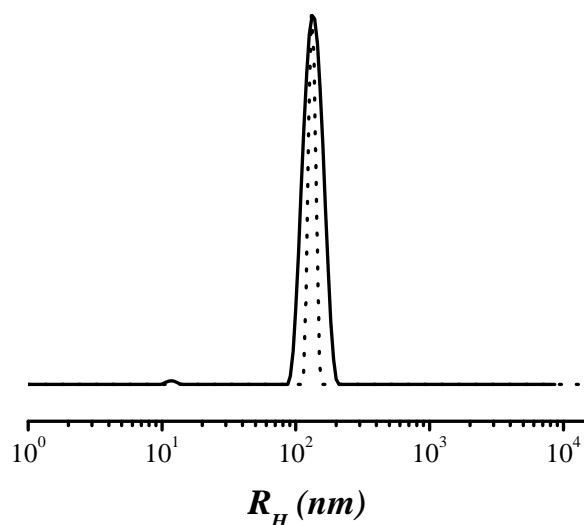

Figure 6-4. Unweighted hydrodynamic radius distribution of PNIPAAm$_{2000}$-b-PAA$_{300}$ at 45 °C before cross-linking (• • •) and at 25 °C after cross-linking (——).
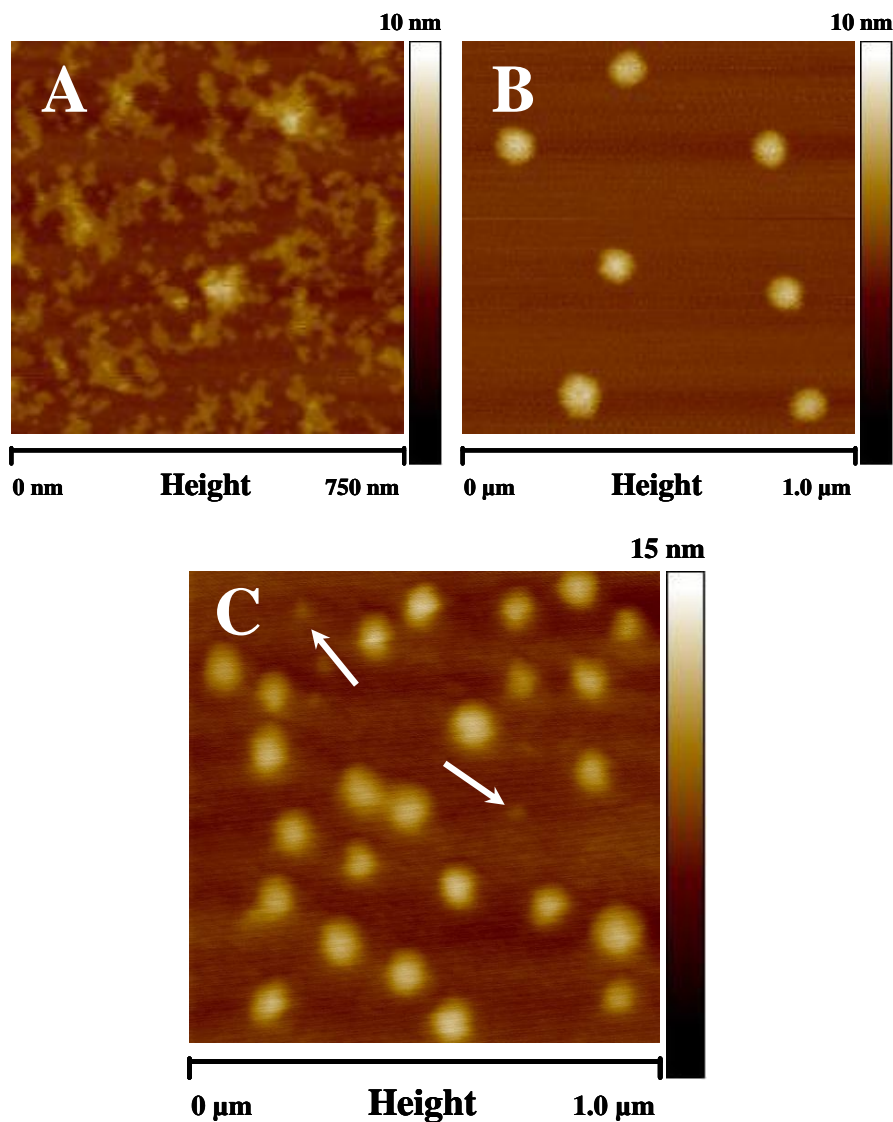
Figure 6-5. Scanning force microscopy height images of PNIPAAm$_{2000}$-b-PAA$_{300}$ and PNIPAAm$_{2000}$-b-PAA$_{500}$ obtained from solutions in pure water pH 7. (A) PNIPAAm$_{2000}$-b-PAA$_{500}$ before cross-linking at 25 °C. (B) PNIPAAm$_{2000}$-b-PAA$_{500}$ before cross-linking at 60 °C. (C) Shell cross-linked PNIPAAm$_{2000}$-b-PAA$_{500}$ at 25 °C.

Scanning force microscopy (SFM) measurements were performed on the PNIPAAm$_{2000}$-b-PAA$_{500}$ in solution before and after cross-linking and the representative images are plotted in Figure 6-5. At room temperature in water the free polymer generates a film on the silicon wafer after spin-casting of the solution (Figure 6-5A). Moreover in the dry state there is a phase separation between the PNIPAAm and the PAA

blocks which are not miscible. Nevertheless the texture is not regular, which might indicate that an equilibrium state was not reached. After heating the solution to 60 °C and spin casting the heated solution on a hot silicon wafer substrate (Figure 6-5B), spherical micelles are observed. Due to the strong interaction with the surface, the particles collapse and flat disk-shaped objects were observed. They have a monodisperse distribution in size and no trace of contamination of free polymer was found on the whole substrate. Figure 6-5C is the SFM image obtained at room temperature after shell cross-linking of the same polymer. It is obvious that the structure obtained at high temperature is kept at room temperature after cross-linking. The objects have a disk-like shape and the same diameter. However few smaller objects are also observed. Some of them are highlighted with arrows. As already seen in DLS images these apparently are small pieces of cross-linked PNIPAAm-b-PAA. The size distribution determined from the SFM is narrow distributed and fit to the one obtained by DLS. The same type of images was obtained for PNIPAAm$_{2000}$-b-PAA$_{300}$ (results not shown).
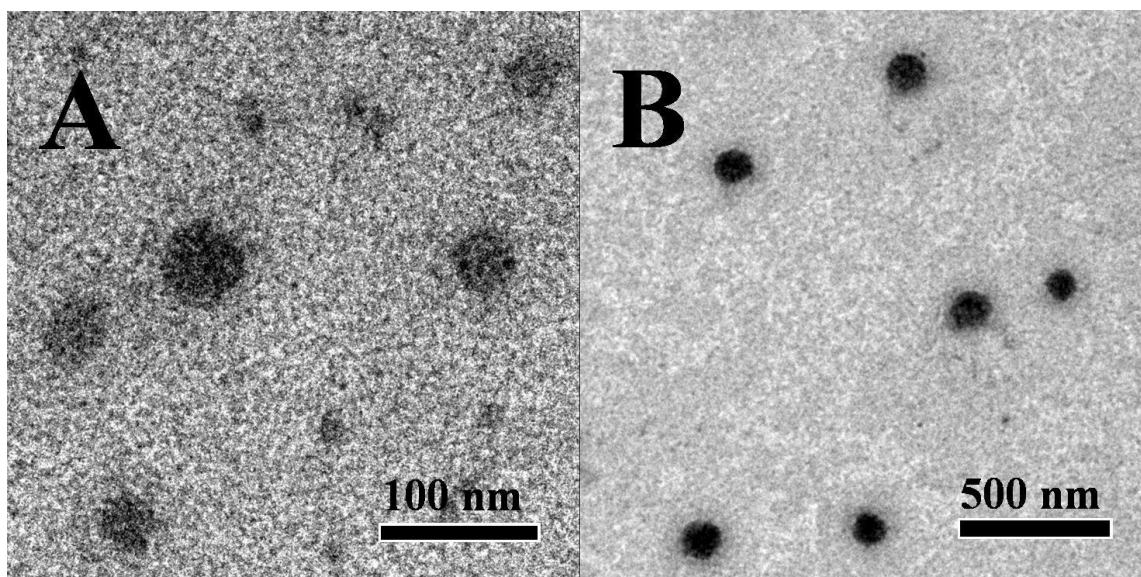
Figure 6-6. Transmission electron micrographs of cross-linked PNIPAAm$_{2000}$-b-PAA$_{300}$ and PNIPAAm$_{2000}$-b-PAA$_{500}$ solutions in water at 25 °C (A) Cross-linked PNIPAAm$_{2000}$-b-PAA$_{500}$. (B) Cross-linked PNIPAAm$_{2000}$-b-PAA$_{300}$.

The results obtained by SFM and DLS were also confirmed by transmission electron microscopy (TEM). Figure 6-6 depicts typical TEM images for the two different shell

cross-linked PNIPAAm-*b*-PAA particles. For both almost spherical particles were observed. The corona of PAA could not be observed clearly due to the low difference of electronic contrast between PAA and PNIPAAm. Small fragments of cross-linked PNIPAAm-b-PAA can also be seen (Figure 6-6A). The average radii are around 30 nm for PNIPAAm$_{2000}$-*b*-PAA$_{500}$ and 65 nm for PNIPAAm$_{2000}$-*b*-PAA$_{300}$ which are much smaller than those obtained by DLS and SFM. This phenomenon can be explained by the fact that only the dense PNIPAAm core is observed. The cross-linking has locked the density of the core reached at high temperature when the PNIPAAm is collapsed.
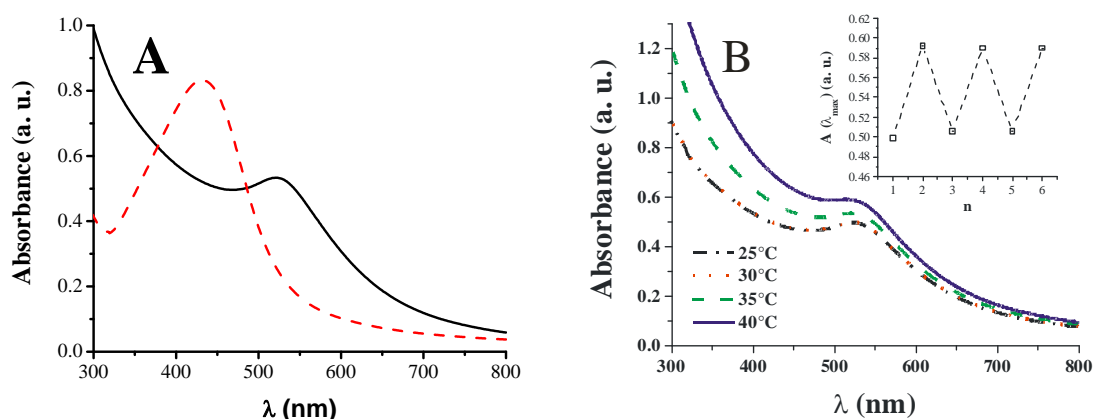
Figure 6-7. UV-Vis absorption spectra of the nano-hybrids based on PNIPAAm$_{2000}$-*b*-PAA$_{500}$. (A) UV absorption spectra in water at 25 ℃ of (——) PNIPAAm$_{2000}$-*b*-PAA$_{500}$ after gold reduction, (– –) PNIPAAm$_{2000}$-*b*-PAA$_{500}$ after silver reduction. (B) Absorption spectra of PNIPAAm$_{2000}$-*b*-PAA$_{500}$ after reduction of gold nanoparticles depending of the temperature (• – •) 25 ℃, (• • •) 30 ℃, (– –) 35 ℃ and (——) 40 ℃. In the inset, variation of the absorbance maximum (λ_{max}= 523 nm) at 25 ℃ and 40 ℃ over 3 heating-cooling cycles.

The temperature response the shell cross-linked micelles in pure water was also investigated by DLS. No contraction of the particles was observed. Instead these particles tend to aggregate (results not shown). This is due to the cross-linking which modifies the charge of the corona. Without cross-linking, at pH 7, about 50% carboxylic group are unprotonated. So the micelles have at high temperature and at neutral or basic pH, a negative charge which shield the hydrophobic interaction and prevent the aggregates

formation. After cross-linking, the carboxylic group is transformed in amide functionality which is neutral and does not respond to pH. The resulting charge on the surface is strongly modified and does not prevent anymore the aggregation when the solution is heated.

Metal/PNIPAAm-*b*-PAA nanohybrids

These SCL micelles were used as a nanoreactor to generate new organic-inorganic nano-hybrids. To prove the efficiency of the vessel, we decided to reduce gold or silver salts to generate in-situ gold or silver nanoparticles respectively. The synthesis was based on classical reduction of the salts with sodium borohydride.[68,78] To obtain the different nano-hybrids, a concentrated aqueous solution of tetrachloroauric acid ($HAuCl_4$) or silver nitrate ($AgNO_3$) was added to the different SCL micelle solution. Then complexation of metal ions with residual acrylic acid and acrylamide moieties was performed in the dark for two hours. In the case of gold, the color of the solutions changes to yellowish afterward which is the evidence of a good interaction between the gold and the polymer. Then to avoid some particles formation outside of the nanoreator the excess of metal was removed by dialysis for two days in the dark prior to the reduction by addition of $NaBH_4$ solution. For silver, the same dialysis treatment was not successful due to a lower interaction of the weak silver cations with the polymer which leads to a total washing of the metal ions. Therefore in this particular case, we decided to reduce the silver ions directly. The different solution colors changed instantaneously to yellow-orange in the case of silver and to violet in the case of gold, proving of the formation of nanoparticles in both cases. The UV-Vis absorption spectra of the obtained nanohybrids are shown in Figure 6-7. Absorption peaks at 522 and 523 nm were detected after reduction gold in the two different SCL micelles and 427 and 432 nm after silver reduction respectively (Figure 6-7A). By increasing the temperature from 25 ℃ to 40 ℃, the UV spectra change. An example for the case of gold-PNIPAAm$_{2000}$-*b*-PAA$_{500}$ nano-hybrids is provided in Figure 6-7B. The peak maximum increases due to the transition of PNIPAAm which modify the refractive index of the hybrids which scatter more leading

to the enhancement of the absorbance. Like for the SCL micelles, nano-hybrids reversibly aggregate at elevated temperature, as shown in the inset, by few heating-cooling cycles at 25 ºC and 40 ºC where the system reach the same absorbance values. These hybrids were also characterized by TEM (Figure 6-8). In the case of PNIPAAm$_{2000}$-b-PAA$_{300}$, it can be clearly seen, for both metals, that practically monodisperse nanoparticles have been generated *in situ* by reduction with NaBH$_4$. These pictures also indicate that particles are homogeneously embedded into the PNIPAAm-b-PAA cross-linked micelle. Moreover, in accord with the UV-Vis measurements, the analysis of TEM image indicates that the metal particles are small with an average diameter of around 2 nm. Finally it seems that none or few nanoparticles only are generated outside the carriers.
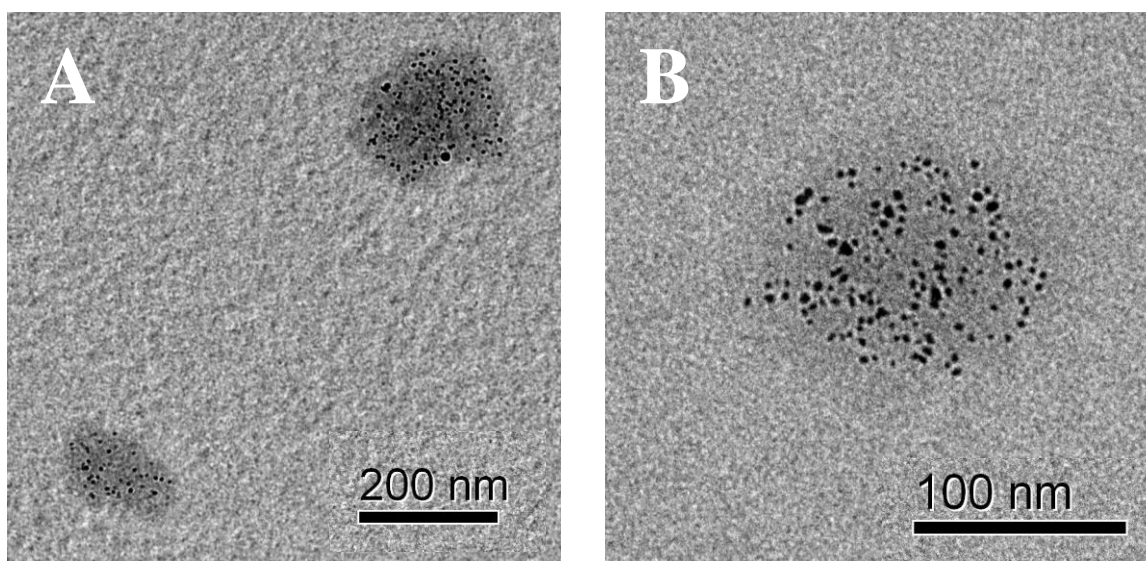
Figure 6-8. Transmission electron microscopy (TEM) of metal-PNIPAAm$_{2000}$-b-PAA$_{300}$ nano-hybrids. (A) Gold-PNIPAAm$_{2000}$-b-PAA$_{300}$ solution in water at 25 °C. (B) higher magnification (C) Silver-PNIPAAm$_{2000}$-b-PAA$_{300}$ solution in water at 25 °C.

In order to evaluate the potential of these robust shell cross-linked micelles to be used as nanocarriers, the catalytic activity of the silver nanocomposite particles was investigated. The reduction of 4-nitrophenol by an excess of NaBH$_4$ has been chosen as model reaction.[69] Kinetics of this reaction can be easily monitored by UV-vis spectroscopy. After addition of silver nano-hybrids, the peak at 400 nm due to the 4-

nitrophenolate ions decreases gradually with time while a new peak appears at 290 nm from the 4-aminophenol produced. From the UV-vis spectra depicted in Figure 6-9 it can be seen that the reaction occurs rapidly and after around 21 min the most part of the nitrophenate ions are reduced. This experiment proves the accessibility and the capacity of the silver nanoparticles inside the shell cross-linked micelle to catalyze the reduction. It also demonstrates that these nano-hybrids can be a very powerful tool for different catalytic reaction.
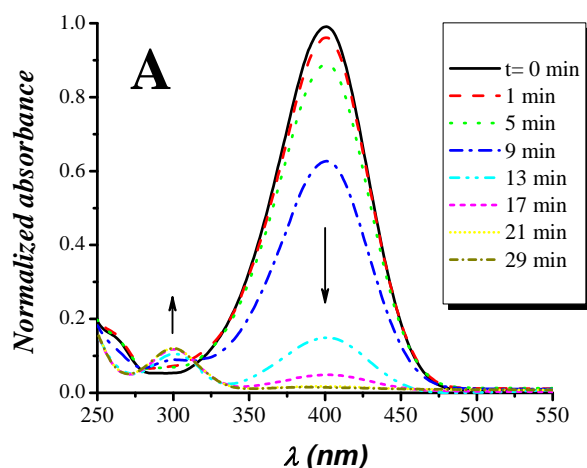
Figure 6-9. Catalytic reduction of 4-nitrophenol by NaBH$_4$ in the presence of silver/PNIPAAm$_{2000}$-*b*-PAA$_{300}$ nano-hybrids at 25 °C. UV-vis spectra measured at different times.

Conclusions

The synthesis of shell cross-linked micelles based on two different PNIPAAm-*b*-PAA block copolymers have been presented. The multi-responsive block copolymers were first self-assembled in neutral water at elevated temperature into spherical micelles. Afterwards TREN, a trifunctional amino compound, was used to cross-link the structure by amidification of the carboxylic groups present in the shell. The efficiency of the cross-linking was demonstrated by DLS, and NMR. Narrow distributed spherical SCM were

observed by SFM and SEM. However a tiny amount of partially cross-linked fragments was also found in the media. The SCM were then utilized as nano-carriers for silver or gold nanoparticles by *in situ* reduction using $NaBH_4$ as reducing agent. Small spherical nanoparticles around 2nm were able to be imaged by TEM inside the SCM. These nanohybrids respond to temperature and aggregate at elevated temperature. Finally the potential of this new nano-carriers was demonstrated by performing the reduction 4-nitrophenol into 4-aminophenol in presence of the silver-PNIPAAm-*b*-PAA nanohybrids which prove the catalytic activity and accessibility of the silver nanoparticles. We believe that the results of the present study prove that these multi-responsive SCM are a good candidate to generate smart nanohybrids for catalytic nanoreactor applications.

Acknowledgements

References

(1)   Cheng, C.; Wei, H.; Shi, B.-X.; Cheng, H.; Li, C.; Gu, Z.-W.; Cheng, S.-X.; Zhang, X.-Z.; Zhuo, R.-X. *Biomaterials* **2008**, *29*, 497-505.

(2)   Karanikolopoulos, N.; Pitsikalis, M.; Hadjichristidis, N.; Georgikopoulou, K.; Calogeropoulou, T.; Dunlap, J. R. *Langmuir* **2007**, *23*, 4214-4224.

(3)   Liu, H.; Jiang, X.; Fan, J.; Wang, G.; Liu, S. *Macromolecules* **2007**, *40*, 9074-9083.

(4)   Yang, C.-C.; Tian, Y.; Jen, A. K. Y.; Chen, W.-C. *Journal of Polymer Science Part A: Polymer Chemistry* **2006**, *44*, 5495-5504.

(5)   Hoffmann, J.; Plötner, M.; Kuckling, D.; Fischer, W.-J. *Sensors and Actuators A: Physical* **1999**, *77*, 139-144.

(6)   Wang, Y.; Wei, G.; Wen, F.; Zhang, X.; Zhang, W.; Shi, L. *Journal of Molecular Catalysis A: Chemical* **2008**, *280*, 1-6.

(7)   Wang, Y.; Wei, G.; Zhang, W.; Jiang, X.; Zheng, P.; Shi, L.; Dong, A. *Journal of Molecular Catalysis A: Chemical* **2007**, *266*, 233-238.

(8)   Shimoboji, T.; Larenas, E.; Fowler, T.; Hoffman, A. S.; Stayton, P. S. *Bioconjugate Chemistry* **2003**, *14*, 517-525.

(9)   Christman, K. L.; Maynard, H. D. *Langmuir* **2005**, *21*, 8389-8393.

(10)   Dimitrov, I.; Trzebicka, B.; Müller, A. H. E.; Dworak, A.; Tsvetanov, C. B. *Progress in Polymer Science* **2007**, *32*, 1275-1343.

(11)   Lupitskyy, R.; Roiter, Y.; Tsitsilianis, C.; Minko, S. *Langmuir* **2005**, *21*, 8591-8593.

(12)   Kuo, P.-L.; Chen, C.-C.; Jao, M.-W. *The Journal of Physical Chemistry B* **2005**, *109*, 9445-9450.

(13)   Rauter, H.; Matyushin, V.; Alguel, Y.; Pittner, F.; Schalkhammer, T. *Macromolecular Symposia* **2004**, *217*, 109-133.

(14)   Kulkarni, S.; Schilli, C.; Mueller, A. H. E.; Hoffman, A. S.; Stayton, P. S. *Bioconjugate Chemistry* **2004**, *15*, 747-753.

(15)   Galaev, I.; Mattiasson, B.; Editors *Smart Polymers for Bioseparation and Bioprocessing*, 2004.

(16)   Gil, E. S.; Hudson, S. M. *Progress in Polymer Science* **2004**, *29*, 1173-1222.

(17)   Yang, H.; Cheng, R.; Wang, Z. *Polymer* **2003**, *44*, 7175-7180.

(18)   Plamper, F. A.; Becker, H.; Lanzendörfer, M.; Patel, M.; Wittemann, A.; Ballauff, M.; Müller, A. H. E. *Macromolecular Chemistry and Physics* **2005**, *206*, 1813-1825.

(19)   Hofs, B.; Keizer, A. d.; Burgh, S. v. d.; Leermakers, F. A. M.; Stuart, M. A. C.; Millard, P. E.; Muller, A. H. E. *Soft Matter* **2008**, *4*, 1473-1482.

(20)   Schilli, C. M.; Zhang, M.; Rizzardo, E.; Thang, S. H.; Chong, Y. K.; Edwards, K.; Karlsson, G.; Muller, A. H. E. *Macromolecules* **2004**, *37*, 7861-7866.

(21)   Li, G.; Song, S.; Guo, L.; Ma, S. *Journal of Polymer Science Part A: Polymer Chemistry* **2008**, *46*, 5028-5035.

(22)   McCormick, C. L.; Kirkland, S. E.; York, A. W. *Polymer Reviews* **2006**, *46*, 421 - 443.

(23)   Sciannamea, V.; Jerome, R.; Detrembleur, C. *Chemical Reviews* **2008**, *108*, 1104-1126.

(24)   Braunecker, W. A.; Matyjaszewski, K. *Progress in Polymer Science* **2007**, *32*, 93-146.

(25)   Moad, G.; Rizzardo, E.; Thang, S. H. *Polymer* **2008**, *49*, 1079-1131.

(26)   Millard, P.-E.; Barner, L.; Stenzel, M. H.; Davis, T. P.; Barner-Kowollik, C.; Müller, A. H. E. *Macromolecular Rapid Communications* **2006**, *27*, 821-828.

(27)   Zhang, L.; Liu, W.; Lin, L.; Chen, D.; Stenzel, M. H. *Biomacromolecules* **2008**, *9*, 3321-3331.

(28)   O'Reilly, R. K.; Hawker, C. J.; Wooley, K. L. *Chemical Society Reviews* **2006**, *35*, 1068-1083.

(29)   Read, E. S.; Armes, S. P. *Chemical Communications* **2007**, 3021-3035.

(30)   Becker, M. L.; Remsen, E. E.; Pan, D.; Wooley, K. L. *Bioconjugate Chemistry* **2004**, *15*, 699-709.

(31)   Fujii, S.; Cai, Y.; Weaver, J. V. M.; Armes, S. P. *Journal of the American Chemical Society* **2005**, *127*, 7304-7305.

(32)   Joralemon, M. J.; Smith, N. L.; Holowka, D.; Baird, B.; Wooley, K. L. *Bioconjugate Chemistry* **2005**, *16*, 1246-1256.

(33)   Qi, K.; Ma, Q.; Remsen, E. E.; Clark, C. G.; Wooley, K. L. *Journal of the American Chemical Society* **2004**, *126*, 6599-6607.

(34)   Rossin, R.; Pan, D.; Qi, K.; Turner, J. L.; Sun, X.; Wooley, K. L.; Welch, M. J. *J Nucl Med* **2005**, *46*, 1210-1218.

(35)   Sun, G.; Hagooly, A.; Xu, J.; Nyströͫm, A. M.; Li, Z.; Rossin, R.; Moore, D. A.; Wooley, K. L.; Welch, M. J. *Biomacromolecules* **2008**, *9*, 1997-2006.

(36)   Wei, H.; ChengCheng; Chang, C.; Chen, W.-Q.; Cheng, S.-X.; Zhang, X.-Z.; Zhuo, R.-X. *Langmuir* **2008**, *24*, 4564-4570.

(37)   Zhang, L.; Nguyen, T. L. U.; Bernard, J.; Davis, T. P.; Barner-Kowollik, C.; Stenzel, M. H. *Biomacromolecules* **2007**, *8*, 2890-2901.

(38)   Liu, S.; Weaver, J. V. M.; Tang, Y.; Billingham, N. C.; Armes, S. P.; Tribe, K. *Macromolecules* **2002**, *35*, 6121-6131.

(39)   Li, Y.; Du, W.; Sun, G.; Wooley, K. L. *Macromolecules* **2008**, *41*, 6605-6607.

(40)   Joralemon, M. J.; O'Reilly, R. K.; Hawker, C. J.; Wooley, K. L. *Journal of the American Chemical Society* **2005**, *127*, 16892-16899.

(41)   Liu, S.; Weaver, J. V. M.; Save, M.; Armes, S. P. *Langmuir* **2002**, *18*, 8350-8357.

(42)   Stewart, S.; Liu, G. *Chemistry of Materials* **1999**, *11*, 1048-1054.

(43)   Weaver, J. V. M.; Tang, Y.; Liu, S.; Iddon, P. D.; Grigg, R.; Billingham, N. C.; Armes, S. P.; Hunter, R.; Rannard, S. P. *Angewandte Chemie International Edition* **2004**, *43*, 1389-1392.

(44)   Wang, H.; Wang, X.; Winnik, M. A.; Manners, I. *Journal of the American Chemical Society* **2008**, *130*, 12921-12930.

(45)   Perkin, K. K.; Turner, J. L.; Wooley, K. L.; Mann, S. *Nano Letters* **2005**, *5*, 1457-1461.

(46)   Zhou, Y.; Jiang, K.; Chen, Y.; Liu, S. *Journal of Polymer Science Part A: Polymer Chemistry* **2008**, *46*, 6518-6531.

(47)   Murray, R. W. *Chemical Reviews* **2008**, *108*, 2688-2720.

(48)   Schrinner, M.; Proch, S.; Mei, Y.; Kempe, R.; Miyajima, N.; Ballauff, M. *Advanced Materials* **2008**, *20*, 1928-1933.

(49)   Shan, J.; Tenhu, H. *Chemical Communications* **2007**, 4580-4598.

(50)   Shenhar, R.; Norsten, T. B.; Rotello, V. M. *Advanced Materials* **2005**, *17*, 657-669.

(51)   Wilson, R. *Chemical Society Reviews* **2008**, *37*, 2028-2045.

(52)   Grzelczak, M.; Perez-Juste, J.; Mulvaney, P.; Liz-Marzan, L. M. *Chemical Society Reviews* **2008**, *37*, 1783-1791.

(53)   Pelton, M.; Aizpurua, J.; Bryant, G. *Laser & Photonics Review* **2008**, *2*, 136-159.

(54)   Biju, V.; Itoh, T.; Anas, A.; Sujith, A.; Ishikawa, M. *Analytical and Bioanalytical Chemistry* **2008**, *391*, 2469-2495.

(55)   Lu, Y.; Mei, Y.; Schrinner, M.; Ballauff, M.; Moller, M. W.; Breu, J. *The Journal of Physical Chemistry C* **2007**, *111*, 7676-7681.

(56)   Schrinner, M.; Polzer, F.; Mei, Y.; Lu, Y.; Haupt, B.; Ballauff, M.; Göldel, A.; Drechsler, M.; Preussner, J.; Glatzel, U. *Macromolecular Chemistry and Physics* **2007**, *208*, 1542-1547.

(57)   Brust, M.; Walker, M.; Bethell, D.; Schiffrin, D. J.; Whyman, R. *Journal of the Chemical Society, Chemical Communications* **1994**, 801-802.

(58)   Singh, N.; Lyon, L. A. *Chemistry of Materials* **2007**, *19*, 719-726.

(59)   Shan, J.; Nuopponen, M.; Jiang, H.; Kauppinen, E.; Tenhu, H. *Macromolecules* **2003**, *36*, 4526-4533.

(60)   Shan, J.; Nuopponen, M.; Jiang, H.; Viitala, T.; Kauppinen, E.; Kontturi, K.; Tenhu, H. *Macromolecules* **2005**, *38*, 2918-2926.

(61)   Hou, G.; Zhu, L.; Chen, D.; Jiang, M. *Macromolecules* **2007**, *40*, 2134-2140.

(62)   Kang, Y.; Taton, T. A. *Angewandte Chemie International Edition* **2005**, *44*, 409-412.

(63)   Nuopponen, M.; Tenhu, H. *Langmuir* **2007**, *23*, 5352-5357.

(64)   Qu, S.; Zhang, X. W.; Gao, Y.; You, J. B.; Fan, Y. M.; Yin, Z. G.; Chen, N. F. *Nanotechnology* **2008**, 135704.

(65)   Tang, T.; Krysmann, M. J.; Hamley, I. W. *Colloids and Surfaces A: Physicochemical and Engineering Aspects* **2008**, *317*, 764-767.

(66)   Lu, Y.; Spyra, P.; Mei, Y.; Ballauff, M.; Pich, A. *Macromolecular Chemistry and Physics* **2007**, *208*, 254-261.

(67)   Mohan, Y. M.; Lee, K.; Premkumar, T.; Geckeler, K. E. *Polymer* **2007**, *48*, 158-164.

(68)   Mei, Y.; Lu, Y.; Polzer, F.; Ballauff, M.; Drechsler, M. *Chemistry of Materials* **2007**, *19*, 1062-1069.

(69)   Mei, Y.; Sharma, G.; Lu, Y.; Ballauff, M.; Drechsler, M.; Irrgang, T.; Kempe, R. *Langmuir* **2005**, *21*, 12229-12234.

(70)   Petrov, P.; Tsvetanov, C. B.; Jérôme, R. *The Journal of Physical Chemistry B* **2009**, *113*, 7527-7533.

(71)   Yuan, J.; Lu, Y.; Schacher, F.; Lunkenbein, T.; Weiss, S.; Schmalz, H.; Müller, A. H. E. *Chemistry of Materials* **2009**, *21*, 4146-4154.

(72)   Yuan, J.; Schacher, F.; Drechsler, M.; Hanisch, A.; Lu, Y.; Ballauff, M.; Müller, A. H. E. *Chemistry of Materials* **2010**, *22*, 2626-2634.

(73)   Millard, P.-E.; Barner, L.; Reinhardt, J.; Buchmeise, M. R.; Barner-Kowollik, C.; Müller, A. H. E. *Polymer* **2010**, *51*, 4319-4328.

(74)   Kulkarni, S.; Schilli, C.; Grin, B.; Müller, A. H. E.; Hoffman, A. S.; Stayton, P. S. *Biomacromolecules* **2006**, *7*, 2736-2741.

(75)   Cheng, H.; Shen, L.; Wu, C. *Macromolecules* **2006**, *39*, 2325-2329.

(76)   Kwak, J.; Capua, A. D.; Locardi, E.; Goodman, M. *Journal of the American Chemical Society* **2002**, *124*, 14085-14091.

(77)   Kraft, A. *Journal of Chemical Education* **2003**, *80*, 554-null.

(78)   Lu, Y.; Mei, Y.; Drechsler, M.; Ballauff, M. *Angewandte Chemie International Edition* **2006**, *45*, 813-816.

7. New Water-Soluble Smart Polymer-Silica Hybrid Based on Poly(*N*-Isopropylacrylamide)-*b*-Poly(Acrylic Acid)

Pierre-Eric Millard,[1] Jerome J. Crassous,[2] Andreas Hanisch,[1] Adriana M. Mihut,[2] Jiayin Yuan,[1] and Axel H. E. Müller[1]

[1]Makromolekulare Chemie II, [2]Physikalische Chemie I, Universität Bayreuth, 95440 Bayreuth, Germany,

pierre-eric.millard@basf.com; axel.mueller@uni-bayreuth.de
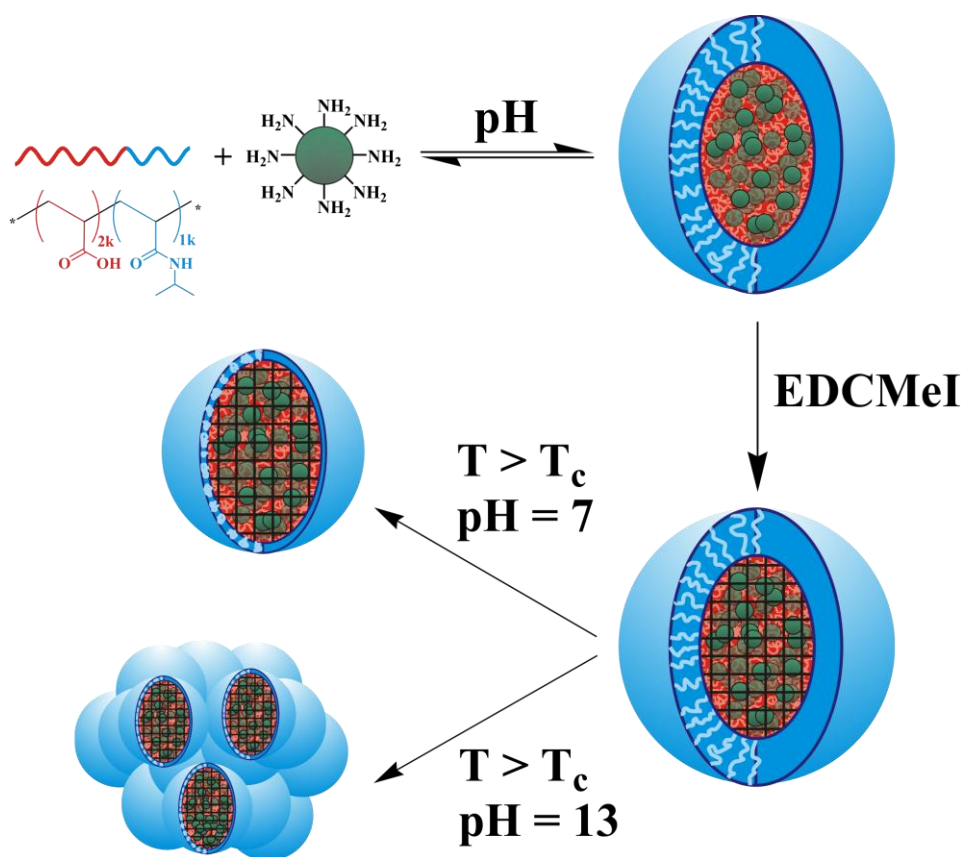
In preparation

Abstract

Smart organic-inorganic nanohybrids are formed in aqueous solution by the interaction of the double hydrophilic multi-responsive block copolymer poly(N-isopropylacrylamide)-*block*-poly(acrylic acid) (PNIPAAm$_{1000}$-*b*-PAA$_{2000}$) and amino functionalized silsesquioxane nanoparticles. We investigate the structure of the complex in dependence of the pH. The presence of nanoparticles strongly modifies the pH response of the block copolymer. The obtained spherical micelles are cross-linked at ambient temperature via amidification between the amino groups of silica particles and the carboxylic groups of the PAA present in the core. These robust nanohybrids are characterized by dynamic light scattering and their structure is revealed by scanning force microscopy (SFM) and transmission electron microscopy (TEM). Finally we demonstrate that their response to temperature can be modulated with the pH.

Introduction

Organic-inorganic hybrid materials have found huge interest, in particular in the areas of biomaterials, optical and mechanical applications. These hybrids combine the properties of both organic and inorganic materials; leading to new materials with unique properties.[1-4] An important class of hybrid materials contains silica or silsesquioxanes as the inorganic component.[5-7] The organic and inorganic components can be simply mixed, e.g., in nanocomposites,[8-10] they can be attached in a covalent way,[11-16] or they can form defined complexes.[17-19] The preparation of polymer-nanoparticle assemblies is not a straightforward task. Due to entropic depletion associated with chain stretching, nanoparticles are commonly not readily miscible with polymers.[20,21] Only strong enthalpic interactions may overcome the entropic penalty and promote the mixing of nanoparticles with polymers. One important driving force is hydrogen bonding or ionic interactions.[22-24]

Much research has been conducted in the promising field of smart materials, i.e., materials that possess the possibility to react on external stimuli like pH, salinity or temperature. These materials offer new applications, for example, in electroactive materials, electrochromic materials, sensors, membranes, drug delivery, emulsifiers, foam stabilizers, detergents, nanocontainers, catalysis, and biohybrid materials.[25-28] Two of them, i.e. poly(*N*-isopropylacylamide) (PNIPAAm) and poly(acrylic acid) (PAA) , have been intensively investigated for their responsive properties.[29] PNIPAAm exhibits a lower critical solution temperature (LCST) in aqueous solution and a sharp reversible phase transition is observed at 32 °C in water.[30,31] PAA responds on changes in pH and ionic strength by changing coil dimensions and solubility.[32,33] Combining these two polymers in PNIPAAm-*b*-PAA block copolymers generates a material which responses to several stimuli and has micellisation properties depending on the solvent, temperature, pH, block lengths and salt concentration.[34,35] Their combination with inorganic materials offers the chance to develop new nanosized smart organic-inorganic materials.[36-43]

An important consideration concerning the practical applications of responsive double hydrophilic block copolymers (DHBCs) is the stability of the complexes in solution. Sturdiness is a key property for instance in drug delivery or catalytic application where

the overall material concentration is really low. The micelles will inevitably disintegrate into unimers when the copolymer concentration falls below the critical micelle concentration (cmc). For therapeutics application, this will lead to premature release of the active compounds.[44] To solve this handicap, different research groups developed cross-linking procedures to maintain the micelle configuration. We can distinguish two types of cross-linked micelles depending on the location of the network: the core [45] or the shell cross-linked[46] micelles.

In the current study, we report the self-organization of a long multi-responsive PNIPAAm-*b*-PAA block-copolymer with amino-functionalized silsesquioxane nanoparticles. The self-assembly is triggered by pH and spherical hybrid micelles are obtained. We investigate the complexation using pH-turbidimetric titration and dynamic light scattering titration techniques. The locking of the structure is carried out by cross-linking reaction where the silsesquioxane nanoparticles act as a new multifunctional cross-linker. The characterization of the generated robust objects is investigated by dynamic light scattering (DLS), scanning force microscopy (SFM) and transmission electron microscopy (TEM). Finally we explore the response to pH and temperature of these new organic-inorganic nanohybrids.

Experimental

Materials

All chemicals and solvents where purchased from Sigma-Aldrich, Acros and Fluka at the highest available purity and used as received. PNIPAAm$_{1000}$-b-PAA$_{2000}$ described here was obtained by reversible addition-fragmentation chain transfer (RAFT) polymerization. 3-Benzylsulfanyl thiocarbonylsulfanyl propionic acid (BPATT) was used as chain transfer agent (CTA) and the reaction was carried out in two steps by synthesis and purification of a PAA macroCTA and then polymerization of the PNIPAAm block. The all procedure was performed in aqueous media at ambient temperature by using γ-irradiation to initiate the polymerization. Details of the polymerization process have been described elsewhere.[47]

Amino-Functionalized Silica Nanoparticles Synthesis

A solution of 3-aminopropyltriethoxysilane (APTES) in methanol was condensed with an aqueous solution of hydrofluoric acid. In a typical run 4.06 mL of an aqueous solution of hydrofluoric acid (3 wt%) were added to 25 g of APTES in 125 mL methanol. The reaction mixture was stirred for 3.5 hours before the solvent was removed via high vacuum. The amino-functionalized silica nanoparticles were obtained as a glassy solid after high vacuum drying at 40 °C over night. Characterization by Matrix Assisted Laser Desorption Ionization − Time of Flight (MALDI-ToF) Mass Spectrometry revealed narrow and monomodal molecular weight distribution. A number average molecular weight of 2600 g·mol^{-1} was determined which correspond to an average of 23.6 amino groups per molecules.

Cross-Linking Procedure

In a typical procedure 15 mg of PNIPAAm$_{1000}$-b-PAA$_{2000}$ ($\overline{M}_{n, th}$ = 257 kg·mol^{-1}) was dissolved in deionized water. A tiny amount of KOH solution was added to reach basic pH and a sonic bath filled of cold water was used to accelerate the process. After full dissolution, 128.6 mg of amino-functionalized silica nanoparticles (10 molar equivalents)

of amino groups compared to acrylic acid moieties) were added. The pH was adjusted to pH 6 by addition of a diluted HCl solution, a turbid solution was obtained. Then the polymer concentration was adjusted to 0.5 g·L^{-1} by addition of deionized water. At room temperature under stirring, 2 Eq. compared to the acrylic acid units of 1-[3-(dimethylamino)propyl]-3-ethylcarbodiimide methiodide (EDCMeI) powder were introduced (69.4 mg). The solution was stirred overnight to complete the cross-linking process. The solution was then dialyzed several days against water to remove the residual urea compound generated from the EDCMeI and the non associated silica nanoparticles.

Characterization

pH-turbidimetric titration measurements were achieved using a titrator (Titrando 809, Metrohm, Herisau, Switzerland) equipped with a turbidity sensor (λ_0 = 523 nm, Spectrosense, Metrohm). The pH was determined with a Mettler Toledo MP 220 pH meter with an InLab 423 electrode. The pH meter was calibrated with buffer standard solutions of pH 4, 7, and 10. The titration was done using a hydrochloric acid solution 0.1 mol·L^{-1} using a dynamic addition.

Dynamic Light Scattering (DLS) was performed at 25 °C using an ALV DLS/SLS-SP 5022F compact goniometer system with an ALV 5000/E correlator and a He-Ne laser (λ = 632.8 nm; Peters ALV, Lange n, Germany). The intensity fluctuations were detected at 90°. Measurements were repeated five times with an accumulation time of 30 s. By means of CONTIN analysis of the intensity autocorrelation functions the intensity weighted hydrodynamic radii were derived from the collective diffusion coefficients by the Stokes-Einstein relation.

Dynamic light scattering titrations were performed with the same DLS setup and a computer controlled titrator (Titrando 809, Metrohm). Both instruments were synchronized by employing homemade software and hardware synchronization. Measurements were carried out in homemade glass cells consisting of a cylindrical scattering cell connected to a three-necked reservoir containing the solution, the stirrer (Methrom), and the micro-pH electrode (Metrohm) as well as the titration tube (Methrom), which was immersed in the solution. Sample preparation followed the same protocol as above. Five DLS measurements per titration step were performed at an angle

184

of 90° with correlation times of 30 s. The different titration parameters like the stirring speed and the stirring time as well as the lag time between the stirring period (equilibration period) and the actual LS measurement time were optimized to prevent any kinetic effects. Starting from a basic solution of polymer and silsesquioxane nanoparticles 10 µL addition volume per addition step of a hydrochloric solution 1M were mostly used for one DLS titration experiment. The concentration of the titrant (polymer and silsesquioxane nanoparticles) was high enough to ensure only minor dilution effects of the micellar solution. During each titration step, vigorous stirring was performed for 30 s, followed by a lag time of 30 s between the addition step and the LS measurement of the quiescent solution.

Scanning force microscopy (SFM) measurements were performed with a Dimension 3100 Metrology SFM (Digital Instruments, Veeco Metrology Group) operated in tapping mode by using silicon tips with a spring constant of 40 N·m^{-1} and a resonance frequency in the range between 200 and 300 kHz. Scan rates were between 0.5 and 1 Hz and a resolution of 256×256 were used for image recording. Samples were prepared on silicon wafers by spin casting at 2000 rpm from 0.1 wt% polymer solution in water.

Transmission electron microscopy (TEM) images were taken on a Zeiss EM EF-TEM instrument operated at 200 kV. A 5 µL droplet of a diluted solution (~0.01 g·L^{-1}) in water, was dropped onto a copper grid (200 mesh) coated with carbon film, followed by drying at room temperature for a short time.

ζ-Potential and Size Measurements were measured on a Malvern Instruments Zetasizer Nano ZS with a 4 mW He-Ne laser (633 nm) and a detection angle of 173°. Size distributions were determined by fitting the experimental correlation curve to a multiexponential using the CONTIN algorithm. ζ-potentials were calculated via the Smoluchowski equation.

Results and Discussion

PNIPAAm-*b*-PAA and Silsesquioxane Nanoparticles Self-Assembly

Reversible addition-fragmentation chain transfer polymerization (RAFT) initiated by γ-radiation in water has been proven to be very effective to obtain very long polymers with narrow molecular weight distribution and with a low amount of termination even at high conversion.[48] Therefore a PNIPAAm-*b*-PAA with a degree of polymerization of 1000 for PNIPAAm block and 2000 for PAA block ($\overline{M}_{n, th}$ = 257 kg·mol^{-1}) was obtained with a rather low polydispersity (PDI = 1.40).

Table 7-1. Hydrodynamic radii of PNIPAAM$_{1000}$-*b*-PAA$_{2000}$ obtained by DLS under different conditions of pH and temperature

Temperature (°C)	pH	R_H (nm)
25	7	Not evaluated
40	7	85
25	4	43
40	4	Aggregation
25	2	Aggregation

Due to the nature of the two blocks, this block-copolymer can respond to several external stimuli, like temperature, pH and ionic strength.[34] Selected results of behaviour are highlighted in Table 7-1. In aqueous solution at neutral or basic pH and room temperature, PNIPAAm$_{1000}$-*b*-PAA$_{2000}$ is fully soluble and exists as random coils. When the temperature is raised above the cloud point (T_{cl}) spherical micelles are formed;[49] hydrophobic PNIPAAm forming the micellar core and hydrophilic PAA block generating the corona, which prevents the full aggregation of the system. In our particular system, a hydrodynamic radius (R_H) of 85 nm was determined by dynamic light scattering (DLS). The phase transition is fully reversible and after cooling down, the solution is again fully transparent. By changing the pH to acidic (pH 4) at ambient temperature, micelles are

186

also formed. A complex based on hydrogen bonding interaction between the carboxylic group of the PAA and the amide group of the NIPAAm is obtained. Monodisperse and narrow distributed objects of $R_H = 43$ nm can be observed (Entry 3 of Table 7-1). Under acidic conditions, an increase of temperature above T_{cl} leads to the aggregation of the system. Moreover lowering the pH to pH 2 or below generates at ambient temperature macroscopic particles too.

The addition of amino-functionalized silsesquioxane nanoparticles strongly modifies the behaviour of PNIPAAm-*b*-PAA. These silica particles were synthesized via condensation of 3-aminopropyltriethoxysilane (APTS) in methanol solution catalyzed by hydrofluoric acid. This process allows the generation of narrow distributed small inorganic particles (d $\approx$ 3 nm). A number-average molecular weight of 2600 g·mol^{-1} was determined by MALDI-ToF which corresponds to approximately 23.6 amino groups per particles. Because of the tiny size and high functionality, the silica particles can be uniformly dispersed in water and behave as single dissolved molecules to form a transparent colloidal solution. These properties are significantly different from those of hydrophilic silica particles prepared from tetraethoxysilane.
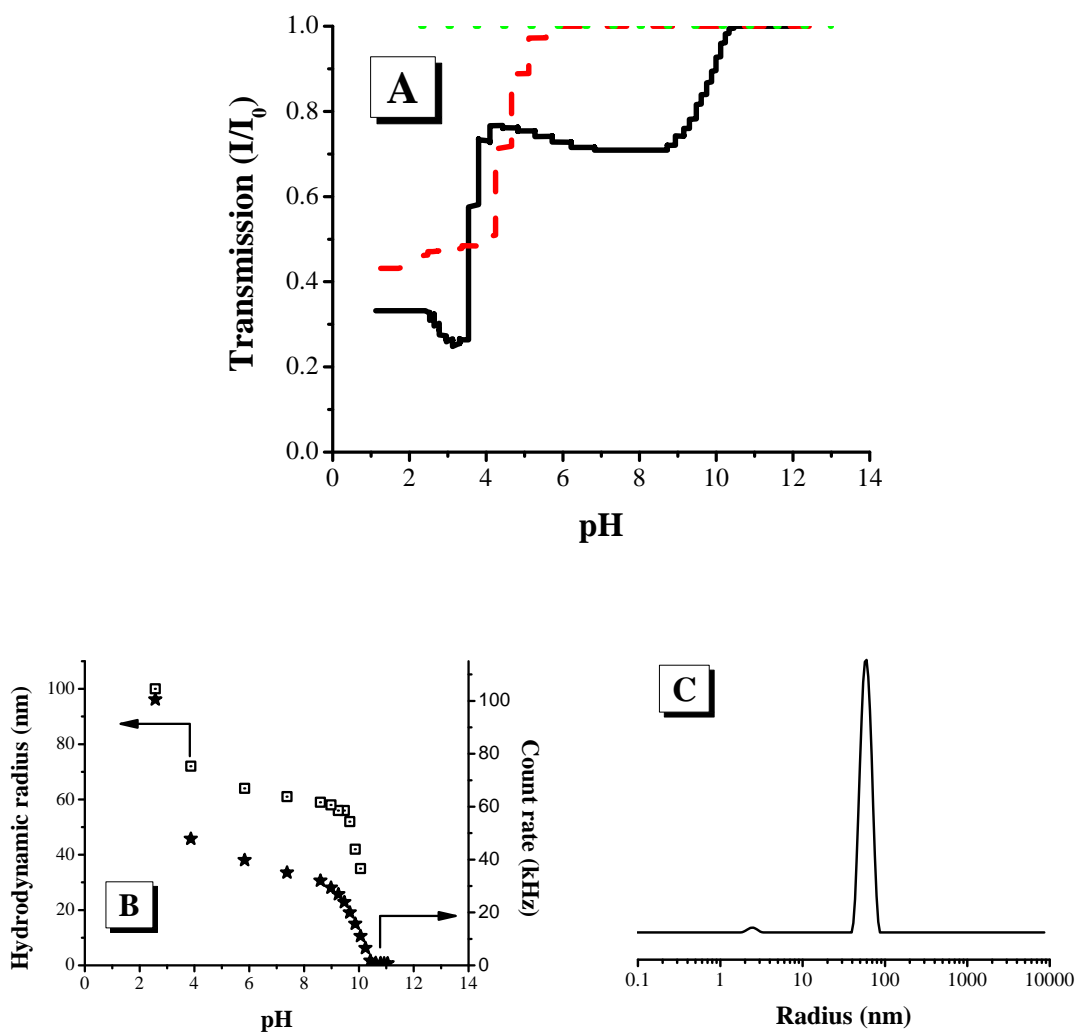
Figure 7-1. Self-assembly of PNIPAAm$_{1000}$-*b*-PAA$_{2000}$ and amino-functionalized silsesquioxane nanoparticles trigger by the pH. (A) pH-turbidimetric titration in water of PNIPAAm$_{1000}$-*b*-PAA$_{2000}$ (——), amino-functionalized silsesquioxane nanoparticles (– –) and their complex with a ratio [NH$_2$]/[AA] of 10 (• • •). (B) Dynamic light scattering titration of the hybrid for a ratio [NH$_2$]/[AA] of 10 with (⊡) the hydrodynamic radius and (★) the count rate. (C) Unweighted radius distribution determined for the same complex at pH 7.4.

The complexation in water of PNIPAAm$_{1000}$-*b*-PAA$_{2000}$ and amino-functionalized silsesquioxane with a ratio [NH$_2$]/[AA] of 10 was investigated by pH-turbidimetric titration and DLS titration (Figure 7-1). When the two components were mixed at high

pH (pH $\geq$ 12) a clear transparent solution is observed (Figure 7-1A). No insoluble complex is formed in alkaline solution, where PAA is fully ionized and the amino-residues are in a neutral state. However by adding HCl a turbid dispersion is obtained. A transition occurs at pH 10.5 and micelles are obtained without any traces of macroscopic aggregates present. At this pH, some of the amino groups are protonated and a complex with carboxylate units occurred. Micelles composed of a core of PAA and silica particles surrounded by a PNIPAAm corona are formed. Decreasing the pH, leads to more and more protonation of the NH_2 and to a stronger complex. However, at lower pH, the carboxylate units are protonated to carboxylic acid moieties. When the pH is decreased below pH 4, another transition is detected by turbidimetry. The transmission drops drastically and a highly turbid solution is obtained. At this point the PNIPAAm chains start to interact with PAA by hydrogen bonding between the amide groups and the carboxylic moieties. Subsequent addition of HCl leads to the system's aggregation. Finally it is important to notice that this behaviour is fully reversible and the disintegration of the nanohybrids can be simply performed by adding sodium hydroxide to the system.

The response to pH of PNIPAAm$_{1000}$-b-PAA$_{2000}$ in presence amino-functionalized silica particles is strongly different to the one of the single components alone in water, which proved that the complexation between the amino and the acrylate residues occurs. The silsesquioxane solution is fully transparent over the full range of pH. The pH-turbidimetric titration curve obtained for the pure PNIPAAm$_{1000}$-b-PAA$_{2000}$ is in good agreement to the results observed by DLS (Table 7-1) when the pH is varied. Above pH 5.5, the solution is clear and the block copolymer is fully soluble in water. Then a transition is observed and micelles are formed. This type of complexation of silica particles and PAA was already demonstrated in our group. Hydroxy-diglycidylamino-functionalized silsesquioxane particles form complexes with a large variety of structures based on PAA like homopolymer,[17] block-copolymer,[39] star-polymer[24] or polymer brush.[22]

Similar results for the complexation in water of PNIPAAm$_{1000}$-b-PAA$_{2000}$ and amino-functionalized silsesquioxane were observed by DLS titration (Figure 7-1B). Above pH 10.5, the count rate is extremely low, no complex or aggregates can be detected. Then by

adding HCl micelles were observed. The hydrodynamic radius, R_H, increases when the pH decreases until pH 2.5 where macroscopic aggregation occurred. The radius distribution (Figure 7-1C), recorded at pH 7.4, shows a narrow distribution with an average hydrodynamic radius $R_H = 61$ nm and the absence of large aggregates. A small secondary peak at 3 nm can be also seen, which appears sometimes in the radius distribution and which can stems from residual silica particles, which do not participate to the formation of the complex.
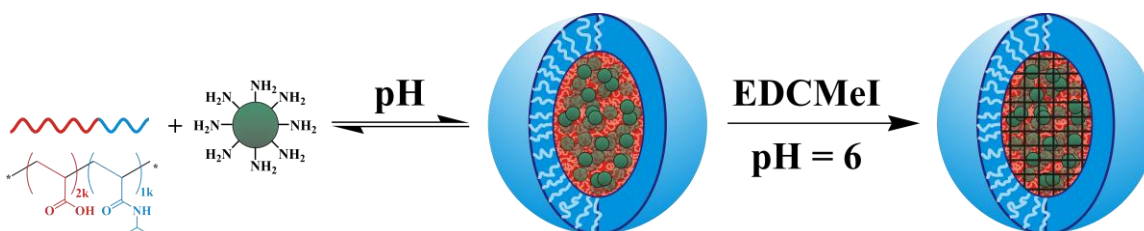
Scheme 7-1. Schematic representation of the preparation of PNIPAAm-*b*-PAA - silica nanohybrids. PNIPAAm-*b*-PAA and amino-functionalized silsesquioxane are first self-assembled as spherical micelles in water by tuning the pH below 10.5. The micelles are crosslinked at pH 6 by addition of 1-[3-(dimethylamino)propyl]-3-ethylcarbodiimide methiodide (EDCMeI).

Silica/PNIPAAm-*b*-PAA Nanohybrids

To keep this micellar structure even at high pH and make robust objects, the nanohybrids were cross-linked via amidification reaction. The cross-linking occurs in the core of the micelle. Compared to shell cross-linking this strategy prevents intermicellar coupling. The reaction was carried out at pH=6 in presence of 1-[3-(dimethylamino)propyl]-3-ethylcarbodiimide methiodide (EDCMeI) which promotes the amidification (Scheme 7-1). Two equivalents of this compound compared to the acrylic acid moieties were used to ensure a good cross-linking density. Four different [NH$_2$]/[AA] ratios were investigated: 10, 5, 2 and 1. In all cases, the complexation between the silica particles and the block-copolymer occurred at pH 6 and core-crosslinked nanohybrids were obtained.
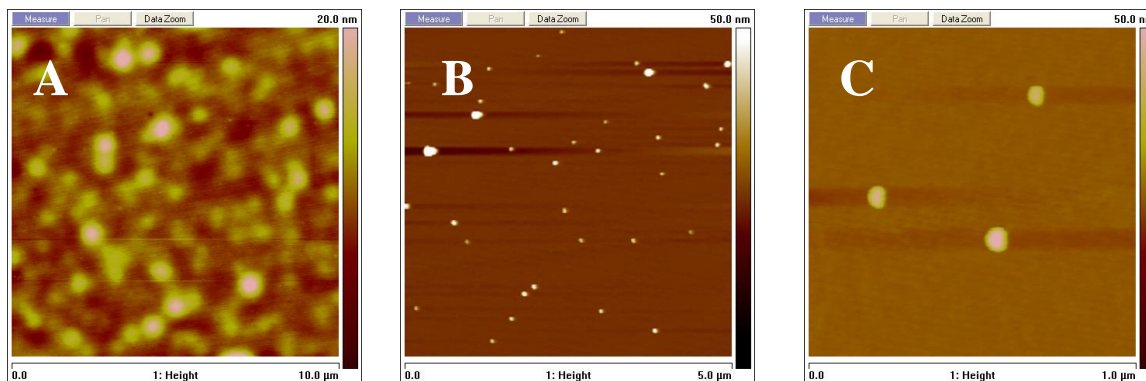
Figure 7-2. Scanning force microscopy of PNIPAAm$_{1000}$-*b*-PAA$_{2000}$ and amino-functionalized nanohybrids (A) before cross-linking, (B) and (C) after cross-linking at different magnifications.

Figure 7-2 shows tapping mode scanning force microscopy (SFM) images of PNIPAAm-b-PAA/silsesquioxane complexes at neutral pH when a ratio [NH$_2$]/[AA] = 5 is used. Before cross-linking (Figure 7-2A), the structure is not really clear, large and very flat spherical objects are observed (average length of 500 nm and height of 9 nm). These results can be explained by the strong interaction of materials with the mica substrate which destroys the integrity of the complex and leads to undefined structures. After cross-linking (Figure 7-2B-C), well-defined spherical objects are seen. An average height of 30 nm and a diameter of 80 nm were evaluated. No free partially cross-linked fragment was detected. However few larger structures of 300 nm were also seen. The difference of results, before and after cross-linking, proves that the amidification reaction was efficient to lock the structure of the organic-inorganic nanohybrids.

Table 7-2. Hydrodynamic radii PNIPAAM$_{1000}$-*b*-PAA$_{2000}$ - silica nanoparticles nanohybrids after cross-linking obtained by DLS at pH 7 under different [NH2]/[AA] ratio

$\dfrac{[NH_2]}{[AA]}$	$\dfrac{R_H}{(nm)}$
10	157
5	137
2	127
1	59

An overview of the different hydrodynamic radii obtained by DLS of the cross-linked structures depending on the [NH$_2$]/[AA] ratio can be found in Table 7-2. It can be clearly seen that R$_H$ is smaller when the number of silica particles added to the block-copolymer decreases. A variation from 157 nm to 59 nm was found. It is also interesting notice that R$_H$ before and after core cross-linking exhibits a strong variation. In the case of [NH$_2$]/[AA] = 10 at neutral pH R$_H$ = 61 nm, whereas after reaction the hydrodynamic radius is almost three times higher. This phenomenon can be explained by the transformation of the carboxylic groups and amino residues present in amide functionality which decreases the original ionic interactions. Moreover after cross-linking there is an excess of amino group present. At neutral pH, they are in a protonated form (NH3+) and they behave as a polyelectrolyte which tends to expand due to the charge density.
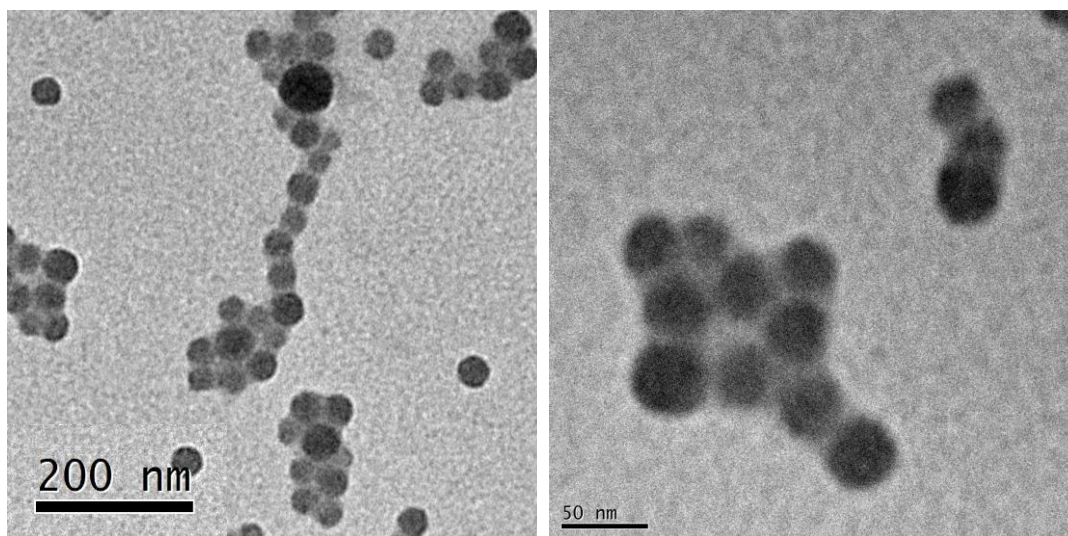
Figure 7-3. Silica-PNIPAAm$_{1000}$-b-PAA$_{2000}$ core cross-linked micelles for a [NH2]/[AA] ratio of 2 at different magnification.

Figure 7-3 shows transmission electron microscopy images of the cross-linked nanohybrids for a ratio [NH$_2$]/[AA] = 2. Small spherical objects are observed. The size is smaller than the one obtained by DLS. This is due to the high contrast of the core compared to the corona which allows detecting only the PAA-silica core. The super-structures seen in SFM are also present; however their number declines with the ratio. For [NH$_2$]/[AA] = 1 none of them were detected.

Table 7-3. Response to temperature of silica/PNIPAAm$_{1000}$-b-PAA$_{2000}$ core cross-linked micelles at [NH$_2$]/[AA] = 10 in water.

Conditions	$\dfrac{R_H}{nm}$	$\dfrac{\zeta}{mV}$
25°C, pH=7	173	+18
40°C, pH=7	124	+60
25°C, pH=13	139	+1
40°C, pH=13	Aggregation	——

The response to temperature of these robust micelles was also explored. Depending of the pH, the behavior can be tuned. At neutral pH, the hydrodynamic radius decreases above the LCST when at high pH, the hybrids aggregate (Table 7-3). This can be explained by the charges present in the micelle as demonstrated by zeta potential measurements. At pH 7, the residual amino groups are protonated, a charge is observed (ζ = +18 mV) which prevents the aggregation when the temperature is raised. In basic solution (pH 13), the hybrid is stable which proves the efficiency of the crosslinking. Moreover, amino groups are deprotonated, no charge is detected to avoid the destabilization of the system.

Conclusions

A high molecular weight PNIPAAm-*b*-PAA was used to complex amino-functionalized silsesquioxane nanoparticles. Around neutral pH, the carboxylate groups of PAA interact with the protonated amino groups present on the silica and they formed the core of a spherical micelle which is stabilized by thermoresponsive PNIPAAm block. The structure was cross-linked via amidification reaction between the carboxylic group and the amino residues to generate robust nano-objects. DLS, SFM and TEM confirmed the locking of micelles. Narrow distributed spherical SCM were observed. However a tiny amount of superstructure was also found in the media. Finally to illustrate the potential of these new organic-inorganic nanohybrids, we demonstrated that the response to temperature in aqueous media was able to be trigger by the pH. At high pH, the objects aggregate; whereas at neutral pH, due to the residual ammonium present in the core, the size of nanohybrids decreases. We believe that the strategy developed can be really convenient and straightforward to generate well-defined water soluble polymer-silica nanohybrids.

Acknowledgements

References

(1)   *Hybrid Materials: Synthesis, Characterization, and Applications*; Kickelbick, Guido ed.; Wiley-VCH: Weinheim, 2007.

(2)   Paul, D. R.; Robeson, L. M. *Polymer* **2008**, *49*, 3187-3204.

(3)   Tjong, S. C. *Materials Science and Engineering: R: Reports* **2006**, *53*, 73-197.

(4)   Daniel, M.-C.; Astruc, D. *Chemical Reviews* **2004**, *104*, 293-346.

(5)   Kawakami, Y.; Kakihana, Y.; Miyazato, A.; Tateyama, S.; Hoque, M. In *Advances in Polymer Science*, 2010.

(6)   Wu, J.; Mather, P. T. *Polymer Reviews* **2009**, *49*, 25 - 63.

(7)   Ogoshi, T.; Chujo, Y. *Composite Interfaces* **2005**, *11*, 539-566.

(8)   Han, J. T.; Xu, X.; Cho, K. *Langmuir* **2005**, *21*, 6662-6665.

(9)   Lee, C.-K.; Don, T.-M.; Lai, W.-C.; Chen, C.-C.; Lin, D.-J.; Cheng, L.-P. *Thin Solid Films* **2008**, *516*, 8399-8407.

(10)   Stelzig, S. H.; Klapper, M.; Müllen, K. *Advanced Materials* **2008**, *20*, 929-932.

(11)   Muthukrishnan, S.; Plamper, F.; Mori, H.; Müller, A. H. E. *Macromolecules* **2005**, *38*, 10631-10642.

(12)   Zhao, Y.; Perrier, S. *Macromolecules* **2007**, *40*, 9116-9124.

(13)   Yuan, J.; Xu, Y.; Walther, A.; Bolisetty, S.; Schumacher, M.; Schmalz, H.; Ballauff, M.; Müller, A. H. E. *Nat Mater* **2008**, *7*, 718-722.

(14)   Ranjan, R.; Brittain, W. J. *Macromolecular Rapid Communications* **2008**, *29*, 1104-1110.

(15)   Yamada, Y.; Qiao, K.; Bao, Q.; Tomida, D.; Nagao, D.; Konno, M.; Yokoyama, C. *Catalysis Communications* **2009**, *11*, 227-231.

(16)   Feng, J.; Li, Y.; Yang, M. *Sensors and Actuators B: Chemical* **2010**, *145*, 438-443.

(17)   Mori, H.; Müller, A. H. E.; Klee, J. E. *Journal of the American Chemical Society* **2003**, *125*, 3712-3713.

(18)   Mori, H.; Lanzendörfer, M. G.; Müller, A. H. E.; Klee, J. E. *Langmuir* **2004**, *20*, 1934-1944.

(19)   Liu, G.; Ji, H.; Yang, X.; Wang, Y. *Langmuir* **2008**, *24*, 1019-1025.

(20)   Balazs, A. C.; Emrick, T.; Russell, T. P. *Science* **2006**, *314*, 1107-1110.

(21)   Mackay, M. E.; Tuteja, A.; Duxbury, P. M.; Hawker, C. J.; Van Horn, B.; Guan, Z.; Chen, G.; Krishnan, R. S. *Science* **2006**, *311*, 1740-1743.

(22)   Retsch, M.; Walther, A.; Loos, K.; Müller, A. H. E. *Langmuir* **2008**, *24*, 9421-9429.

(23)   Kind, L.; Plamper, F. A.; Göbel, R.; Mantion, A.; Müller, A. H. E.; Pieles, U.; Taubert, A.; Meier, W. *Langmuir* **2009**, *25*, 7109-7115.

(24)   Schumacher, M.; Ruppel, M.; Kohlbrecher, J.; Burkhardt, M.; Plamper, F.; Drechsler, M.; Müller, A. H. E. *Polymer* **2009**, *50*, 1908-1917.

(25)   Schmaljohann, D. *Advanced Drug Delivery Reviews* **2006**, *58*, 1655-1670.

(26)   Roy, D.; Cambre, J. N.; Sumerlin, B. S. *Progress in Polymer Science* **2010**, *35*, 278-301.

(27)   Stuart, M. A. C.; Huck, W. T. S.; Genzer, J.; Muller, M.; Ober, C.; Stamm, M.; Sukhorukov, G. B.; Szleifer, I.; Tsukruk, V. V.; Urban, M.; Winnik, F.; Zauscher, S.; Luzinov, I.; Minko, S. *Nat Mater* **2010**, *9*, 101-113.

(28)   Harper, M.; Hu, J. *Journal of Intelligent Material Systems and Structures, pp. 859-885 vol. 21:* **2010**.

(29)   Gil, E. S.; Hudson, S. M. *Progress in Polymer Science* **2004**, *29*, 1173-1222.

(30)   Yang, H.; Cheng, R.; Wang, Z. *Polymer* **2003**, *44*, 7175-7180.

(31)   Dimitrov, I.; Trzebicka, B.; Müller, A. H. E.; Dworak, A.; Tsvetanov, C. B. *Progress in Polymer Science* **2007**, *32*, 1275-1343.

(32)   Plamper, F. A.; Becker, H.; Lanzendörfer, M. G.; Patel, M.; Wittemann, A.; Ballauff, M.; Müller, A. H. E. *Macromolecular Chemistry and Physics* **2005**, *206*, 1813-1825.

(33)   Hofs, B.; de Keizer, A.; van der Burgh, S.; Leermakers, F. A. M.; Cohen Stuart, M. A.; Millard, P.-E.; Müller, A. H. E. *Soft Matter* **2008**, *4*, 1473-1482.

(34)   Schilli, C. M.; Zhang, M.; Rizzardo, E.; Thang, S. H.; Chong, Y. K.; Edwards, K.; Karlsson, G.; Müller, A. H. E. *Macromolecules* **2004**, *37*, 7861-7866.

(35)   Li, G.; Song, S.; Guo, L.; Ma, S. *Journal of Polymer Science Part A: Polymer Chemistry* **2008**, *46*, 5028-5035.

(36)   Berger, S.; Synytska, A.; Ionov, L.; Eichhorn, K.-J.; Stamm, M. *Macromolecules* **2008**, *41*, 9669-9676.

(37)   Huang, J.; Hu, X.; Zhang, W.; Zhang, Y.; Li, G. *Colloid & Polymer Science* **2008**, *286*, 113-118.

(38)   Isojima, T.; Lattuada, M.; Vander Sande, J. B.; Hatton, T. A. *ACS Nano* **2008**, *2*, 1799-1806.

(39)   Schumacher, M.; Ruppel, M.; Yuan, J.; Schmalz, H.; Colombani, O.; Drechsler, M.; Müller, A. H. E. *Langmuir* **2009**, *25*, 3407-3417.

(40)   Yan, E.; Ding, Y.; Chen, C.; Li, R.; Hu, Y.; Jiang, X. *Chemical Communications* **2009**, 2718-2720.

(41)   Motornov, M.; Roiter, Y.; Tokarev, I.; Minko, S. *Progress in Polymer Science* **2010**, *35*, 174-211.

(42)   Park, C.-Y.; Lee, Y.-G.; Oh, C.; Oh, S.-G. *Journal of Industrial and Engineering Chemistry* **2010**, *16*, 32-38.

(43)   Tsyalkovsky, V.; Burtovyy, R.; Klep, V.; Lupitskyy, R.; Motornov, M.; Minko, S.; Luzinov, I. *Langmuir* **2010**, *26*, 10684-10692.

(44)   Zhang, L.; Liu, W.; Lin, L.; Chen, D.; Stenzel, M. H. *Biomacromolecules* **2008**, *9*, 3321-3331.

(45)   O'Reilly, R. K.; Hawker, C. J.; Wooley, K. L. *Chemical Society Reviews* **2006**, *35*, 1068-1083.

(46)   Read, E. S.; Armes, S. P. *Chemical Communications* **2007**, 3021-3035.

(47)   Millard, P.-E.; Barner, L.; Reinhardt, J.; Buchmeiser, M. R.; Barner-Kowollik, C.; Müller, A. H. E. *Polymer* **2010**, *51*, 4319-4328.

(48)   Millard, P.-E.; Barner, L.; Stenzel, M. H.; Davis, T. P.; Barner-Kowollik, C.; Müller, A. H. E. *Macromolecular Rapid Communications* **2006**, *27*, 821-828.

(49)   Kulkarni, S.; Schilli, C.; Grin, B.; Müller, A. H. E.; Hoffman, A. S.; Stayton, P. S. *Biomacromolecules* **2006**, *7*, 2736-2741.

List of Publications

13 Crassous, J. J.; **Millard P.-E.**; Mihut, A. M.; Polzer, F.; Drechsler, M.; Ballauff, M.; Schurtenberger, P.: Colloidal Molecules Formation through Asymmetric Self-Assembly of Oppositely Charged Composite Microgels and Gold Nanoparticles, *in preparation*

12 Crassous, J. J.; **Millard, P.-E.**; Mihut, A. M.; Witterman, A.; Drechsler, M.; Ballauff, M.; Schurtenberger, P.: Biomimetic Self-Assembly of Oppositely Charged Polyelectrolytes Brushes and Cationic Gold Particles into Giant Hollow Fibers, *submitted to advanced materials*

11 **Millard, P.-E.;** Crassous, J. J.; Yuan, J.; Mihut, A.; Hanisch, A.; Müller, A. H. E,: New Water-Soluble Smart Polymer-Silica Hybrids Based on Poly(*N*-isopropylacrylamide)-*b*-Poly(Acrylic Acid), *in preparation*

10 **Millard, P.-E.**; Crassous, J. J.; Mihut, A. M., Yuan, J.; Müller, A. H. E,: Poly(*N*-Isopropylacrylamide)-*b*-Poly(Acrylic Acid) Shell Cross-Linked Micelles Formation and Application to the Synthesis of Metal-Polymer Hybrids, *in preparation*

9 Penott-Chang, E. K.; Walther, A.; **Millard, P.-E.**; Jäger, A. Jäger, E.; Müller, A. H. E.; Guterres, S. S.; Pohlmann, A. R.: Amphiphilic diblock copolymer and polycaprolactone blends to produce new vesicular nanocarriers, *accepted in J. Biomed. Nanotechnol.*

8 **Millard, P.-E.**; Barner, L.; Reinhardt, J.; Stenzel M. H.; Buchmeiser, M. R.; Davis, T. P.; Barner-Kowollik, C.; Müller, A. H. E.: Synthesis of Water-Soluble Homo- and Block Copolymers by RAFT Polymerization under γ-Irradiation in Aqueous Media, *Polymer*, 51(19), 4319 (**2010**)

7 **Millard, P.-E.**; Mougin, N. C.; Böker, A.; Müller, A. H. E.: Controlling the Fast ATRP of *N*-Isopropylacrylamide in Water, *Controlled/Living Radical Polymerization: Progress in ATRP*, ACS Washington DC, Ed: Matyjaszewski, K.; 1023, 127 **(2009)**

6 Walther, A.; **Millard, P.-E.**; Goldmann, A. S.; Lovestead, T. M.; Schacher, F.; Barner-Kowollik, C.; Müller, A. H. E.: Bis-Hydrophilic Block Terpolymers via RAFT Polymerization: Toward Dynamic Micelles with Tunable Corona Properties, *Macromolecules*, 41(22), 8608 **(2008)**

5 **Millard, P.-E.**; Mougin, N.; Böker, A.; Müller, A. H. E.: Fast ATRP of *N*-isopropylacrylamide in water and its application to bioconjugates, *Polym. Prepr.*, 49(2), 121 **(2008)**

4 Goldmann, A. S.; **Millard, P.-E.**; Quénemer, D.; Davis, T. P.; Stenzel, M. H.; Barner-Kowollik, C.; Müller, A. H. E.: Access to cyclic polystyrenes *via* a combination of reversible addition fragmentation chain transfer (RAFT) polymerization and click chemistry, *Polym. Prepr.*, 49(2), 1 **(2008)**

3 Hofs, B.; de Keizer, A.; van der Burgh, S.; Leermakers, F. A. M.; Cohen Stuart, M. A.; **Millard, P.-E.**; Müller, A. H. E.: Complex coacervate core micro-emulsions, *Soft Matter*, 4(7), 1473 **(2008)**

2 Goldmann, A. S.; Quémener, D.; **Millard, P.-E.**; Davis, T. P.; Stenzel, M. H.; Barner-Kowollik, C.; Müller, A. H. E.: Access to cyclic polystyrenes *via* a combination of reversible addition fragmentation chain transfer (RAFT) polymerization and click chemistry, *Polymer*, 49(9), 2274 **(2008)**

1 **Millard, P.-E.**; Barner, L.; Stenzel, M. H.; Davis, T. P.; Barner-Kowollik, C.; Müller, A. H. E.: RAFT Polymerization of *N*-Isopropylacrylamide and Acrylic Acid under γ-Irradiation in Aqueous Media, *Macromol. Rapid Commun.*, 27(11), 821 **(2006)**

Acknowledgments

Only with the help and the support of the people around me, I was able to complete this thesis. I am thankful to all of them.

First and foremost, I would like to express all my gratitude to my supervisor Prof. Axel Müller. He gave me a great opportunity to work in his excellent laboratory on a topic of choice. I want to thank him for sharing his scientific knowledge, for his patience and for his confidence in letting me develop different projects independently with just as little guidance as necessary. This has helped me in exploring many different fields of chemistry. It was a great chance to work with him.

I had a wonderful time throughout the last years. I am particularly grateful to all the opportunities I have been offered. Presenting my work at numerous national and international conferences, having the possibility of spending time overseas and being able to cooperate with a number of groups have been a great experience and enriched my personality and my scientific skills.

Many thanks go out to the MCII group and people from other chairs at Uni Bayreuth who have helped me making this dissertation become reality. The open and direct support from many sides was an enormous help for my PhD. They also participated to the very good atmosphere present. In particular, I want to thank Sabine Wunder to introduce me to the liquid chromatography techniques and with whom I shared plenty of good times. I thank also Jérôme Crassous with whom I worked closely during a part of my PhD, I have really appreciated all our scientific discussions and all the fun we had together. I acknowledge Jiayin Yuan and Youyong Xu, my fume hood neighbors who have supported me and my RAFT smells daily. I thank also Markus Burkhardt and Felix Shacher who have shared my office. A special thank you goes to the French connection, Alexandre Terrenoire, Andre Xavier, Sandrine Tea and Christophe Rochette. I am grateful to all my colleagues for the pleasant time we spend together, Anja Goldmann, Adriana Mihut, Felix Plamper, Manuela Schumacher, Sergey Nosov, Andreas Walther, Markus Ruppel, André Pfaff, André Gröschel, Andreas Hanisch, Stephan Reinicke, Alexander Schmaltz, Stephan Weiß, Markus Müllner, Annette Krökel, Holger Schmalz,

Erklärung

Die vorliegende Arbeit wurde von mir selbstständig verfasst und ich habe keine anderen als die angegebenen Hilfsmittel benutzt. Ferner habe ich nicht versucht, anderweitig mit oder ohne Erfolg eine Dissertation einzureichen oder mich der Doktorprüfung zu unterziehen.

Bayreuth, den 27.07.2010

Pierre-Eric Millard